Design, Synthesis and Study of Polycyclic Aromatic Hydrocarbons and their Cation Radicals

Tushar Navale
Marquette University

DESIGN, SYNTHESIS AND STUDY OF POLYCYCLIC AROMATIC HYDROCARBONS AND THEIR CATION RADICALS

by

Tushar Shivram Navale, B.Sc., M.Sc.

A Dissertation submitted to the Faculty of the Graduate School,
Marquette University,
in Partial Fulfillment of the Requirements for
the Degree of Doctor of Philosophy

Milwaukee, Wisconsin

May 2012

ABSTRACT

DESIGN, SYNTHESIS AND STUDY OF POLYCYCLIC AROMATIC HYDROCARBONS AND THEIR CATION RADICALS

Tushar Shivram Navale, B.Sc., M.Sc.

Marquette University, 2011

The unifying theme of most of optoelectronic devices revolves around the charge carrier mobility of the organic materials used in the conductive layers, which is a measure of how easily the electron/hole moves in a particular π conjugated organic material. When π conjugated materials are incorporated in these devices, molecules are generally layered in random orientation. Consequently, the efficiency of charge transport in the conducting layers of these devices is governed not only by the intramolecular electron/hole transport through the backbone of the molecule but also by the intermolecular electron/hole transport between the molecules and hence packing of these molecules plays a critical role in the efficiency of these devices. Although significant progress has been made in understanding the charge transport mechanisms in various polycyclic aromatic hydrocarbons (PAHs), the usefulness of such materials in functional devices remains limited; hence design and synthesis of new PAHs to better understand the charge transport mechanisms remains an active area of research.

A novel series of methoxydibenzochrysenes was designed and synthesized utilizing ferric chloride mediated oxidative cyclodehydrogenation as a key step. We have also shown that numerous 9,10-diarylphenanthrenes and dibenzo[g,p]chrysenes can be prepared from a readily available tetraarylethylenes using 1 and 2 equivalents of 2,3-dichloro-5,6-dicyano-1,4-benzoquinone (DDQ), respectively. A similar oxidative cyclodehydrogenation strategy was used for synthesizing a highly soluble, larger derivative of hexa-*peri*-hexabenzocoronene (HBC), where twelve carbon-carbon bonds are formed in a single step. Deployment of fluorenes at the periphery of the HBC core not only imparts solubility to the structure, but also allows the new PAHs to be functionalized further to make bigger PAHs.

X-ray crystal structure determination of octamethoxydibenzochrysene cation radical and 1,4,5,8-tetramethoxyanthracene dimer cation radical, in addition to their neutral structures, allowed us to delineate the effect of electron removal on their bond length changes. Definitive X-ray crystallographic evidence is obtained for a single hole to be uniformly distributed on the three equivalent 1,2-dimethoxybenzenoid (or veratrole) rings in the hexamethoxytriptycene cation radical. This conclusion is further supported by electrochemical analysis and by the observation of an intense near-IR transition in its electronic spectrum, as well as by comparison of the spectral and electrochemical characteristics with the model compounds containing one and two dimethoxybenzene

rings. A new class of intervalance cation radicals from *p*-diaryloxybenzenes was also studied.

ACKNOWLEDGEMENTS

Tushar Shivram Navale, B.Sc., M.Sc.

I would like to sincerely thank Prof. Rajendra Rathore for his assistance and guidance in getting my graduate career started on the right foot and providing me with the foundation for becoming a synthetic organic chemist. His pursuit for the science and his enthusiasm for the research have made deep impression on me.

I also thank my committee members Dr. James Gardinier, Dr. Adam Fiedler and Dr. Daniel Sem for spending their precious time to read my dissertation and provide feedback on it. I like to thank Prof. S. H. Mashraqui – my M.Sc. advisor, for introducing me to the laboratory research and motivating me to pursue doctoral studies.

I would like to acknowledge the funding sources – Marquette University, Department of Chemistry and Prof. Eisch research fellowship.

I wish to thank Dr. Sergey Lindeman for the X-ray crystallography. I also want to thank Rathore group members with whom I worked for all their help during my stay at Marquette. I would particularly like to thank Vijay for sharing his immense Chemistry knowledge and experience. I also thank my friends specially Chiran Doshi, Vaibhav Tale, Ronak Dholakia and Esteban Di Masi for their support.

I want to thank all my teachers who have taught me Chemistry: my junior college teacher at DMJC, Ale (especially Devkar sir), my undergraduate teachers at the D. G. Ruparel College, Mumbai (especially Dr. R. Manjrekar, Dr. N. R. Pai and Dr. K. Waghmode) and my graduate teachers at the University Department of Chemistry (UDC), Kalina (especially Dr. A. V. Karnik).

I am grateful to my Mother- Nirmala and Father-Shivram, for their faith in me and allowing me to be as ambitious as I wanted. It was under their watchful eye that I gained so much drive and an ability to tackle challenges head on. Also, I thank Shubhangi, Praveen, Dayanand and Manisha for providing me with unending encouragement and support. Finally, I thank all those who directly or indirectly contributed towards the completion of this thesis in its final form.

TABLE OF CONTENTS

LIST OF FIGURES

General Introduction

Chapter 1A

Chapter 2A

Chapter 2B

Chapter 3

Chapter 4

LIST OF TABLES

Chapter 1A

Chapter 1B

Chapter 2A

Chapter 2B

Chapter 3

LIST OF SCHEMES

Chapter 1A

Chapter 1B

Chapter 2A

Chapter 2B

Chapter 3

Chapter 4

INTRODUCTION

Reactive organic cation radicals are critical intermediates in many organic reactions[1-3], while stable cation radicals are of contemporary interest in organic material science, since they represent the smallest unit that carry a delocalized positive charge, mainly intended for molecular devices such as electrical and photoconductors, ferro-magnets, sensors, optical switches etc.[4,5]

The unifying theme of most of optoelectronic devices revolves around the charge carrier mobility of the organic materials used in the conductive layers, which is a measure of how easily the electron/hole moves in a particular π conjugated organic material[6]. When π conjugated materials are incorporated in these devices, molecules are generally layered in random orientation (Fig. 1)[7-10]. Consequently, the efficiency of charge transport in the conducting layers of these devices is governed not only by the intramolecular electron/hole transport through the backbone of the molecule but also by the intermolecular electron/hole transport between the molecules and hence packing of these molecules plays a critical role in the efficiency of these devices. Although significant progress has been made in understanding the charge transport mechanisms in various polycyclic aromatic hydrocarbons (PAHs), the usefulness of such materials in functional devices remains limited; hence design and synthesis of new PAHs to better understand the charge transport mechanisms remains an active area of research.

Thus, designing better conductive organic materials for photovoltaic applications requires thorough studies to develop a necessary understanding of structure-function relationships for both electron and hole transport along the conjugated chains[11-12], and

through cofacially stacked aromatic π systems[7-10, 13-16]. In this regard, we[13-19] and others[7-10] have been investigating the structural factors governing the interchain charge transport using a variety of cofacially arrayed molecules with varying degrees of interchain overlap.

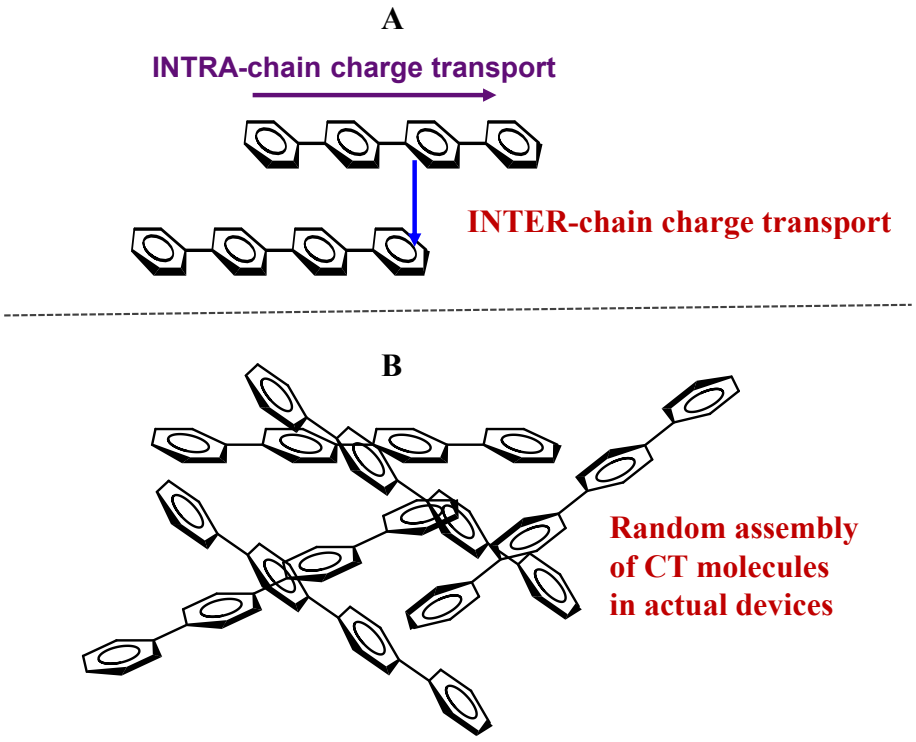

Figure 1. (A) Cartoon diagram showing the intrachain versus interchain charge transport (CT) in poly-*p*-phenylene wires and (B) their randomized assembly in amorphous bulk material

This challenging task of the design and synthesis of new functional materials for long-range charge transport requires the development of a state-of-the-art understanding of fundamental molecular units, such as a cation radical, dimer cation radical and anion radical, that are responsible for charge transport in large molecular assemblies. Usual spectroscopic techniques such as UV-vis, IR, and ESR are available for structural determination of organic cation radicals. The definitive X-ray structural analysis has not been

commonly used owing to the difficulty in preparation and isolation of single crystals suitable for X-ray analysis, which is understandable as presence of both cationic and radical centers usually lead to highly labile species[17]. Rathore and coworkers have recently shown that various polycyclic aromatic hydrocarbons such as substituted benzenes, naphthalenes, anthracenes, pyrenes, poly-phenylenes, hexa-peri-hexabenzo-coronenes etc.[18-20] forms stable cation radicals or hole carriers.

The one electron oxidation of variety of aromatic donors (**D**) generates paramagnetic cation radicals ($\mathbf{D}^{+\bullet}$) which can spontaneously associate with their neutral counterpart to form stabilized dimeric cation radicals $[\mathbf{D,D}]^{+\bullet}$ (i.e., eq 1)

$$\mathbf{D} + \mathbf{D}^{+\bullet} \rightleftharpoons \left[\mathbf{D,D}\right]^{+\bullet} \qquad (1)$$

With the help of ESR spectroscopic information, Lewis and Singer[21] were first to postulate the sandwich like geometry for the naphthalene dimer cation radical, they considered the unpaired electron to be delocalized between both the aromatic rings. Later, Brocklchurst and Rodgers[22,23] examined numerous dimer cation radicals and showed that the dimer cation radicals have characteristic broad absorption bands in the near IR region (NIR) in addition to the absorption bands in the visible region ascribed to the monomeric cation radical in their absorption spectrum. These broad NIR bands were then called charge resonance bands and the corresponding electronic transition was termed as charge resonance transition.[22] For example, Rathore and Coworkers[24] have shown that the treatment of a blue solution of a highly robust octamethylbiphenylene cation radical ($\mathbf{OMB}^{+\bullet}$ $SbCl_6^-$), prepared from neutral octamethylbiphenylene (**OMB**) and nitrosonium hexachloroantimonate (NO^+ $SbCl_6^-$) as an oxidant in dichloromethane at 22 ^oC, with an incre-

mental amounts of neutral OMB at 22 ^{o}C produces a dimer cation radical, the accompanying spectral changes are shown in the Figure 2 A.

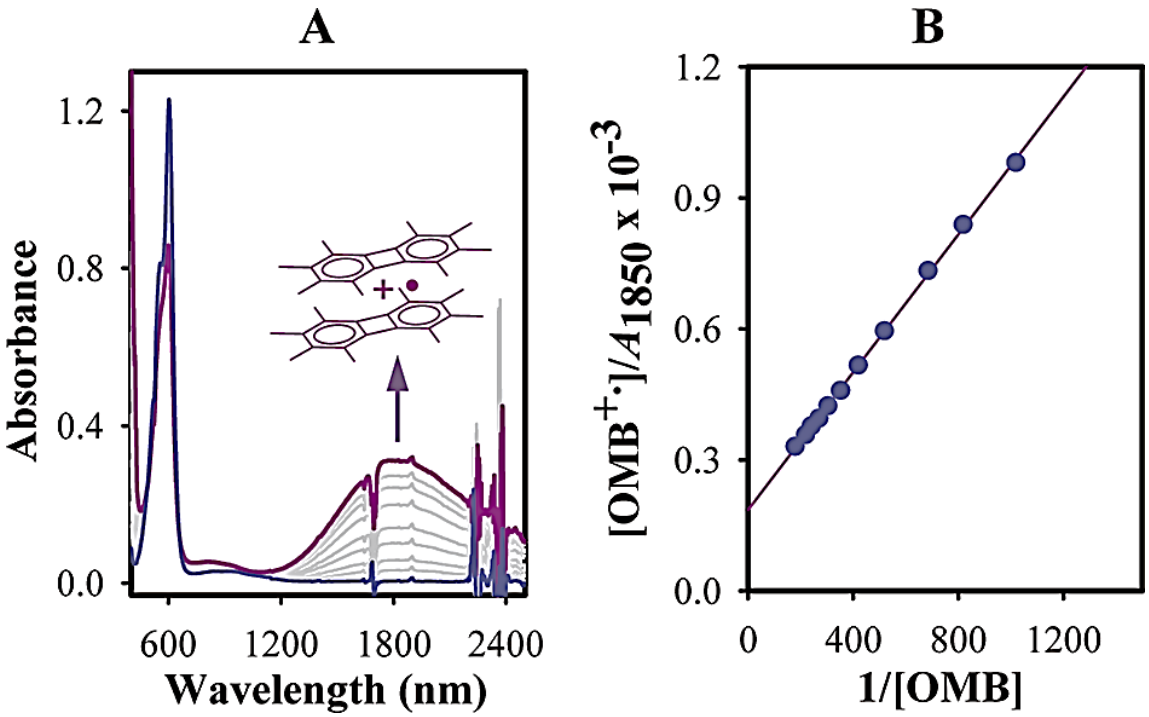

Figure 2. (A) UV-vis spectral changes upon the incremental addition of neutral **OMB** to a dichloromethane solution of the **OMB**$^{+\bullet}$ $SbCl_6^-$ monomer cation radical salt at 22^{o}C. (B) Benesi-Hildebrand plot for the experiment in A.

The characteristic difference between the monomer cation radical and dimer cation radical of **OMB** is that the dimer cation radical shows the presence of charge resonance transit-ion in near IR (NIR) region, which is completely lacking in its mono-mer cation radical. The quantitative formation of **(OMB)$_2$**$^{+\bullet}$ dimer cation radical was carried out using the Bensi-Hildebrand procedure, Figure 2 B,[25] which provided the value for dimerization constant, K_{dimer} = 300±50 M^{-1}.

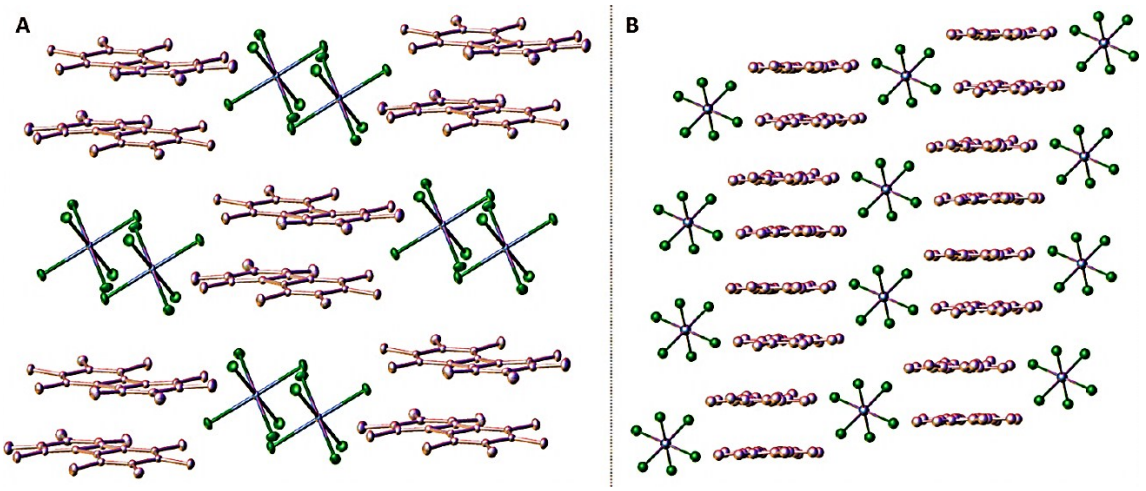

Figure 3. (A) Packing of pairs of **OMB**$^{+\bullet}$ cations with pairs of $SbCl_6^-$ anions in the crystal structure of **OMB**$^{+\bullet}$ **SbCl$_6^-$**. (B) Infinite stacks of octamethylbiphenylenes separated by columns of hexachloroantimonate anions in the crystal structure of **(OMB)$_2^{+\bullet}$ SbCl$_6^-$**.

To establish the delocalization of single positive charge in **OMB** dimer cation radical, we crystallized both monomer and dimer cation radicals as the corresponding hexachloroantimonate salts. After examining the subtle bond length changes in monomer and dimer cation radicals, it was confirmed that the single hole in **OMB** dimer cation radical is equally distributed over two cofacially arrayed **OMB** moieties. The packing arrangement of monomeric **OMB**$^{+\bullet}$ $SbCl6^-$ shows that they are packed in pairs of **OMB** species separated by pairs of $SbCl_6^-$ anions in infinite alternating stacks (Figure 3 A). In contrast, **OMB** molecules in crystals of **(OMB)$_2^{+\bullet}$** $SbCl_6^-$ were arranged in infinite stacks and were separated by intertwined columns of $SbCl_6^-$ counter anions (Figure 3 B).

The X-ray crystallography of numerous intervalence monochromophoric benze-noid cation radicals has shown that the benzenoid donors generally assemble in 1 D stacks (Figure 4A).[26] To improve the dimensionality of the charge transport in solid state assemblies, multichromophoric molecules, in which multiple arene moieties are electro-nically coupled are necessary (Figure 4 B). Rathore and coworkers[19] have demon-strated

that a sandwich like geometry is not mandatory for actual electronic commu-nication to occur between two aromatic moieties in a dimer cation radical. For example, they have shown that phenylenes oriented even at 120^{o} have effective electronic commu-nication as judged by progressive decrease in the first oxidation potential in **EANT** (1.44 V) and **TRIP** (1.34 V) when compared to model **CHP** (1.61V).

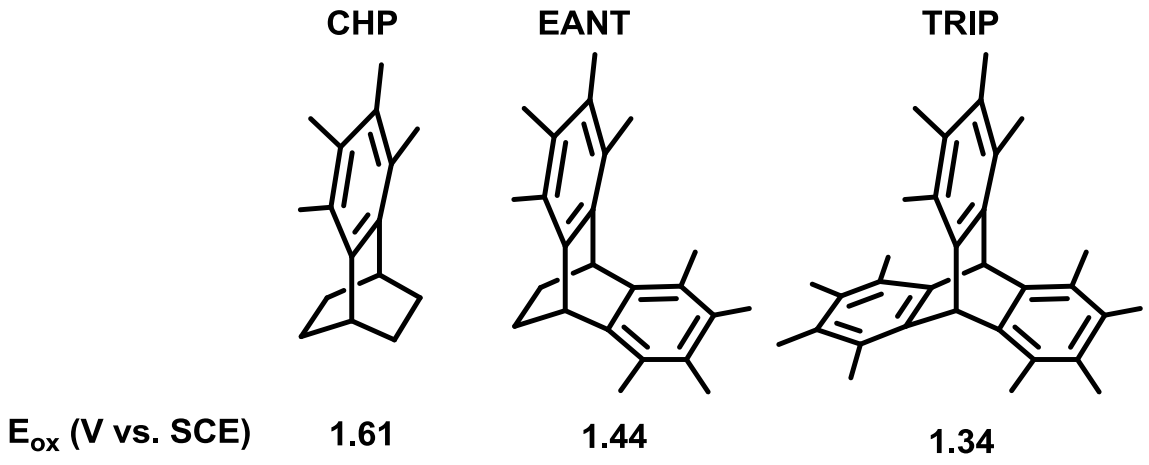

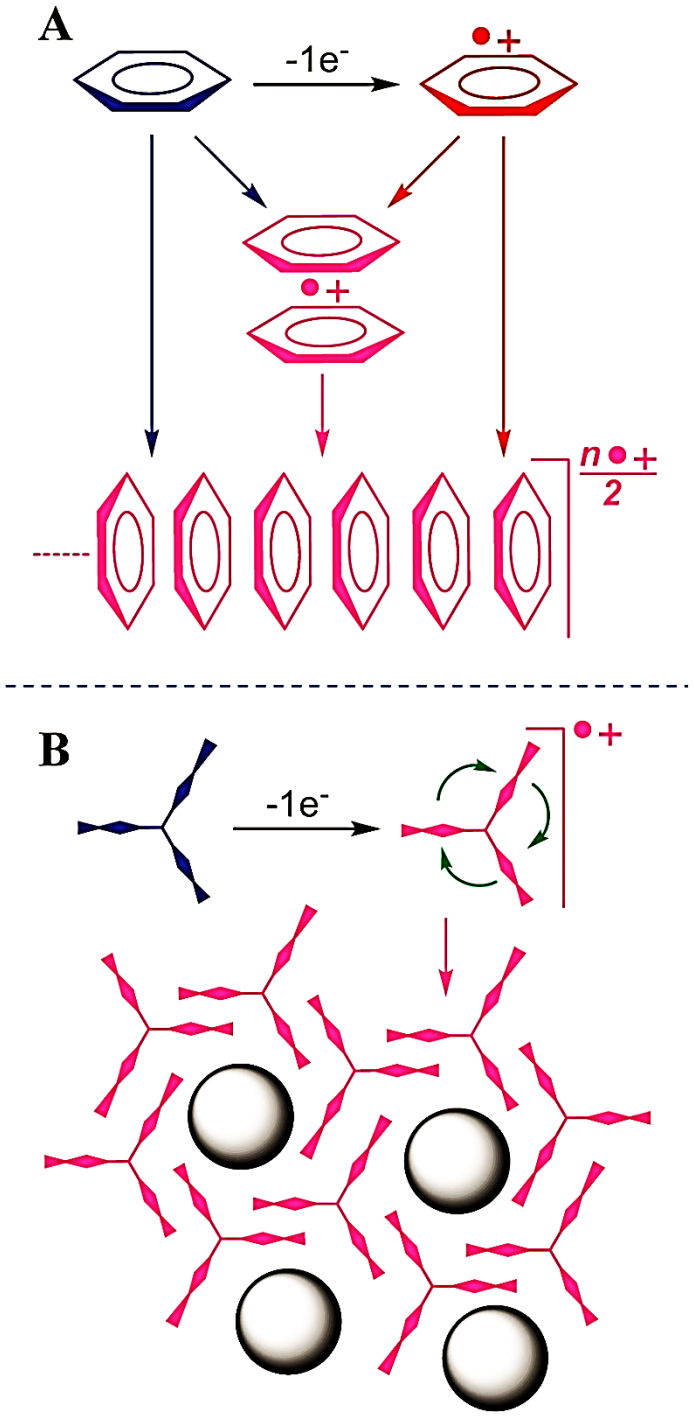

Figure 4. Cartoon diagrams showing (**A**) the 1D stacking of the mixedvalence benzenoid cation radicals and (**B**) the 2D assembly of polychromophoric cation radicals with holes (shown by shaded black spheres) for counteranions in which a single charge is delocalized on all electronically coupled chromophores. Note that the holes in 2D assemblies, shown by shaded black spheres, may allow the incorporation of counteranions and other guest molecules.

According to the discussion above, we undertook not only the preparation but also the isolation of cation radicals of various methoxydibenzochrysenes, 1,4,5,8-tetramethoxyanthracene, hexamethoxy-triptycene, and cycloannulated diaryloxyethers to understand the charge delocalization in these systems. Moreover, we discovered that readily-available tetraarylethylenes can be sequentially transformed into 9,10-diarylphenanthrenes and dibenzochrysenes using one and two equivalents of DDQ, respecti-vely, in dichloromethane containing methanesulfonic acid, in excellent yields. The efficient access to substituted dibenzochrysenes from tetraarylethylenes further established the versatility of this procedure over the existing multi-step syntheses of dibenzochrysenes. Moreover, the ready regeneration of DDQ from easily recovered reduced DDQ-H_2 continues to advance the use of DDQ/H^+ for the oxidative C-C bond formation reactions. Similarly, ferric trichloride mediated oxidative cyclodehydrogenation strategy was used for synthesizing a highly soluble, larger derivative of hexa-*peri*-hexabenzocoronene (HBC), where twelve carbon-carbon bonds are formed in a single step. Deployment of fluorenes at the periphery of the HBC core not only imparts solubility to the structure, but also allows the new PAHs to be functionalized further to make bigger PAHs. Results obtained from these studies are presented in the following four chapters.

Chapter 1A: Octamethoxydibenzochrysene: Isolation and X-ray crystallographic characterization of a twisted polyaromatic cation radical.

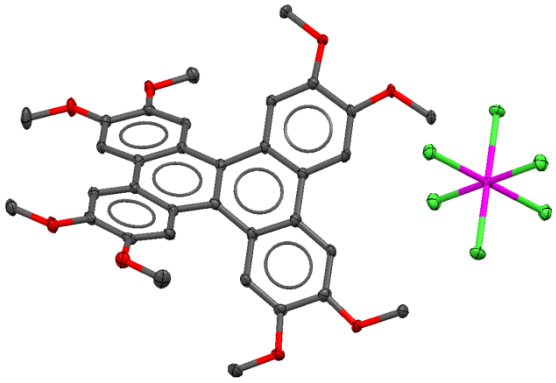

The isolation and X-ray crystal structure determination of octamethoxydibenzochrysene (**3**) cation radical together with DFT calculations allow us to delineate evidence that the complex structural changes (i.e. elongation and shortening of various bonds) in a polyaromatic hydrocarbon can be predicted based on the positioning of the largest bonding and antibonding character of the HOMO.

Chapter 1B: A Practical Synthesis of 1,4,5,8-Tetramethoxyanthracene from Cheap and Readily Available 1,8-Dihydroxyanthraquinone and X-Ray Crystal Structure Characterization of its Dimer Cation Radical

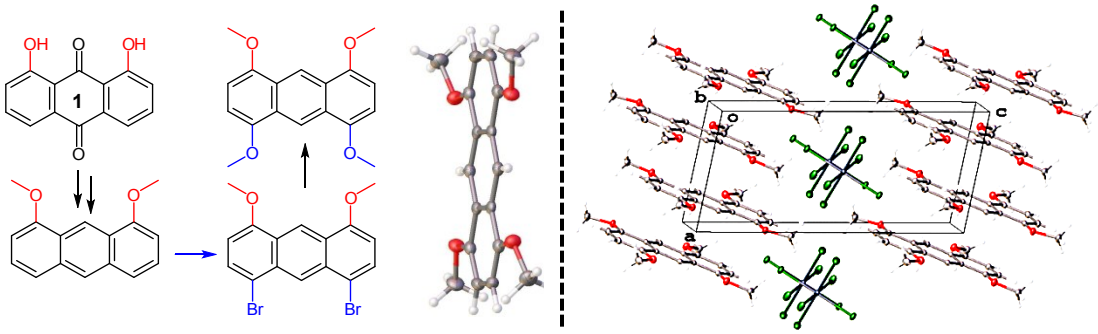

The preparation of gram quantities of 1,4,5,8-tetramethoxyanthracene (**6**) from commercially available and cheap 1,8-dihydroxyanthraquinone is described. The key

steps in the synthesis of **6** involve bromination of 1,8-dimethoxy-anthracene (**4**) to form 1,8-dibromo-4,5-dimethoxyanthracene (**5**) followed by Cu(I) catalyzed replacement of bromo substituents with methoxy groups. The contrasting reports concerning the preparation of 1,8-dimethoxyanthracene (**4**) from 1,8-dimethoxyanthraquinone (**2**) using Zn dust in refluxing acetic acid are also discussed.

The Isolation and X-ray crystal structure determination of 1,4,5,8-tetramethoxy-anthracene dimer cation radical allowed us to delineate that the single hole is uniformly distributed over two 1,4,5,8-Tetramethoxyanthracene moieties.

Chapter 2A: X-ray Structural Characterization of Charge Delocalization onto the Three Equivalent Benzenoid Rings in Hexamethoxytriptycene Cation Radical.

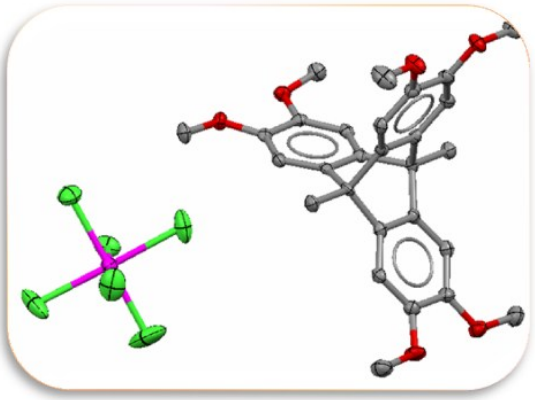

Definitive X-ray crystallographic evidence is obtained for a single hole (or a polaron) to be uniformly distributed on the three equivalent 1,2-dimethoxybenzenoid (or veratrole) rings in the hexamethoxytriptycene cation radical. This conclusion is further supported by electrochemical analysis and by the observation of an intense near IR transition in its electronic spectrum, as well as by comparison of the spectral and electrochemical characteristics with the model compounds containing one and two dimethoxybenzene rings.

Chapter 2B: Preparation and Optoelectronic properties of a new class of Intervalance Cation Radicals from *p*-Diaryloxybenzenes.

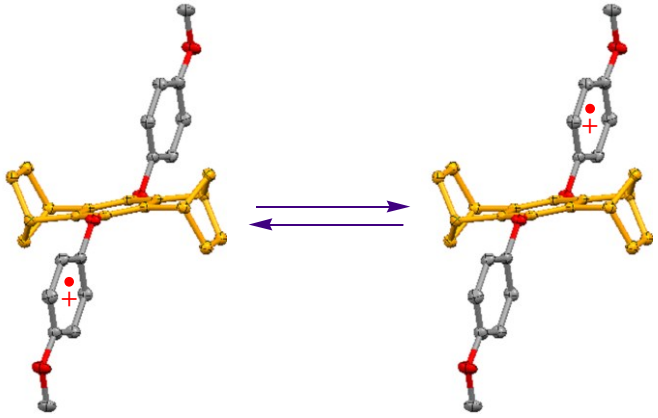

We have demonstrated that bis-cycloannulated *p*-diaryloxybenzenes can be easily synthesized from readily available starting materials using Ullmann ether synthesis. These biaryl ethers (**5-10**) underwent reversible electrochemical oxidation and formed stable cation radical salts. Appearance of two $1e^-$ oxidation waves for **6-8** separated by ~100 mV indicates the effective electronic coupling between two aryl groups. Observance of near-IR transition in the electronic spectrum of **4-7** cation radicals and X-ray crystal determination for $\mathbf{8}^{++}$ together with DFT calculations attest that single charge is delocalized evenly on terminal aryl groups.

Chapter 3: Sequential Oxidative Transformation of Tetraarylethylenes to 9,10-diaryl-henanthrenes and Dibenzo[g,p]-chrysenes using DDQ as an Oxidant.

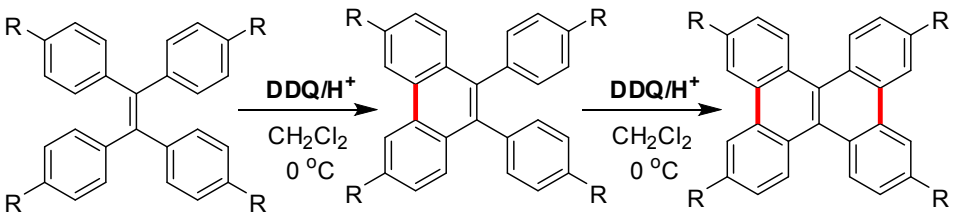

Readily-available tetraarylethylenes can be sequentially transformed into 9,10-diarylphenanthrenes and dibenzochrysenes using one and two equivalents of DDQ, respectively, in dichloromethane containing methanesulfonic acid, in excellent yields. The efficient access to substituted dibenzochrysenes from tetraarylethylenes further establishes the versatility of this procedure over the existing multi-step syntheses of dibenzochrysenes. Moreover, the ready regeneration of DDQ from easily recovered reduced DDQ-H_2 continues to advance the use of DDQ/H^+ for the oxidative C-C bond formation reactions.

Chapter 4: Synthesis and Photophysical Properties of Highly Soluble hexa-peri-hexabenzocoronenes (HBC)

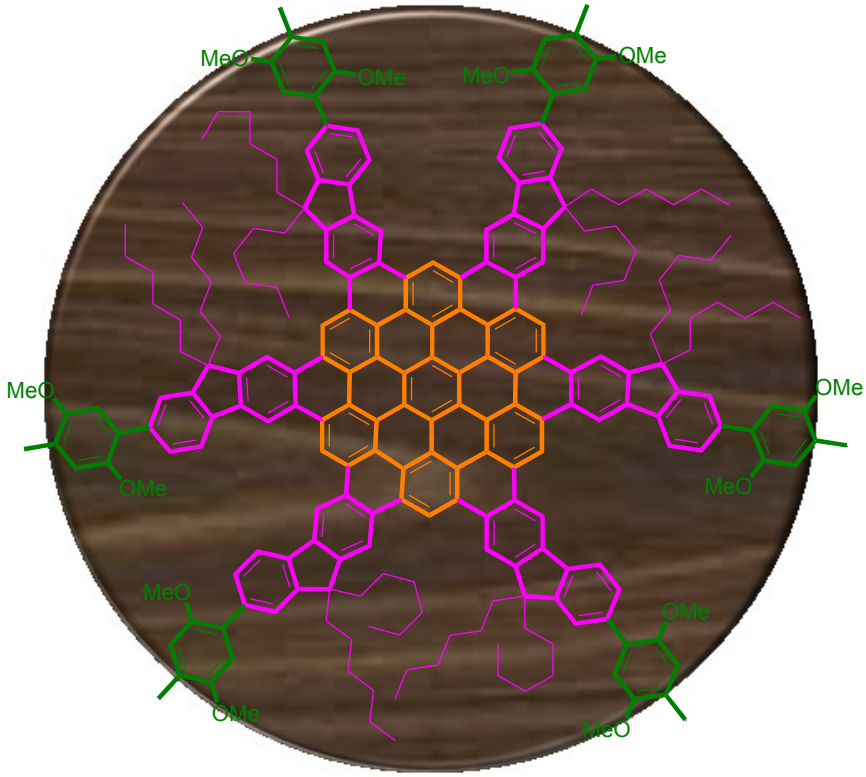

Synthesis of a highly soluble hexa-peri-hexabenzocoronene (HBC) based polycyclic aromatic hydrocarbon (PAH) is described. Deployment of fluorenes at the

periphery of the HBC core not only imparts solubility to the structure, but also allows the new PAHs to be functionalized further to make bigger PAHs or attach electroactive groups in order to study the intramolecular charge transport phenomena.

CHAPTER 1A

Octamethoxydibenzochrysene: Isolation and X-ray crystallographic characterization of a twisted polyaromatic cation radical

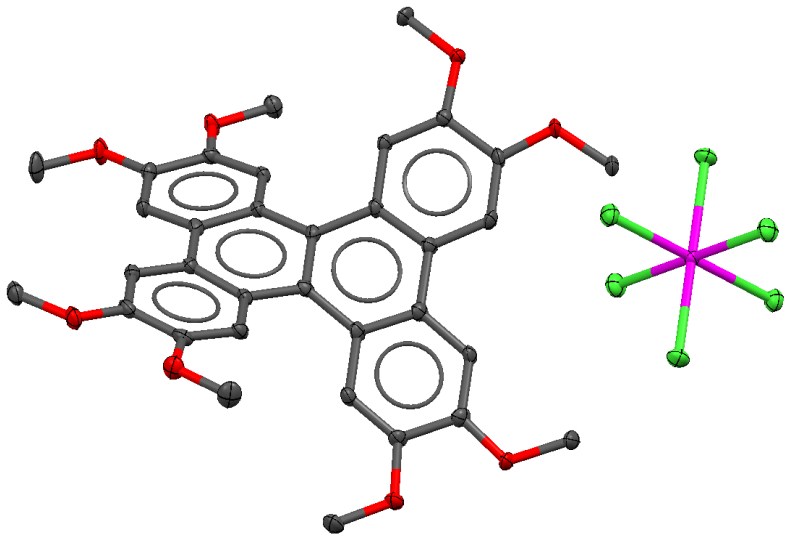

Abstract: The isolation and X-ray crystal structure determination of octamethoxydibenzochrysene (3) cation radical together with DFT calculations allow us to delineate evidence that the complex structural changes (i.e. elongation and shortening of various bonds) in a polyaromatic hydrocarbon can be predicted based on the positioning of the largest bonding and antibonding character of the HOMO.

INTRODUCTION

The study of polyaromatic hydrocarbons has attracted considerable attention since these molecules hold potential to serve as building blocks for the preparation of functional electronic and optoelectronic devices.[1] Of these, dibenzochrysene, a twisted polyaromatic hydrocarbon, and its derivatives have been explored by Swager and coworkers[2] and others[3] for the preparation of sensors, non-linear optical and liquid-crystalline materials, etc. The aromaticity and structure of parent dibenzochrysene and its dication (formed by 2-electron oxidation) has been probed both theoretically[4] and experimentally,[5] however, the structural information is completely lacking.

Our continuing interest in the design and syntheses of stable organic cation radicals, or hole carriers, which are of fundamental importance to organic materials science,[6] prompted the synthesis of octamethoxydibenzochrysene (**3**), and isolation and X-ray crystallographic characterization of its cation-radical salt. The availability of the X-ray structural data on the first cationic dibenzochrysene allows us to provide definitive evidence as to how a hole (formed by 1-e^- oxidation) induces complex bond length changes in a polyaromatic hydrocarbon as well as a verification of the experimentally observed structural changes by DFT calculations. The details of these preliminary findings are described herein.

RESULTS and DISCUSSION

The octamethoxydibenzochrysene (**3**) was obtained by an oxidative cyclodehydrogenation of tetrakis(3,4-dimethoxy-phenyl)ethylene (**2**) using $FeCl_3$ as an oxidant in a mixture of dichloromethane and nitromethane in 60% isolated yield. The tetraveratrylethylene (**2**), in turn, was prepared from McMurry coupling of the corresponding tetramethoxybenzophenone[7] (**1**) in 92% yield (see Scheme 1). The structure of **3** was established by $^{1}H/^{13}C$ NMR spectroscopy and further confirmed by X-ray crystallography (see Scheme 2 and ESI for the experimental details).

Scheme 1. Synthesis of octamethoxydibenzochrysene (**3**) and its ORTEP diagrams with twisted structure (thermal elipsoids: 50% probability).

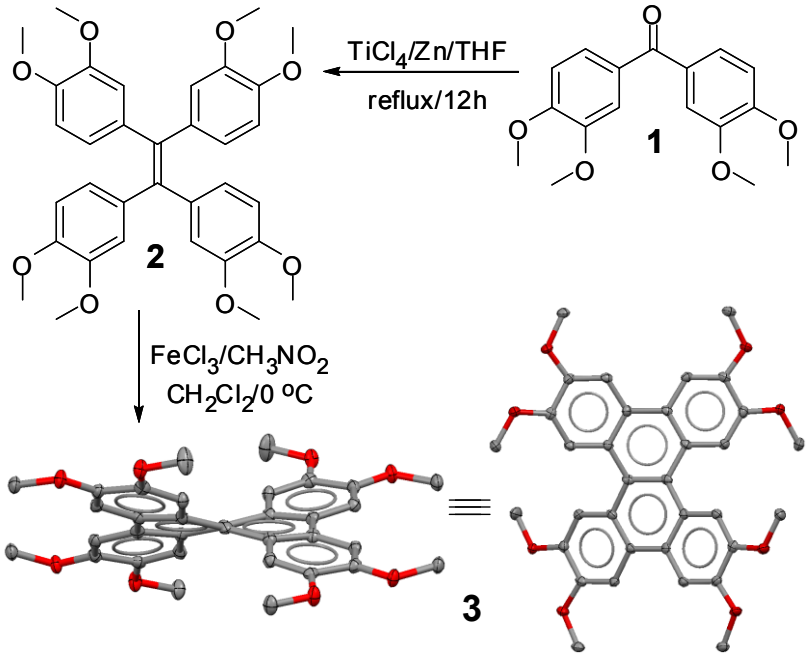

The electron donor strength of octamethoxydibenzo-chrysene (**3**) was

evaluated by electrochemical oxidation at a platinum electrode as a 2 x 10^{-3} M solution in dichloromethane containing 0.2 M *n*-Bu_4NPF_6 as the supporting electrolyte. The cyclic voltammograms of **3**, if terminated before the start of the third oxidation event, showed two reversible oxidation waves (Fig. 1A), which consistently met the reversibility criteria at various scan rates of 25-500 mV/s, as they all showed cathodic/anodic peak current ratios of i_a/i_c=1.0 (theoretical) as well as the differences between anodic and cathodic peak potentials of E_{pa}-E_{pc} ~ 70 mV at 22 ^{o}C (Fig. 1B). The reversible oxidation potentials of **3** were calibrated with ferrocene as internal standard (E_{ox} = 0.45 V vs SCE) and were found to be 0.91 and 1.27 V vs. SCE corresponding to the formation of monocation and dication, respectively. It is noted that the third oxidation wave in the cyclic voltammogram of **3** displays a quasi-reversible oxidation wave (E_{ox3} = 1.69 V) which, in turn, distort the other waves corresponding to the first and second oxidation events (see Fig. 1A).

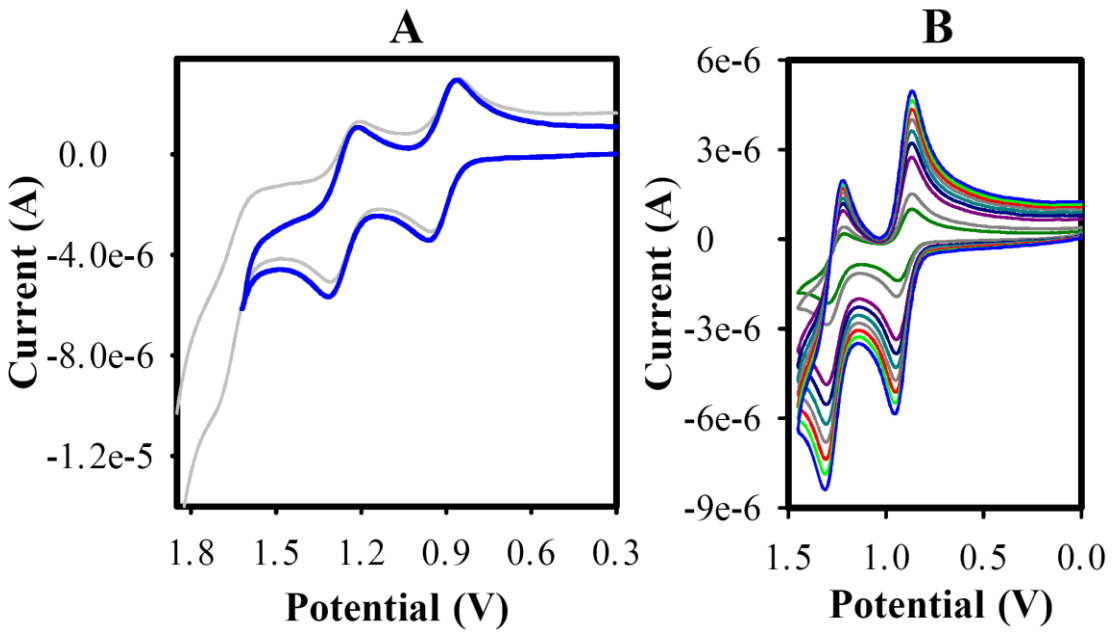

Figure 1. (A) Cyclic voltammograms of 2 x 10^{-3} M **3** in CH_2Cl_2 containing 0.2 M *n*-Bu_4NPF_6 at a scan rate of 200 mV/s and (B) cyclic voltammograms of **3** at scan rates of 25-500 mV/s at 22 °C.

The electrochemical reversibility of **3** and its relatively low oxidation potential permits its ready oxidation to the corresponding cation radical using either a hydroquinone ether cation radical (**CRET**$^{+\bullet}$ $SbCl_6^-$; E_{red} = 1.11 V vs. SCE)[8] or magic blue (**MB**$^{+\bullet}$ $SbCl_6^-$; E_{red} = 1.15 V vs. SCE)[9] as oxidants.

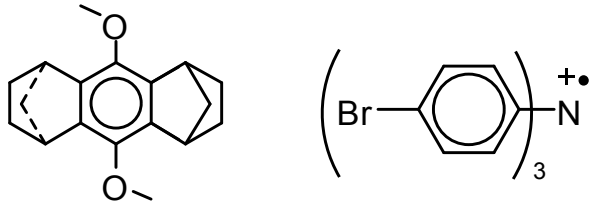

CRET$^{+\bullet}$ **MB**$^{+\bullet}$

E^{o}_{red} 1.11 1.15 (V *vs.* SCE)

Thus, Fig. 2A shows the spectral changes attendant upon the reduction of blue-colored **MB**$^{+\bullet}$ (λ_{max} = 728 nm, log ε_{728} = 4.45) by incremental additions of sub-stoichiometric amounts of **3** in dichloromethane at 22 °C. The presence of multiple isosbestic points at λ = 355, 387, 564, and 783 nm (see Figure 2A) indicates a simple electron transfer from **3** to **MB**$^{+\bullet}$ without decomposition of **3**$^{+\bullet}$. Furthermore, a plot of formation of **3**$^{+\bullet}$ (i.e. an increase in the absorbance at 890 nm against the increments of added **3**, Fig. 2B) established that **MB**$^{+\bullet}$ was completely consumed after the addition of 1 equiv of **3**; and the resulting highly structured absorption spectrum of the **3**$^{+\bullet}$ [with intense absorption bands at λ_{max} = 890 (log ε_{890} = 4.37), 513, 458, and

394 nm and relatively weak bands at λ_{max} = 636 (log ε_{634} = 3.67) and 784 nm] remained unchanged upon further addition of neutral **3**, i.e., eq 1.

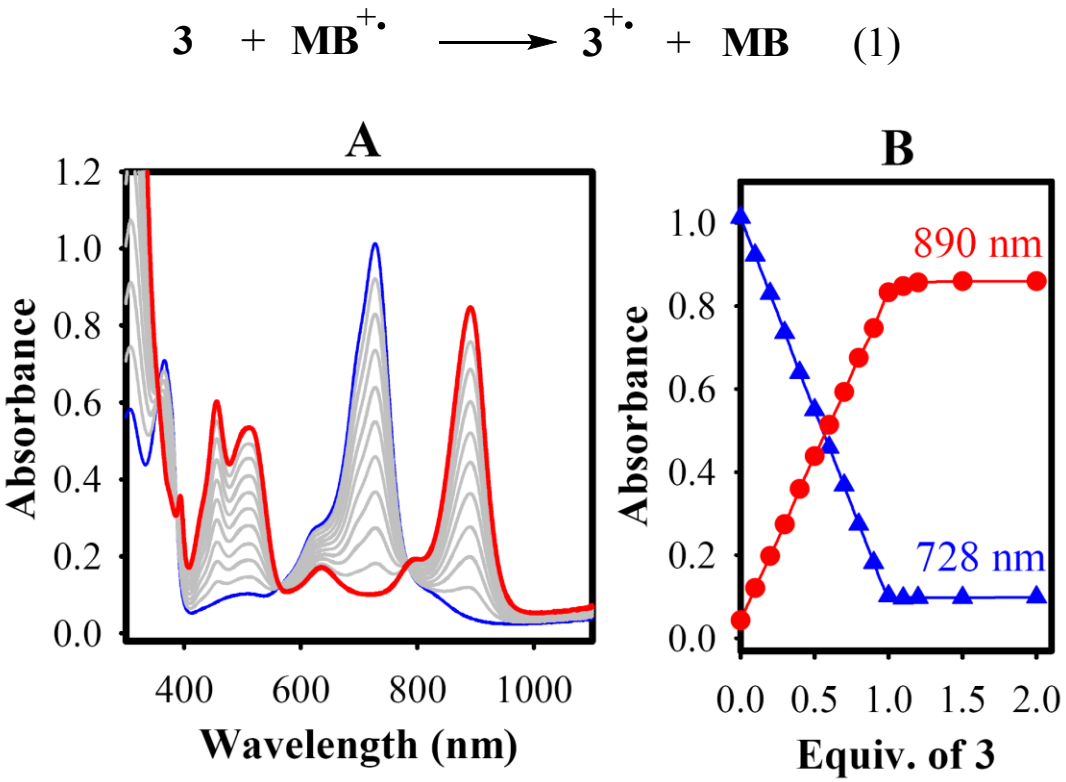

Figure 2. (**A**) The spectral changes observed upon the reduction of 3.6 x 10^{-5} M $\mathbf{MB}^{+\bullet}$ by an incremental addition of substoichiometric amounts of **3** in CH_2Cl_2 at 22 °C. (**B**) A plot of depletion of absorbance of $\mathbf{MB}^{+\bullet}$ (blue triangles, at 728 nm) and an increase of the absorbance of $\mathbf{3}^{+\bullet}$ (red circles, at 890 nm) against the equivalents of added neutral **3**.

It is noted that although an identical spectrum of $\mathbf{3}^{+\bullet}$ was obtained when $\mathbf{CRET}^{+\bullet}$ was treated with an equimolar amount of **3**, a clean spectral titration plot with isosbestic point could not be obtained owing to an overwhelming overlap of the absorption band of $\mathbf{CRET}^{+\bullet}$ at 518 nm with that of $\mathbf{3}^{+\bullet}$ (see ESI). It is further noted that the intensely colored solution of $\mathbf{3}^{+\bullet}$, obtained according to eq. 1 or using

CRET$^{+\bullet}$, was stable at ambient temperature and did not show any decomposition during a 48-h period at 22 ^{o}C, as confirmed by UV-vis spectroscopy. Moreover, a reduction of **3**$^{+\bullet}$ with zinc dust regenerated the neutral **3** quantitaitively as confirmed by ^{1}H NMR spectroscopy.

The high stability of **3**$^{+\bullet}$ $SbCl_6^-$ in solution prompted us to attempt the isolation of its crystalline salt as follows. For example, an excellent crop of dark-colored crystals, suitable for X-ray crystallographic studies, were obtained by a slow diffusion of toluene in a dichloromethane solution of **3**$^{+\bullet}$ $SbCl_6^-$, obtained using a 1:1 mixture of **3** and **CRET**$^{+\bullet}$ $SbCl_6^-$, during a period of 24 h at ~0 ^{o}C.

The crystal structure of **3**$^{\bullet+}$ $SbCl_6^-$ revealed that cationic dibenzochrysene moieties form infinite stacks along the z axis with non-equivalent interplanar separations of 3.31 and 3.44 Å. The robust π-π stacking arrangements amongst the molecules of the cationic **3** leads to a clathrate structure with large channels that are filled with $SbCl_6^-$ counter anions and multiple dichloromethane molecules (see Fig. 3A/B). In contrast, the packing in the crystal structure of neutral **3** is dominated not by π-π but by CH···π interactions amongst the methoxy groups and the electron-rich aromatic rings of the neighboring molecules. The resulting honeycomb-like layers, formed perpendicular to the crystallographic x-axis, are interspaced by disordered dichloromethane molecules (see Fig. 3D); and the layers are separated by copious amounts of acetonitrile molecules (see Fig. 3C).[#]

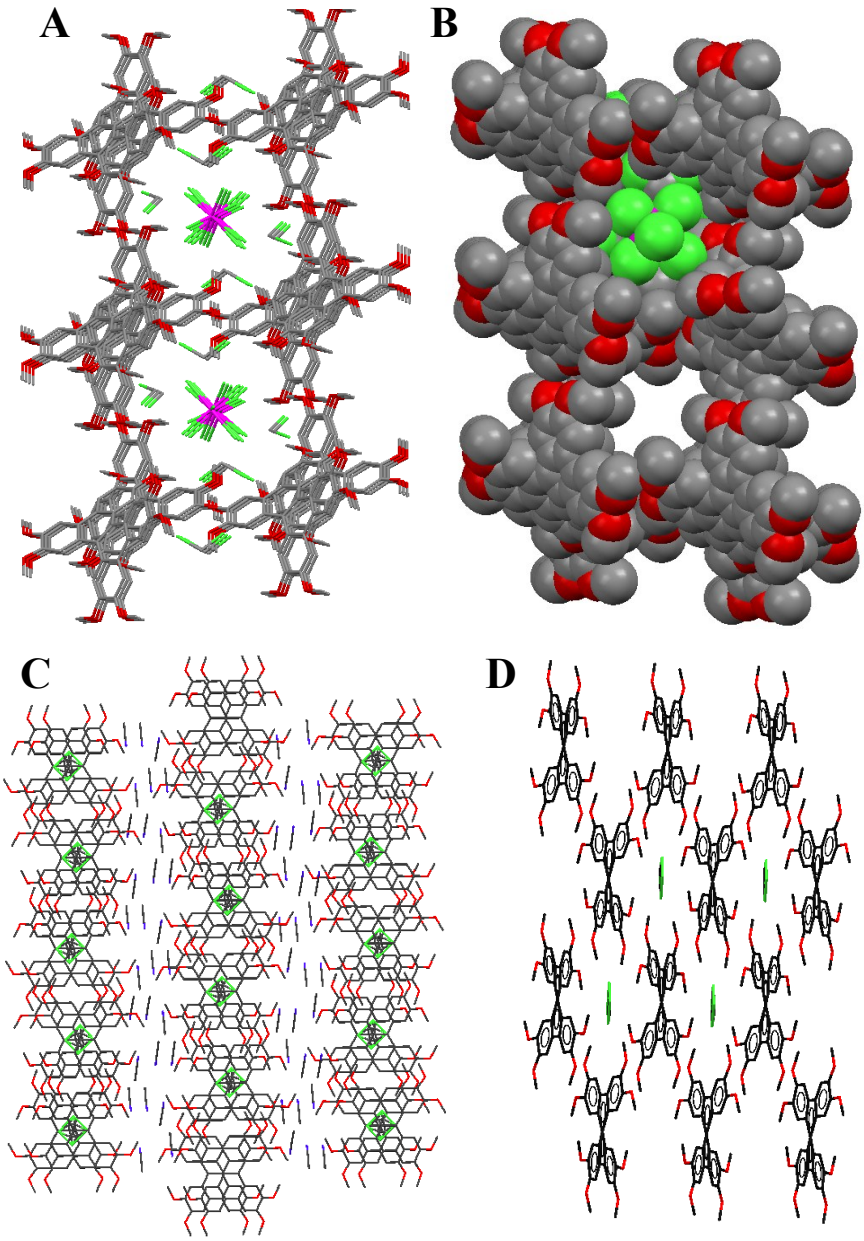

Fig. 3. (**A**) The packing diagram of $\mathbf{3}^{\bullet+}$ SbCl6^{-} showing that the channels formed by stacked $\mathbf{3}^{\bullet+}$ are filled with $SbCl_6^-$ and CH_2Cl_2 molecules. (**B**) Space filling representation of the packing diagram of $\mathbf{3}^{\bullet+}$ $SbCl_6^-$ where one of the channels is shown without $SbCl_6^-$ and CH_2Cl_2 molecules. (**C**) The packing diagram of neutral **3** showing the layered structure where the layers are separated by acetonitrile molecules. (**D**) The arrangement of **3** with embedded CH_2Cl_2 molecules within a single layer of neutral **3**.

An inspection of the bond length changes in the cation radical $\mathbf{3}^{+\bullet}$, together with a comparison of its neutral form, points to the following salient features. (i) Neutral **3** has a crystallographic 2-fold symmetry and its planarity is substantially distorted by twisting around the central C=C bond (denoted as **A**, see Table 1) by 25.8º and around the central bonds of "biphenyl" fragments (denoted by **I**) by 11.4º. One electron oxidation of **3** results only in a minor amplification of the distortions as judged by the slightly increased twist angles of 29.1 and 11.9º for bonds **A** and **I**, respectively. (ii) As in various other aryl-methyl ether cation radicals,[10] O-C(ar) bonds (denoned as **J** and **L**) in $\mathbf{3}^{+\bullet}$ exhibit shortening by ~1.3 pm due to an increased p-π dative interaction. (iii) Although, the rearrangement of the lengths of various bonds (i.e. elongation and shortening) in the polyaromatic moiety in $\mathbf{3}^{+\bullet}$ has a complex character (see Table 1), the changes clearly correspond to the predominant contributions from the resonance structures I/II, as judged by the significant lengthening of bonds **A**, **C**, **F**, **I**, and **M** and shortening of bonds **B**, **G**, **J**, and **L** and only a minor contribution from the resonance structures III/IV (see below).

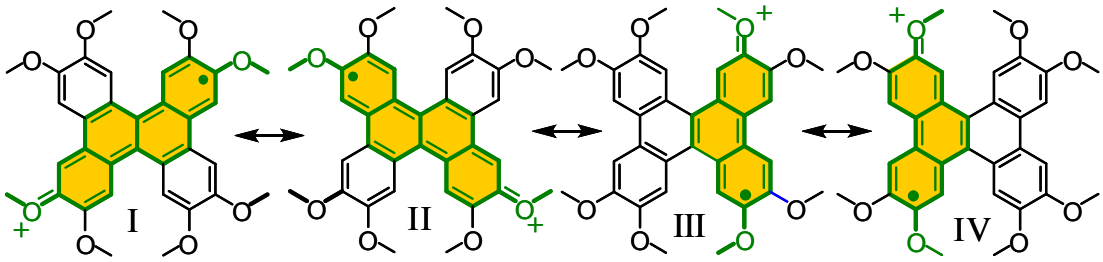

Table 1. Experimental and theoretical bond lengths of the neutral and cation radical of **3** presented in picometers (pm). Numbering scheme for the skeleton of **3** and its HOMO, obtained by DFT calculations at B3LYP/6-31G* level.

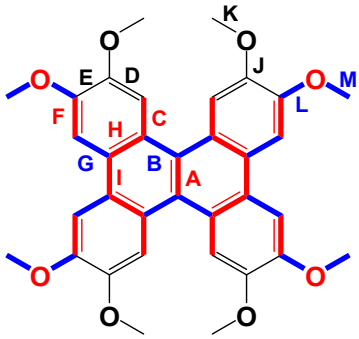

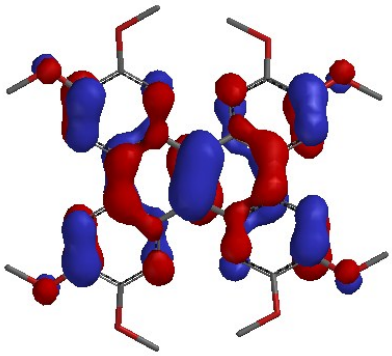

Bond Type	**B3LYP/6-31G***			**X-Ray Data**		
Bond[1]	**3**	**$3^{+\bullet}$**	Δ	**3**	**$3^{+\bullet}$**	Δ
A	140.3	144.0	+3.7	141.4	143.0	+1.6
B	145.8	144.1	-1.7	145.5	143.9	-1.4
C	142.2	142.4	+0.2	141.5	142.3	+0.8
D	138.1	138.0	-0.1	136.9	136.9	0.0
E	142.4	143.0	+0.6	141.9	142.5	+0.6
F	138.1	139.3	+1.2	137.8	138.2	+0.4
G	141.7	140.4	-1.3	142.0	140.1	-1.9
H	141.7	142.2	+0.5	141.6	141.6	0.0
I	145.2	146.3	+1.1	145.3	146.5	+1.2
J	136.3	135.1	-1.2	137.0	135.8	-1.2
K	141.6	142.3	+0.7	143.3	143.2	-0.1
L	136.2	134.1	-2.1	136.3	134.9	-1.4
M	141.6	142.7	+1.1	142.9	144.2	+1.3
σ	--	--	--	0.5	0.4	--

[1]Average of equivalent bonds.

A further examination of the positioning of the HOMO in octamethoxydibenzochrysene (**3**) in Table 1 suggests that the methoxy substituents at 3,6,11,14 positions should have little or no influence in stabilizing the cation radical of **3**. In order to verify this conjecture, we have undertaken the syntheses of hitherto unknown 2,5,10,13-tetramethoxybenzochrysene (**4**) and 3,6,11,14-tetramethoxybenzochrysene (**5**) (see Schemes 2 and 3) and compared their redox properties with octamethoxydibenzochrysene **3** and parent (unsubstituted) dibenzochrysene as follows.

While dibenzochrysene **5** was easily obtained via oxidative cyclodehydrogenation of the corresponding tetrakis(3-methoxyphenyl)ethylene using $FeCl_3$. The required tetrakis(3-methoxyphenyl)ethylene in turn was prepared form the 3,3'-dimethoxybenzophenone via a standard McMurry coupling (Scheme 3). However, the dibenzochrysene **4** could not be accessed from the corresponding tetranisylethylene [or tetrakis(4-methoxyphenyl)ethylene] via oxidative cyclodehydrogenation using $FeCl_3$ as an oxidant (see Chapter 5 and 6). We therefore accessed **4** by adopting the procedure of Swager and coworkers as follows. Thus, the required bis(biaryl)acetylene was easily prepared from 2-iodobiaryl followed by a reaction with $FeCl_3$ easily afforded dibenzochrysene **4** in modest yield (see Scheme 2). Both **4** and **5** were characterized by $^{1}H/^{13}C$ NMR spectroscopy and by X-ray crystallography (see Schemes 2 and 3)

Scheme 2. Synthesis of 2,5,10,13-tetramethoxydibenzochrysene (**4**) and its ORTEP diagrams with twisted structure.

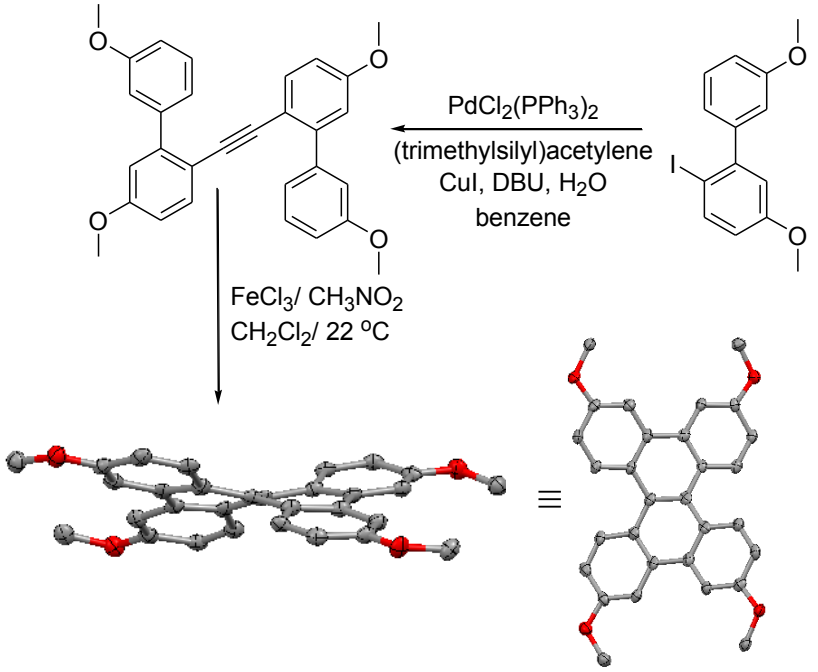

Scheme 3. Synthesis of 3,6,11,14-tetramethoxydibenzochrysene (**5**) and its ORTEP diagrams with twisted structure.

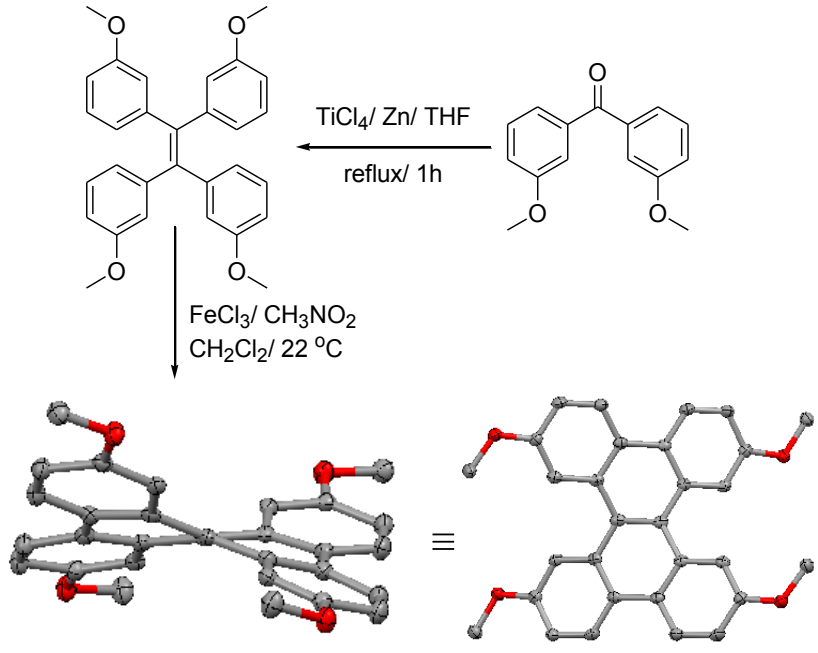

Cyclic Voltammograms of various dibenzochrysenes were recorded at a

platinum electrode as a 2 x 10^{-3} M solution in dichloromethane containing 0.2 M *n*-Bu_4NPF_6 as the supporting electrolyte. The reversible first oxidation potentials of **3, 4, 5** and **6** were calibrated with ferrocene as internal standard (E_{ox} = 0.45 V vs SCE). First oxidation potentials of **3**, **4**, **5** and **6** were reversible and consitently met the criteria of reversibility over 50 mV to 500 mV scan rate. The second oxidation wave of **5** and **6** shows the quasi-reversible behaviour.

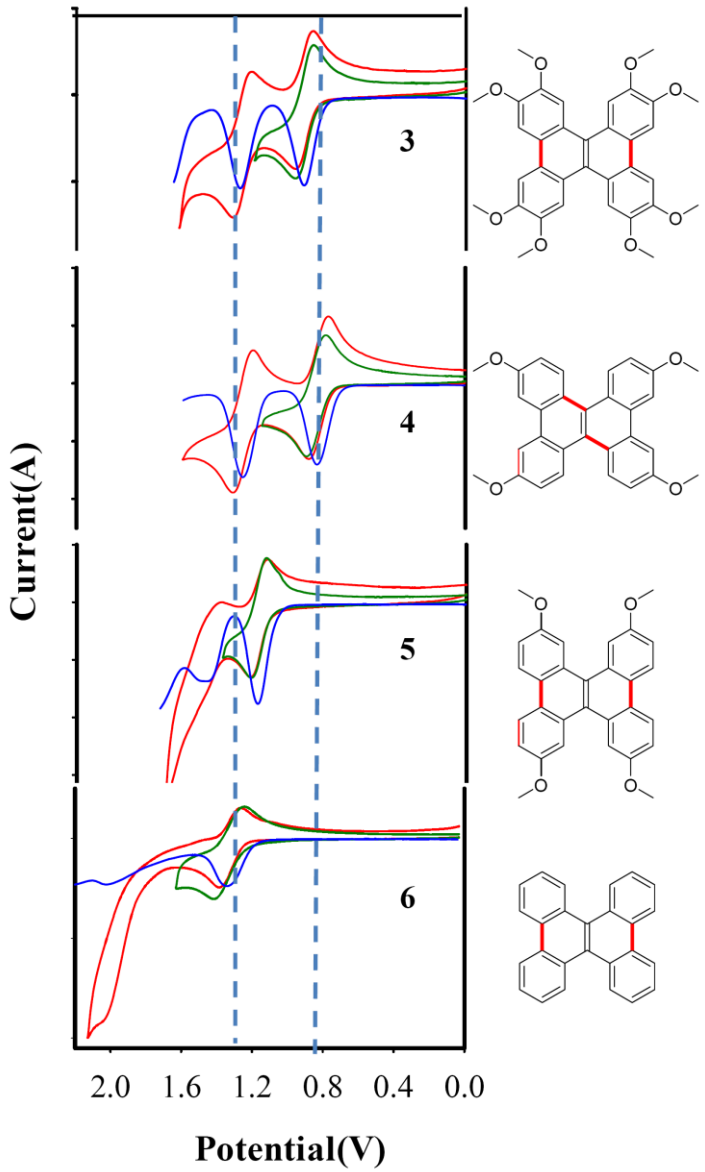

Figure 4. Cyclic voltammograms of 2 x 10^{-3} M **3, 4, 5** and **6** in CH_2Cl_2 containing 0.2 M *n*-Bu_4NPF_6 at a scan rate of 200 mV/s

Table 2. The comparison of first and second oxidation potentials of **3**, **4**, **5** and **6**.

Compd.	$E_{ox1(V\ vs\ SCE)}$	$E_{ox2(V\ vs\ SCE)}$	ΔE_{ox}
3	0.914	1.274	0.360
4	0.850	1.258	0.408
5	1.178	1.448	0.270
6	1.330	1.866	0.530

Incorporation of methoxy substituents in a molecule is expected to decrease its oxidation potential by the virtue of the electron donating nature of methoxy substituents. Interestingly, when parent dibenzochrysene (**6**), with reversible first oxidation potentail at 1.33 V, was substituted at 3,6,11, and 14 positions with methoxy groups (i.e. dibenzochrysene **5**), shows an E_{ox1} value of 1.18 V, however, when it was substituted with methoxy groups at 2,5,10, and 13 positions (i.e. dibenzochrysene **4**) its E_{ox1} value decreases to 0.85 V. Such a dramatic difference in E_{ox1} values of **4** (085 V) and **5** (1.18 V) clearly attests that methoxy groups at 2,5,10, and 13 positions have much larger influence (~480 mV) in stabilizing the cation radical of **4** as compared to 3,6,11, and 14 substituted dibenzochrysene (~152 mV). Moreover, introduction of additional four methoxy groups in 2,5,10,13-

tetramethoxydibenzochrysene (**4**) at 3,6,11, and 14 positions (i.e. octamethoxydibenzochrysene **3**), does not decrease its first oxidation potential (see Table 1). In fact a slight increases in the E_{ox1} values of **3** from 0.85 V to 0.91 V suggest that additional methoxy groups have a negative effect in stabilizing the cationic charge in **3**. The structure/redox property relationship of various dibenzochrysenes in Table 3 is in complete accord with the positioning of HOMO on dibenzochrysene.

We also generated the cation radicals of **4-6**, as described above, and their spectra are displayed in Figures 5-7 and Figure 8 shows the comparison of the absorption spectra of various dibenzochrysenes.

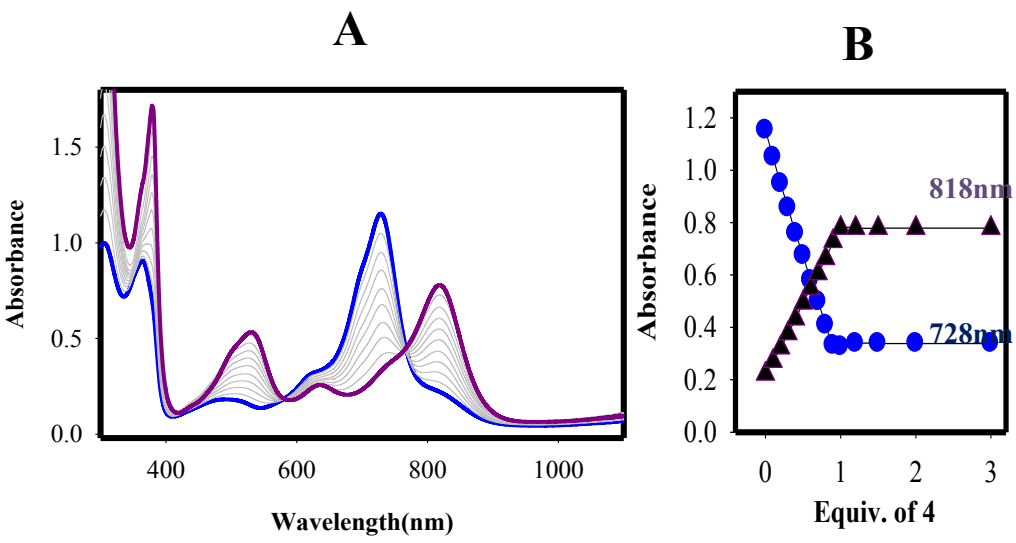

Figure 5. (**A**) The spectral changes observed upon the reduction of 4.08 x 10^{-5} M $\mathbf{MB}^{+\bullet}$ by an incremental addition of substoichiometric amounts of **4** in CH_2Cl_2 at 22 ^{o}C. (**B**) A plot of depletion of absorbance of $\mathbf{MB}^{+\bullet}$ (blue circles, at 728 nm) and an increase of the absorbance of $\mathbf{4}^{+\bullet}$ (brown trialgles, at 818 nm) against the equivalents of added neutral **4**.

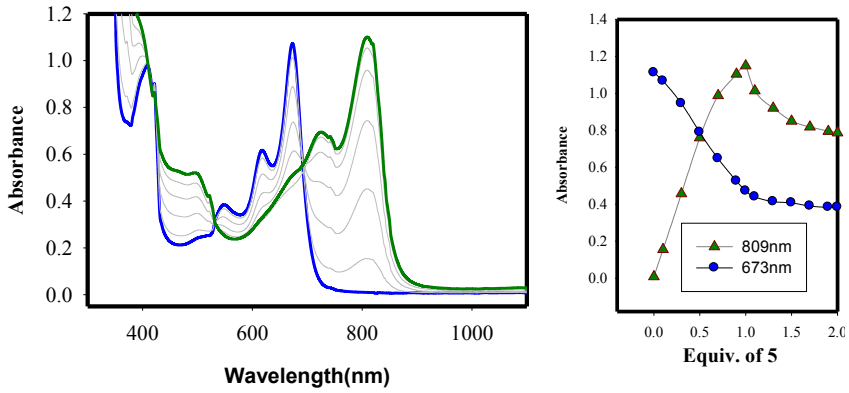

Figure 6. (**A**) The spectral changes observed upon the reduction of 1.18 x 10^{-4} M **NAP**$^{+\bullet}$ by an incremental addition of substoichiometric amounts of **5** in CH_2Cl_2 at 22 ^{o}C. (**B**) A plot of depletion of absorbance of **NAP**$^{+\bullet}$ (blue circles, at 673 nm) and an increase of the absorbance of **5**$^{+\bullet}$ (green triangles, at 673 nm) against the equivalents of added neutral **5**.

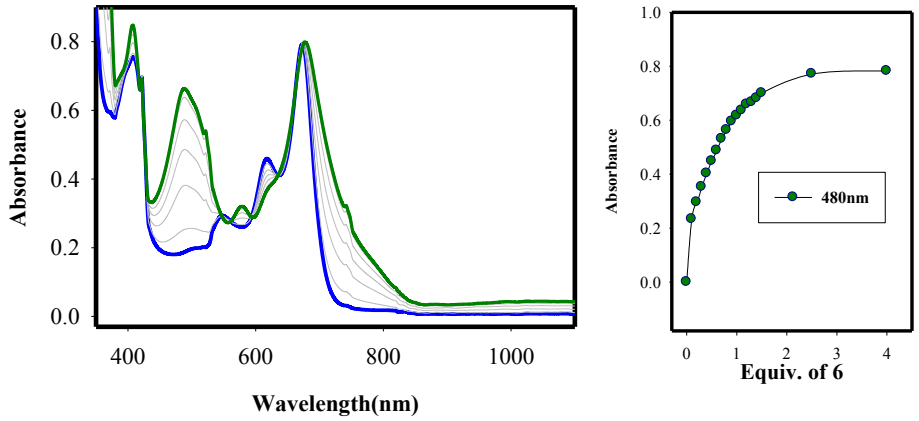

Figure 7. (**A**) The spectral changes observed upon the reduction of 8.60 x 10^{-5} M **NAP**$^{+\bullet}$ by an incremental addition of substoichiometric amounts of **6** in CH_2Cl_2 at 22 ^{o}C. (**B**) A plot of an increase of the absorbance of **6**$^{+\bullet}$ (green circles, at 480 nm) against the equivalents of added neutral **6**.

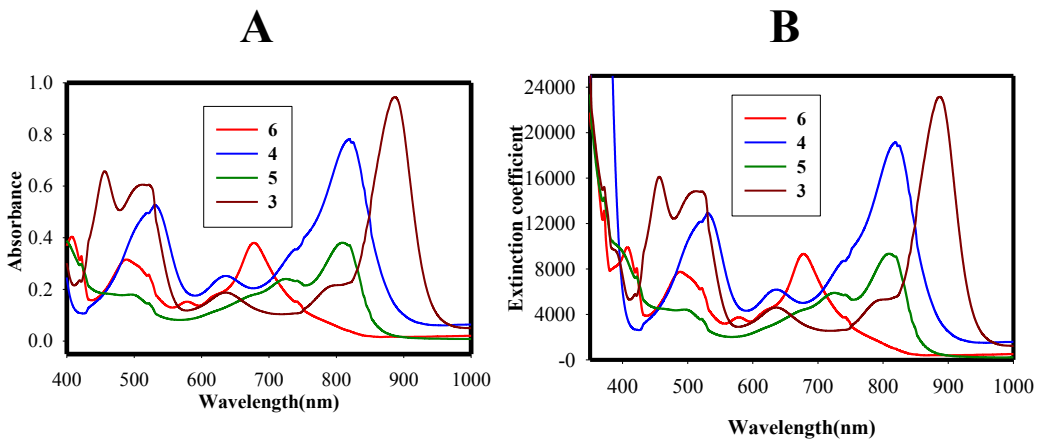

Figure 8. (**A**) $\mathbf{3}^{+\bullet}$, $\mathbf{4}^{+\bullet}$, $\mathbf{5}^{+\bullet}$ and $\mathbf{6}^{+\bullet}$ spectras observed upon the reduction of 3.60 x 10^{-5} M $\mathbf{MB}^{+\bullet}$(for **3** and **4**) or 3.60 x 10^{-5} M $Nap^{+\bullet}$ (for **5** and **6**) by an incremental addition of substoichiometric amounts of **3, 4, 5** and **6** in CH_2Cl_2 at 22 ^{o}C. (**B**) A plot of extinction coefficient of $\mathbf{3}^{+\bullet}$, $\mathbf{4}^{+\bullet}$, $\mathbf{5}^{+\bullet}$ and $\mathbf{6}^{+\bullet}$.

SUMMARY and CONCLUSIONS

In summary, octamethoxydibenzochrysene (**3**) is easily accessed from readily available starting materials and it undergoes reversible electrochemical oxidation and forms a highly robust cation-radical salt. The X-ray crystal structure determination of $\mathbf{3}^{+\bullet}$ $SbCl_6^-$ as well as neutral **3** together with DFT calculations provides unequivocal evidence that an introduction of a cationic charge (or polaron) in polyaromatic hydrocarbon **3** leads to a complex elongation and shortening of the various bonds. The observed bond length changes in $\mathbf{3}^{+\bullet}$ can be readily reconciled by the positioning of the largest bonding and antibonding character of the HOMO in neutral **3**. The close packing of the molecules of the cationic **3** in the crystals produces large channels akin to those found in zeolites and may allow the preparation

of potentially useful conducting materials by utilizing electro-active counter anions.[11]

EXPERIMENTAL

General Experimental Methods and Materials. All reactions were performed under argon atmosphere unless otherwise noted. All commercial reagents were used without further purification unless otherwise noted. Dichloromethane was repeatedly stirred with fresh aliquots of conc. sulfuric acid (~10 % by volume) until the acid layer remained colorless. After separation it was washed successively with water, aqueous sodium bicarbonate, water, and aqueous sodium chloride and dried over anhydrous calcium chloride. The dichloromethane was distilled twice from P_2O_5 under an argon atmosphere and stored in a Schlenk flask equipped with a Teflon valve fitted with Viton O-rings. The hexanes and toluene were distilled from P_2O_5 under an argon atmosphere and then refluxed over calcium hydride (~12 h). After distillation from CaH_2, the solvents were stored in Schlenk flasks under an argon atmosphere. Tetrahydrofuran (THF) was dried initially by distilling over lithium aluminum hydride under an argon atmosphere. The THF was further refluxed over metallic sodium in the presence of benzophenone until a persistent blue color was obtained and then it was distilled under an argon atmosphere and stored in a Schlenk flask equipped with a Teflon valve fitted with Viton O-rings. NMR spectra were recorded on 300 and 400 MHz NMR spectrometers.

Cyclic Voltammetry (CV). The CV cell was of an air-tight design with high vacuum Teflon valves and Viton O-ring seals to allow an inert atmosphere to be maintained without contamination by grease. The working electrode consisted of an adjustable

platinum disk embedded in a glass seal to allow periodic polishing (with a fine emery cloth) without changing the surface area (~1 mm2) significantly. The reference SCE electrode (saturated calomel electrode) and its salt bridge were separated from the catholyte by a sintered glass frit. The counter electrode consisted of a platinum gauze that was separated from the working electrode by ~3 mm. The CV measurements were carried out in a solution of 0.1 to 0.2 M supporting electrolyte (tetra-*n*-butylammonium hexafluorophosphate, TBAH) and 2-5 x 10^{-3} M substrate in dry dichloromethane under an argon atmosphere. All the cyclic voltammograms were recorded at a sweep rate of 200 mV sec^{-1}, unless otherwise specified and were IR compensated. The oxidation potentials ($E_{1/2}$) were referenced to SCE, which was calibrated with added (equimolar) ferrocene ($E_{1/2}$ = 0.450 V *vs*. SCE). The $E_{1/2}$ values were calculated by taking the average of anodic and cathodic peak potentials in the reversible cyclic voltammograms.

Preparation of $3^{+\bullet}$ $SbCl_6^-$ single crystals using $CRET^{+\bullet}$ $SbCl_6^-$.

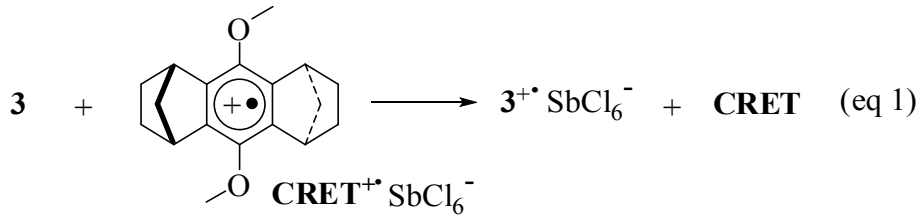

A 20-mL tube fitted with a Schlenk adaptor was charged with **CRET**$^{+\bullet}$ $SbCl_6^-$ (30 mg, 0.05 mmol), and a solution of octamethoxydibenzochrysene **3** (28 mg, 0.05 mmol) in anhydrous dichloromethane (10 mL) was added under an argon atmosphere at 22 ^{o}C. The solution immediately took on a green coloration and it was stirred for 5 min to yield a dark-green solution of cation radical [**3**$^{+\bullet}$ $SbCl_6^-$]. The solution was carefully layered with

dry toluene (10 mL) and placed in a refrigerator (~0 ^{o}C) which after 2 days, produced dark-colored needles of the cation radical salt suitable for X-ray structure analysis.

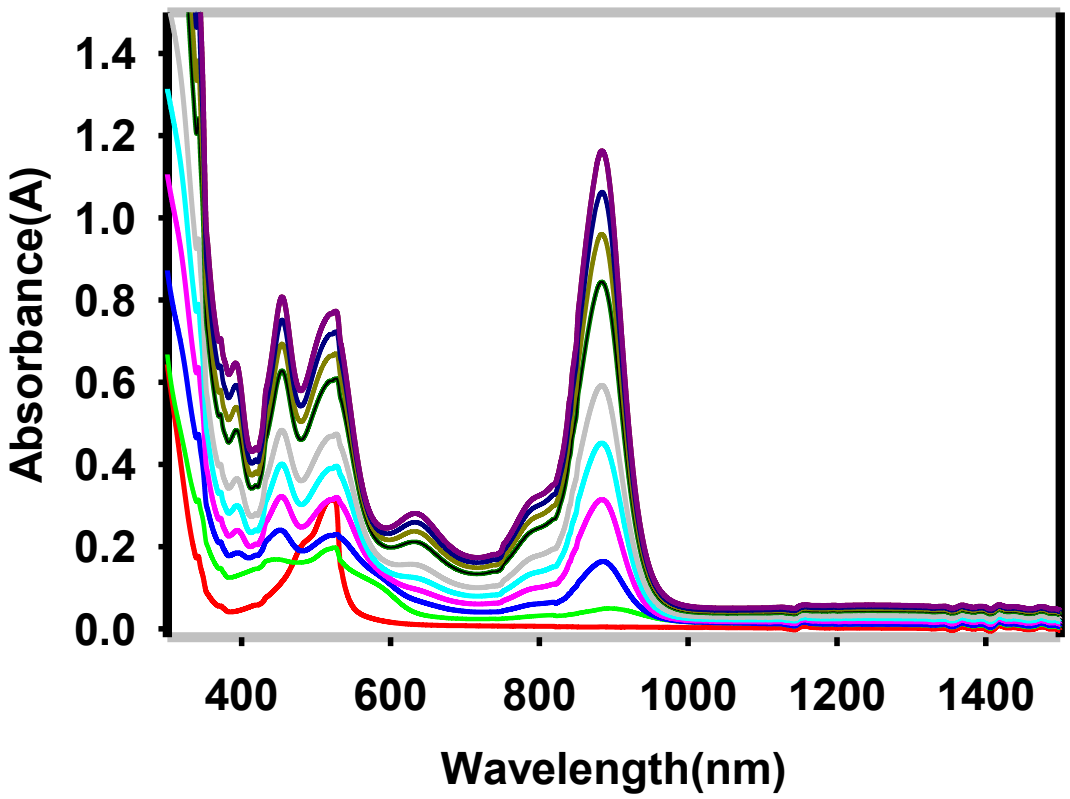

Figure E1. The spectral changes observed upon the reduction of 4.2 x 10^{-5} M **CRET**$^{+\bullet}$ (red line) by an incremental addition of substoichiometric amounts of **3** in CH_2Cl_2 at 22 ^{o}C.

Tetraveratrylethylene (2).

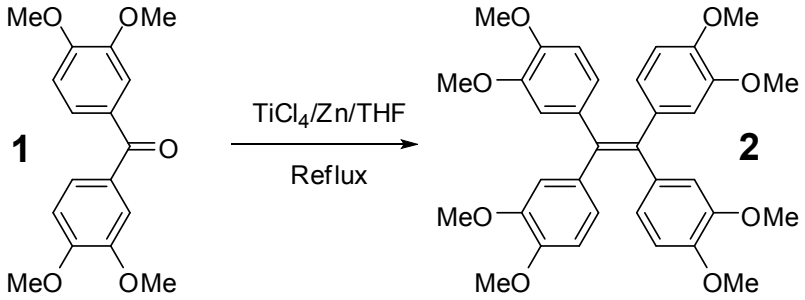

To chilled (~0 ^{o}C) anhydrous tetrahydrofuran (200 mL) was added $TiCl_4$ (6 ml, 54 mmol) dropwise with the aid of a dropping funnel under an argon atmosphere. To the resulting mixture was added Zn dust (4.4 g, 68 mmol) and dry pyridine (0.2 g, 2.5 mmol) and the resulting black suspension thus obtained was warmed to room temperature and then refluxed for two hours. A solution of tetramethoxybenzo-phenone [M. A. Silvestri, M. Nagarajan, E. De Clercq, C. Pannecouque, M. Cushman, *J. Med. Chem.* 2004, **47**, 3149] (6 g, ~20 mmol) in tetrahydrofuran (50 mL) was added dropwise to the above black reaction mixture during a course of 30 min while refluxing and the resulting mixture was refluxed for an additional 12 h. The resultant mixture was cooled to room temperature and quenched with 10 % aqueous K_2CO_3 (50 mL). The organic layer was separated and the aqueous suspension was extracted with dichloromethane (4 x 50 mL). The combined organic layers were dried over anhydrous MgSO4, filtered and evaporated to afford pale yellow solid which was purified by crystallization from a 1:1 mixture of dichloromethane and methanol to afford tetraveratrylethylene **2** [S. M. Ali, J. W. A. Findlay, A. B. Turner, *J. Chem. Soc., Perkin Trans 1* 1976, 407.] in 92% yield. M.p. 168-170 ^{o}C; ^{1}H NMR ($CDCl_3$, 400 MHz) δ: 3.54 (s, 12H), 3.82 (s, 12H), 6.57-5.65 (m, 12H); ^{13}C NMR ($CDCl_3$, 400 MHz) δ: 55.83, 55.89, 110.43, 114.97, 124.05, 136.91, 139.15, 147.59, 148.15.

Octamethoxydibenzochrysene (3).

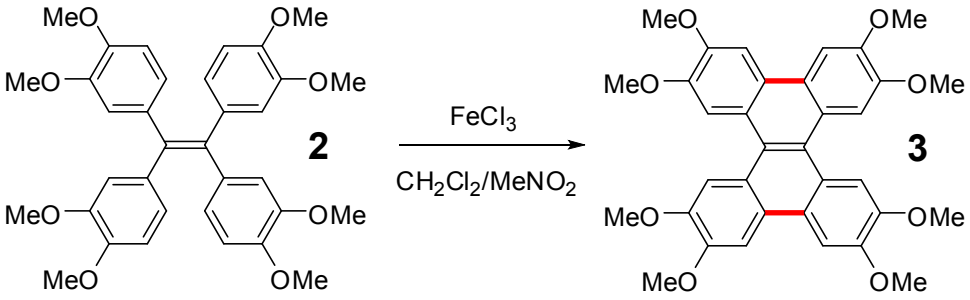

Tetraveratrylethylene (**2**) (572 mg, 1 mmol) was dissolved in dry dichloromethane (30 mL) and cooled to ~0 ^{o}C in an ice bath under an argon atmosphere. A solution of ferric chloride (1.43 g, 8.82 mmol) in nitromethane (20 mL) was added dropwise into the above mixture. When the addition was completed, the ice bath was removed and the resulting mixture was stirred for 1 h at room temperature. [Note that throughout the reaction period, a slow stream of argon was passed though the reaction mixture to remove gaseous HCl formed in the reaction.] The reaction was quenched by addition of methanol (20 mL) followed by water (20 mL). The organic layer was separated and the aqueous layer was extracted with dichloromethane (3 x 25 mL). The combined dichloromethane extracts were dried over anhydrous $MgSO_4$, filtered and evaporated to produce a pale yellow solid. Recrystallization of the solid from dichloromethane/methanol afforded **3** as a pale yellow solid in 60% yield. M.p. 321-323 ^{o}C; ^{1}H NMR ($CDCl_3$, 400 MHz) δ: 4.10 (s, 12H), 4.18 (s, 12H), 7.88 (s, 4H), 8.21 (s, 4H); ^{13}C NMR ($CDCl_3$, 400 MHz) δ: 56.22, 56.40, 104.70, 109.63, 123.64, 124.79, 125.48, 148.40, 148.88.

Synthesis of Bis(3-methoxyphenyl)methanol.

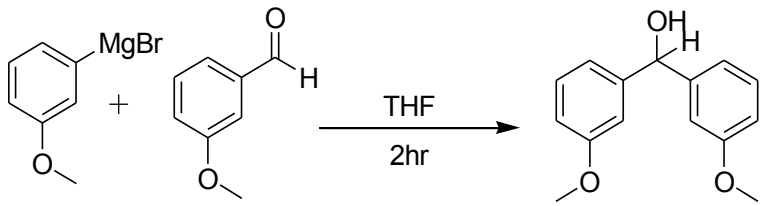

Magnesium turnings (1.73 g, 72.2 mmol) were heated for 30 minutes (40- 60 ^{o}C) under argon atmosphere. One Iodine crystal was added followed by 10 mL THF to heated magnesium. 3-Bromoanisole (4.25 g, 24.0 mmol) was dissolved in 25 mL of THF with few drops of 1,2-dibromoethane under argon, transferred to the dropping funnel and added to the schlenk flask containing magnesium. After complete addition resulting solution was refluxed for 4 h, cooled down to room temperature and added (with the help of cannula) to another schlenk flask containing 3-methoxy-benzaldehyde in 50 mL THF. Resulting mixture was stirred for 1.5 h, after completion, reaction mixture was poured onto ammonium chloride solution, extracted with DCM, dried over MgSO4, evaporated under vacuum to yield yellow oil which was purified by silica column chromatography using ethyl acetate: Hexane (10: 90) mixture to give 4.1 g of bis (3-methoxyphenyl) methanol with 87% yield (0.7 g 3-methoxy-benzaldehyde was also recovered). ^{1}H NMR ($CDCl_3$, 400 MHz) δ: 2.98 (s, 1H), 3.79 (s, 6H), 5.73 (s, 1H), 6.80- 6.86 (dd, 2H, J = 6.2 Hz), 6.95- 7.02 (m, 4H), 7.27 (t, 2H, J = 6.2 Hz); ^{13}C NMR ($CDCl_3$, 400 MHz) δ: 52.26, 76.00, 122.14, 113.03, 118.99, 129.57, 145.50, 159.71.

Synthesis of bis-(3-methoxyphenyl) ketone.

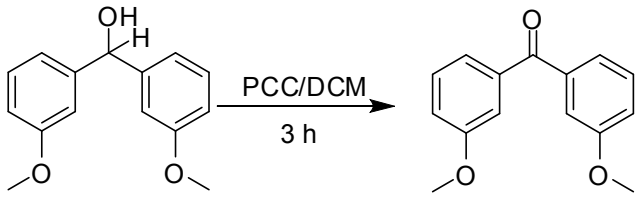

To a suspension of 5.16 g (23.94 mmol) of pyridinium chlorochromate (PCC) in 30 mL of dichloromethane was added a solution of 3.9 g (15.9 mmol) of bis-(3-methoxyphenyl)-methanol in 20 mL of dichloromethane. After the resultant mixture was stirred for 3 h at

20 ^{o}C, 100 mL of anhydrous ether was added. Resulting mixture was filtered through short pad of packed celite and evaporated under vacuum to get brown colored liquid which was purified by silica gel column chromatography using ethyl acetate and hexane (10:90) to get 3.6 g of bis(3-methoxyphenyl)ketone as an oil in 92% yield. ^{1}H NMR ($CDCl_3$, 400 MHz) δ: 3.83 (s, 6H), 7.08-7.13 (m, 2H), 7.30-7.38 (m, 6H); ^{13}C NMR ($CDCl_3$, 400 MHz) δ: 55.54, 114.40, 118.96, 122.94, 129.31, 138.99, 159.64, 196.36.

Synthesis of tetrakis(3-methoxyphenyl)ethylene.

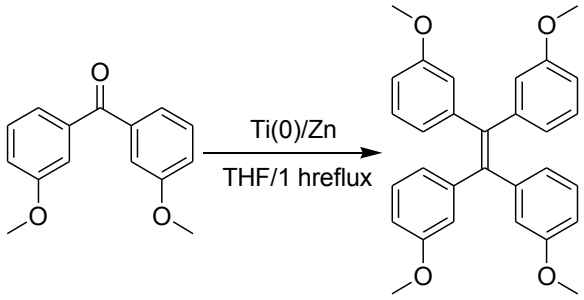

Bis-(3-methoxyphenyl)ketone (1.1 g, 4.54 mmol) was dissolved in 150 mL THF and cooled in ice-acetone bath followed by addition of $TiCl_4$ (4.08 mL, 36.56 mmol) after all fumes were ceased Zinc poweder (2.62 g, 40.2 mmol) was added in portions and resulting solution was refluxed for 1 h. After completion, reaction mixture was cooled in ice-acetone bath followed by dropwise addition of 10 % K_2CO_3 (100 mL), resulting mixture was stirred for 30 minutes followed by multiple extractions with ether, collected ether layers were washed with water, dried over magnesium sulfate, evaporated under vacuum to afford crude product which was purified by silica column chromatography to give tetrakis-(3-methoxy-phenyl)ethylene in 56% yield. ^{1}H NMR ($CDCl_3$, 400 MHz) δ: 3.58 (s, 12H), 6.63- 6.73 (m, 12H), 7.05 (t, 4H); ^{13}C NMR ($CDCl_3$, 400 MHz) δ: 55.13, 112.82, 116.51, 123.83, 128.75, 140.98, 144.87, 159.09.

Synthesis of 3,6,11,14-tetramethoxydibenzochrysene.

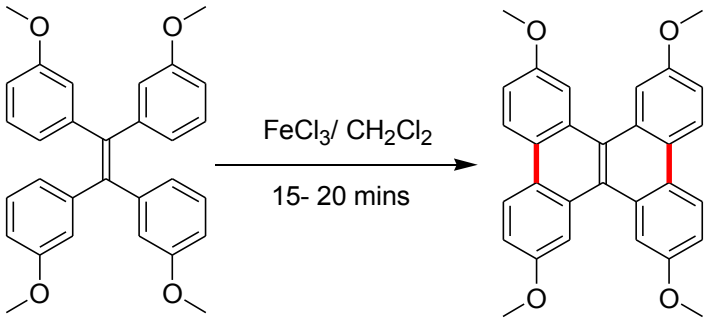

Tetrakis-(3-methoxyphenyl)ethylene (1.0 mmol) was dissolved in dry dichloromethane followed by addition of excess of $FeCl_3$ (~10.0 mmol), resulting mixture was stirred for 15- 20 minutes at room temperature. After complete consumption of tetrakis-(3-methoxy-phenyl)ethylene, reaction was quenched with methanol followed by aqueous workup to afford 3,6,11,14-tetramethoxydibenzochrysene as pale yellow colored solid in good yield (82 %). ^{1}H NMR ($CDCl_3$, 400 MHz) δ: 3.93 (s, 12H), 7.28 (dd, 4H, J = 9.0 Hz, 2.6 Hz), 8.23 (d, 4H, J = 2.6 Hz), 8.51 (d, 4H, J = 9.0 Hz); ^{13}C NMR ($CDCl_3$, 400 MHz) δ: 55.74, 110.24, 116.45, 124.90, 125.25, 128.77, 129.93, 157.77.

Synthesis of 3,3'-dimethoxybiphenyl.

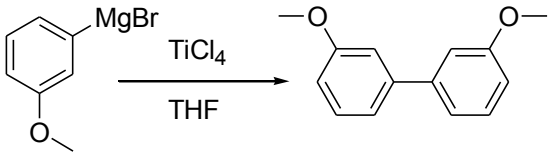

Magnesium turnings (0.52 g, 21.8 mmol) were transferred to the schlenk flask which was warmed to 40-50 ^{o}C for 15 minutes. 3-Bromo-anisole (3.7 g, 19.8 mmole) dissolved in 40 mL THF was transferred to the schlenk flask containing magnesium turnings (at room temperature). Resulting solution was refluxed for 30 minutes and subsequently cooled to -78 ^{o}C. $TiCl_4$ (5.63 g, 29.7 mmol) was then added dropwise to the above mixture at 0 ^{o}C

(after transferring it to the ice bath). Stirring was continued for additional 30 minutes under the high flow of argon. After completion, reaction was quenched by pouring it over saturated solution of ammonium chloride followed by extraction with dichloromethane (3 x 25 mL). Combined organic layers were washed with water, dried over MgSO4, and evaporated under vacuum to afford 3,3'-dimethoxybiphenyl in nearly quantitative yield as light-brown liquid. ^{1}H NMR ($CDCl_3$, 400 MHz) δ: 3.87 (s, 6H), 6.91 (d, 2H, *J* = 8.2 Hz), 7.13 (s, 2H), 7.19 (d, 1H, *J* = 8.2 Hz), 7.36 (t, 1H, *J* = 8.2 Hz); ^{13}C NMR ($CDCl_3$, 400 MHz) δ: 55.50, 112.99, 113.12, 119.89, 129.92, 142.81, 160.06.

Synthesis of 2-bromo-5,3'-dimethoxybiphenyl.

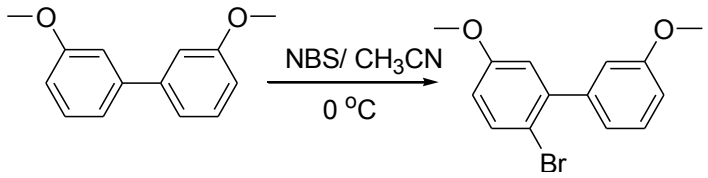

3,3'-Dimethoxybiphenyl (4.2 g, 19.60 mmol) was dissolved in acetonitrile (40 mL) and cooled to 0 °C. A solution of *N*-bromosuccinamide (3.48 g, 19.6 mmol) in acetonitrile (40 mL) was added dropwise to the above solution over a period of 1 h and the resulting mixture was stirred for an additional 30 min. The reaction mixture was diluted with water (50 mL) and extracted with dichloromethane (3 x 50 mL). The dichloromethane layer was dried over anhydrous $MgSO_4$ and evaporated to afford a pale-yellow liquid in nearly quantitative yield. ^{1}H NMR ($CDCl_3$, 400 MHz) δ: 3.80 (s, 3H), 3.85 (s, 3H), 6.79 (dd, 1H, *J* = 8.77 Hz, 3.0 Hz), 6.90 (d, 1H, *J* = 3.0 Hz), 6.92- 7.01 (m, 3H), 7.35 (t, 1H, *J* = 7.6 Hz), 7.54 (d, 1H, *J* = 8.77 Hz); ^{13}C NMR ($CDCl_3$, 400 MHz) δ: 55.42, 55.65, 113.05, 113.38, 114.92, 115.10, 116.70, 121.83, 129.16, 133.83, 142.54, 143.32, 158.87, 159.22.

Synthesis of 2-iodo-5,3'-dimethoxybiphenyl.

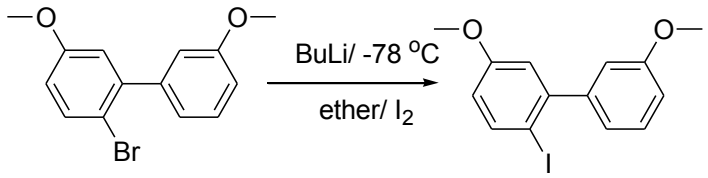

2-Bromo-5,3'-dimethoxybiphenyl (4.85 g, 16.54 mmol) was dissolved in 100 mL dry ethyl ether and cooled to -78 ^{o}C subsequently 2.5 M butyl lithium (6.9 mL, 17.4 mmol) was added dropwise. Resulting solution was stirred for 1 h at -78 ^{o}C and 1.2 h at -40 ^{o}C followed by dropwise addition of iodine (10.56 g, 41.7 mmol) dissolved in 80 mL ethyl ether. Resulting solution was stirred for 30 minutes at -78 ^{o}C and 15 minutes at room temperature before pouring onto ice cooled sodium bisulfate solution, followed by multiple extractions with dichloromethane to get 2-iodo-5,3'-dimethoxy-buiphenyl in excellent yield, the compound was used without purification for the further step. ^{1}H NMR ($CDCl_3$, 400 MHz) δ: 3.81 (s, 3H), 3.86 (s, 3H), 6.67 (dd, 1H, J = 8.8 Hz, 3.0 Hz), 6.89-6.99 (m, 4H), 7.36 (t, 1H, *J* = 7.8 Hz), 7.81 (d, 1H, 8.8 Hz); ^{13}C NMR ($CDCl_3$, 400 MHz) δ: 55.45, 55.57, 87.07, 114.97, 115.37, 115.98, 121.74, 129.19, 140.13, 145.52, 147.45, 159.17, 159.84.

Synthesis of bis-biarylacetylene.

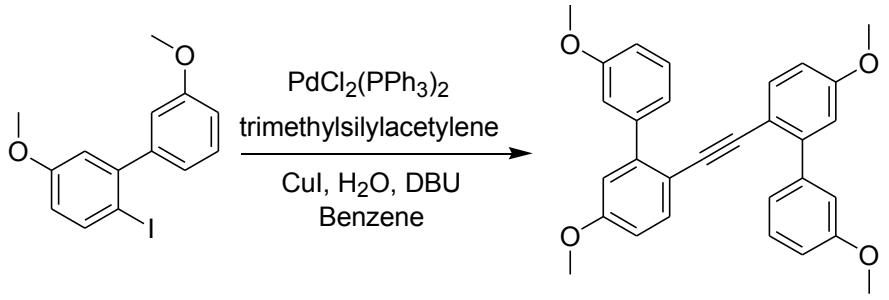

2-Iodo-5,3'-dimethoxy-biphenyl(3.5 g, 10.3 mmol), $PdCl_2(PPh_3)_2$ (0.43 g, 0.6 mmol), CuI(0.195 g, 1.0 mmol), DBU (9.39 g, 61.8 mmol) and water (4.1 mmol) were mixed under an argon atmosphere. To this mixture was added trimethylsilylacetylene (0.504 g, 5.1 mmol) at room temperature over the course of 5 minutes. Resulting mixture was then refluxed for 18 h followed by general aqueous workup afforded bis-biarylacetylene in 44% yield. ^{1}H NMR ($CDCl_3$, 400 MHz) δ: 3.80 (s, 6H), 3.83 (s, 6H), 6.81 (dd, 2H, *J* = 8.6 Hz, 2.7 Hz), 6.88-6.92 (m, 4H), 7.13-7.18 (m, 4H), 7.26-7.32 (m, 4H); ^{13}C NMR ($CDCl_3$, 400 MHz) δ: 55.45, 55.95, 90.79, 113.24, 113.69, 114.61, 114.67, 114.87, 121.92, 129.06, 134.38, 141.99, 144.79, 159.27, 159.45.

Synthesis of 2,7,10,15-tetramethoxydibenzochrysene:

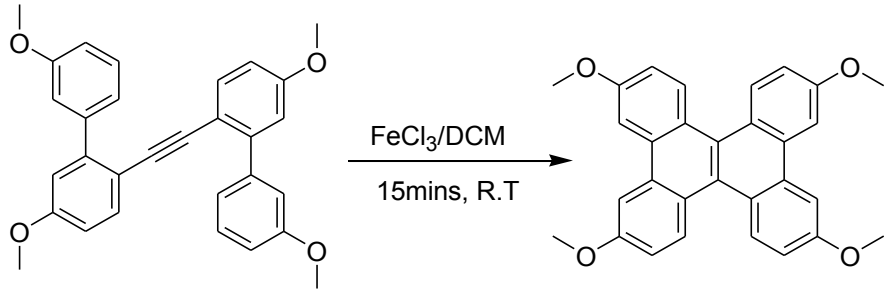

Bisbiarylacetylene (2.0 mmol) was dissolved in dry dichloromethane followed by addition of excess of $FeCl_3$ (~10.0 mmol), resulting mixture was stirred for 15- 20 minutes at room temperature. After complete consumption of bisarylacetylene, reaction was quenched with 20 mL methanol followed by aqueous workup afforded 2,7,10,15-tetramethoxydibenzochrysene as a colorless solid in good yield (73%). ^{1}H NMR ($CDCl_3$, 400 MHz) δ: 4.04 (s, 12H), 7.23 (dd, 4H, *J* = 9.1 Hz, 2.6 Hz), 7.99 (d, 4H, *J* = 2.6 Hz), 8.52 (d, 4H, *J* = 9.1 Hz); ^{13}C NMR ($CDCl_3$, 400 MHz) δ: 55.74, 106.31, 115.29, 124.19, 124.67, 130.50, 131.69, 157.93.

EXPERIMENTAL SPECTRA

^{1}H and ^{13}C NMR spectra of various compounds

^{1}H NMR spectrum of Tetraveratrylethylene (2).

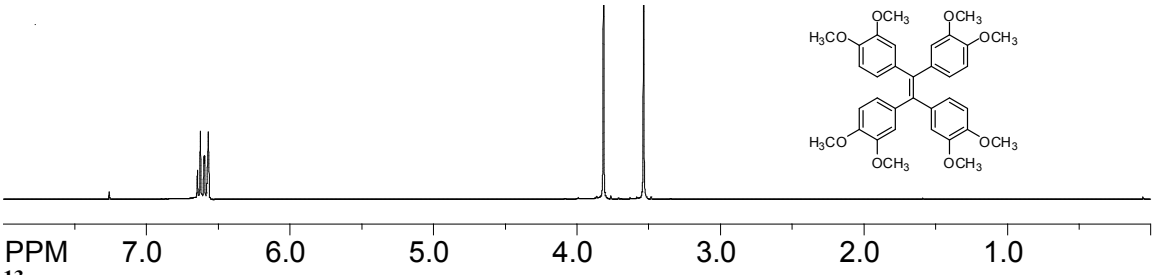

^{13}C NMR spectrum of Tetraveratrylethylene (2).

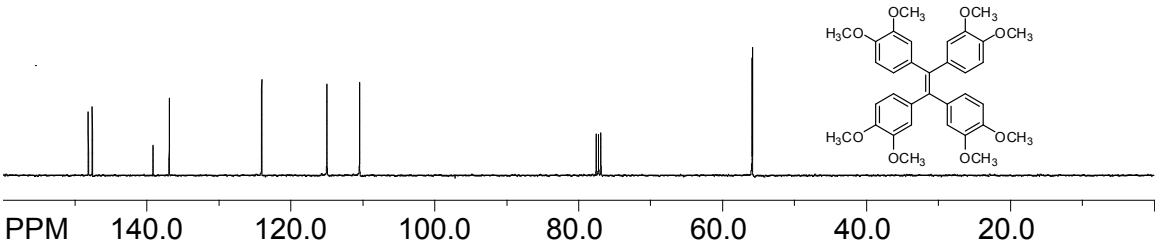

^{1}H NMR spectrum of Octamethoxydibenzochrysene (3).

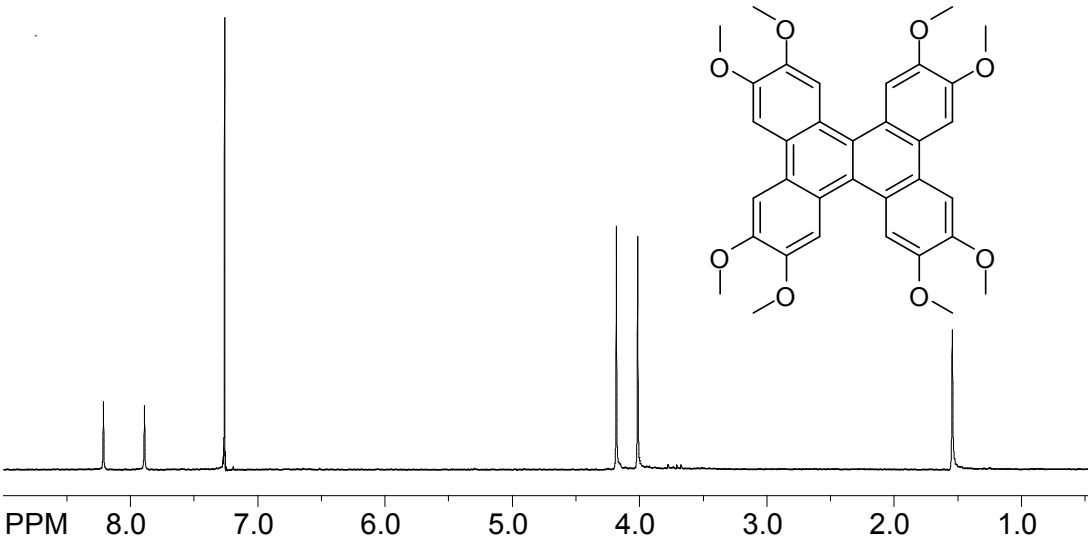

^{13}C NMR spectrum of Octamethoxydibenzochrysene (3).

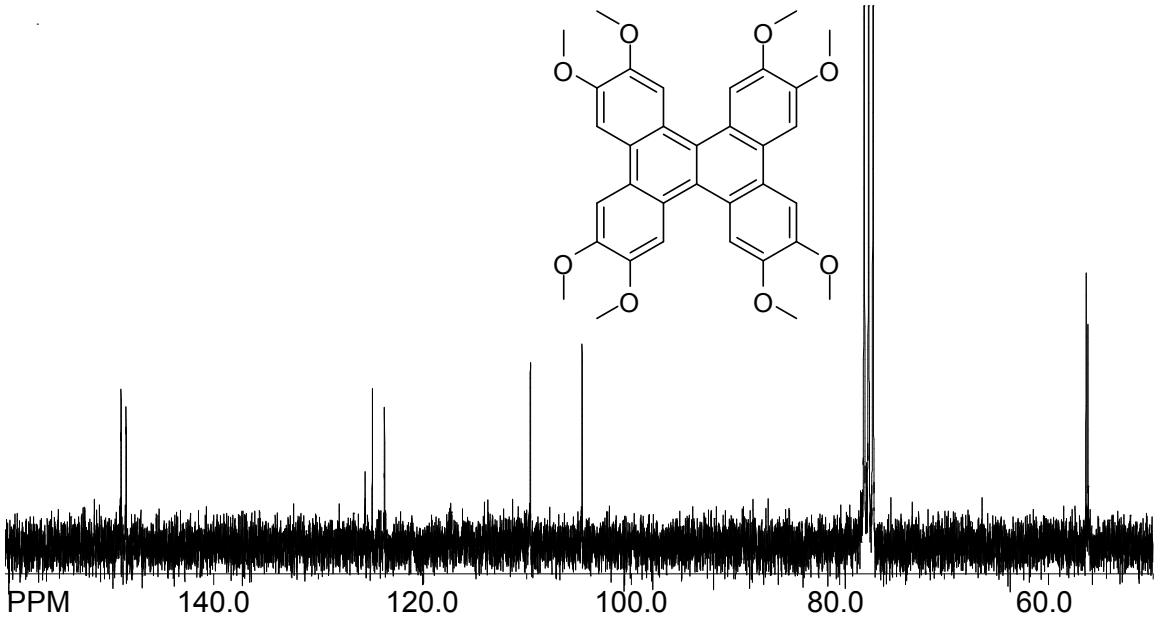

^{1}H NMR of Bis(3-methoxyphenyl)methanol:

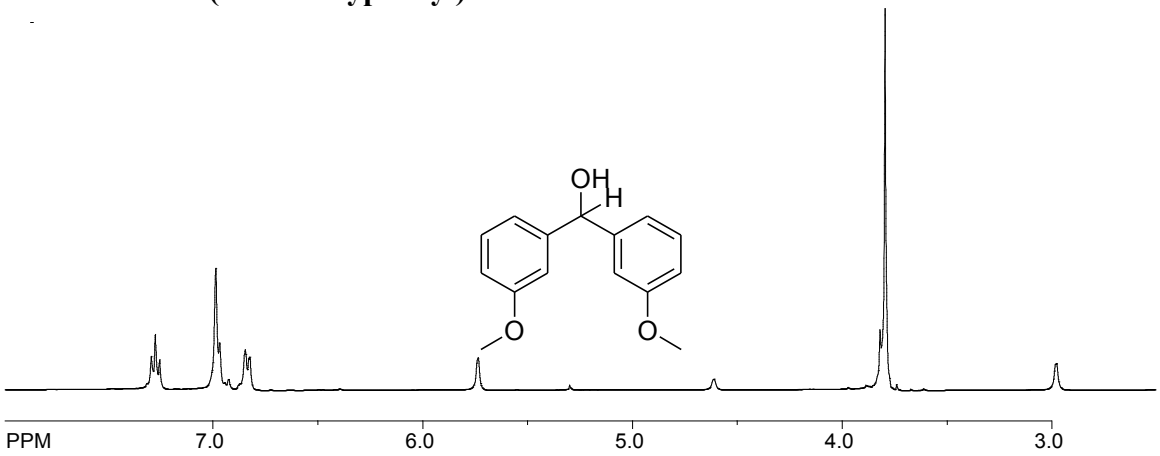

^{13}C NMR of Bis(3-methoxyphenyl)methanol:

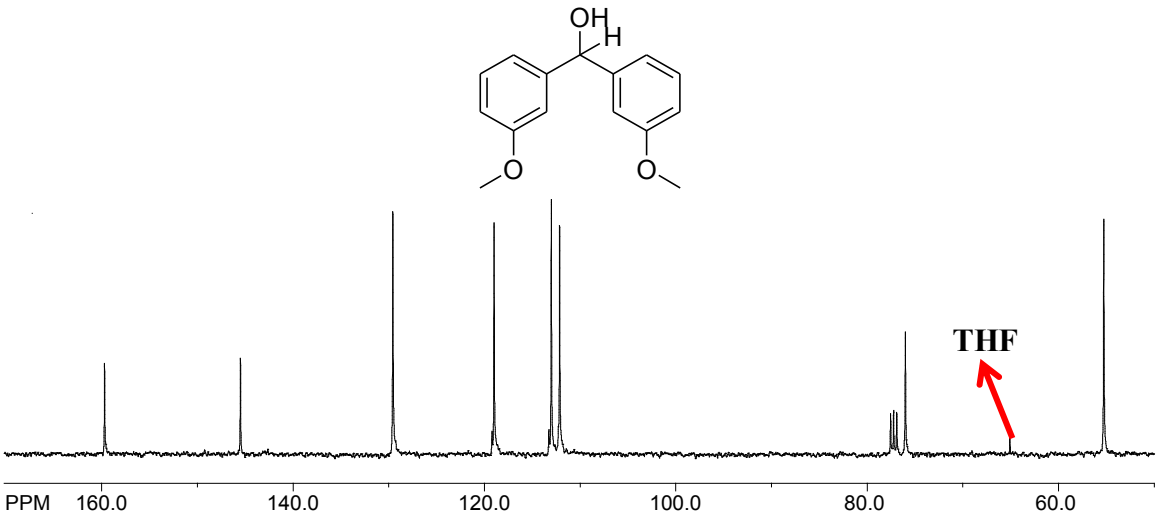

^{1}H NMR of Bis(3-methoxyphenyl)ketone:

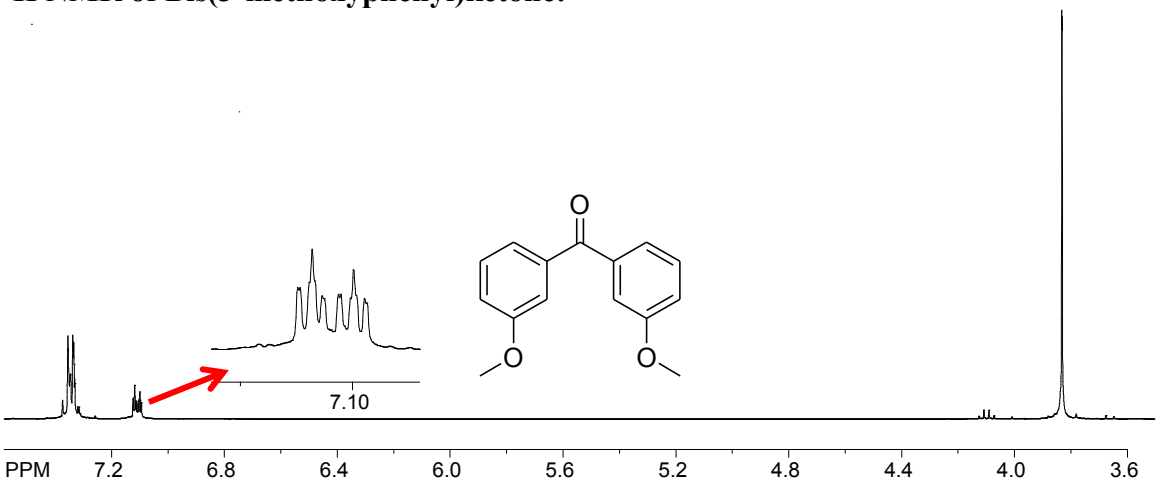

^{13}C NMR of Bis(3-methoxyphenyl)ketone:

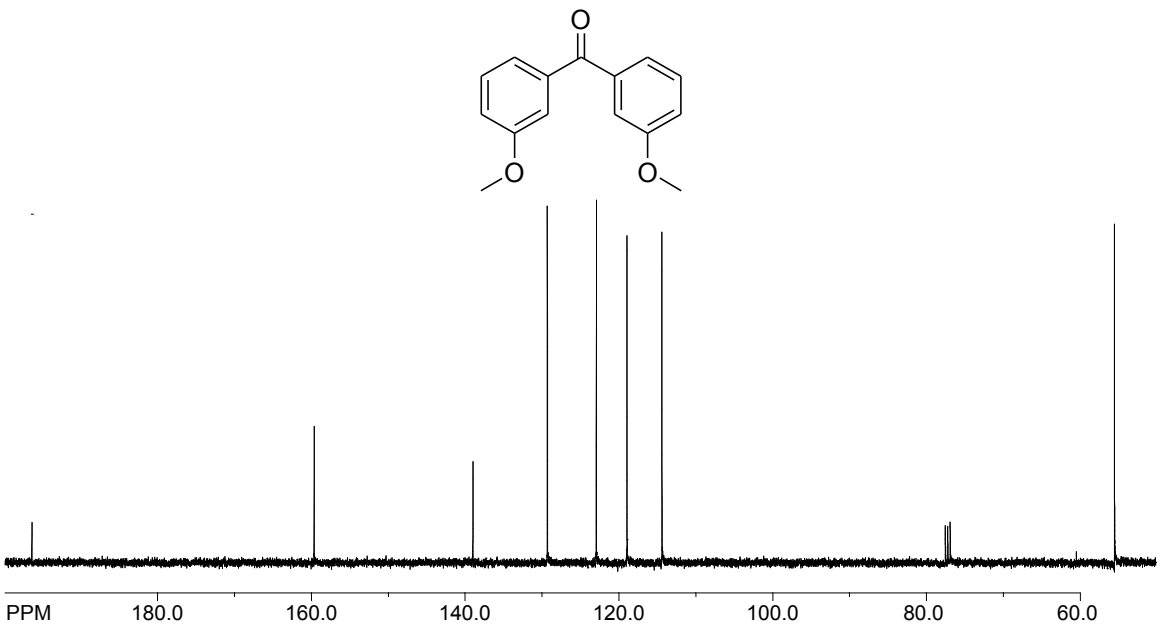

^{1}H NMR of tetrakis-(3-methoxy-phenyl)-ethylene:

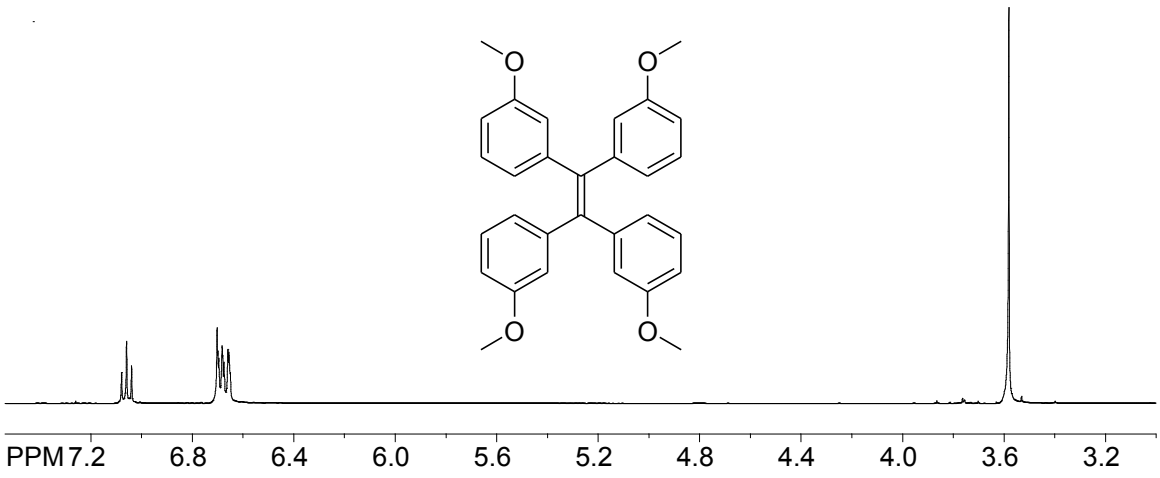

^{13}C NMR of tetrakis-(3-methoxy-phenyl)-ethylene:

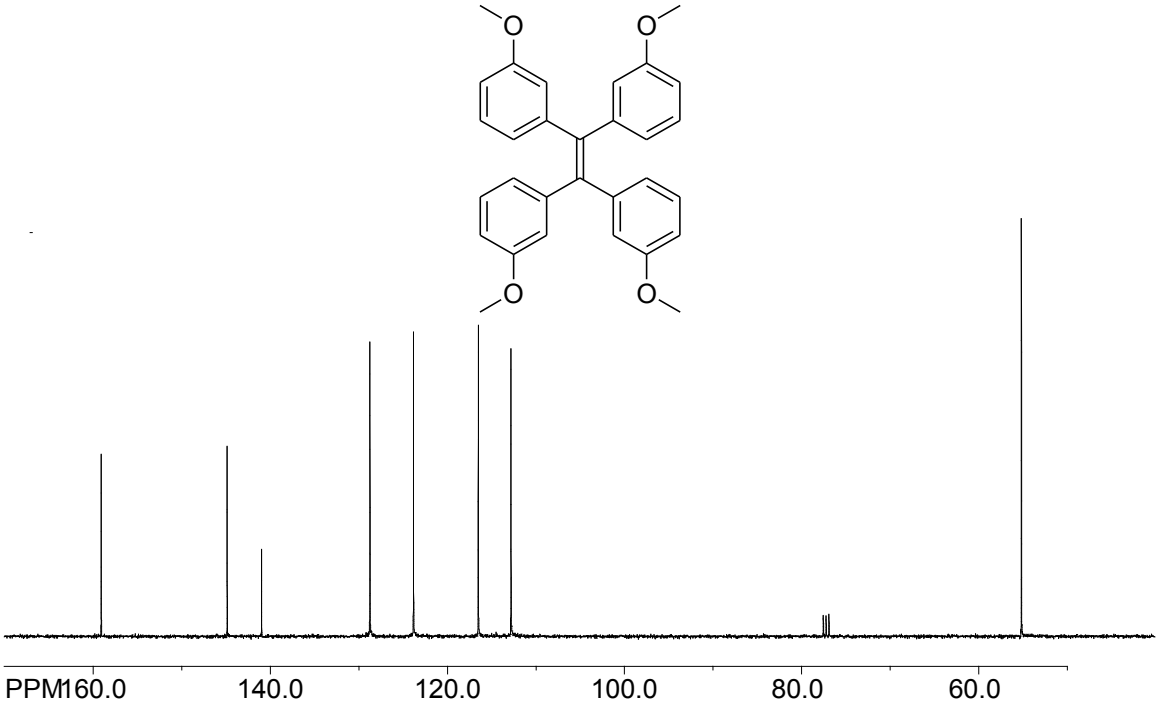

^{1}H NMR of 3,6,11,14-tetramethoxydibenzochrysene:

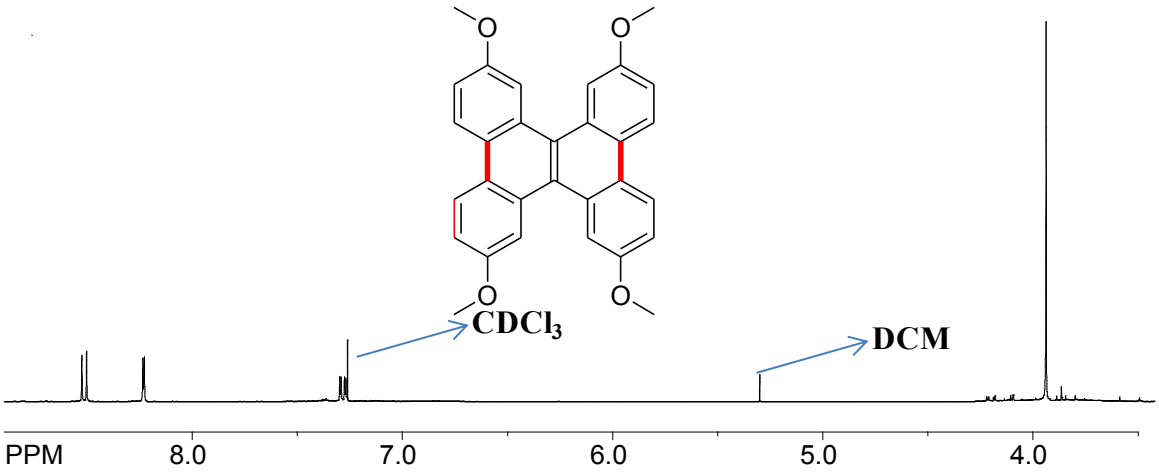

Zoomed NMR of 3,6,11,14-tetramethoxydibenzochrysene:

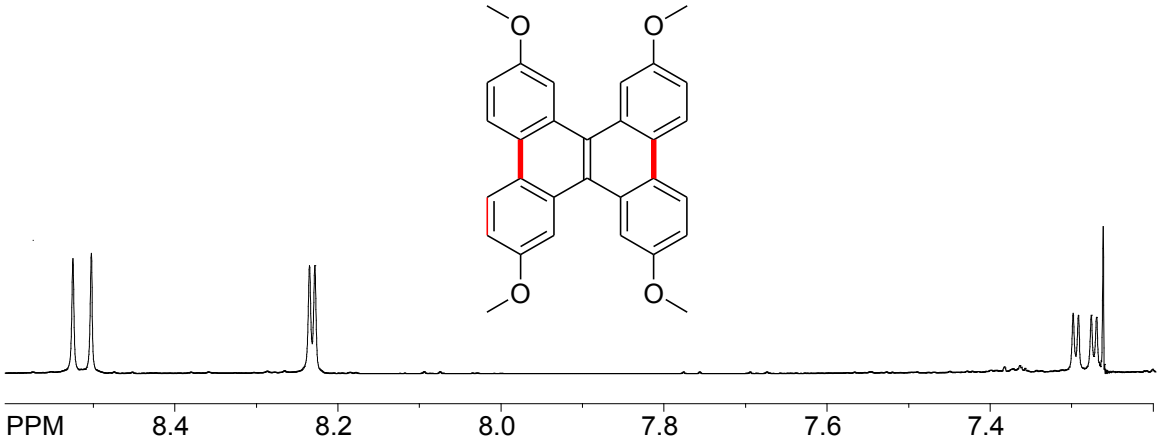

^{13}C NMR of 3,6,11,14-tetramethoxydibenzochrysene:

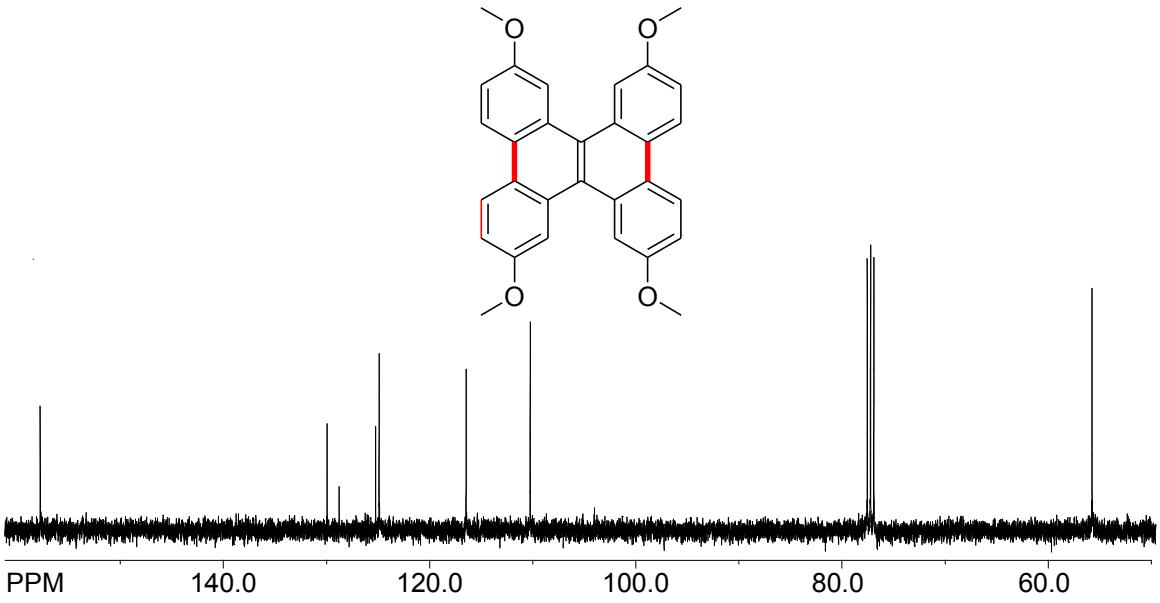

^{1}H NMR of 3,3'-dimethoxy-biphenyl:

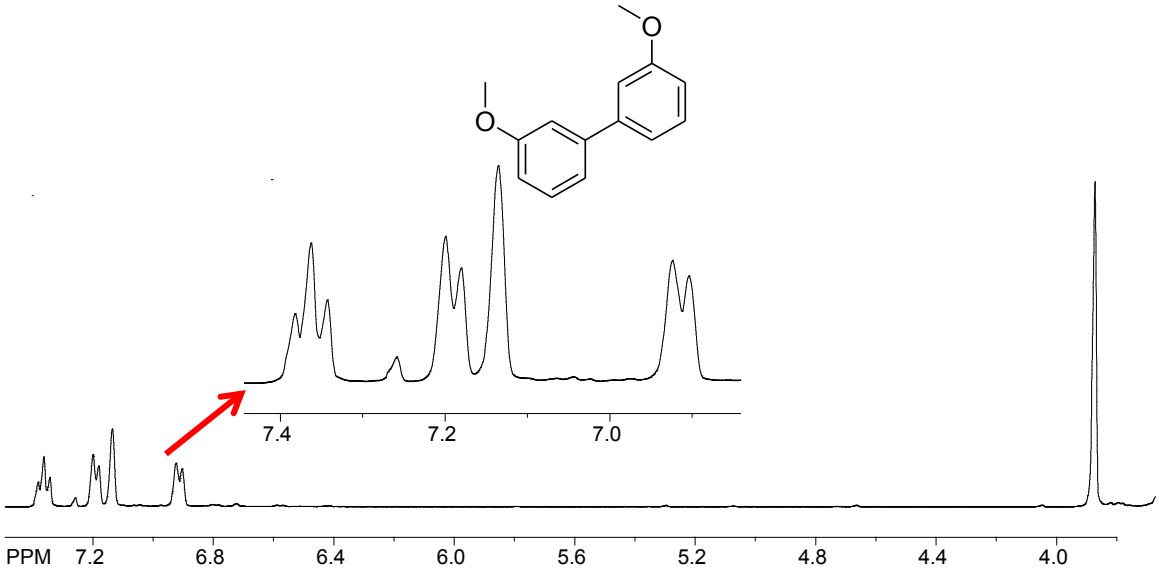

^{13}C NMR of 3,3'-dimethoxy-biphenyl:

^{1}H NMR of 2-bromo-5,3'-dimethoxy-biphenyl:

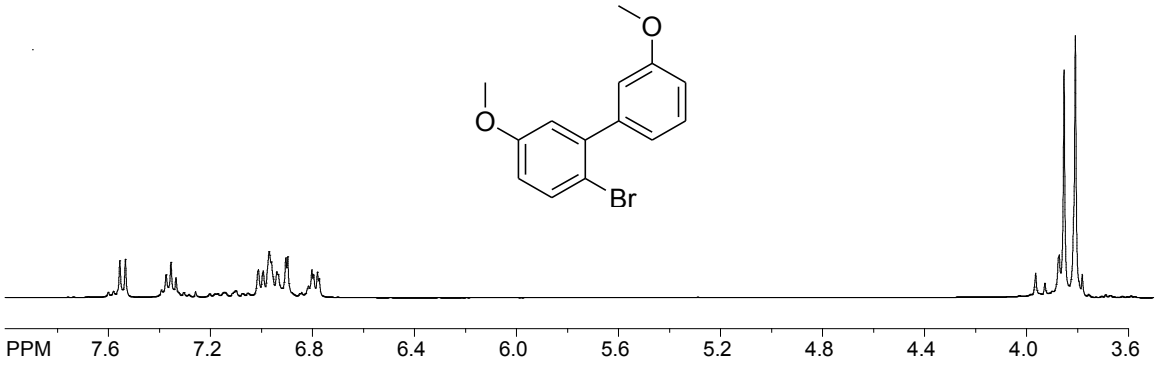

^{13}C NMR of 2-bromo-5,3'-dimethoxy-biphenyl:

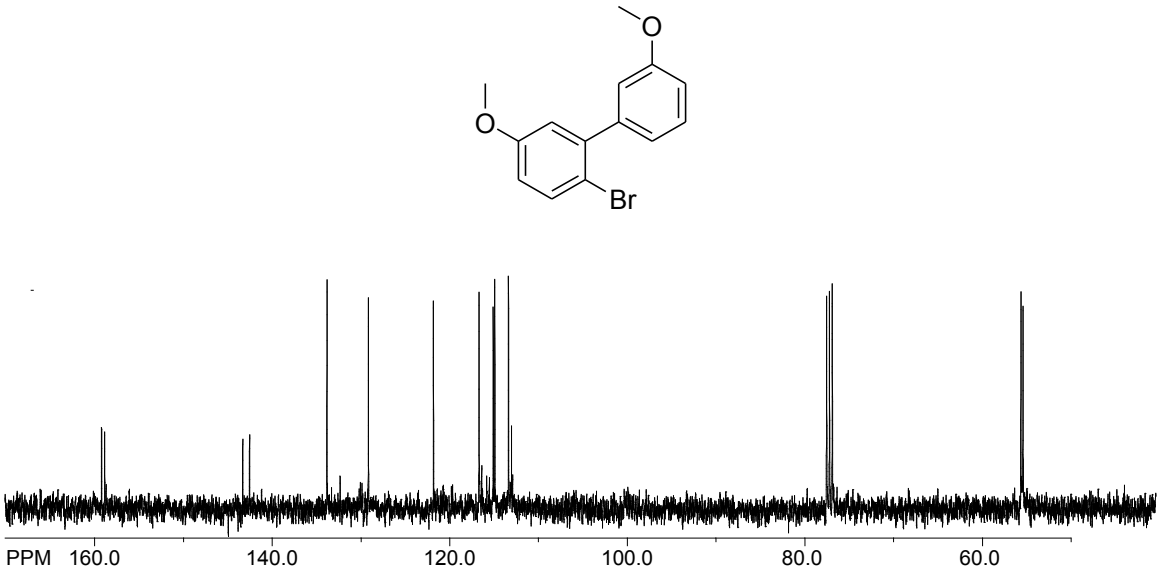

^{1}H NMR of 2-iodo-5,3'-dimethoxybiphenyl:

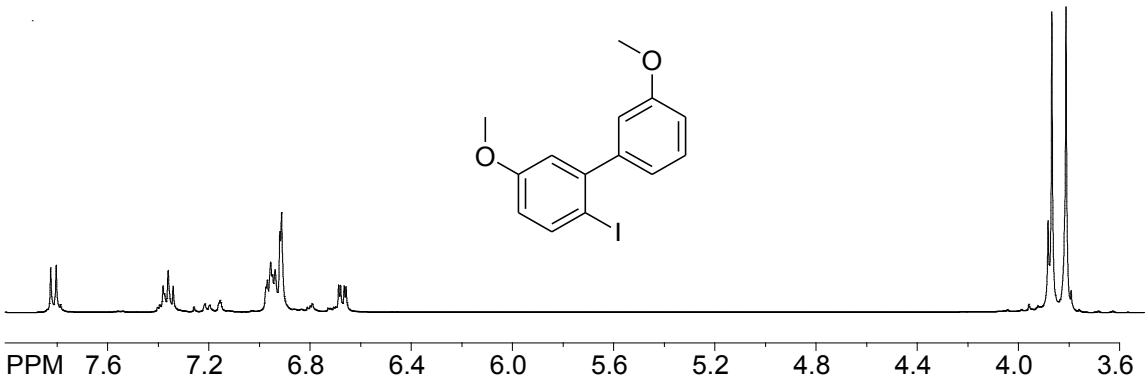

^{13}C NMR of 2-iodo-5,3'-dimethoxy-biphenyl:

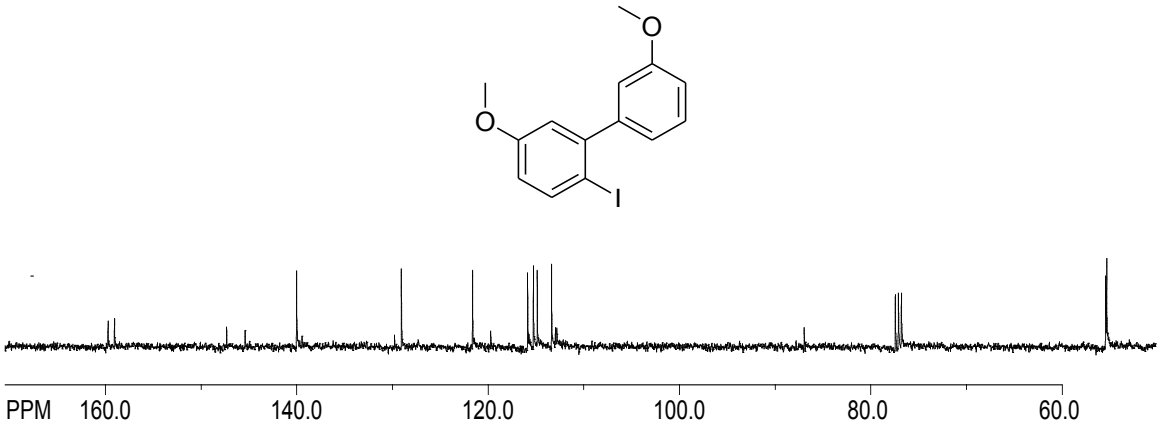

^{1}H NMR of Bis-biphenylacetylene:

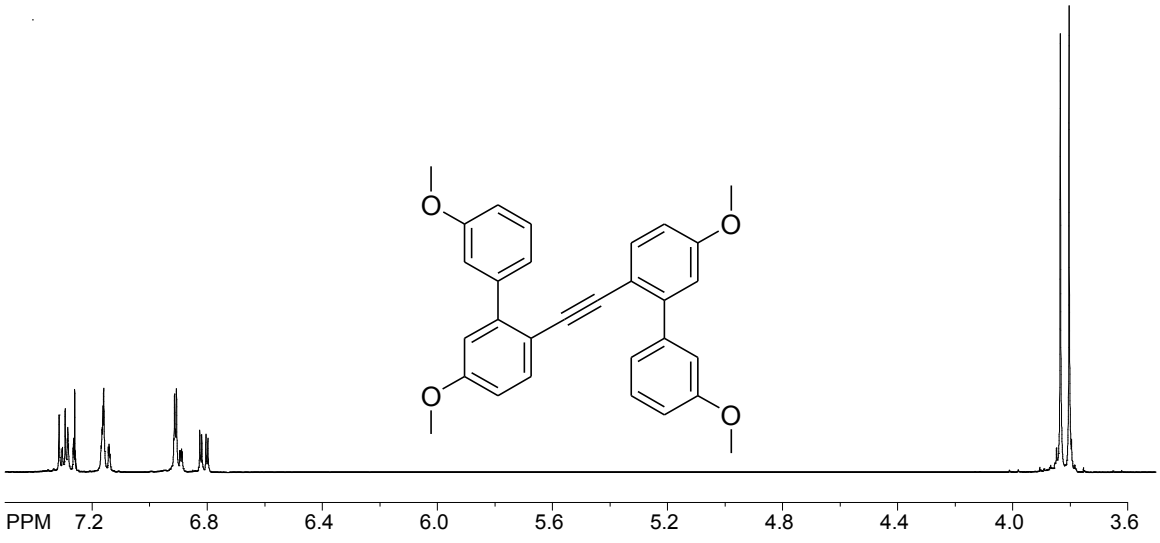

Zoomed ^{1}H NMR of Bis-biphenyl-alkyne:

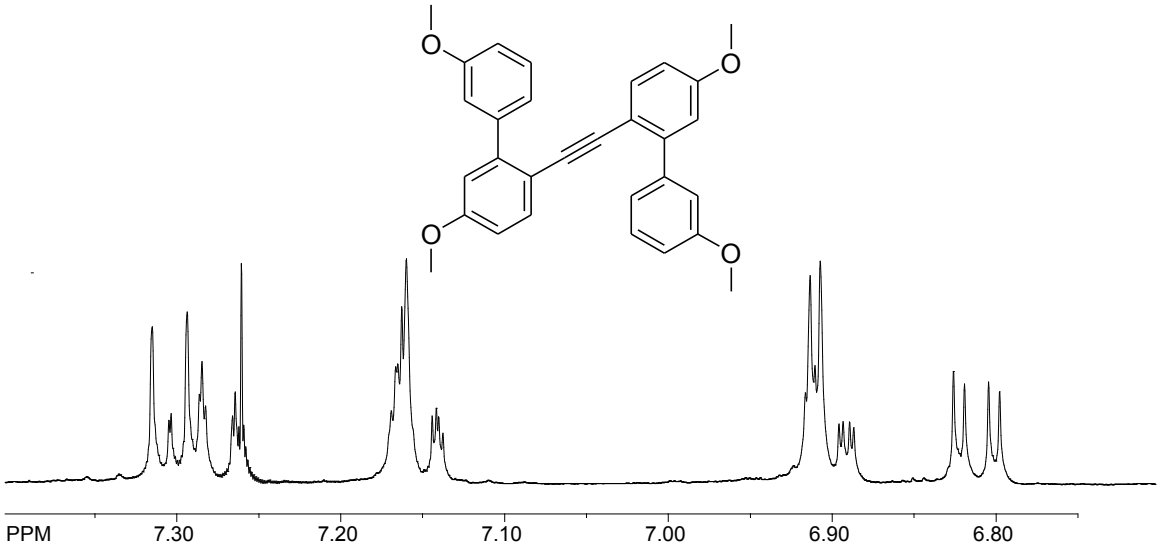

^{13}C NMR of Bis-biphenyl-alkyne:

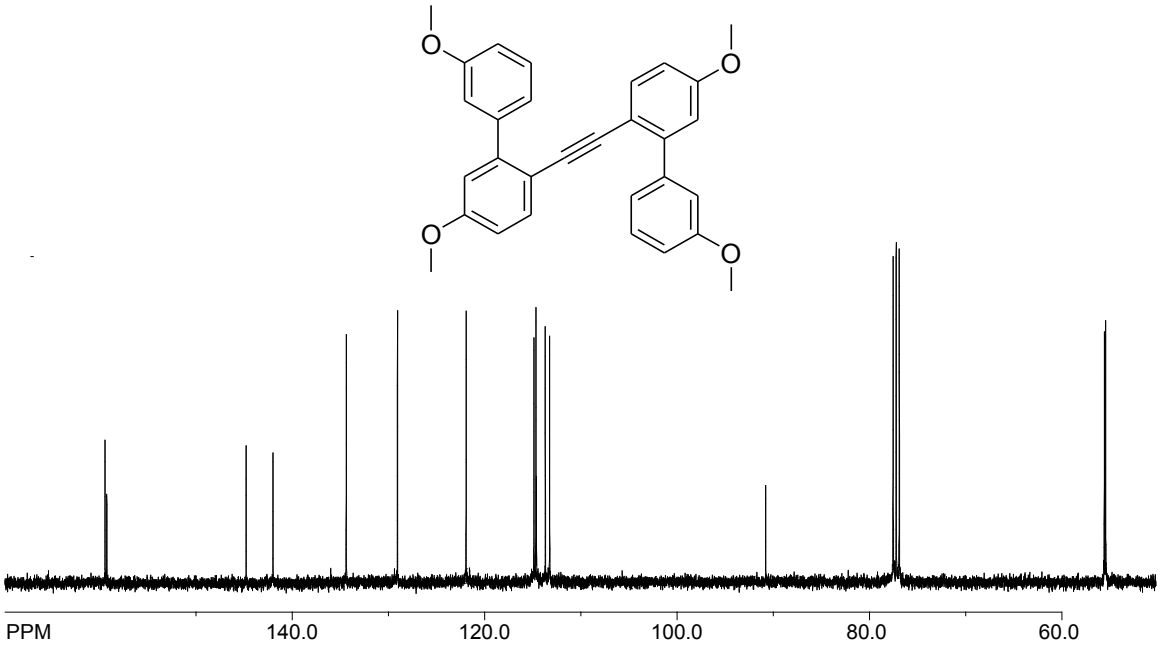

^{1}H NMR of 2,7,10,15-tetramethoxydibenzochrysene:

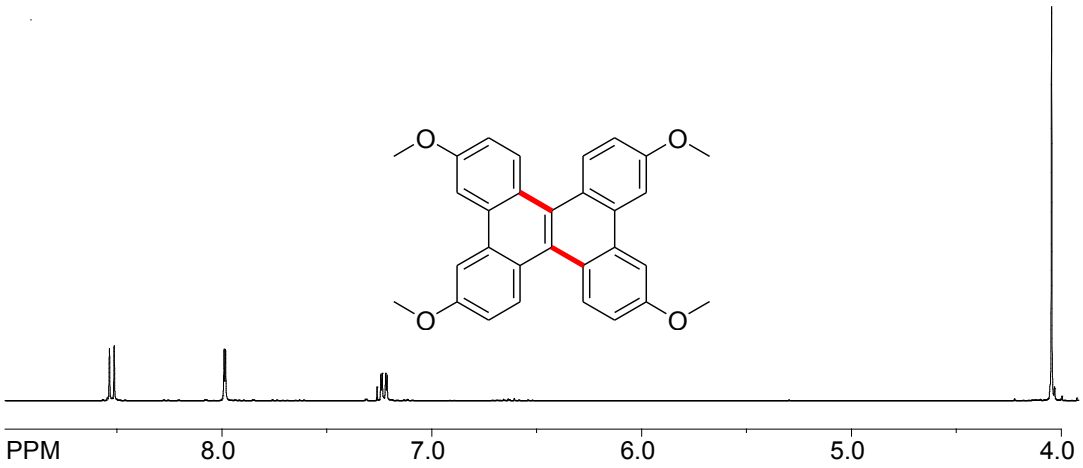

Zoomed ^{1}H NMR of 2,7,10,15-tetramethoxydibenzochrysene:

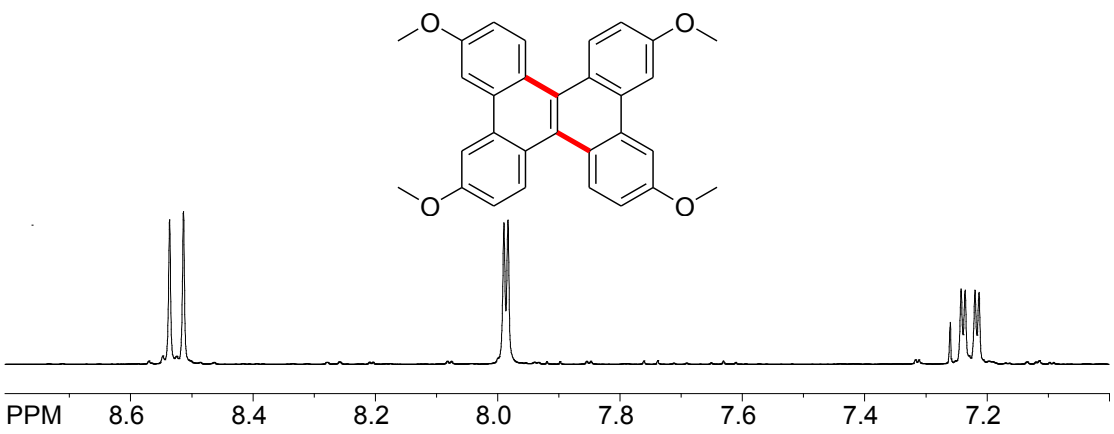

^{13}C NMR of 2,7,10,15-tetramethoxydibenzochrysene:

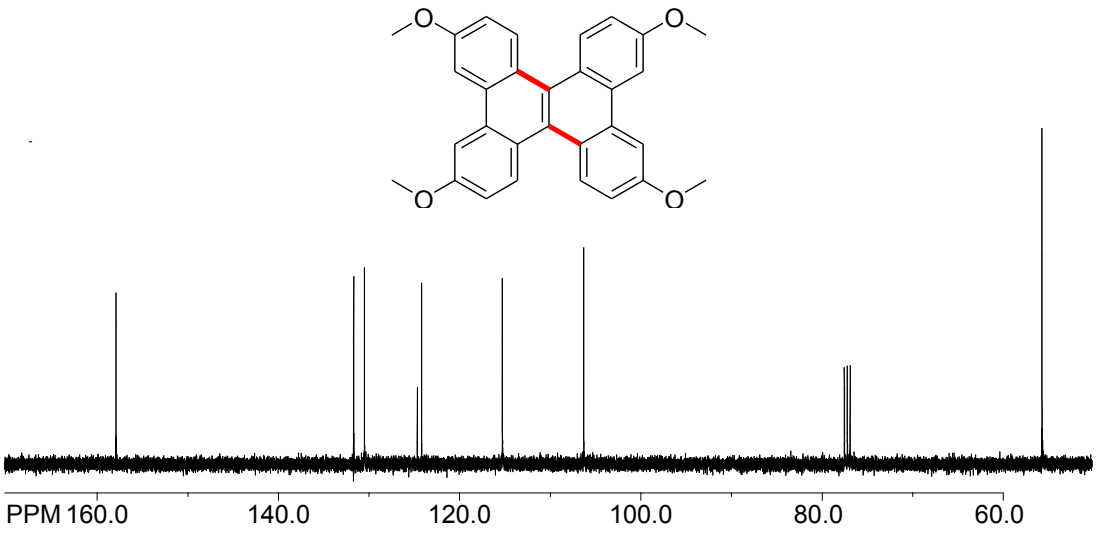

Table 3. **Crystal data and structure refinement for Octamethoxy-dibenzochrysene (3)**

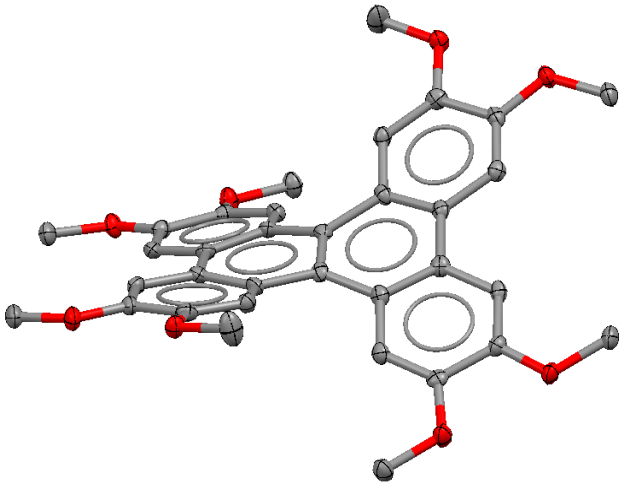

Identification code	raj2z	
Empirical formula	C43 H46 Cl2 N4 O8	
Formula weight	817.74	
Temperature	100(2) K	
Wavelength	1.54178 Å	
Crystal system	Monoclinic	
Space group	C 2/c	
Unit cell dimensions	a = 31.6750(8) Å	α= 90°.
	b = 7.3983(2) Å	β= 106.7180(10)°.
	c = 18.0078(4) Å	γ = 90°.
Volume	4041.60(17) $Å^3$	
Z	4	
Density (calculated)	1.344 Mg/m^3	
Absorption coefficient	1.930 mm^{-1}	
F(000)	1720	
Crystal size	0.25 x 0.12 x 0.08 mm^3	
Theta range for data collection	2.91 to 62.57°.	
Index ranges	-36<=h<=34, 0<=k<=8, 0<=l<=20	
Reflections collected	6231	
Independent reflections	3114 [R(int) = 0.0174]	
Completeness to theta = 62.57°	98.6 %	
Absorption correction	Semi-empirical from equivalents	
Max. and min. transmission	0.8609 and 0.6440	
Refinement method	Full-matrix least-squares on F^2	
Data / restraints / parameters	3114 / 0 / 342	
Goodness-of-fit on F^2	1.066	
Final R indices [I>2sigma(I)]	R1 = 0.0817, wR2 = 0.2344	
R indices (all data)	R1 = 0.0944, wR2 = 0.2397	
Largest diff. peak and hole	0.506 and -0.612 $e.Å^{-3}$	

Table 4. **Crystal data and structure refinement for Octamethoxydibenzochrysene Cation Radical [$3^{+\bullet}$ $SbCl_6^-$]**

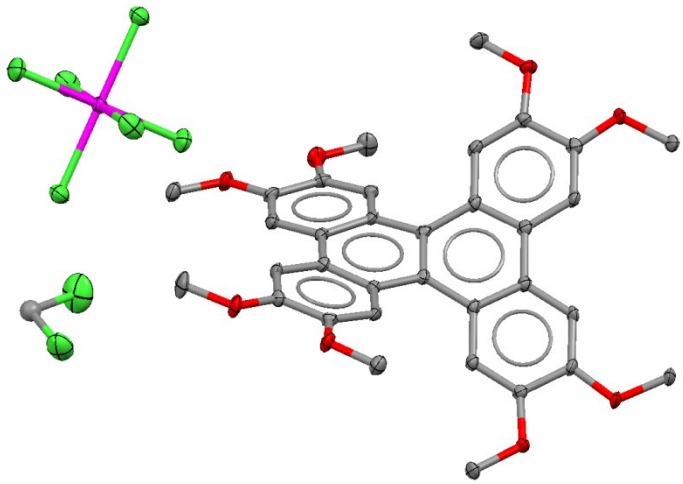

Identification code	raj3d	
Empirical formula	C36 H36 Cl10 O8 Sb	
Formula weight	1072.90	
Temperature	100(2) K	
Wavelength	1.54178 Å	
Crystal system	Triclinic	
Space group	P -1	
Unit cell dimensions	a = 13.6451(5) Å	α= 61.672(2)°.
	b = 14.0770(5) Å	β= 62.275(2)°.
	c = 14.3621(5) Å	γ = 70.899(2)°.
Volume	2129.38(13) $Å^3$	
Z	2	
Density (calculated)	1.673 Mg/m^3	
Absorption coefficient	11.327 mm^{-1}	
F(000)	1074	
Crystal size	0.42 x 0.07 x 0.07 mm^3	
Theta range for data collection	3.60 to 62.76°.	
Index ranges	-13<=h<=15, -13<=k<=15, 0<=l<=16	
Reflections collected	16984	
Independent reflections	6159 [R(int) = 0.0343]	
Completeness to theta = 62.76°	98.7 %	
Absorption correction	Numerical	
Max. and min. transmission	0.5044 and 0.0874	
Refinement method	Full-matrix least-squares on F^2	
Data / restraints / parameters	6159 / 0 / 644	
Goodness-of-fit on F^2	1.039	
Final R indices [I>2sigma(I)]	R1 = 0.0277, wR2 = 0.0714	
R indices (all data)	R1 = 0.0307, wR2 = 0.0728	
Largest diff. peak and hole	0.703 and -0.605 $e.Å^{-3}$	

Table 5. **Crystal data and structure refinement for 2,7,10,15-tetramethoxydibenzochrysene**.

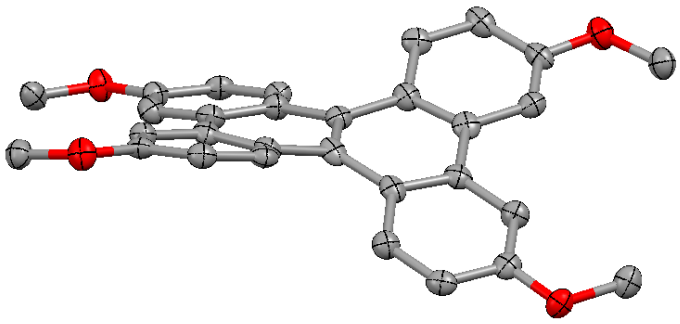

Identification code	raj17e5	
Empirical formula	C30 H24 O4	
Formula weight	448.49	
Temperature	100(2) K	
Wavelength	1.54178 Å	
Crystal system	Monoclinic	
Space group	P 21/c	
Unit cell dimensions	a = 10.7741(11) Å	α= 90°.
	b = 28.847(2) Å	β= 109.098(7)°.
	c = 7.3526(9) Å	γ = 90°.
Volume	2159.4(4) $Å^3$	
Z	4	
Density (calculated)	1.380 Mg/m^3	
Absorption coefficient	0.728 mm^{-1}	
F(000)	944	
Crystal size	0.22 x 0.12 x 0.03 mm^3	
Theta range for data collection	3.06 to 67.42°.	
Index ranges	-12<=h<=11, 0<=k<=34, 0<=l<=8	
Reflections collected	50907	
Independent reflections	4316 [R(int) = 0.1129]	
Completeness to theta = 67.42°	98.4 %	
Absorption correction	Semi-empirical from equivalents	
Max. and min. transmission	0.9785 and 0.8563	
Refinement method	Full-matrix least-squares on F^2	
Data / restraints / parameters	4316 / 0 / 314	
Goodness-of-fit on F^2	1.032	
Final R indices [I>2sigma(I)]	R1 = 0.0899, wR2 = 0.2530	
R indices (all data)	R1 = 0.1140, wR2 = 0.2743	
Largest diff. peak and hole	0.356 and -0.354 e.$Å^{-3}$	

Table 6. **Crystal data and structure refinement for 3,6,11,14-tetramethoxydibenzochrysene**

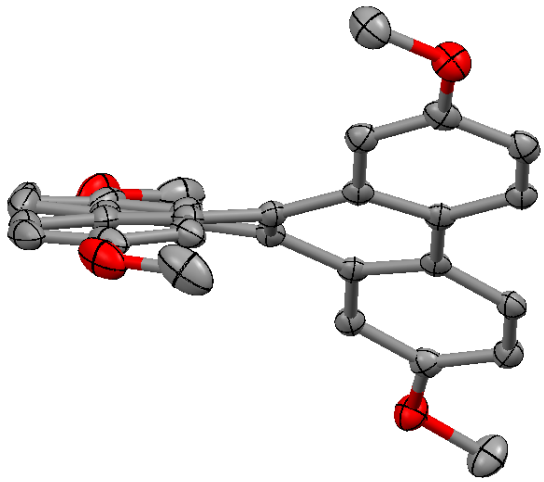

Identification code	raj17d	
Empirical formula	C30 H24 O4	
Formula weight	448.49	
Temperature	100(2) K	
Wavelength	1.54178 Å	
Crystal system	Monoclinic	
Space group	P 2/c	
Unit cell dimensions	a = 17.8332(5) Å	α= 90°.
	b = 15.2005(4) Å	β= 97.269(2)°.
	c = 24.3655(7) Å	γ = 90°.
Volume	6551.8(3) $Å^3$	
Z	12	
Density (calculated)	1.364 Mg/m^3	
Absorption coefficient	0.720 mm^{-1}	
F(000)	2832	
Crystal size	0.32 x 0.23 x 0.02 mm^3	
Theta range for data collection	2.50 to 67.60°.	
Index ranges	-21<=h<=21, 0<=k<=18, 0<=l<=28	
Reflections collected	51909	
Independent reflections	11574 [R(int) = 0.0426]	
Completeness to theta = 67.60°	98.6 %	
Absorption correction	Semi-empirical from equivalents	
Max. and min. transmission	0.9858 and 0.8024	
Refinement method	Full-matrix least-squares on F^2	
Data / restraints / parameters	11574 / 0 / 932	
Goodness-of-fit on F^2	0.999	
Final R indices [I>2sigma(I)]	R1 = 0.0462, wR2 = 0.1130	
R indices (all data)	R1 = 0.0718, wR2 = 0.1290	
Extinction coefficient	0.00012(2)	
Largest diff. peak and hole	0.230 and -0.250 $e.Å^{-3}$	

CHAPTER 1B

A Practical Synthesis of 1,4,5,8-Tetramethoxyanthracene from Cheap and Readily Available 1,8-Dihydroxyanthraquinone And X-Ray Crystal Characterization of its Dimer Cation Radical

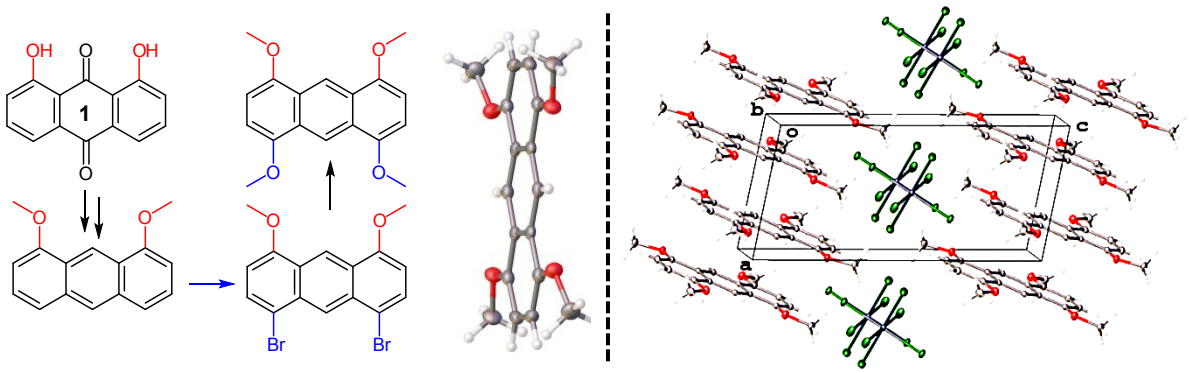

Abstract: The preparation of gram quantities of 1,4,5,8-tetramethoxyanthracene (**6**) from commercially available and cheap 1,8-dihydroxyanthraquinone is described. The key steps in the synthesis of **6** involve bromination of 1,8-dimethoxy-anthracene (**4**) to form 1,8-dibromo-4,5-dimethoxyanthracene (**5**) followed by Cu(I) catalyzed replacement of bromo substituents with methoxy groups. The contrasting reports concerning the preparation of 4 from 1,8-dimethoxyanthraquinone (**2**) using Zn dust in refluxing acetic acid are also discussed.

The Isolation and X-ray crystal structure determination of 1,4,5,8-Tetramethoxyanthracene dimer cation radical in addition to DFT calculations allowed us to delineate that the single hole is uniformly distributed over two 1,4,5,8-Tetramethoxyanthracene moieties.

INTRODUCTION

Our continued interest in the design and synthesis of polycyclic aromatic hydrocarbons (such as substituted benzenes, naphthalenes, anthracenes, pyrenes, poly-*p*-phenylenes, polyfluorenes, hexa-*peri*-hexabenzocoronenes, etc.),[1] which form stable cation radicals (or hole carriers) prompted us to examine the redox characteristics of the well-known 1,4,5,8-tetramethoxyanthracene (**6**).[2] Unfortunately, the existing syntheses of tetramethoxyanthracene **6** proved to be rather tedious and difficult despite the fact that it has been extensively utilized for the preparation of novel belt-like iptycenes,[3] iptycene-quinones,[4] triptycenes,[5] and liquid crystalline materials.[6]

All of the existing synthetic strategies for the preparation of **6** are not amenable to access large quantities of **6** because they involve expensive starting materials/reagents and suffer from low yields. For example, the first synthesis of **6** was carried out using diaminoanthrarufin in 6 steps in rather poor yield.[7] The tediousness and irreproducibility of this route[7] led Miller and coworkers[8] to devise an alternative strategy which involved a cycloaddition reaction of 1,4-dimethoxybenzocyclobutanol with benzoquinone. Unfortunately, the Miller synthesis[8] is accomplished in 9 steps and a number of these steps require chromatographic separations and are rather low yielding. A one-step synthesis of **6** is known,[9] unfortunately, however, this synthesis uses a strong base, generated from 2,2,6,6-tetramethylpiperdine and methyllithum and requires careful chromatography to produce relatively low-yield (~15-25 %) of **6**.

Herein, we report a facile preparation of 1,4,5,8-tetramethoxyanthracene (**6**) in gram-scale from cheap and commercially-available 1,8-dihydroxyanthraquinone (**1**) and

cheap reagents (e.g. zinc dust, NBS, and CuBr) in four high-yielding steps without the need for chromatographic separations (i.e. Scheme 1).

RESULTS and DISCUSSION

Scheme 1 Synthetic route for the preparation of multi-gram quantities of **6**.

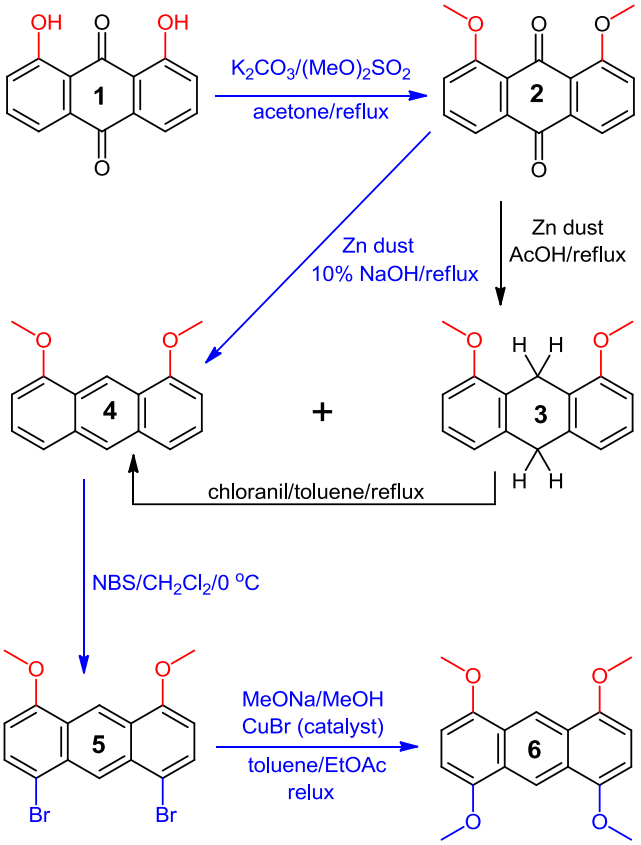

A methylation of dihydroxyanthraquinone **1** was performed in refluxing acetone using anhydrous potassium carbonate as a base and dimethylsulphate as the methylating reagent for 24 h. The isolation of **2** in a large-scale (i.e. 50-100 mmol scale) synthesis was significantly improved by avoiding an aqueous workup (see Experimental Section).

The next step in our synthesis required a reduction of quinone **2** to anthracene **4**. A search of the literature revealed the existence of contrasting reports[10,11] for a direct transformation of **2** to **4**. For example, Müller and coworkers[10] reported that a reduction of **2** with a large excess of zinc dust in refluxing acetic acid produces dihydroanthracene **3**. However, a recent report by Chen and coworkers[11] claimed that a reduction of **2**, under same conditi-ons as Müller's do not produce **3** but the corresponding dimethoxyanthracene **4**, i.e. Scheme 2.

Scheme 2 Contrasting reports concerning the preparation of **4**.

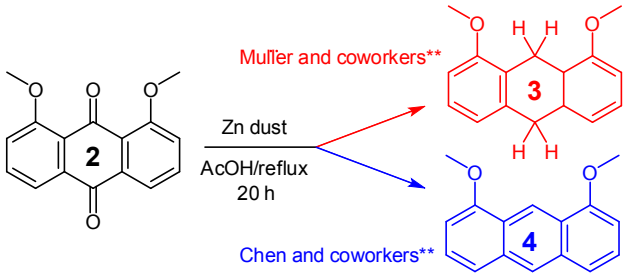

In order to find the cause of these conflicting reports, we carefully examined the reduction of **2** with Zn dust in acetic acid. For example, a mixture of **2** (10 mmol), Zn dust (15 equivalent, 150 mmol) and acetic acid (50 mL) was refluxed under an argon atmosphere. The 2-mL aliquots of the above reaction mixture were removed every 10 min and quenched with water (10 mL). The water layer was extracted with dichloro-methane (3 x 5 mL) and the CH_2Cl_2 layers were dried over anhydrous magnesium sulphate and evaporated in vacuo. The ^{1}H NMR analysis of these aliquots, collected during a course of ~3 h, showed that they contained a mixture of starting anthraquinone

2, dihydroantharacene **3** and only small amounts of anthracene **4**. A plot of the formation **3** and **4** and disappearance of starting anthraquinone **2** with time is shown in Figure 1.

Figure 1 A plot of consumption of anthraquinone **2** (blue square) and concomitant formation of dihydroanthracene **3** (red circles) and anthracene **4** (pink diamonds) in the presence of zinc dust in refluxing acetic acid during the course of 3 h.

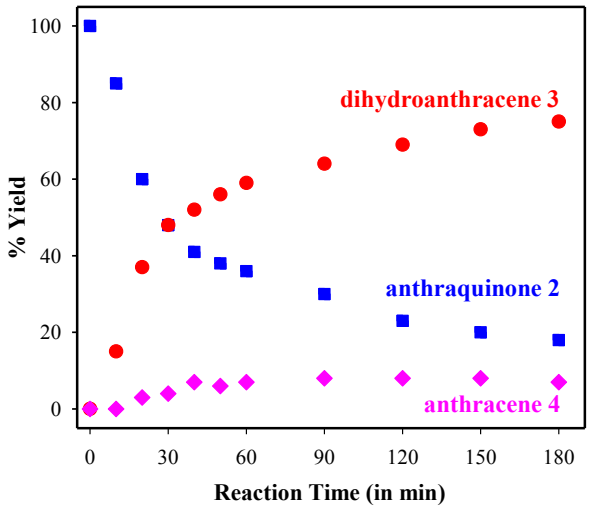

Figure 1 clearly demonstrates that anthracene **4** is a relatively minor product (<8%) while the major product (>92%) is dihydroanthracene **3** under these reaction conditions. It is also important to note that anthracene **4** does not undergo a reduction to dihydroanthr-acene **3** under these reaction conditions. For example, a purified sample of anthracene **4** (1 mmol) and zinc dust (15 mmol) in acetic acid (10 mL) was refluxed for 24 h without any change and **4** was recovered quantitatively after aqueous workup. Moreover, a timely reduction of **2** to a mixture of **3** and **4** (~9:1), in nearly quantitative yield, can be accomplished in ~8 h in refluxing acetic acid in the presence of ~15 equi-valent of Zn dust (see Experimental section).

A mixture of **3** and **4**, obtained above, can be cleanly converted to the corresponding anthracene **4** by a reaction with chloranil in refluxing toluene during a course of 2-3 h.[12] It is also noteworthy that anthracene **4** can be prepared directly form **2** by its reaction with zinc dust (6 equivalents) in 10% aqueous NaOH solution at reflux for 24 h in quantitative yield.[13]

Generally, the electrophilic aromatic substitution reactions of anthracene and various anthracene derivatives occur at highly reactive 9,10-positions. We, however, conjectured that electron donating methoxy groups at 1,8-positions may activate sufficiently the 4,5-positions in **4** to carry out a selective bromination at the desired sites using a mild brominating agent. Indeed, a bromination of **3** with 2 equivalents of NBS in dichloromethane at ~0 ^{o}C afforded the desired dibromoanthracene **5** in excellent yield. The pure dibromoanthracene **5** was easily obtained by a simple crystallization from a mixture of dichloromethane and methanol.

Interestingly, **5** can also be prepared from a 9:1 mixture of dihydroanthracene **3** and anthracene **4**, obtained above. For example, a bromination of a 9:1 mixture of **3** and **4** using NBS in dichloromethane afforded the crude dihydrodibromo derivative **7**, which was subjected, without further purification, to a dehydrogenation reaction with chloranil in refluxing toluene for 18 h. The resulting anthracene **5** was purified by crystallization from a mixture of dichloromethane and methanol to afford pure **5** in a 79% yield, i.e. Scheme 3.

Scheme 3 Alternative synthesis of dibromodimethoxyantharene **5**.

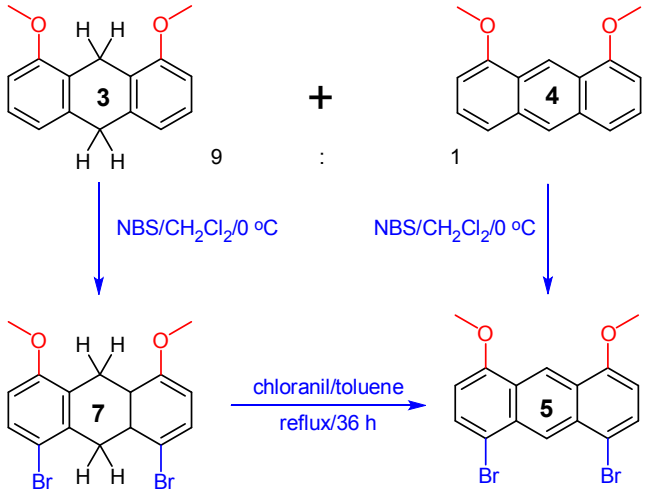

The availability of large quantities of dibromodimethoxyanthracene **5**, via 2 different routes (i.e. Schemes 1 and 3), allowed us to develop a simple procedure for the conversion of its bromo substituents into methoxy groups. After some experimentation, it was uncovered that refluxing of a mixture of **5** in toluene containing large excess of sodium methoxide, catalytic amounts of Cu(I)Br and ethyl acetate (5%) for 24 h afforded clean tetramethoxyanthracene **6** in excellent yield. The resulting crude tetramethoxy-anthracene **6** was sufficiently pure and, if needed, an analytical sample of **6** can be obtained by a simple recrystallization from a mixture of chloroform and toluene. The structure of **6** was established by $^{1}H/^{13}C$ NMR spectroscopy, mass spectrometry, and further confirmed by X-ray crystallography (Figure 2).

Figure 2 A. An ORTEP diagram of tetramethoxyanthracene **6** with the thermal ellipsoid at 50% probability. **B.** A packing diagram of **6** in its crystals.

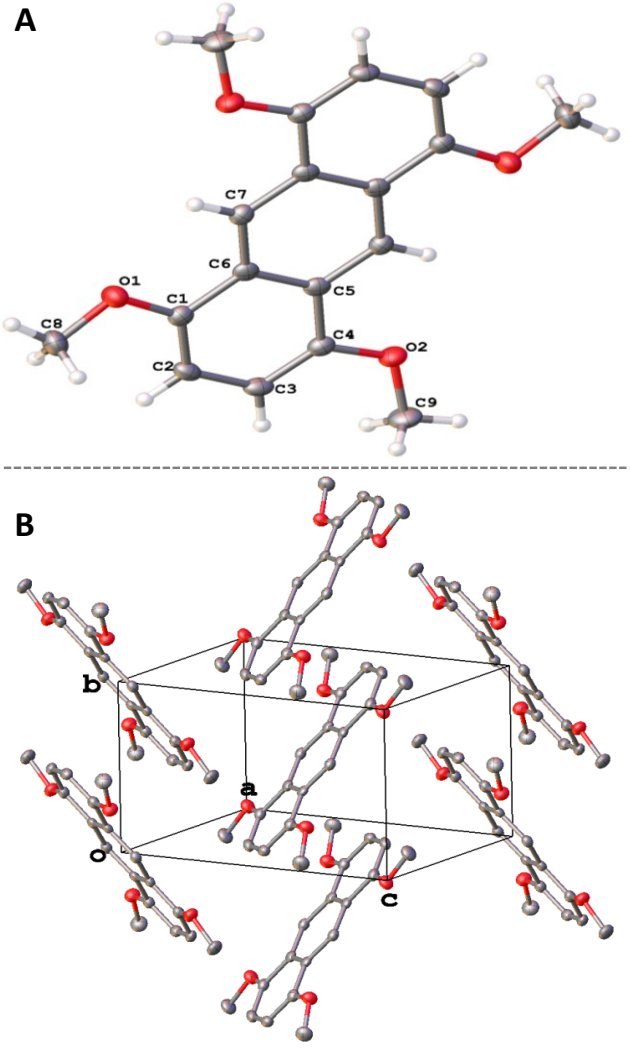

The anthracene **6** crystallizes in centrosymmetric space group and makes stacks along the y axis where parallel terminal rings of the neighboring molecules overlap with an interplanar separation of 3.46 Å. These stacks of **6** are arranged in a herringbone fashion in its crystal with numerous edge-to-face contacts between the molecules from the different stacks. The packing of **6** in crystals is governed by both π,π-stacking (i.e. within each stack of **6**) and by CH**…**O interactions between the adjacent stacks.[14]

In summary, we have demonstrated that commercially available 1,8-dihydroxyanthraquinone (**1**) can be successfully utilized for an efficient 4-step synthesis of 1,4,5,8-tetramethoxyanthracene (**6**) in excellent overall yield. The molecular structure of **6** was confirmed by X-ray crystallography. The ready-availability of **6** facilitated the evaluation of its redox properties and exploration for the usage in photovoltaic applications.

The Isolation and X-ray crystal structure determination of 1,4,5,8-Tetramethoxyanthracene dimer cation radical

Easy access of large quantities of 1,4,5,8-tetramethoxyanthracene in analytical pure form coupled with our continued interest in the design and synthesis of polycyclic aromatic hydrocarbons (PAHs) such as substituted naphthlenes, anthracenes, pyrenes, poly-*p*-phenylenes, hexa-*peri*-hexabenzocorornenes (HBCs) etc.,[15] which yield stable cation radicals or dimer cation radicals urged us to examine the possibility of isolation and X-ray crystal structure determination of 1,4,5,8-tetramethoxyanthracene, many of whose derivatives have been explored for contemporary materials.[16,17]

Herein, we now report that 1,4,5,8-tetramethoxyanthracene **6** can be quantitatively oxidized to its cation radical using a stable aromatic oxidant.[18] The cation radical of **6** was found to be stable at room temperature, numerous attempts to isolate the mono cation radical of **6** failed owing to the poor quality of the crystals. We then crystallized a dimer cation radical, $(\mathbf{6})_2^{+\bullet}$ using one equivalent $\mathbf{CRET}^{+\bullet}SbCl_6^-$ and two equivalents of **6**. Careful analysis of the dimer cation radical showed that the single hole is uniformly distribu-

ted between two molecules of **6**, furthermore the DFT calculations corroborated this results. The details of these preliminary findings are discussed herein.

The electron donor strength and initial cation radical stability of **6** were evaluated by its electrochemical oxidation at platinum electrode as a 2.5 x 10^{-3} M solution in dichloromethane containing 0.1 M *n*-Bu_4NPF_6 as a supporting electrolyte. The cyclic voltammogrames of **6** showed two reversible oxidation waves which consistently met the reversibility criteria at various scan rates ranging from 100-1000 mV/s (Fig. 3 A and 3 B), as they all showed cathodic/anodic pear current ratios of $i_a/i_c = 1.0$ (theoretical) as well as the differences between anodic and cathodic peak potentials E_{pa}-$E_{pc} = 70$ mV at 22°C. The reversible oxidation potentials of **6** were calibrated with ferrocene as an internal standard ($E_{ox} = 0.45$ V vs SCE) and were found to be 0.78 and 1.25 V vs. SCE corresponding to the formation of monocation and dication, respectively.

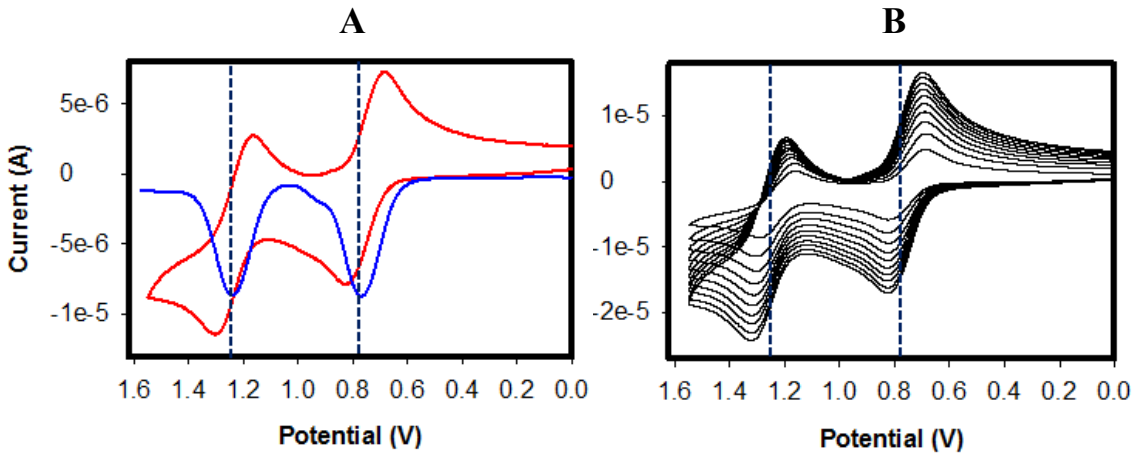

Figure 3. (**A**) Cyclic voltammograms (red trace) at a scan rate of 200 mV/s and square wave (blue trace) of 2.5 x 10^{-3} M **6** in CH_2Cl_2 containing 0.1 M *n*-Bu_4NPF_6 and (**B**) cyclic voltammograms of **6** at scan rates of 100-1000 mV/s at 22 °C.

The electrochemical reversibility of **6** and its relatively low oxidation potential permits its ready oxidation to the corresponding cation radical using either a hydroquinone ether cation radical (**CRET**$^{+\bullet}$ $SbCl_6^-$; E_{red} = 1.11 V vs. SCE)[18] as an oxidant.

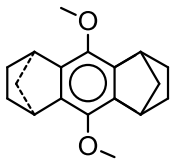

CRET$^{+\bullet}$

E^{o}_{red} 1.11 (V *vs.* SCE)

Thus, Fig. 4 A shows the spectral changes attendant upon the reduction of orange-colored **CRET**$^{+\bullet}$ (λ_{max} = 518 nm, ε_{518} = 7300 M^{-1} cm^{-1}) by incremental additions of sub-stoichiometric amounts of **6** in dichloromethane at 22 °C, i.e. eq 1. The presence of two isosbestic points at λ = 444 and 541 nm (see Figure 4A) indicates a simple unclu-ttered electron transfer from **6** to **CRET**$^{+\bullet}$ without decomposition of **6**$^{+\bullet}$. Further-more, a plot of formation of **6**$^{+\bullet}$ (i.e. an increase in the absorbance at 1414 nm against the increm-ents of added **6**, Fig. 4B) established that **CRET**$^{+\bullet}$ was completely consumed after the addition of 1 equivalent of **6**; and the resulting highly structured absorption spectrum of the **6**$^{+\bullet}$ [with intense absorption bands at λ_{max} = 1414 (ε_{890} = 28900 M^{-1} cm^{-1}), 310, and 392 and relatively weak bands at λ_{max} = 562, 613, 678, and 1182 nm (ε_{613} = 2610 M^{-1} cm^{-1})]. Further addition of neutral **6** to above solution of **6**$^{+\bullet}$ (blue trace) resulted in minute increase in the bands at 562, 613, 678, 1182, and 1414 nm, while the band centered at 392 nm grew considerably (pink trace), Fig. 5.

$$\mathbf{6} + \mathbf{CRET}^{+\cdot} \longrightarrow \mathbf{6}^{+\cdot} + \mathbf{CRET} \quad (1)$$

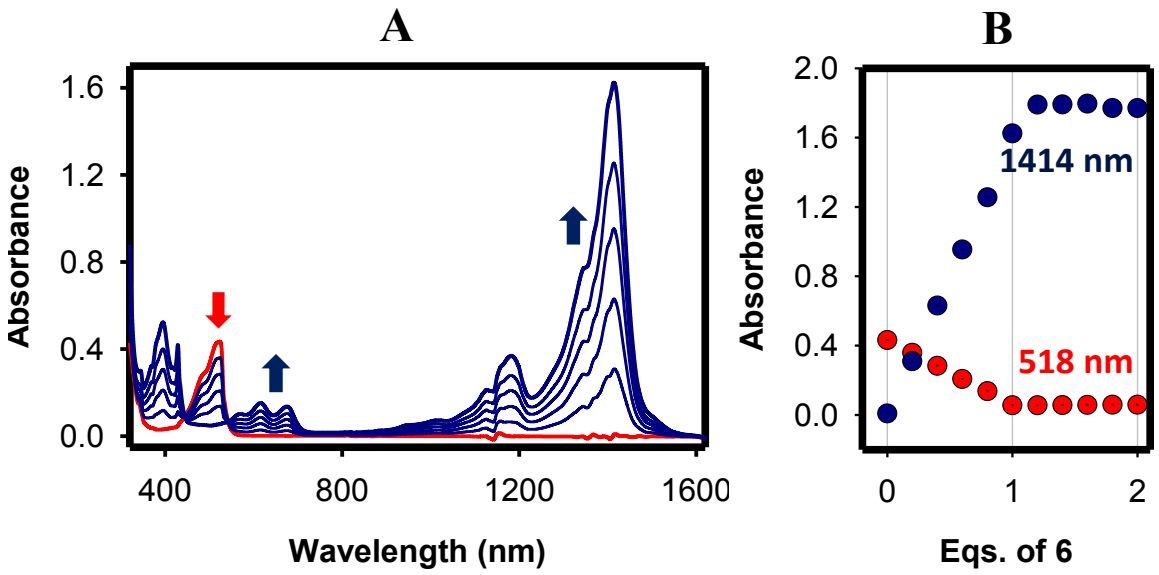

Figure 4. (**A**) The spectral changes observed upon the reduction of 5.48 x 10^{-5} M **CRET**$^{+\bullet}$ by an incremental addition of substoichiometric amounts of **6** in CH_2Cl_2 at 22 ^{o}C. (**B**) A plot of depletion of absorbance of **CRET**$^{+\bullet}$ (red circles, at 518 nm) and an increase of the absorbance of **6**$^{+\bullet}$ (blue circles, at 1414 nm) against the equivalents of added neutral **6**.

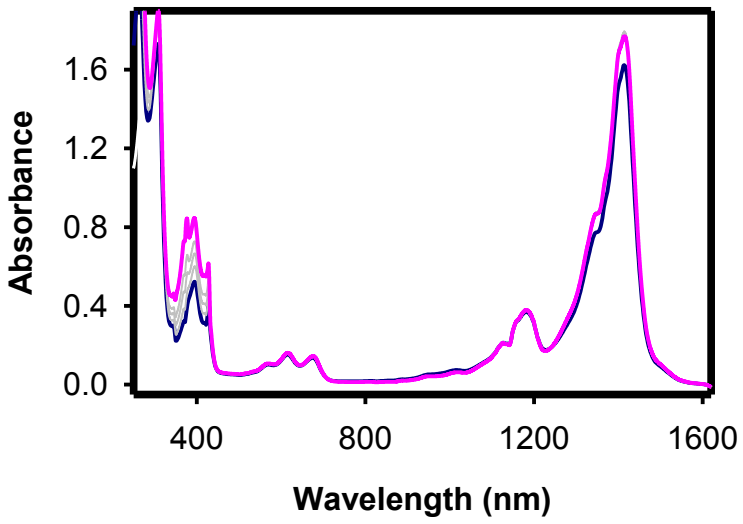

Figure 5. The spectral changes observed upon incremental addition of neutral **6** to 5.48 x 10^{-5} M **6**$^{+\bullet}$ (blue trace) in CH_2Cl_2 at 22 ^{o}C.

It is further noted that the intensely colored solution of $\mathbf{6}^{+\bullet}$, obtained according to eq. 1 using $\mathbf{CRET}^{+\bullet}$, was stable at ambient temperature and did not show any decomposition during a 48 h period at 22 ^{o}C, as confirmed by UV-vis spectroscopy. Moreover, a reduction of $\mathbf{6}^{+\bullet}$ with zinc dust regenerated the neutral **6** quantitaitively as confirmed by ^{1}H NMR spectroscopy.

The high stability of $\mathbf{6}^{+\bullet}$ $SbCl_6^-$ in solution prompted us to attempt the isolation of its crystalline salt. The treatment of one equivalent of **6** with equimolar $\mathbf{CRET}^{+\bullet}$ $SbCl_6^-$ at room temparature resulted in a dark blue colored solution of $\mathbf{6}^{+\bullet}$ $SbCl_6^-$. This dark blue solution was layered with hexanes or toluene in separate Schlenk tubes and allowed to crystallize at -10^{o}C for 24 hours, unfortunately very weakly diffracting, tiny dark blue/black crystals of $\mathbf{6}^{+\bullet}$ $SbCl_6^-$ were isolated and were found to be unsuitable for precise X-ray crystallographic analysis. Repeated attempts to crystallize $\mathbf{6}^{+\bullet}$ $SbCl_6^-$ using different oxidant such as NO^+ $SbCl_6^-$ and NO^+ PF_6^- did not provide any good quality crystals. Interestingly, the treatment of one equivalent of **6** with half equivalent of $\mathbf{CRET}^{+\bullet}$ $SbCl_6^-$ at room temperature resulted in a blue colored solution, which was layered with hexane and allowed to crystallize at -10^{o}C for 24 hours to obtain a good quality, blue crystals. X-ray crystallography established the 2:1 stoichiometry for **6** and $SbCl_6$ anion, that is a dimer cation radical $\mathbf{6_2}^{+\bullet}$ $SbCl_6^-$. The dimer cation radicals form more-or-less regular stacks along x axis with two symmetrically non-equivalent interplanar separations of 3.346 and 3.380 Å.

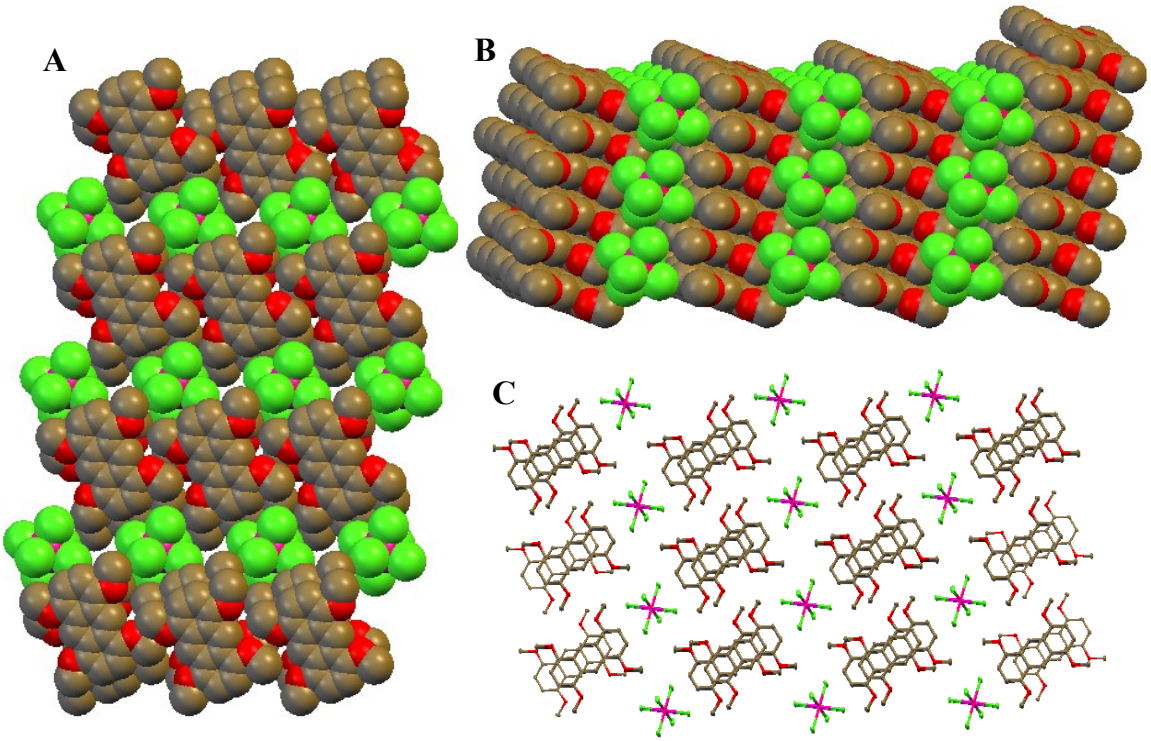

Fig. 6. (**A**) The packing diagram of $\mathbf{6}_2^{+\bullet}$ $SbCl_6^-$ showing 2:1 stoichiometry of **6** and $SbCl_6$ anion. (**B**) Space filling representation of the packing diagram of $\mathbf{6}_2^{+\bullet}$ $SbCl_6^-$ showing the alternate stacks of $\mathbf{6}_2^{+\bullet}$ and SbCl6$^-$. (**C**) The packing diagram (ellipsoid representation) of $\mathbf{6}_2^{+\bullet}$ SbCl6$^-$, showing the layered structure.

Availability of both neutral and dimer cation radical crystal structures of **6** allowed us to relate the bond length changes upon an electron removal. An inspection of bond length changes confirmed the shortening of bonds labeled **A**, **C**, and **F** bonds, and lengthening of bonds labeled **B** and **G**, while the bonds labeled as **D** and **E** showed insignificant alterations. As in various other aryl-methyl ether cation radicals,[19] O-C(ar) bonds (denoted as **F**) in $\mathbf{6}_2^{+\bullet}$ exhibit shortening by ~1.3 pm due to an increased p-π dative interaction. Greater shortening in bonds labeled as **A** and **C** in addition to extra lengthening in bonds labeled as **B** suggest quinoidal stabilization of a cationic charge.

Table 1. Experimental and theoretical bond lengths of the neutral and dimer cation radical of **6** presented in picometers (pm). Numbering scheme for the skeleton of **6** and its HOMO, obtained by DFT calculations at B3LYP/6-31G* level.

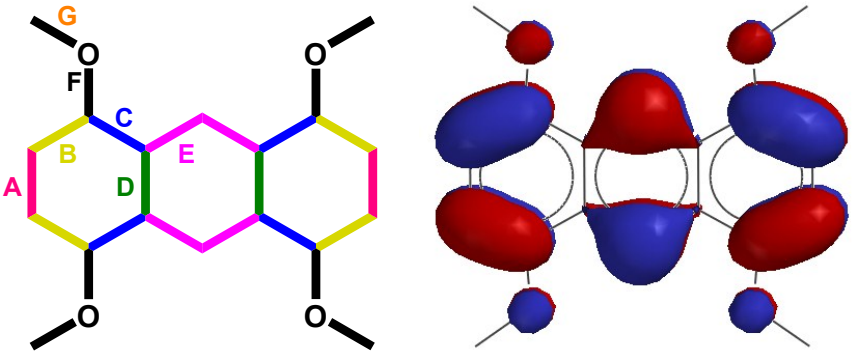

Bond Type	**B3LYP/6-31G***			**X-Ray Data**		
Bond[1]	**6**	$\mathbf{6_2^{+\bullet}}$	Δ	**6**	$\mathbf{6_2^{+\bullet}}$	$\Delta(\mathbf{6_2^{+\bullet}} - \mathbf{6})$
A	142.8	141.3	-1.5	142.3	141.2	-1.1
B	137.2	138.5	+1.3	135.8	138.1	+2.3
C	144.2	143.7	-0.5	143.7	143.5	-0.2
D	143.9	143.9	0.0	142.4	143.6	+1.2
E	140.2	140.1	-0.1	139.4	140.0	+0.6
F	136.7	135.5	-1.2	137.5	136.2	-1.3
G	142.2	142.8	+0.6	142.1	143.2	+1.1
σ	--	--	--	0.2	0.2	--

[1]Average of equivalent bonds.

To corroborate this observations, we performed DFT calculations on $\mathbf{6}^{+\bullet}$ (see Table 2) and $\mathbf{6_2}^{+\bullet}$ (see Table 1) at B3LYP/6-31G* level. Comparison of the bond length changes, obtained by DFT calculations, in $\mathbf{6}^{+\bullet}$ (mono cation radical) and $\mathbf{6_2}^{+\bullet}$ (dimer cation radical) suggest the same trend in the lengthening (bonds labeled as **B** and **G**) and shortening (bonds labeled as **A**, **F** and **C**) of bonds. It is noteworthy that the bond length changes in $\mathbf{6_2}^{+\bullet}$ are roughly half that of $\mathbf{6}^{+\bullet}$, which is understandable as in $\mathbf{6}^{+\bullet}$ a single hole is delocalized on a single molecules of **6** while in $\mathbf{6_2}^{+\bullet}$ a single hole is delocalized between two molecules of **6**. Bond length changes observed (i.e. by X-ray crystallography) in **6** and $\mathbf{6_2}^{+\bullet}$ were found to be in accordance with the bond length changes predicted by DFT calculations, see Table 1.

Table 2. Theoretical bond lengths of the neutral and cation radical of **6** presented in picometers (pm). Numbering scheme for the skeleton of **6** is same as described in Table 1.

Bond Type	**B3LYP/6-31G***		
Bond[1]	**6**	$\mathbf{6}^{+\bullet}$	$\Delta(\mathbf{6}^{+\bullet}\mathbf{-6})$
A	142.8	139.9	-2.9
B	137.2	139.7	+2.5
C	144.2	143.3	-0.9
D	143.9	143.8	-0.1
E	140.2	140.1	-0.1
F	136.7	134.2	-2.5

G	142.2	143.4	+1.2

SUMMARY and CONCLUSIONS

In summary, 1,4,5,8-tetramethoxyanthracene (**6**) is easily accessed from readily available starting materials and it undergoes reversible electrochemical oxidation and forms a highly robust cation-radical salt. The X-ray crystal structure determination of $\mathbf{6_2}^{+\bullet}$ $SbCl_6^-$ as well as neutral **6** together with DFT calculations provides unequivocal evidence that a single hole is completely delocalized onto two 1,4,5,8-tetramethoxyanthracene molecules. We also observed that an introduction of a cationic charge (or polaron) in polycyclicaromatic hydrocarbon **6** leads to a complex elongation and shortening of the various bonds.

EXPERIMENTAL

Melting points are uncorrected. IR spectra were recorded using KBr disks on a Nicolet 560 Magna infrared spectrometer. NMR spectra were obtained on a Varian NMR spectrometer (300 MHz) as $CDCl_3$ solutions using TMS as an internal standard reference. GC-MS spectra were obtained on a Fisons 8000 Trio instrument at an ionization potential of 70 eV. TLC experiments were carried out on pre-coated silica gel plates (hexanes–

EtOAc, 4:1). Solvents and reagents such as dimethyl sulphate, *N*-bromosuccinimide (NBS), tetrachloro-*p*-benzoquinone (chloranil), zinc dust, and sodium metal were purchased from commercial sources.

Anhydrous tetrahydrofuran (THF) was prepared by refluxing commercial THF over lithium aluminum hydride under an argon atmosphere for 24 hours followed by distillation under an argon atmosphere. It was stored in a Schlenk flask equipped with a Teflon valve fitted with Viton O-rings. Dichloromethane was repeatedly stirred with fresh aliquots of conc. sulfuric acid (~10 % by volume) until the acid layer remained colorless. After separation, it was washed successively with water, aqueous sodium bicarbonate, water, and aqueous sodium chloride, and dried over anhydrous calcium chloride. The dichloromethane was distilled twice from P_2O_5 under an argon atmosphere and stored in a Schlenk flask equipped with a Teflon valve fitted with Viton O-rings. The hexanes and toluene were distilled from P_2O_5 under an argon atmosphere and then refluxed over calcium hydride (~12 hr). After distillation from CaH_2, the solvents were stored in Schlenk flasks under an argon atmosphere. NMR spectra were recorded on 300 and 400 MHz NMR spectrometers.

Cyclic Voltammetry (CV). The CV cell was of an air-tight design with high vacuum Teflon valves and Viton O-ring seals to allow an inert atmosphere to be maintained without contamination by grease. The working electrode consisted of an adjustable platinum disk embedded in a glass seal to allow periodic polishing (with a fine emery cloth) without changing the surface area (~1 mm^2) significantly. The reference SCE electrode (saturated calomel electrode) and its salt bridge were separated from the catholyte by a sintered glass frit. The counter electrode consisted of platinum gauze that

was separated from the working electrode by ~3 mm. The CV measurements were carried out in a solution of 0.1 to 0.2 M supporting electrolyte (tetra-*n*-butylammonium hexafluorophosphate, TBAH) and the substrate in dry dichloromethane under an argon atmosphere. All the cyclic voltammograms were recorded at a sweep rate of 200 mV sec^{-1}, unless otherwise specified and were IR compensated. The oxidation potentials ($E_{1/2}$) were referenced to SCE, which was calibrated with added (equimolar) ferrocene ($E_{1/2}$ = 0.450 V *vs*. SCE). The $E_{1/2}$ values were calculated by taking the average of anodic and cathodic peak potentials in reversible cyclic voltammograms or directly from square-wave voltammograms in irreversible cyclic voltammograms.

Synthesis of 1,8-dimethoxy-9,10-anthraquinone (2)

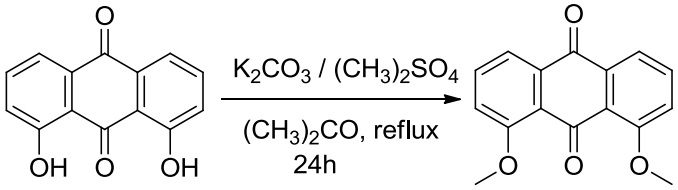

A suspension of 1,8-dihydroxy-9,10-anthraquinone (15.5 g, 65 mmol) and K_2CO_3 (22.0 g, 162 mmol) in anhydrous acetone (400 mL) under an argon atmosphere was gently refluxed . A solution of dimethyl sulfate (20.5 g, 162 mmol) in acetone (~50 mL) was added dropwise over 30 minutes with the help of a dropping funnel and the resulting mixture was refluxed for an additional 24 hours. After cooling to room temperature, the reaction mixture was filtered and the dark colored K_2CO_3 solid residue was washed with dichloromethane (3 x 150 mL). The combined organic solvent was then passed through a short pad of silica gel and the pad was washed with dichloromethane (3 x 80 mL). The collected organic filtrate was then evaporated under reduced pressure to afford **1,8-**

dimethoxy-9,10-anthraquinone (2) as an yellow solid in excellent yield. (15.6 g, 90 %).

Note 1. An aqueous work-up should be avoided as it complicates the isolation of **2** because of formation of emulsion. Yield: 15.6 g, 90%; m p 222-224 ^{o}C (lit[11] 223-224 ^{o}C). IR (KBr): 1664, 1587, 1434, 1318, 1239, 1061, 977, 743 cm^{-1}; ^{l}H NMR ($CDCl_3$): δ = 4.01 (s, 6H), 7.30 (dd, 2H, *J* = 8.4 Hz, 1.0 Hz), 7.61-7.66 (t, 2H, *J* = 8.0 Hz), 7.83 (dd, 2H, *J* = 7.7 Hz, 1.0 Hz). ^{13}C NMR ($CDCl_3$): δ = 56.60, 118.12, 118.95, 124.05, 133.98, 134.79, 159.49, 182.98, 184.09; MS (70 eV): m/z = 268 [M^+], 253 [M^+- CH_3], 236, 225, 209, 180, 164, 152, 139, 76.

Synthesis of 1,8-dimethoxyanthracene (4)

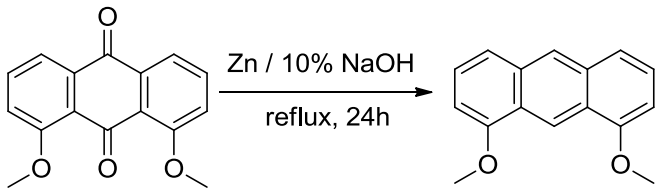

To a suspension of **2** (8.0 g, 30 mmol) in 10% aqueous NaOH solution (150 mL) was added zinc powder (11.8 g, 180 mmol). The mixture was heated for 24 h with vigorous stirring and then the reaction mixture was vacuum filtered. The insoluble filtered cake was washed with water (3 x 100 mL) and dried under vacuum. The resulting pale yellow solid was dissolved in dichloromethane (100 mL) and the solution was passed through a short pad of silica gel. The filtrate was evaporated in vacuo to afford **4** as the pale yellow solid. Yield: 7.0 g, 88%; m p 198-200 ^{o}C (lit[11]198-200^{o}C); IR (KBr): 1625, 1567, 1464, 1440, 1321, 1265, 1126, 1058, 1070, 789, 737 cm^{-1}; ^{l}H NMR ($CDCl_3$): δ = 4.08 (s, 6H), 6.73 (d, 2H, *J* = 7.3 Hz), 7.37 (t, 2H, *J* = 8.0 Hz), 7.56 (d, 2H, *J* = 8.6 Hz), 8.30 (s, 1H), 9.23 (s,1H); ^{13}C NMR ($CDCl_3$): δ = 55.68, 101.72, 115.86, 120.37, 124.61, 125.32, 125.82, 133.06, 156.09.

Synthesis of 1,8-dibromo-4,5-dimethoxyanthracene (5)

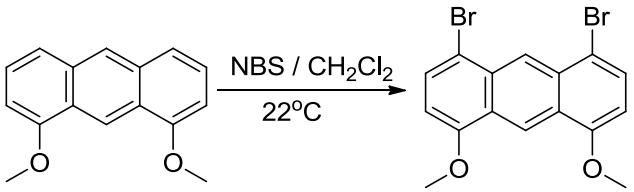

To a pre-chilled solution of **4** (4.0 g, 16.8 mmol) in CH_2Cl_2 (200 mL) in an ice-salt bath (~0 ^oC) was added *N*-bromosuccinimide (5.98 g, 33.6 mmol) in small portions over a 15 min period. After addition, the temperature was slowly allowed to rise to room temperature and the mixture was stirred for an additional 3 h. The resulting reaction mixture was diluted with CH_2Cl_2 (150 mL) and washed with 5% HCl (50 mL) followed by water (3 x 150 mL). The organic layer was separated, dried over anhydrous $MgSO_4$ and evaporated under reduced pressure to afford **5** as pale green solid. Yield: 6.1 g, 92%; m p 272-274 ^oC; IR (KBr): 1613, 1461, 1386, 1318, 1263, 1221, 1148, 1091, 1073, 806, 610, 600 cm^{-1}; 1H NMR ($CDCl_3$): δ = 4.06 (s, 6H), 6.62 (d, 2H, *J* = 8.1 Hz), 7.72 (d, 2H, *J* = 8.1 Hz), 9.0 (s, 1H), 9.25 (s, 1H); ^{13}C NMR ($CDCl_3$): δ = 55.97, 102.97, 113.62, 117.77, 125.53, 125.89, 130.07, 131.54, 155.82; MS (70 eV): m/z = 396 [M+], 381 [M+-CH_3], 353, 338, 310, 198, 150, 75.

Synthesis of 1,4,5,8-tetramethoxyanthracene (6)

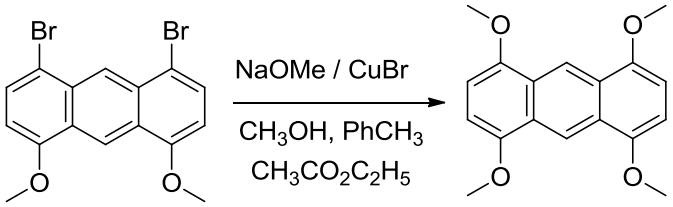

Freshly cut sodium metal (11.0 g, 500 mmol) was added portion wise to a 500-mL Schlenk flask containing dry methanol (100 mL) under an argon atmosphere at 22 ^oC and the resulting mixture was refluxed until the complete dissolution of the sodium metal. To

this solution was added 4,5-dibromo-1,8-dimethoxyanthracene (2.0 g, 5.0 mmol), toluene (100 mL), ethyl-acetate (5.0 mL), and copper(I) bromide (0.70 g, 5.0 mmol), successively. The reaction mixture was then refluxed with rapid stirring for 24 h. After which time, solvent was evaporated under reduced pressure and the residue was dissolved in CH_2Cl_2 (~300 mL) and washed with 10% HCl (100 mL) followed by water (2 x 100 mL). The organic layer was dried over anhydrous $MgSO_4$ and evaporated under reduced pressure to afford an yellow-green solid which was triturated with cold dichloromethane to afford 1,4,5,8-tetramethoxy-anthracene as yellow solid. Analytically pure sample can be obtained by crystallization using a 1: 1 mixture of chloroform/toluene.

Yield: 1.40 g, 93%; m p 296-298 ^oC (lit[9] 298-300 ^oC); IR (KBr): 1631, 1471, 1327, 1258, 1129, 1083, 806 cm^{-1}; ^1H NMR ($CDCl_3$): δ = 4.03 (s, 12H), 6.63 (s, 4H), 9.10 (s, 2H); ^{13}C NMR (CDCl3): δ = 55.83, 101.47, 115.37, 125.39,150.00; MS (70 eV): m/z = 298 [M^+], 283 [M^+-CH_3], 268 [M^+-$2CH_3$], 253 [M^+-$3CH_3$], 237, 225, 149, 134.

Synthesis of 1,8-dimethoxy-9,10-dihydroanthracene (3) contaminated with 4

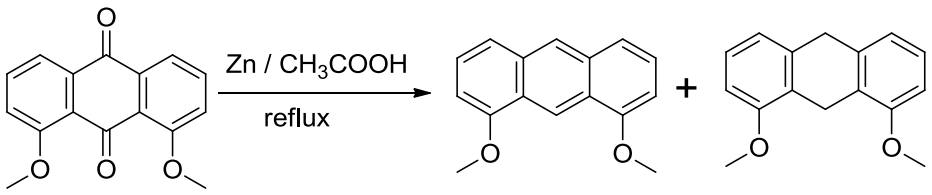

To a suspension of **2** (12.0 g, 45 mmol) in glacial acetic acid (200 mL) was added zinc dust (44.0 g, 675 mmol) in one portion. The reaction mixture was refluxed for 3-4 hours. After the reaction was complete, the mixture was cooled to room temperature and vacuum filtered to remove the zinc dust. The solid cake was washed with dichloromethane (5 x 80 mL), collected filtrate was washed with water (200 mL), sodium

bicarbonate (2 x 100 mL) and again with water (100 mL). The organic layer was dried over $MgSO_4$ and evaporated under reduced pressure to afford a mixture containing 1,8-dimethoxy-9,10-dihydroanthracene (**3**) and 1,8-dimethoxyanthracene (**4**) in ~9:1 ratio as the yellow solid. Yield: 10.0 g, 94% (**3** + **4**); ^{1}H NMR ($CDCl_3$): δ = 3.90 (s, 6H), 3.94 (t, 2H, *J* = 3.0 Hz), 4.03 (t, 2H, *J* = 3.0 Hz), 6.77 (d, 2H, *J* = 8.30 Hz), 6.90 (d, 2H, *J* = 7.5 Hz), 7.19 (t, 2H, *J* = 8.1 Hz); remaining small signals were easily assigned to **3**; ^{13}C NMR ($CDCl_3$): δ = 22.14, 35.27, 55.59, 107.63, 120.07, 124.29, 126.67, 137.05, 157.07; remaining small signals were easily assigned to **3**; MS (70 eV): m/z = 240 [M^+], 225 [M^+-CH_3], 209, 194, 178, 165, 152, 139, 112. **Note:** The dihydroanthracene **3**, contaminated with ~10% anthracene **4** was used for the next step without further separation/purification.

Synthesis of 4,5-dibromo-1,8-dimethoxy-9,10-dihydroanthracene (7)

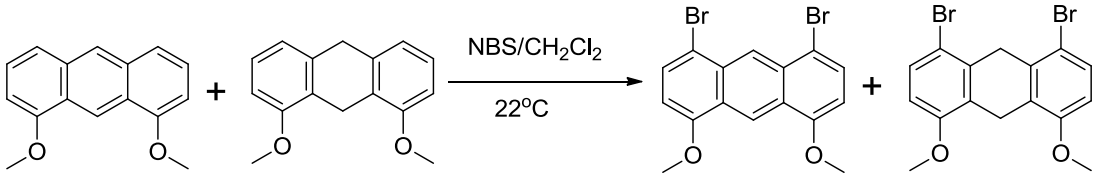

To a solution containing a 9:1 mixture of 1,8-dimethoxy-9,10-dihydroanthracene and 1,8-dimethoxy-anthracene (9.4 g, 39.0 mmol) in dry CH_2Cl_2 (200 mL) was added NBS (13.90 g, 78.0 mmol) in small portions over 15 minutes at 0 ^oC under argon atmosphere. After addition, the temperature was slowly allowed to rise to room temperature and the mixture was stirred for an additional 3 hours. Reaction mixture was then diluted with dichloromethane (200 mL) and washed with 5% HCl (100 mL) followed by water (3 x 150 mL). The organic layer was separated, dried over $MgSO_4$ and evaporated under reduced pressure to afford a mixture containing 4,5-dibromo-1,8-dimethoxy-9,10-

dihydroanthracene and 4,5-dibromo-1,8-dimethoxyanthracene in 9:1 ratio, as the greenish yellow colored solid (14.0 g, 90%). Yield: 14.0 g, 90% (**7** + **5**); ^{1}H NMR ($CDCl_3$): δ = 3.86 (s, 6H), 3.92 (t, 2H, *J* = 3.04 Hz), 4.05 (t, 2H, *J* = 3.04 Hz), 6.65 (d, 2H, *J* = 8.7 Hz), 7.43 (d, 2H, *J* = 8.7 Hz); remaining small signals were easily assigned to **5**; MS (70 eV): m/z = 398 [M^+], 383 [M^+-CH_3], 367, 302, 286, 238, 223, 195, 152, 119.

Note: The dihydroanthracene **7**, contaminated with ~10% anthracene **5** was used for the next step without further separation/purification.

Alternate synthesis of 4,5-dibromo-1,8-dimethoxy-anthracene (5)

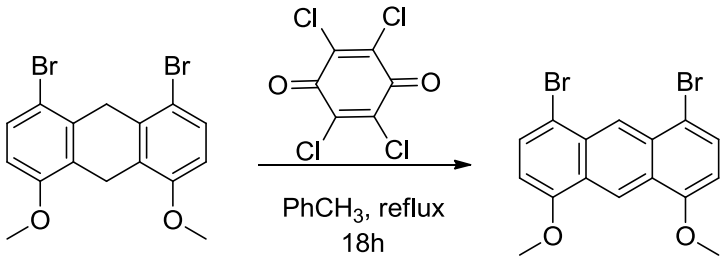

A mixture of 4,5-dibromo-1,8-dimethoxy-9,10-dihydroanthracene and 4,5-dibromo-1,8-dimethoxy-anthracene (9.0 g, 22.6 mmol) and p-chloranil (5.9 g, 24.0 mmol) in 200 mL toluene was refluxed for 18 hours under argon atmosphere. The solvent was evaporated to get a green colored residue which was diluted with dichloromethane (~400 mL) and washed with 10% NaOH (3 x 100 mL) followed by water (2 x 100 mL). The separated organic layer was dried over $MgSO_4$ and the solvent was removed under reduced pressure to afford green solid which was further purified by tituration with dichloromethane (7.1 g, 79 %) and was identical to the sample obtained above.

Alternate synthesis of 1,8-dimethoxyanthracene (4)

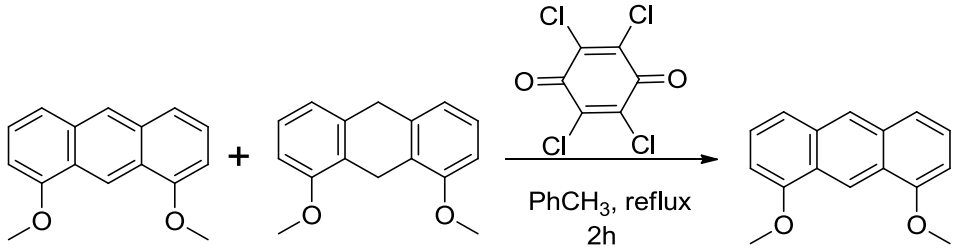

A 9:1 mixture of dihydroanthracene **3** and anthracene **4** (4.0 g, 16.6 mmol) and chloranil (4.1 g, 16.6 mmol) in toluene (100 mL) was refluxed for 2 h under an argon atmosphere. The solvent was evaporated under reduced pressure to afford an yellow-green colored residue which was diluted with dichloromethane (200 mL) and washed with 10% aqueous NaOH (3 x 100 mL) followed by water (2 x 100 mL). The organic layer was dried over anhydrous $MgSO_4$, filtered and the solvent was removed under reduced pressure to afford pure **4** light yellow solid (3.7 g, 93%). The sample of anthracene **4** obtained herein by dehydrogenation was identical to that obtained above by reduction of **2** by zinc dust in aqueous NaOH.

X-ray Crystal Structure Analysis of 6

All diffraction intensity data were collected with a Bruker Smart Apex CCD diffractometer at 173(2) K using Cu-radiation (1.54178 Å). All structures were solved using direct methods, completed by difference. Fourier syntheses, and refined by full matrix least squares procedures. Crystallographic data, details for data collections, and refinement methods for each structure are summarized below.

Yellow crystals of **6** were grown from a mixture of chloroform and toluene. A shiny crystal with dimensions (0.28 x 0.035 x 0.03 mm^3) was selected for data collection. Empirical formula $C_{18}H_{18}O_4$; Formula weight 298.32; Crystal system = monoclinic;

Space group *P21/n*; $Z = 2$; Unit cell dimensions $a = 10.9438(13)$ Å, $b = 5.9802(5)$ Å, $c = 11.6812(14)$ Å; $\alpha = 90^{o}$, $\beta = 110.272(14)^{o}$, $\gamma = 90^{o}$; $V = 717.14(13)$ Å^3; D (calculated) = 1.382 g cm^{-3}; $m = 0.097$ mm^{-1}. The total number of reflections measured was 4234, of which 1739 reflections were symmetrically nonequivalent. Final residuals were $R_1 = 0.0470$ and w$R_2 = 0.1034$ for 1452 reflections with $I > 2\sigma(I_0)$.

EXPERIMENTAL SPECTRA

^{1}H and ^{13}C NMR Spectra for Various Intermediates

^{1}H NMR spectra of **1,8-dimethoxy-9,10-anthraquinone (2)**

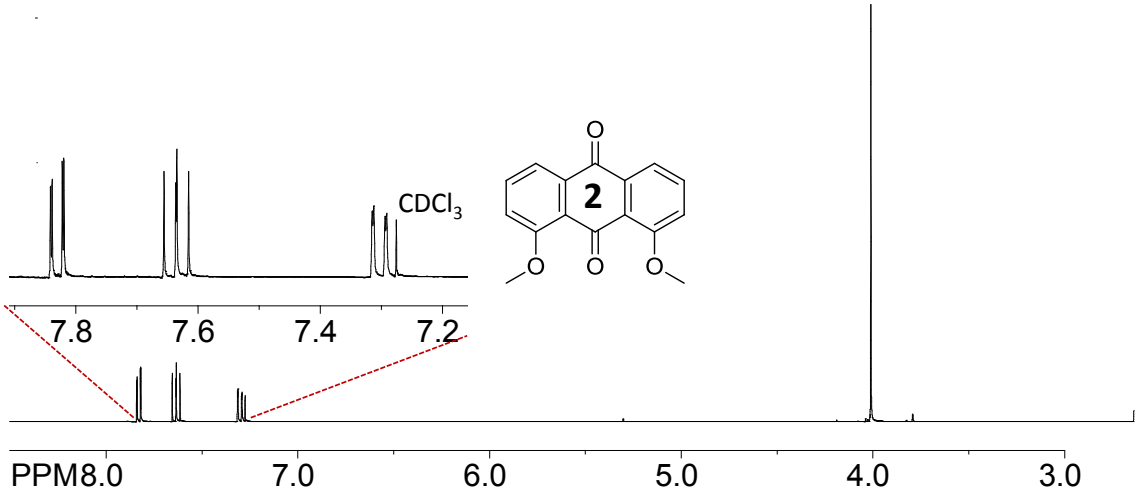

^{13}C NMR spectra of **1,8-dimethoxy-9,10-anthraquinone (2)**

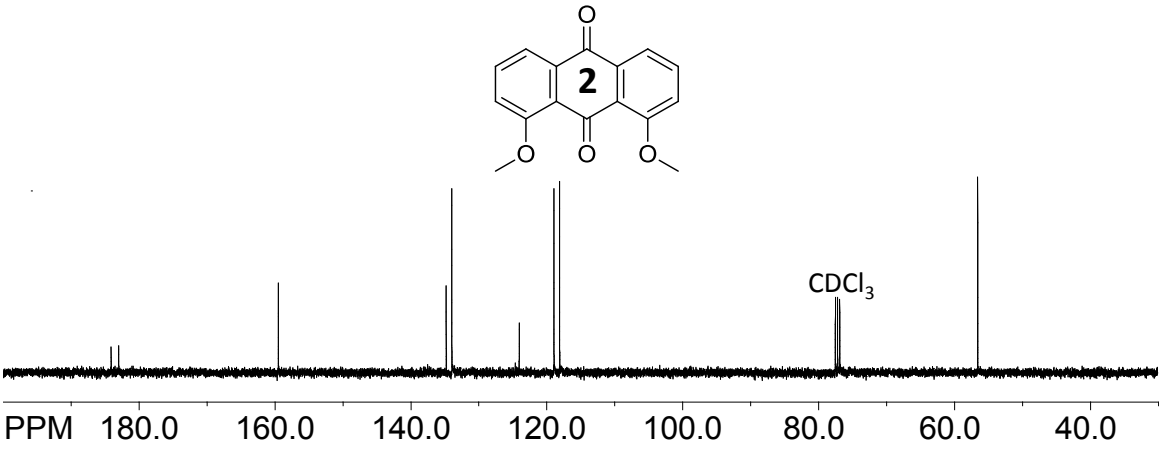

^{1}H NMR spectra of **1,8-dimethoxyanthracene (4)**

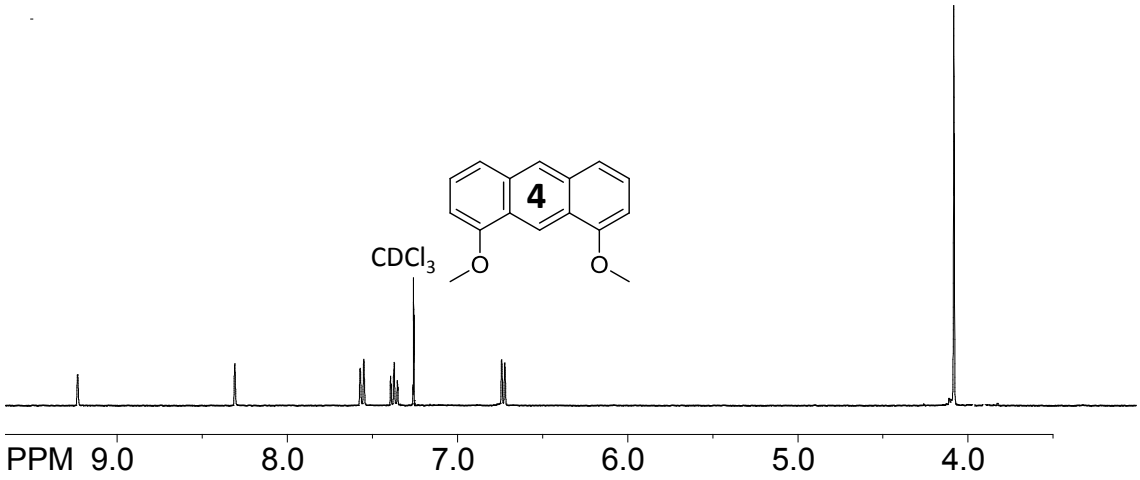

^{13}C NMR spectra of **1,8-dimethoxyanthracene (4)**

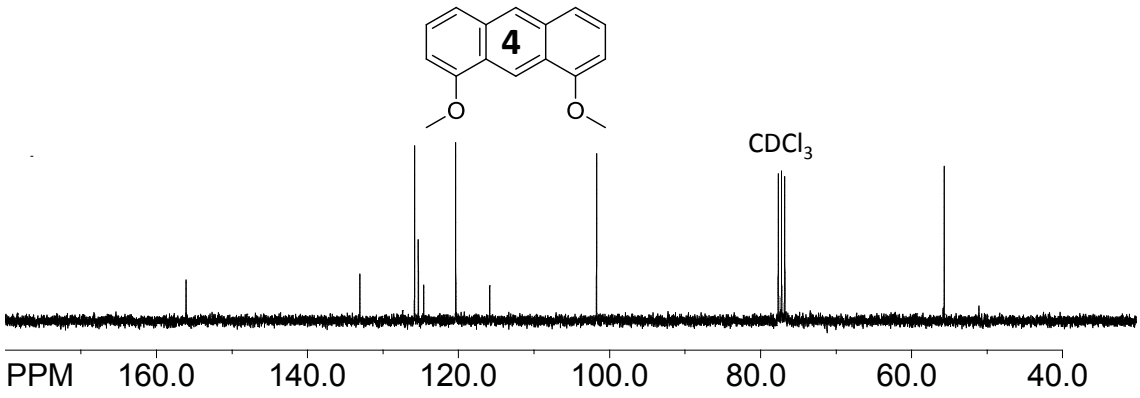

^{1}H NMR spectra of **4,5-dibromo-1,8-dimethoxyanthracene (5)**

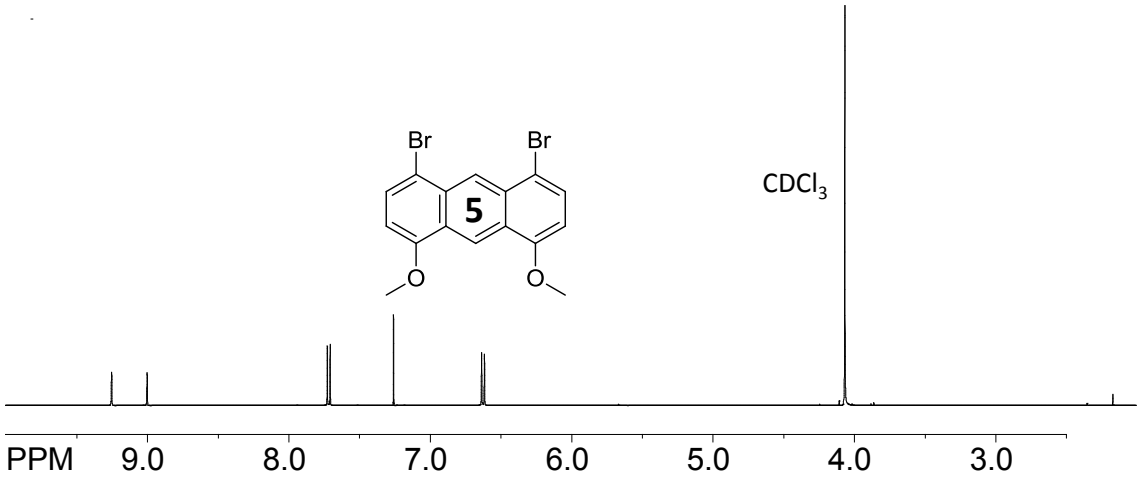

^{13}C NMR spectra of **4,5-dibromo-1,8-dimethoxyanthracene (5)**

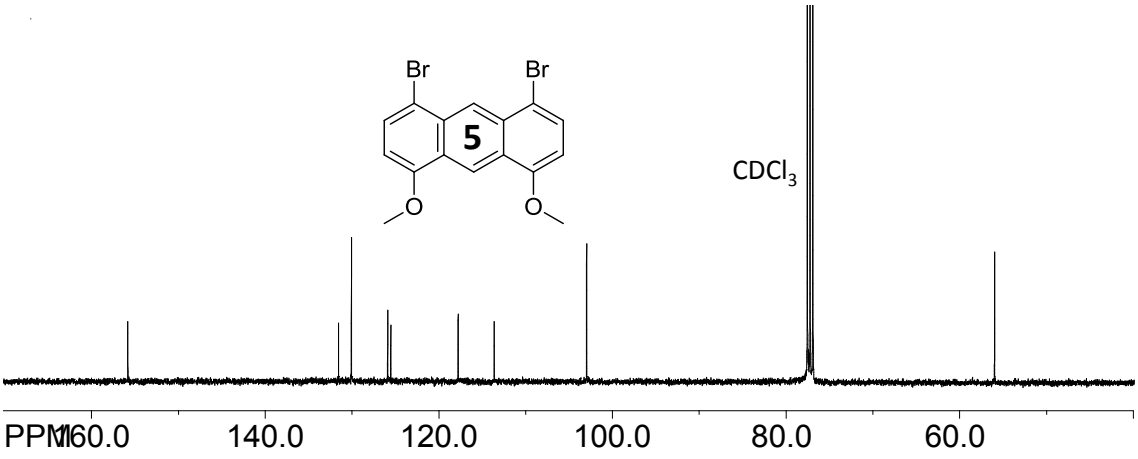

^{1}H NMR spectra of **1,4,5,8-tetramethoxyanthracene (6)**

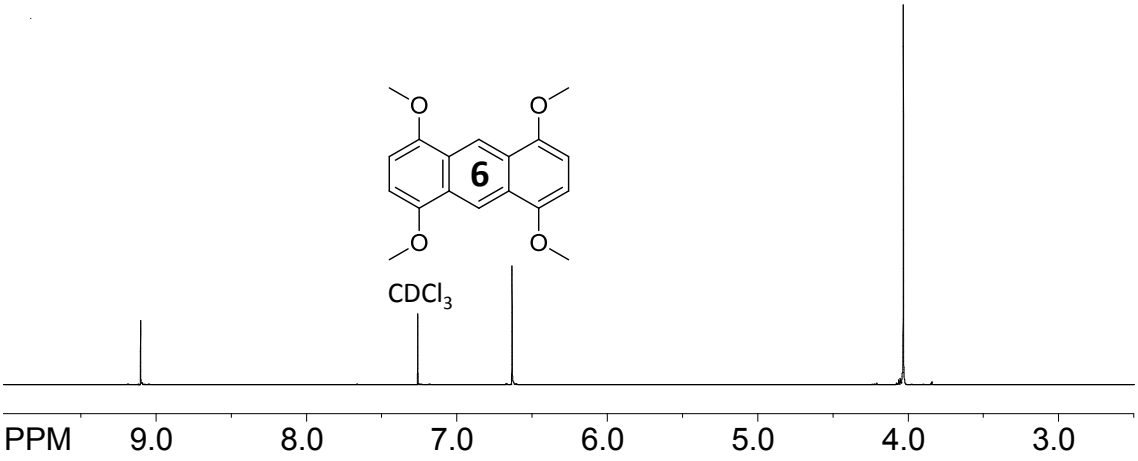

^{13}C NMR spectra of **1,4,5,8-tetramethoxyanthracene (6)**

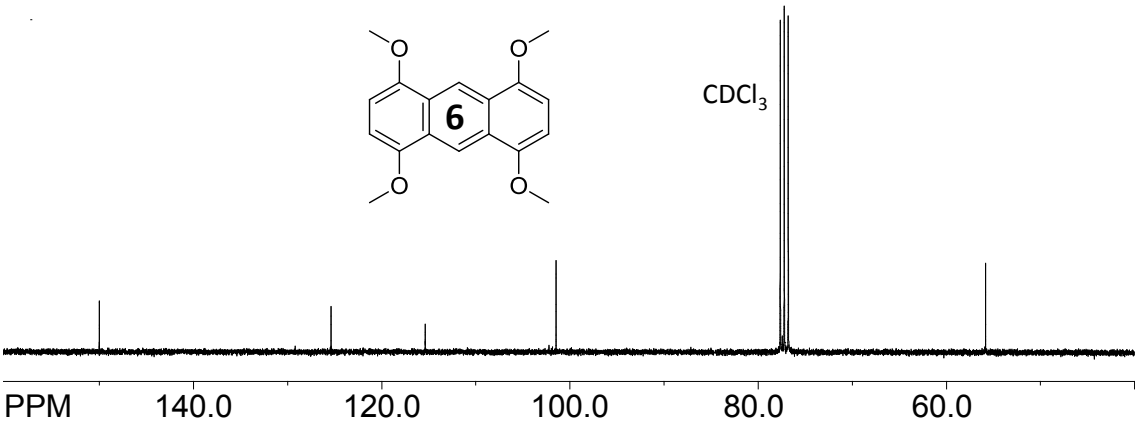

^{1}H NMR spectra of a mixture containing **1,8-dimethoxy-9,10-dihydroanthracene (3)** and **1,8-dimethoxyanthracene (4)**

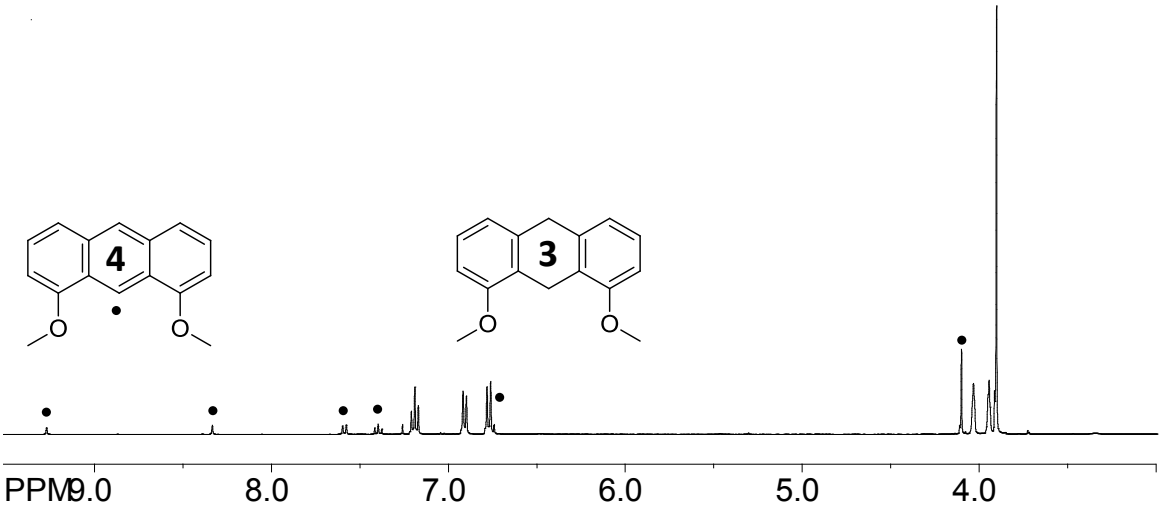

^{13}C NMR spectra of a mixture containing **1,8-dimethoxy-9,10-dihydroanthracene (3)** and **1,8-dimethoxyanthracene (4)**

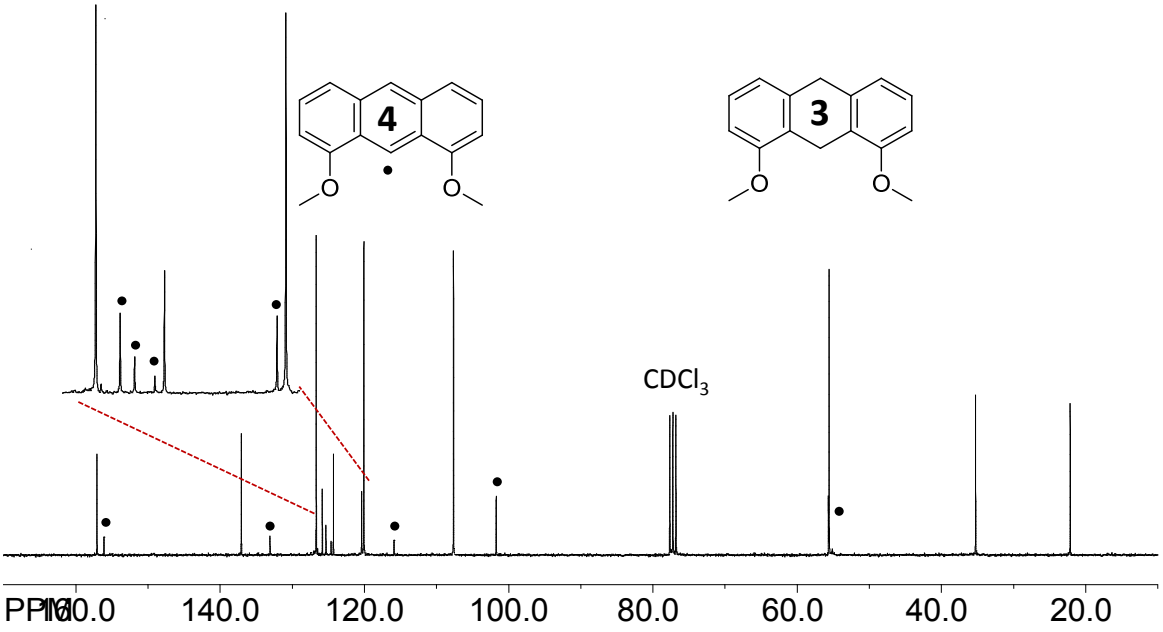

^{1}H NMR spectra of a mixture containing **4,5-dibromo-1,8-dimethoxy-9,10-dihydroanthracene (7)** and **4,5-dibromo-1,8-dimethoxyanthracene (5)**

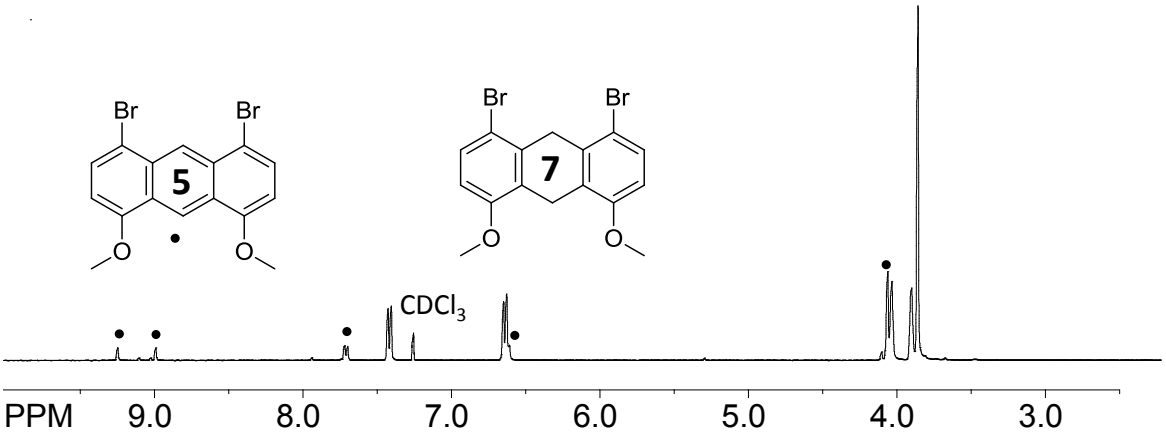

^{13}C NMR spectra of a mixture containing **4,5-dibromo-1,8-dimethoxy-9,10-dihydroanthracene (7)** and **4,5-dibromo-1,8-dimethoxyanthracene (5)**

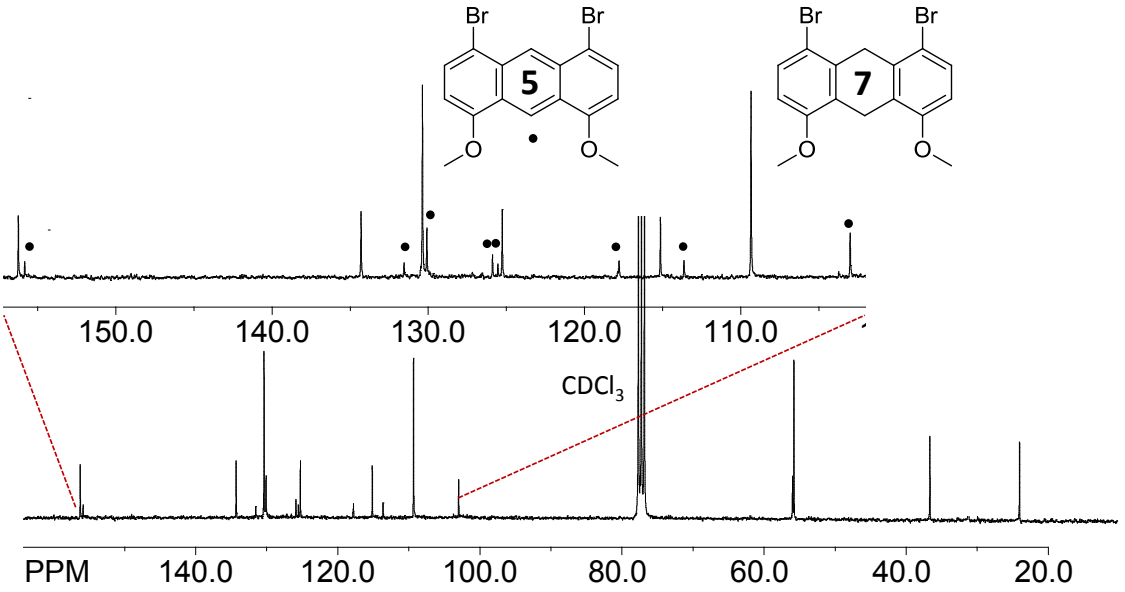

Table 3 Crystal data and structure refinement for raj21v (6)

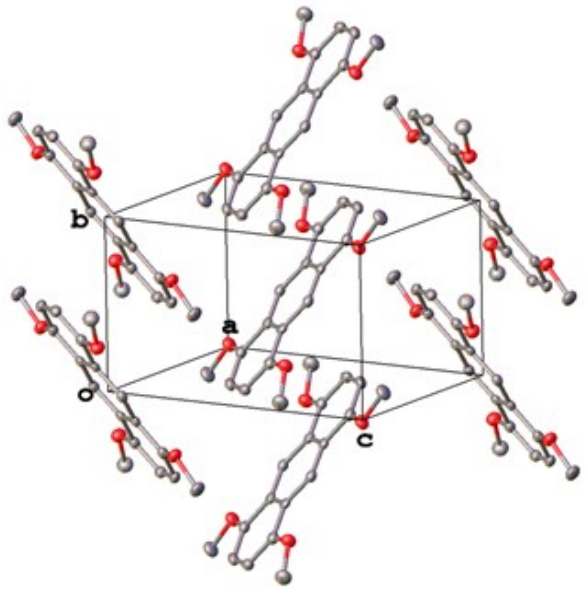

Identification code	raj21v
Empirical formula	$C_{18}H_{18}O_4$
Formula weight	298.32
Temperature/K	101.45(10)
Crystal system	monoclinic
Space group	$P2_1/n$
a/Å	10.9438(13)
b/Å	5.9802(5)
c/Å	11.6812(14)
α/°	90.00
β/°	110.272(14)
γ/°	90.00
Volume/Å^3	717.14(13)
Z	2
ρ_{calc}mg/mm^3	1.382
m/mm^{-1}	0.097
F(000)	316
Crystal size/mm^3	0.28 × 0.035 × 0.03
2Θ range for data collection	7.44 to 59.18°
Index ranges	$-13 \leq h \leq 14$, $-8 \leq k \leq 8$, $-16 \leq l \leq 13$
Reflections collected	4234
Independent reflections	1739[R(int) = 0.0337]
Data/restraints/parameters	1739/0/103

Goodness-of-fit on F^2	1.090
Final R indexes [I>=2σ (I)]	$R_1 = 0.0470$, $wR_2 = 0.1034$
Final R indexes [all data]	$R_1 = 0.0771$, $wR_2 = 0.1239$
Largest diff. peak/hole / e $Å^{-3}$	0.217/-0.242
Flack Parameter	N/A

Table 4 Crystal data and structure refinement for raj21x ($6_2^{+\bullet}$)

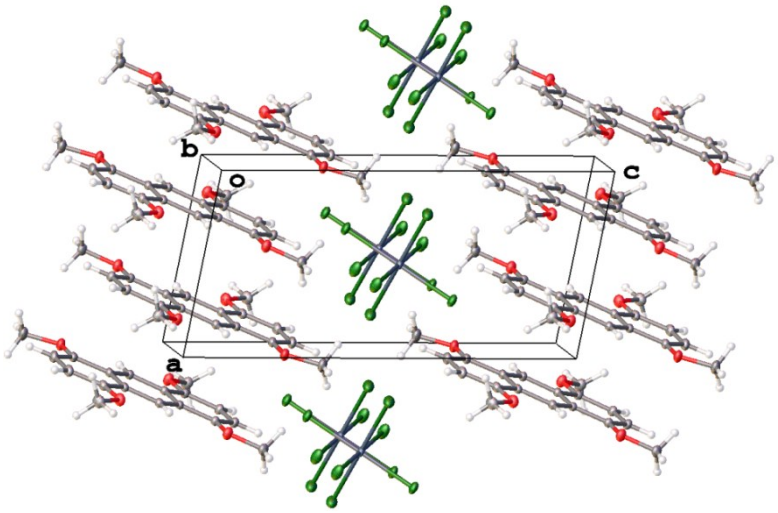

Identification code	raj21x
Empirical formula	$C_{36}H_{36}O_8Cl_6Sb$
Formula weight	931.10
Temperature/K	100.6(8)
Crystal system	triclinic
Space group	P-1
a/Å	6.9953(2)
b/Å	9.5006(3)
c/Å	14.4133(4)
α/°	95.409(2)
β/°	101.434(3)
γ/°	90.981(3)
Volume/$Å^3$	934.09(5)
Z	1
$\rho_{calc}mg/mm^3$	1.655

m/mm^{-1}	1.219
F(000)	469
Crystal size/mm^3	0.2511 × 0.0603 × 0.0362
2Θ range for data collection	6.88 to 91.24°
Index ranges	$-13 \leq h \leq 12$, $-19 \leq k \leq 18$, $-28 \leq l \leq 28$
Reflections collected	51016
Independent reflections	15732[R(int) = 0.0372]
Data/restraints/parameters	15732/0/236
Goodness-of-fit on F^2	1.068
Final R indexes [I>=2σ (I)]	$R_1 = 0.0343$, $wR_2 = 0.0710$
Final R indexes [all data]	$R_1 = 0.0457$, $wR_2 = 0.0785$
Largest diff. peak/hole / e $Å^{-3}$	1.147/-1.282

CHAPTER 2A

X-ray Structural Characterization of Charge Delocalization onto the Three Equivalent Benzenoid Rings in Hexamethoxytriptycene Cation Radical

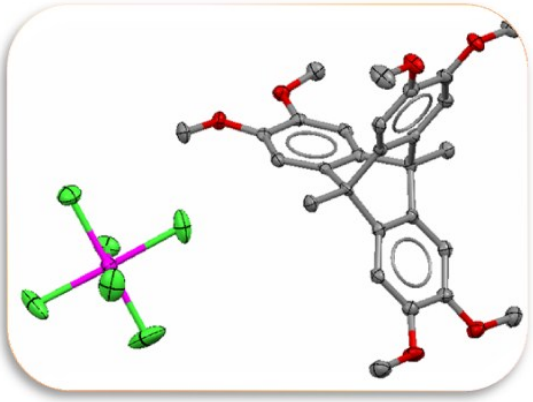

Abstract. Definitive X-ray crystallographic evidence is obtained for a single hole (or a polaron) to be uniformly distributed on the three equivalent 1,2-dimethoxybenzenoid (or veratrole) rings in the hexamethoxytriptycene cation radical. This conclusion is further supported by electrochemical analysis and by the observation of an intense near IR transition in its electronic spectrum, as well as by comparison of the spectral and electrochemical characteristics with the model compounds containing one and two dimethoxybenzene rings.

INTRODUCTION

Interactions between aromatic rings via π-stacking are at the origin of many phenomena of organic material science[1] and biological chemistry including the electron transport in DNA through stacked π-bases.[2] It has been noted in a number of recent studies that electronic coupling amongst the cofacially oriented aryl moieties does not necessarily require a perfect sandwich-like geometry. For example, we[3] and others have shown[4] that a hole (formed by the removal of a single electron) can hop amongst multiple cofacially oriented aryl moieties in various hexaarylbenzene derivatives as judged by the appearance of a characteristic near infrared (NIR) intervalence transition in the absorption spectra of their cation radicals. From this standpoint, triptycene and its derivatives are fundamentally important molecules in which the three equivalent benzenoid rings are cofacially oriented at an angle of ~120^{o}. It has been shown with the aid of esr and photoelectron spectroscopy that there is significant electronic coupling amongst the three benzenoid rings in triptycene and its derivatives.[5] It is also important to note that the triptycene scaffold is being extensively explored[6] for the preparation of modern materials for the potential usage in the emerging areas of molecular electronics and nanotechnology.[7]

Our continued interest in the design, syntheses, and exploration of electronic coupling in the cofacially-arrayed polybenzenoid structures[8] led us to isolate a crystalline cation-radical salt of a hexamethoxytriptycene derivative (**3**), which provides definitive (X-ray) structural evidence that a single hole (or a polaron) is distributed evenly on the three equivalent 1,2-dimethoxybenzene (or veratrole) rings. Furthermore, the effective electronic coupling amongst the three cofacially-oriented veratrole rings in **3**

is further corroborated by comparison of the spectral and electrochemical characteristics with the model compounds containing one and two dimethoxybenzene rings (i.e. **1** and **2**).

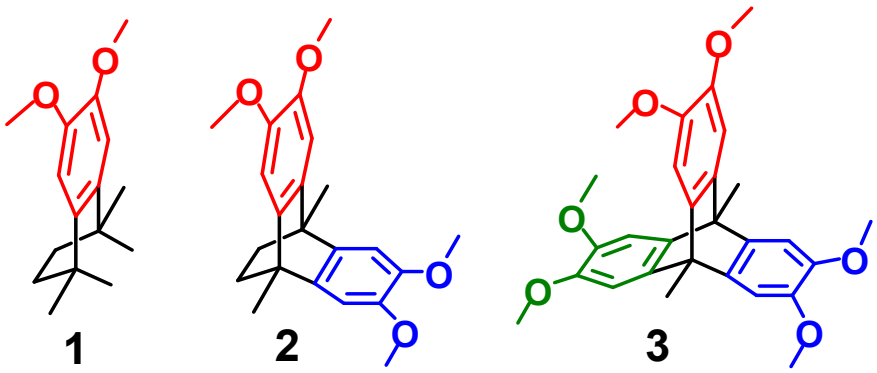

RESULTS and DISCUSSION

The syntheses of **1-3** were easily accomplished by the adaptation of standard literature procedures; and the relevant details along with the ^{1}H and ^{13}C NMR spectral data are summarized in the Experimental Section.

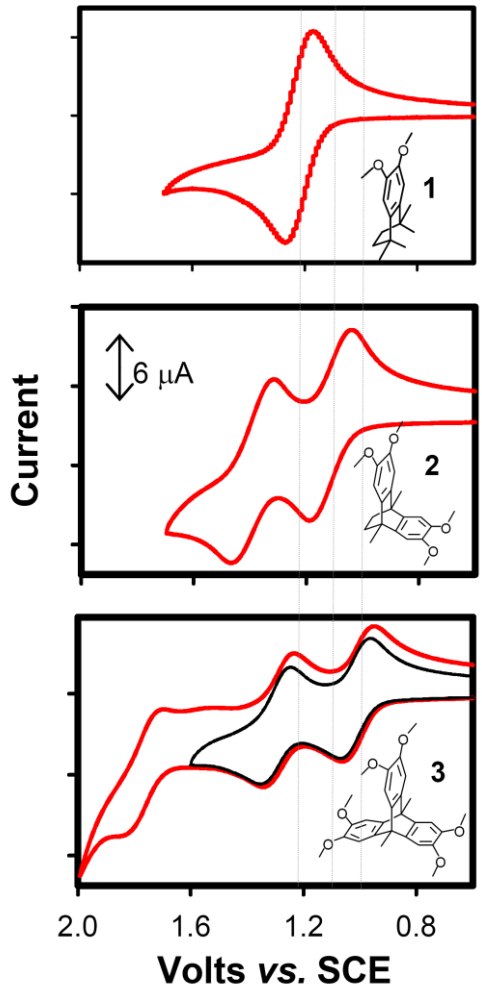

Figure 1. Cyclic voltammograms of **1**, **2**, and **3** (5 mM) in CH_2Cl_2 (containing 0.2 M nBu$_4$NPF$_6$ as the supporting electrolyte) measured at a scan rate of ν = 200 mV s^{-1} at 22 ^{o}C.

The electrochemical oxidations of **1-3** at a platinum electrode in CH_2Cl_2 were reversible at varying scan rates of 25–400 mV s^{-1}; all anodic/cathodic peak current ratios were I_a/I_c = 1.0 (theoretical) at room temperature (Figure 1). A quantitative evaluation of the CV peaks and peak currents with added ferrocene (as an internal standard, E_{ox} = 0.45 V vs. SCE) revealed that the first wave in the reversible cyclic voltammograms of **1-3** correspond to the production of the mono cation radical (by transfer of one electron) at

E_{ox1} = 1.22, 1.11, and 1.00 (V vs. SCE), respectively. The second oxidation in **2** (E_{ox2} = 1.39 V) and the second and third oxidations in **3** (E_{ox2} = 1.29 and E_{ox3} = 1.78 V) occur at relatively higher potentials (see Figure 1), and thus are indicative of the effective electronic coupling amongst the cofacially oriented veratrole moieties.[9] As such, the lowered first oxidation potentials of **2** and **3** by ~110 and ~220 mV, respectively, as compared to the model donor **1** attest to the significant stabilization of the cationic charge by the cofacially-arrayed veratrole rings in **2** and **3**.[9]

The electrochemical reversibility and relatively low oxidation potentials of **1**-**3** allow the generation of their cation radicals in solution using a hydroquinone ether cation radical ($CRET^{+\bullet}$, E_{red} = 1.11 V vs. SCE; λ_{max} = 518 nm; ε_{518} = 7300 M^{-1} cm^{-1})[10] or a hindered naphthalene cation radical ($NAP^{+\bullet}$, E_{red} = 1.34 V vs. SCE; λ_{max} = 672, 616, 503, and 396 nm; ε_{672} = 9300 M^{-1} cm^{-1})[11] as stable (aromatic) one-electron oxidants.

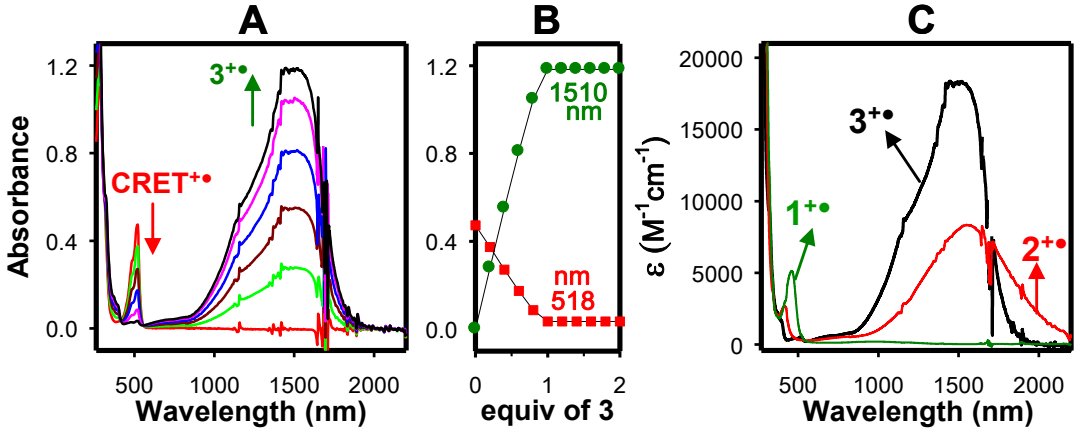

Figure 2. **A**: The spectral changes upon the reduction of 6.5 x 10^{-5} M $CRET^{+\bullet}$ by an incremental addition of substoichiometric amounts of **3** in CH_2Cl_2 at 22 °C. **B**: A plot of depletion of absorbance of $CRET^{+\bullet}$ (red squares, at 518 nm) and an increase of the absorbance of $\mathbf{3}^{+\bullet}$ (green circles, at 1510 nm) against the equivalent of added neutral **3**. **C**: A comparison of the absorption spectra of **1**-**3** cation radicals in CH_2Cl_2 at 22 °C.

Thus, Figure 2A shows the spectral changes attendant upon an incremental addition of sub-stoichiometric amounts of **3** to a solution of $CRET^{+\bullet}$ in dichloromethane at 22 °C. A plot of formation of the $\mathbf{3}^{+\bullet}$ (i.e. increase in the absorbance at 1510 nm) against the increments of added neutral **3** (see Figure 2B), established that $CRET^{+\bullet}$ was completely consumed after the addition of 1 equiv. of **3**; and the resulting absorption spectrum of $\mathbf{3}^{+\bullet}$ [λ_{max} = 408, 1510 nm; ε_{1510} = 18300 M^{-1} cm^{-1}] remained unchanged upon further addition of neutral **3** (i.e. eq 1).[12]

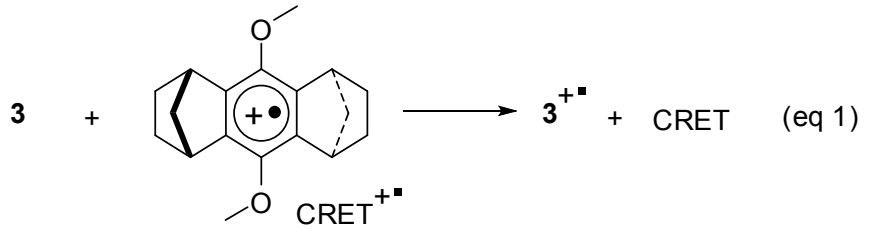

Similarly, the cation radical spectra of **1** and **2** were generated using $NAP^{+\bullet}$ and/or $CRET^{+\bullet}$ and are compared with the cation radical spectrum of triptycene **3** in Figure 2C. The observation of intense NIR transitions in the absorption spectra of bichromophoric $\mathbf{2}^{+\bullet}$ [λ_{max} = 420, 1560 nm; ε_{1560} = 8400 M^{-1} cm^{-1}] and trichromophoric $\mathbf{3}^{+\bullet}$ [λ_{max} = 1510 nm] should be contrasted with a singular lack of any absorption beyond 500 nm in the absorption spectrum of the monochromophoric cation radical $\mathbf{1}^{+\bullet}$ [λ_{max} = 461 nm; ε_{461} = 5200 M^{-1} cm^{-1}] (Figure 2C). Moreover, the fact that the NIR transition in $\mathbf{3}^{+\bullet}$ (λ_{max} = 1510 nm) is roughly twice as intense as in $\mathbf{2}^{+\bullet}$ (λ_{max} = 1560 nm) is most likely due to the increased probability of the hole migration over the three veratrole rings in $\mathbf{3}^{+\bullet}$ as opposed to only the two rings in $\mathbf{2}^{+\bullet}$.[13]

The cation radicals of donors **1**-**3**, obtained according to eq 1, are highly persistent at ambient temperatures and did not show any decomposition during a 12-h period at ~22 °C, as confirmed by UV-vis spectral analysis. The single crystals of the $\mathbf{3}^{+\bullet}$, suitable for

X-ray crystallography, were obtained by a slow diffusion of toluene into the dichloromethane solutions of $\mathbf{3}^{+\bullet}$ $SbCl_6^-$, prepared using equimolar NO^+ $SbCl_6^-$ as a 1-e^- oxidant, at -10 ^oC during the course of 2 days (see Experimental Section). Note that the repeated attempts to obtain single crystals of $\mathbf{1}^{+\bullet}$ $SbCl_6^-$ and $\mathbf{2}^{+\bullet}$ $SbCl_6^-$, suitable for X-ray crystallography, have been thus far unsuccessful.

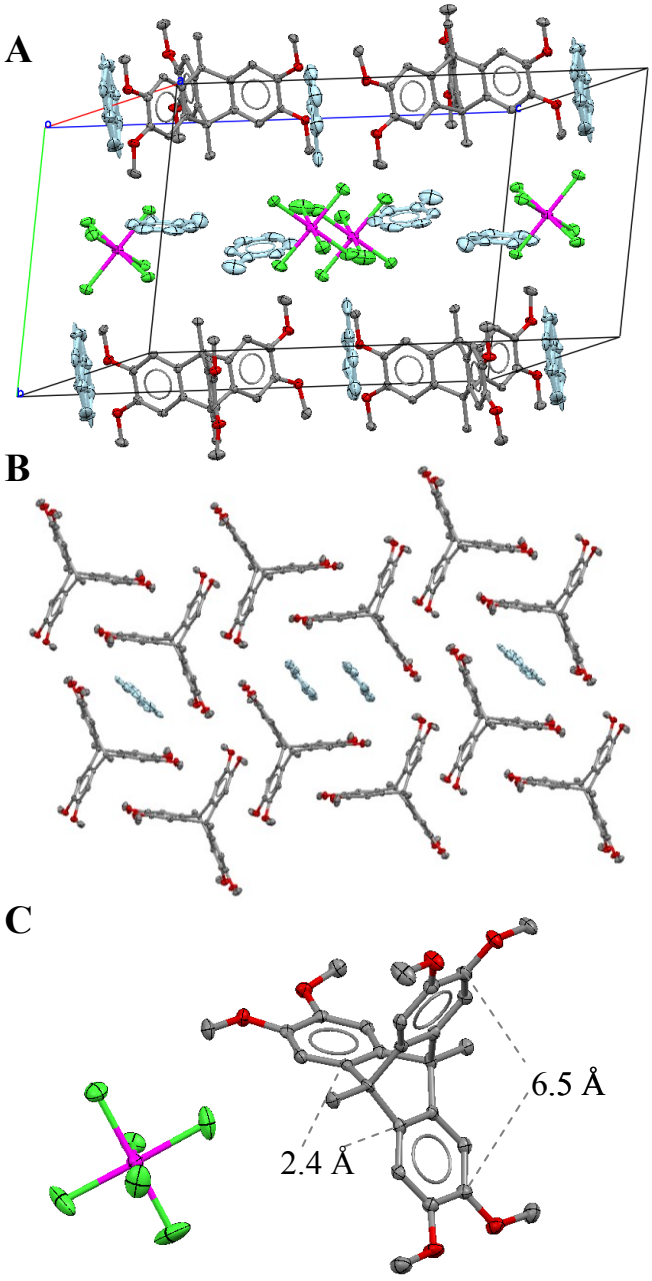

Figure 3. **A.** The packing diagram of $\mathbf{3}^{+\bullet}$ $SbCl_6^-$ cation radical showing the toluenes and $SbCl_6^-$ counter anions embedded between the layers of cationic triptycenes and additional toluene molecules. **B.** The arrangement of cationic triptycenes and toluene molecules within a single layer. **C.** An ORTEP diagram of $\mathbf{3}^{+\bullet}$ $SbCl_6^-$ showing the closest (2.4 Å) and farthest (6.5 Å) separation between the veratrole moieties in the cationic triptycene.[15]

The crystallographic analysis[14] of the highly-colored crystals of $\mathbf{3}^{+\bullet}$ $SbCl_6^-$ revealed that cationic triptycenes pack in layers in the crystallographic plane ***ac*** with embedded toluene molecules; and in between these layers lie the hexachloroantimonate anions and additional solvent (i.e. toluene) molecules (Figure 3A). Within a layer, each independent molecule of the cationic triptycene ($\mathbf{3}^{+\bullet}$) makes a centrosymmetric dimer over the centers of symmetry [0 0 0] and [0 0 ½] by forming a pseudo-½-translation along the z-axis (i.e. Figure 3B). These dimeric units, in turn, form infinite chains along the z-axis in which two out of the three veratrole rings of each cationic triptycene moiety is involved in face-to-face interactions with the neighboring molecules with a center to center distance of ~3.3-3.4 Å. The remaining third veratrole ring of the cationic triptycene makes a somewhat limited contact between the triptycene moieties of the neighboring chains, as well as more distinct face-to-face contacts with the toluene molecules (see Figure 3B).

Table 1. Experimental and theoretical bond lengths of the neutral and cation radical of **3** in picometers (pm).

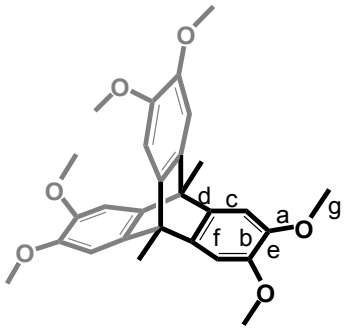

	B3LYP/6-31G*			X-ray Data		
Bond[a]	**3**	**$3^{\bullet+}$**	**Δ ($3^{\bullet+}$-3)**	**3**	**$3^{\bullet+}$**	**Δ ($3^{\bullet+}$-3)**
a	136.6	134.3	-2.3	137.2	135.0	-2.2
b	139.8	139.6	-0.2	139.2	138.4	-0.8
c	139.6	139.5	-0.1	139.0	138.9	-0.1
d	154.2	153.4	-0.8	154.0	153.0	-1.0
e	141.3	143.4	+2.1	141.1	142.3	+1.2
f	139.6	141.2	+1.6	138.8	140.5	+1.7
g	141.5	142.7	+1.2	142.7	143.8	+1.1
σ	--	--	--	0.4	0.6	--

[a] Average of equivalent bonds

A closer look at the structural parameters of the veratrole groups in $\mathbf{3}^{+\bullet}$ suggests that they are identical (within the experimental precision of ~0.006 Å for various C-C/C-O bond lengths) and thus suggests that the cationic charge is evenly distributed over all three veratrole moieties.[15] Furthermore, the bond length changes in the cation radical $\mathbf{3}^{+\bullet}$, together with a comparison of its neutral form, the structure of which was established

by X-ray crystallography,[14] correspond to the predominant contributions from *para*-quinoidal resonance structures **A/B**, as judged by the significant shortening of bonds labeled '**a**' and elongation of bonds labeled '**e**' and '**f**', along with only marginal shortening of the bonds labeled '**b**' and '**c**', (see Scheme 1 and Table 1). It is also noted that the alternate resonance structures **C-E** do not seem to contribute to the stabilization of the cationic charge in any significant way.

Scheme 1. Resonance structures for the stablization of the cationic charge in $\mathbf{3}^{+\bullet}$.

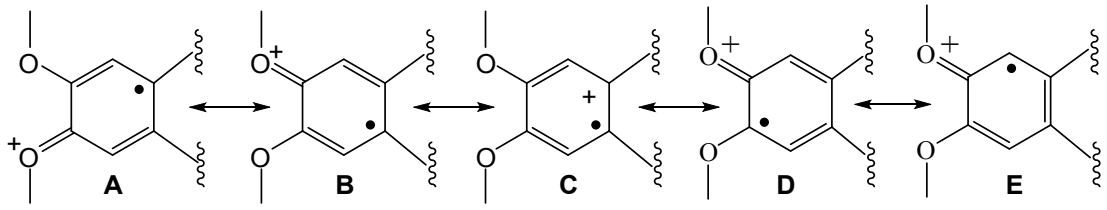

It is noteworthy that the experimental observations of the similar bond length changes in all three veratrole moieties together with a significant shortening of the bonds labeled '**d**' in $\mathbf{3}^{+\bullet}$ were found to be in reasonable agreement with the calculated values obtained using DFT calculations at the B3LYP/6-31G* level (see Table 1).[16] Furthermore, it is noted that the bonds which undergo the most dramatic lengthening (i.e., bonds **e** and **f**) and shortening (i.e., bonds **a**-**d**) in $\mathbf{3}^{+\bullet}$ are the bonds on which the HOMO shows the largest bonding and antibonding character, respectively (see Figure 4).

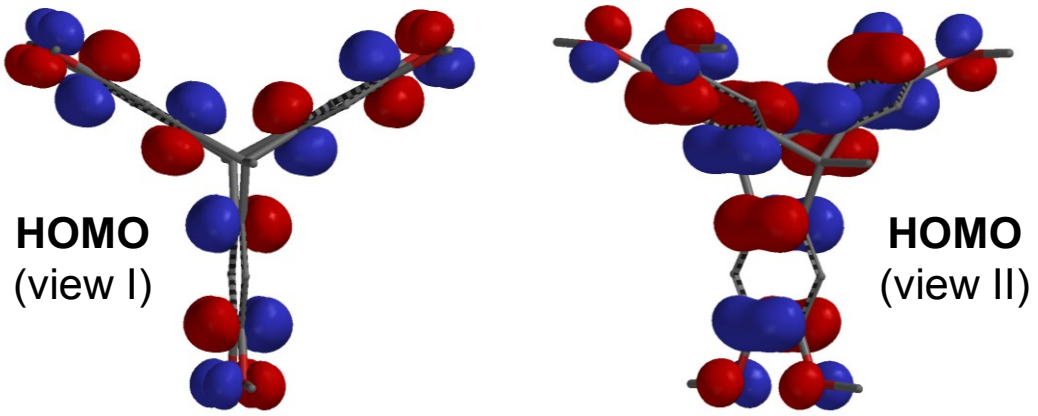

Figure 4. The two views of the HOMO of **3** obtained by DFT calculations at the B3LYP/6-31G* level.

SUMMARY and CONCLUSIONS

In summary, we have demonstrated that hexamethoxytriptycene (**3**) and the model compounds containing one and two veratrole moieties (i.e. **1** and **2**) undergo reversible electrochemical oxidation and form stable cation-radical salts. The significantly lowered first oxidation potentials of bichromophoric **2** and triptycene **3** by ~110 and ~220 mV, respectively, as compared to the monochromophoric donor **1**, as well as the observation of intense NIR transitions in $\mathbf{3}^{+\bullet}$ (λ_{max} = 1510 nm) and $\mathbf{2}^{+\bullet}$ (λ_{max} = 1560 nm), and a complete absence of the NIR transition in monochromophoric $\mathbf{1}^{+\bullet}$, attests to the effective electronic coupling amongst the cofacially-arrayed veratrole rings in **2** and **3**. The isolation and X-ray crystal structure determination of the neutral and cation radical of **3,** as well as the DFT calculations now provide unequivocal evidence that a single charge (or polaron) is evenly distributed over all three veratrole moieties. Efforts are now underway to construct polyaromatic arrays based on the triptycene scaffold to explore their conducting properties as well as potential applications in the emerging areas of molecular electronics and nanotechnology.[7]

EXPERIMENTAL

General Experimental Methods. Anhydrous tetrahydrofuran (THF) was prepared by refluxing the commercial tetrahydrofuran (Aldrich) over lithium tetrahydroaluminate under an argon atmosphere for 24 hours followed by distillation. It was stored under an argon atmosphere in a Schlenk flask equipped with a Teflon valve fitted with Viton O-rings. Dichloromethane (Aldrich) was repeatedly stirred with fresh aliquots of conc. sulfuric acid (~10 % by volume) until the acid layer remained colorless. After separation it was washed successively with water, aqueous sodium bicarbonate, water, and saturated aqueous sodium chloride and dried over anhydrous calcium chloride. The dichloromethane was distilled twice from P_2O_5 under an argon atmosphere and stored in a Schlenk flask equipped with a Teflon valve fitted with Viton O-rings. The hexanes and toluene were distilled from P_2O_5 under an argon atmosphere and then refluxed over calcium hydride (~12 hrs). After distillation from CaH_2, the solvents were stored in Schlenk flasks under argon atmosphere.

Cyclic Voltammetry (CV). The CV cell was of an air-tight design with high vacuum Teflon valves and Viton O-ring seals to allow an inert atmosphere to be maintained without contamination by grease. The working electrode consisted of an adjustable platinum disk embedded in a glass seal to allow periodic polishing (with a fine emery cloth) without changing the surface area (~1 mm^2) significantly. The reference SCE electrode (saturated calomel electrode) and its salt bridge were separated from the catholyte by a sintered glass frit. The counter electrode consisted of a platinum gauze that

was separated from the working electrode by ~3 mm. The CV measurements were carried out in a solution of 0.1 to 0.2 M supporting electrolyte (tetra-*n*-butylammonium hexafluorophosphate, TBAH) and the substrate in dry dichloromethane under an argon atmosphere. All the cyclic voltammograms were recorded at a sweep rate of 200 mV sec^{-1}, unless otherwise specified and were IR compensated. The oxidation potentials ($E_{1/2}$) were referenced to SCE, which was calibrated with added (equimolar) ferrocene ($E_{1/2}$ = 0.450 V *vs*. SCE). The $E_{1/2}$ values were calculated by taking the average of anodic and cathodic peak potentials in the reversible cyclic voltammograms.

Isolation of [$3^{+\bullet}SbCl_6^-$] single crystals.

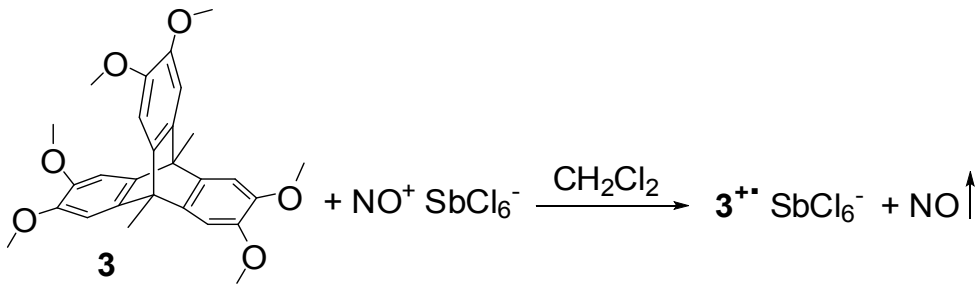

A 25-mL flask fitted with a Schlenk adaptor was charged with nitrosonium hexachloroantimonate ($NO^+SbCl_6^-$) [R. Rathore, C. L. Burns, *J. Org. Chem.* **2003**, *68*, 4071.] (22 mg, 0.06 mmol), and a cold solution of **3** (28 mg, 0.06 mmol) in anhydrous dichloromethane (10 mL) was added under an argon atmosphere at ~0 ^oC. The solution immediately took on a dark-yellow coloration and the solution was stirred (while slowly bubbling argon through the solution to entrain gaseous NO) for 30 min to yield a dark-yellow solution of [$\mathbf{3}^{+\bullet}$ $SbCl_6^-$] which was spectrally identical to that obtained in Figure 1 (see text). The solution was carefully layered with dry toluene (10 mL) and placed in a

refrigerator (-10 ^{o}C) which after 2 days produced dark needle shaped crystals of the $\mathbf{3}^{+\bullet}$ $SbCl_6^-$ suitable for X-ray structure analysis.

Preparation of 1, 2, and 3. The syntheses of **1-3** were accomplished by adapting literature procedures as summarized below:

1,2,3,4-Tetrahydro-6,7-dimethoxy-1,1,4,4-tetramethylnaphthalene (1):

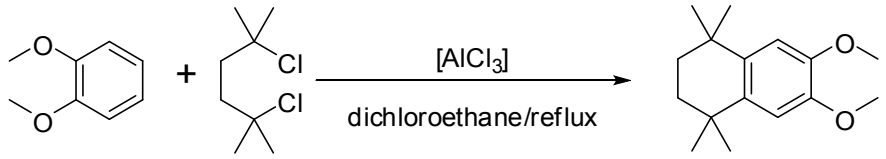

Monochromophoric **1** was prepared by a cycloannulation reaction of 1,2-dimethoxy-benzene (10 mmol) with 2,5-dichloro-2,5-dimethylhexane (12 mmol) in 1,2-dichloro-ethane (10 mL) in the presence of a catalytic amount of $AlCl_3$ (200 mg) at 60 ^{o}C for 8 h. Yield 74%; mp 60-62 ^{o}C; ^{1}H NMR ($CDCl_3$) δ 1.27 (s, 12H), 1.67 (s, 4H), 3.86 (s, 6H), 6.77 (s, 2H); ^{13}C NMR ($CDCl_3$) δ 32.07, 34.22, 35.42, 56.01, 109.37, 137.23, 147.05; GC-MS: *m/z* = 248 (M^+) calcd. for $C_{16}H_{24}O_2$..

^{1}H NMR of 1 in $CDCl_3$

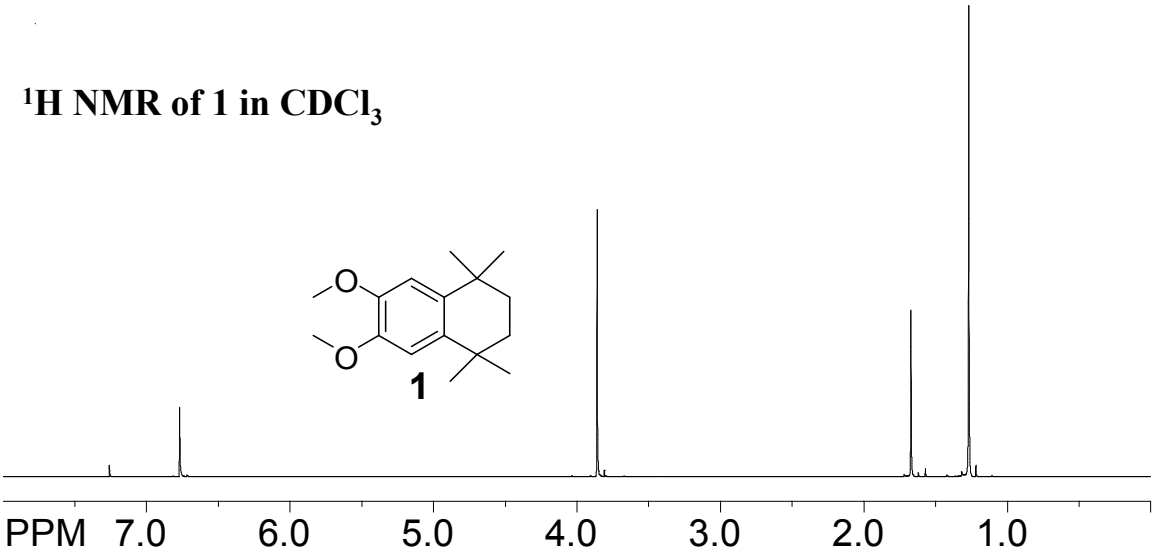

^{13}C NMR of 1 in $CDCl_3$

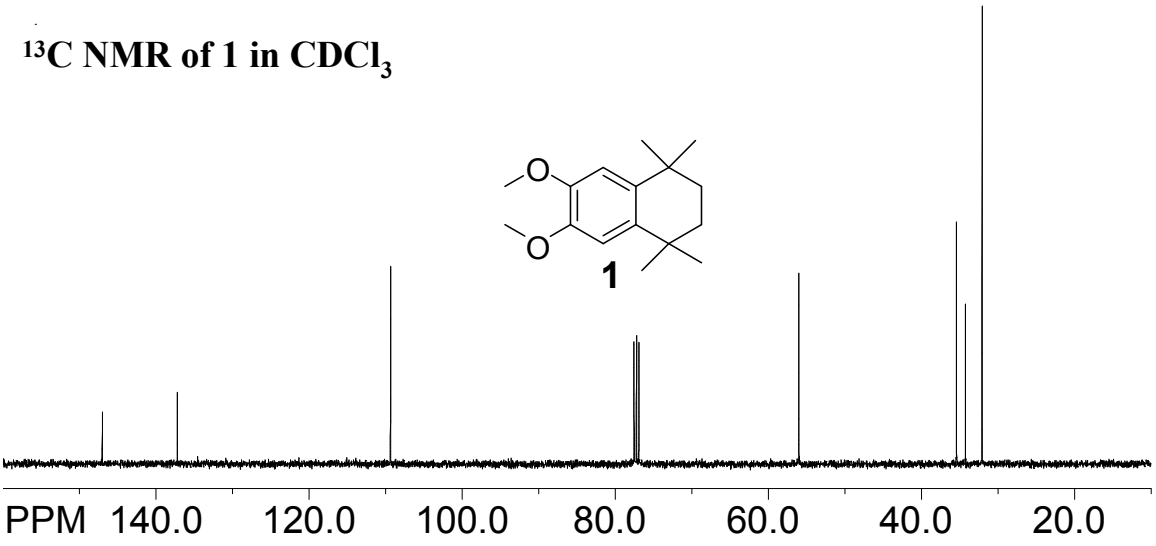

9,10-Dihydro-2,3,6,7-tetramethoxy-9,10-dimethyl-9,10-ethanoanthracene (2):

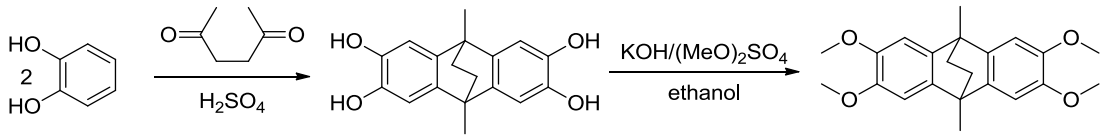

The bichromophoric **2** was prepared by a condensation of 1,2-dihydroxybenzene with 2,5-hexanedione in conc. H_2SO_4 to afford the intermediate 2,3,6,7-tetrahydroxy-9,10-dimethyl-9,10-ethanoanthracene using a literature procedure [Davidson, I. M.; Musgrave, O. C. *J. Chem. Soc.* **1963**, 3154], which was easily methylated using dimethylsulfate and KOH in refluxing ethanol to afford **2** in excellent yield (88%); mp 180-181 ^{o}C; ^{1}H NMR ($CDCl_3$) δ 1.60 (s, 4H), 1.95 (s, 6H), 3.88 (s, 12H), 6.87 (s, 4H); ^{13}C NMR ($CDCl_3$) δ 18.87, 36.54, 41.52, 56.50, 105.70, 139.39, 146.63; GC-MS: *m/z* = 354 (M^+) calcd. for $C_{22}H_{26}O_4$.

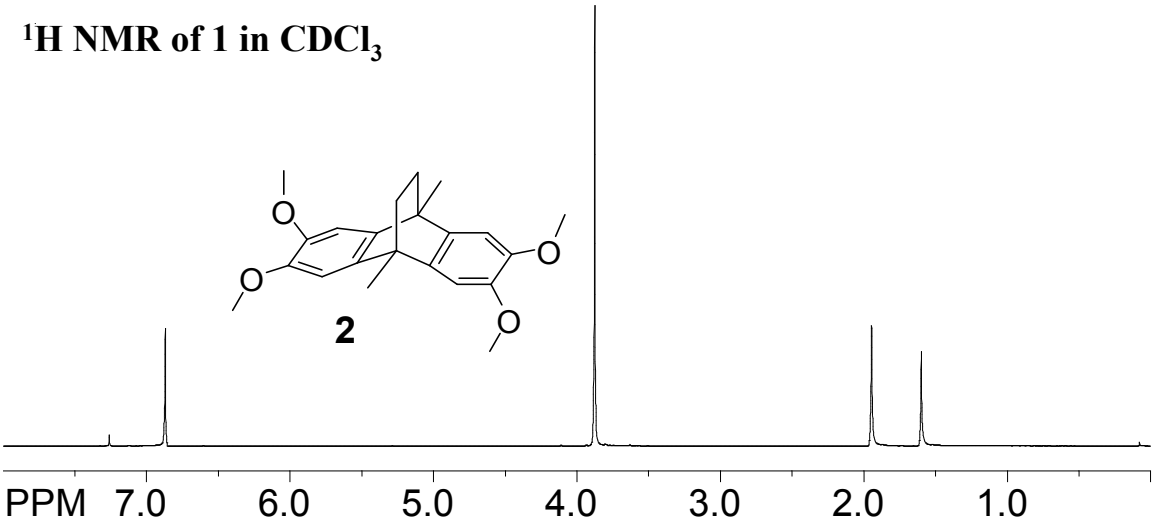

^{13}C NMR of 1 in $CDCl_3$

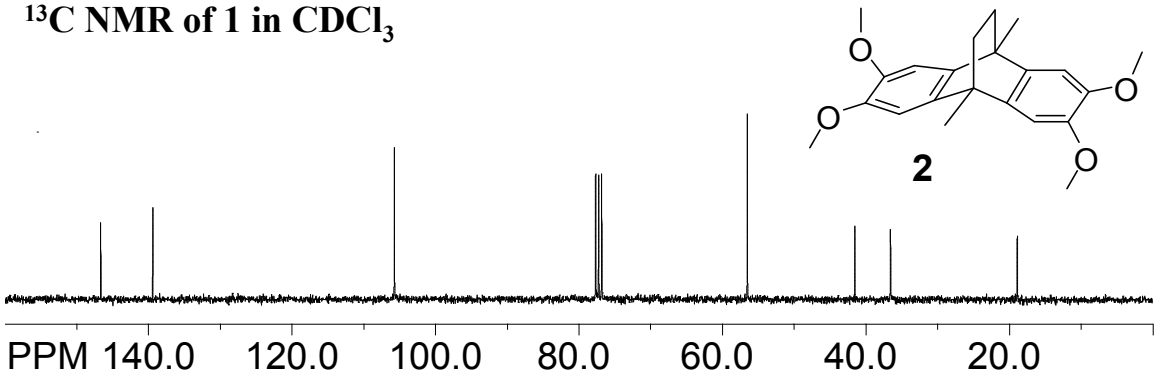

Synthesis of 9,10-dimethyl-2,3,6,7-tetrahydroxyanthracene.

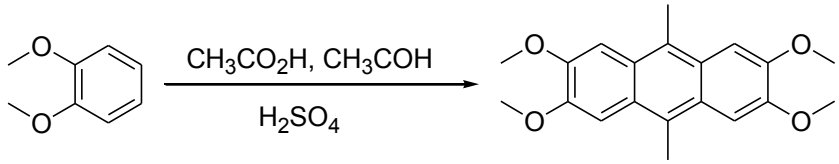

To a cooled solution (~ 0 ^{o}C) of veratole (32 ml, 250 mmol) in acetic acid (125 ml) was slowly added an ice-cold solution of acetaldehyde (21 ml, 375 mmol) in methanol (20 ml). The resulting mixture was then stirred for 1 h and concentrated H_2SO_4 (95%, 125 ml) was added dropwise over 2 h. The reaction mixture was then stirred at 0 ^{o} for 20 h and poured onto ice-water which precipitated the product out as beige solid and collected by vacuum filtration. The product was further purified by recrystallization in chloroform to afford the final product as a yellow solid. Yield: 4.2 g (10 %); m.p. > 350 ^{o}C; ^{1}H NMR ($CDCl_3$) δ: 2.94 (s, 6H), 4.10 (s, 12H), 7.47 (s, 4H). [Reference: Chung, Y.; Duerr, B. F.; McKelvey, T. A.; Nanjappan, P.; Czarnik, A. W. *J. Org. Chem.* **1989**, *54*, 1018-32.]

Synthesis of 4,5-dimethoxybenzenediazonium-2-carboxylate.

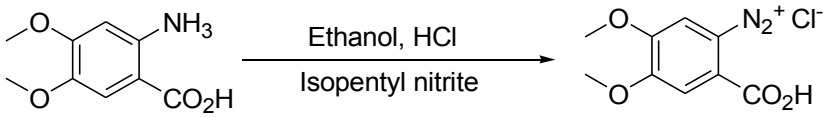

To a ice-cooled suspension of 2-amino-4,5-dimethoxy-benzoic acid (7.5 g, 38 mmol) in ethanol (200 ml) concentrated hydrochloric acid (3.8 ml) was added dropwise and isopentyl nitrite (9 ml) was subsequently added. The reaction mixture was stirred for 15 min and ether (200 ml) was added and stirred for an additional 15 min to precipitate out the product which was filtered and washed with ether to afford a white solid which was quickly used in the next step. Yield: 6.6g (71%). [Reference: Muellner, F. W.; Bauer, L. *J. Heterocyclic Chem.* **1983**, *20*, 1581.]

Synthesis of 9,10-dimethyl-2,3,6,7,14,15-hexamethoxy-9,10-[1'2']benzoanthra-cene or hexamethoxytriptycene (3)

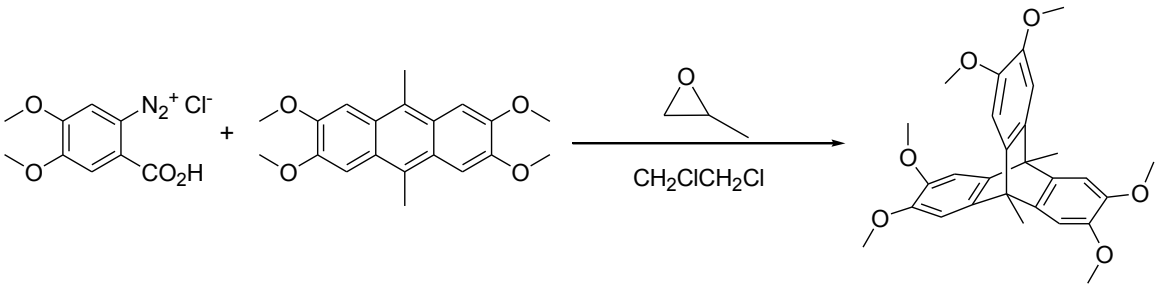

A mixture of 2,3,6,7-tetramethoxyanthracene (2 g, 6.1 mmol), 4,5-dmethoxybenzene-diazonium-2-carboxylate (6.6 g, 27 mmol) and 1,2-epoxypropane (40 ml) in dichloroethane (180 ml) was refluxed for 12 h and then cooled to room temperature. The reaction mixture was concentrated under reduced pressure and the red precipitate was

filtered and washed with acetone. The crude product was further purified by crystallization using acetone to afford a white solid. Yield: 1.64 g (58 %), m.p. 360-362 ^{o}C; ^{1}H NMR ($CDCl_3$) δ 2.38 (s, 6H), 3.85 (s, 18H), 6.93 (s, 6H). ^{13}C NMR ($CDCl_3$) δ 14.22, 47.80, 56.55, 105.92, 142.14, 145.80. [Reference: Zhu, X.-Z.; Chen, C.-F. *J. Am. Chem. Soc.* **2005**, *127*, 13158.]

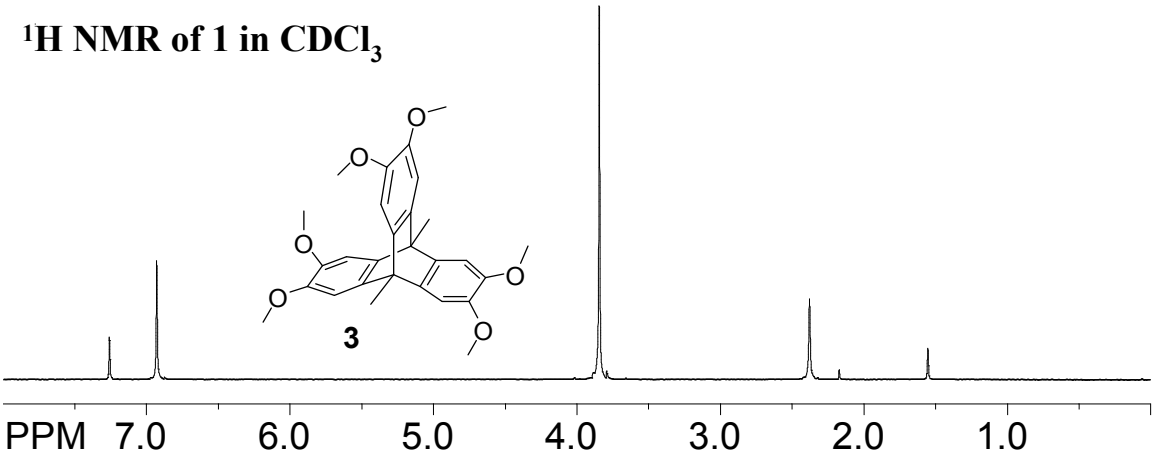

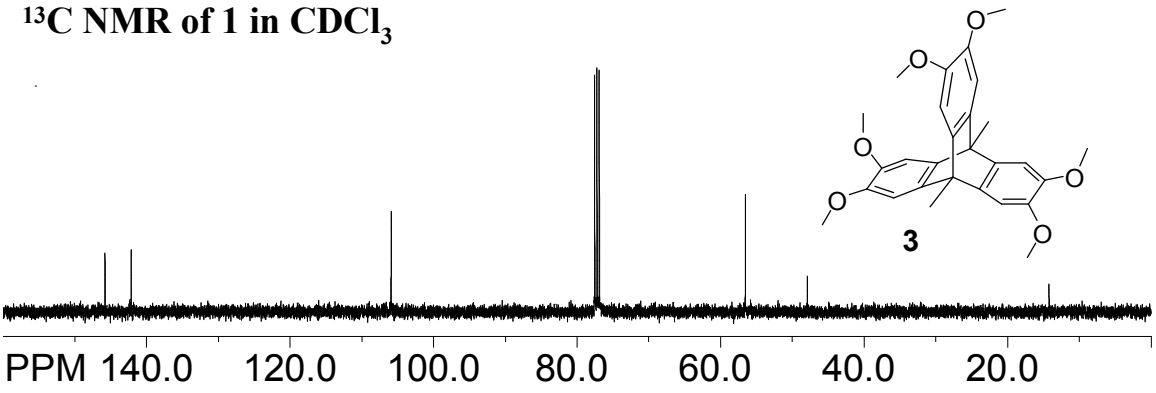

Table 2. **Crystal data and structure refinement for [$3^{+\bullet}SbCl_6^-$] (identification code: raj5za).**

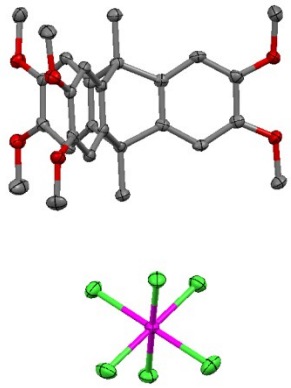

Identification code	raj5za
Empirical formula	C40.25 H44 Cl6 O6 Sb
Formula weight	958.20
Temperature	100(2) K
Wavelength	1.54178 Å
Crystal system	Triclinic
Space group	P -1
Unit cell dimensions	a = 12.5195(2) Å α= 103.8740(10)°.
	b = 12.9701(2) Å β= 93.9200(10)°.
	c = 26.6144(4) Å γ = 90.6470(10)°.
Volume	4184.02(11) $Å^3$
Z	4
Density (calculated)	1.521 Mg/m^3
Absorption coefficient	9.122 mm^{-1}
F(000)	1946
Crystal size	0.22 x 0.05 x 0.04 mm^3
Theta range for data collection	1.71 to 62.46°.
Index ranges	-13<=h<=14, -14<=k<=14, 0<=l<=30
Reflections collected	34690
Independent reflections	12243 [R(int) = 0.0396]
Completeness to theta = 62.46°	98.3 %
Absorption correction	Numerical
Max. and min. transmission	0.7408 and 0.2388
Refinement method	Full-matrix least-squares on F^2
Data / restraints / parameters	12243 / 15 / 1175
Goodness-of-fit on F^2	1.030
Final R indices [I>2sigma(I)]	R1 = 0.0423, wR2 = 0.0925
R indices (all data)	R1 = 0.0590, wR2 = 0.0974
Largest diff. peak and hole	1.023 and -0.592 $e.Å^{-3}$

Table 3. **Crystal data and structure refinement for neutral 3 (identification code: raj5n).**

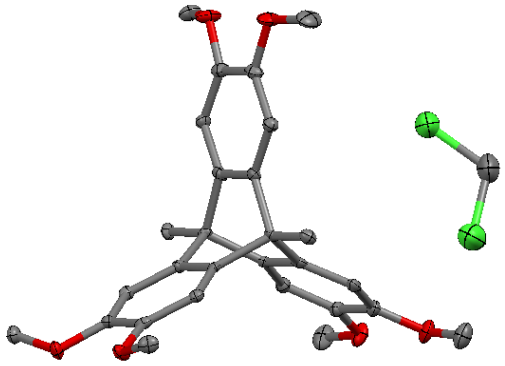

Identification code	raj5n
Empirical formula	C29 H32 Cl2 O6
Formula weight	547.45
Temperature	140(2) K
Wavelength	1.54178 Å
Crystal system	Monoclinic
Space group	P 21
Unit cell dimensions	a = 15.8842(3) Å α= 90°.
	b = 8.8279(2) Å β= 95.7470(10)°.
	c = 18.5716(4) Å γ = 90°.
Volume	2591.10(9) $Å^3$
Z	4
Density (calculated)	1.403 Mg/m^3
Absorption coefficient	2.614 mm^{-1}
F(000)	1152
Crystal size	0.33 x 0.20 x 0.10 mm^3
Theta range for data collection	2.39 to 62.53°.
Index ranges	-18<=h<=17, -10<=k<=9, 0<=l<=21
Reflections collected	21491
Independent reflections	7416 [R(int) = 0.0190]
Completeness to theta = 62.53°	97.8 %
Absorption correction	Semi-empirical from equivalents
Max. and min. transmission	0.7800 and 0.4792
Refinement method	Full-matrix least-squares on F^2
Data / restraints / parameters	7416 / 1 / 667
Goodness-of-fit on F^2	1.021
Final R indices [I>2sigma(I)]	R1 = 0.0485, wR2 = 0.1349
R indices (all data)	R1 = 0.0497, wR2 = 0.1361
Absolute structure parameter	0.036(16)
Largest diff. peak and hole	0.533 and -0.588 $e.Å^{-3}$

CHAPTER 2B

Preparation and Optoelectronic properties of a new class of Intervalance Cation Radicals from *p*-Diaryloxybenzenes

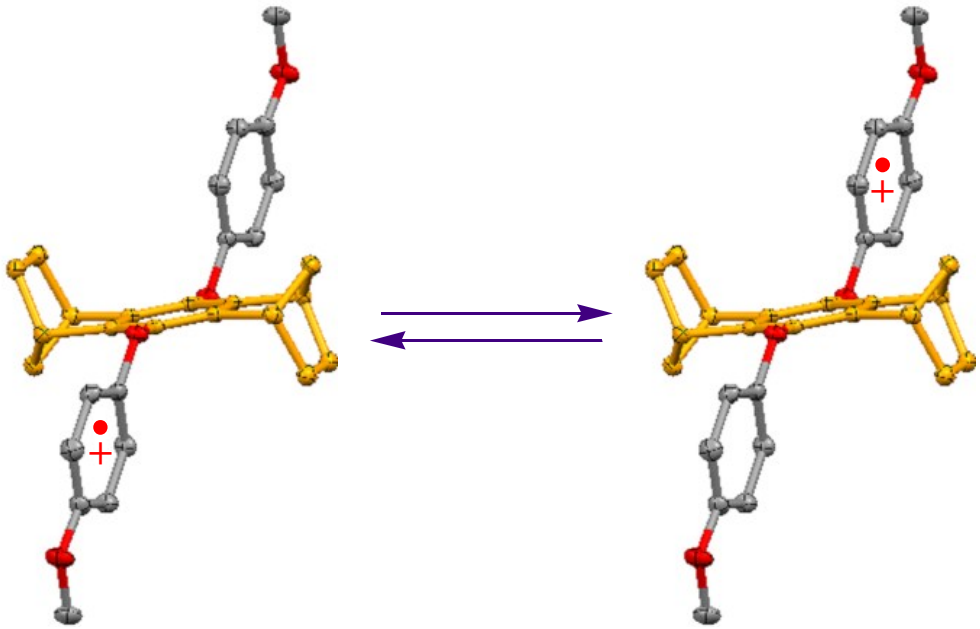

Abstract: Bis-cycloannulated *p*-diaryloxybenzenes can be easily synthesized from readily available starting materials using Ullmann ether synthesis. These biaryl ethers (**5-10**) underwent reversible electrochemical oxidation and formed stable cation radical salts. Appearance of two 1e$^-$ oxidation waves for **6-8** separated by ~100 mV indicates the effective electronic coupling between two aryl groups. Observance of near-IR transition in the electronic spectrum of **4-7** cation radicals and X-ray crystal determination for **8**$^{++}$ together with DFT calculations attest that single charge is localized evenly on terminal aryl groups.

INTRODUCTION

Search for novel materials for improved charge mobilities is continuing with unabated pace owing to their potential for modern photovoltaic applications,[1] beside the exploration of traditional materials such as polyphenylenes and their substituted derivatives,[2] ladder ployfluorenes,[3] polyphenylenevinylenes,[4] polythiophenes,[5] polyacetylenes,[6] hexa-peri-hexabenzocoronenes,[7] etc. as materials for the hole transport layers. One of the many criteria for the choice of hole transport materials demands that they have low oxidation potentials and are able to effectively stabilize the cationic charge and are not subject to rapid decomposition when oxidized. It is well known that aromatic hydrocarbons substituted with electron donating alkoxy groups are oxidized at relatively low oxidation potentials and form stable cation radicals. Recent advances in the ease of preparation of diarylethers prompted us to evaluate the redox behavior of simple benzenoid hydrocarbons bearing various substituents and to evaluate their potential applicability as robust charge carriers, as diaryl ethers are known to show high thermal stability. Accordingly, herein we undertaken a systematic study of diary ethers derived from a cycloannulated hydroquinone (i.e. [1,4:5,8] dimethanooctahydro-9-10-dihydroxy-anthracene, **1**) as follows

Figure 1. List of various cycloannulated ethers

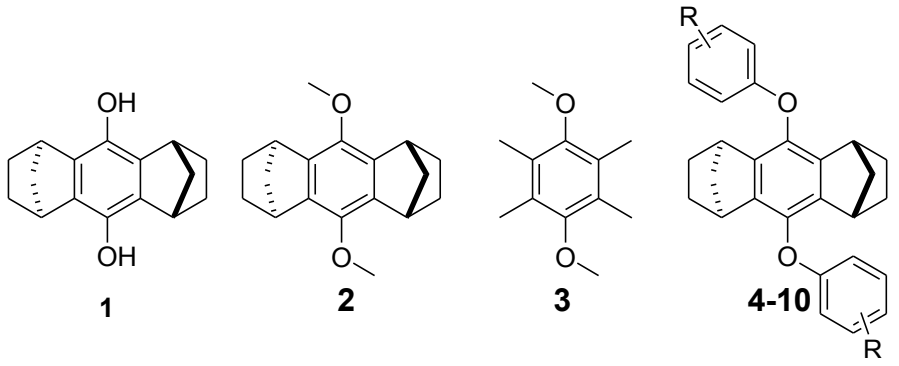

The choice of bicycloheptane-annulated hydroquinone **1** stems from the fact that it's dimethyl ether (**2**) undergoes a highly reversible electrochemical oxidation (E_{ox} = 1.14 V vs. SCE) and forms a robust cation radical salt which can be easily prepared and stored indefinitely.[8] The importance of bicycloheptane annulation in **1** is further emphasized by the fact that simple 2,3,5,6-tetramethyl-1,4-dimethoxybenzene (**3**) is irreversibly oxidized at relatively much higher potential (E_{ox} = 1.45 V vs. SCE) owing to the fact that it does not allow the methoxy groups to lie in the aromatic plane for the effective stabilization of the cationic charge of etheral oxygens.[9] The bicycloheptane annulation of 1,4-dimethoxybenzene allows the methoxy groups to lie in the aromatic plane in its cation radical as well as prevents the loss of alpha-hydrogens which are Bredt's rule protected.[9]

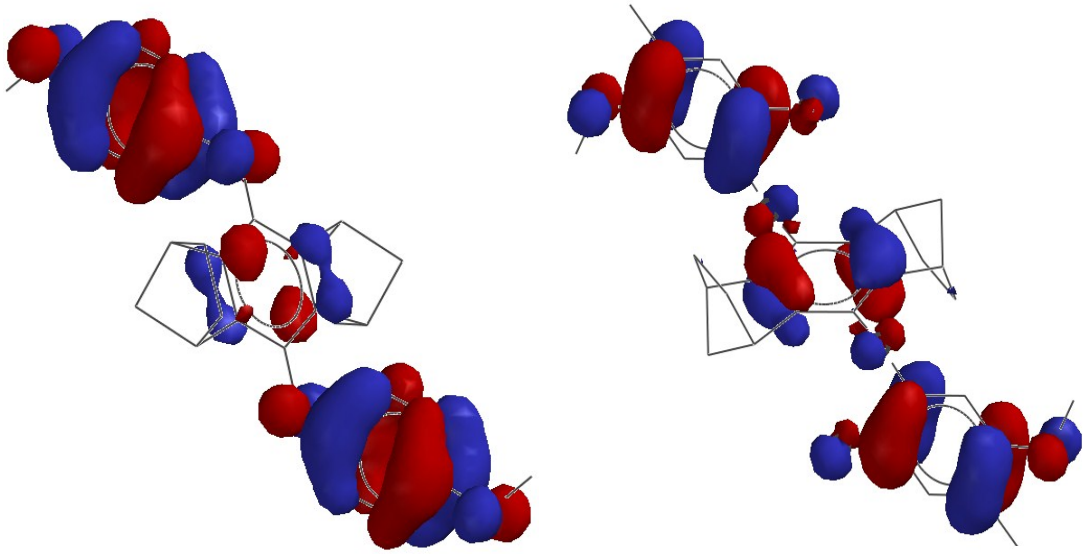

Figure 2. A picture depicting the positioning of HOMO for **6** and **8** obtained by DFT calculations.

Herein it was conjectured that preparation and study of electronic coupling amongst the three benzenoid moieties in various diaryloxy derivatives of **1**, which should be accessible by Cu-catalyzed biaryl ether synthesis, may serve as basis for the future preparation of linear mixed polyaryl ethers as a new class of molecular wires. Before undertaking such a study, we performed density-functional calculations (B3LYP/6-31G* level) on various diaryloxybenzenes which showed that in each case the HOMO resides largely on the aryloxy moieties rather than the central annulated hydroquinone moiety, i.e. Figure 2.

The DFT calculations suggested that these materials may act as inter-valence compounds where a single hole should delocalize onto the aryl groups through the cycloannulated bridge. Accordingly, herein we describe the preparation of a series of diaryloxybenzene ethers (**4**-**10**) and demonstrate for the first time with the aid of cyclic

voltammetry, optical spectroscopy, X-ray crystallography and DFT calculations that these diaryl ethers indeed serve as a new class of intervalence compounds. The details of preliminary findings are described herein.

RESULTS and DISCUSSION

The syntheses of **4**-**10** were achieved by the literature reported Ullmann ether synthesis procedure[10] using Copper oxide and potassium carbonate in a refluxing pyridine i.e. Scheme 1.

Scheme 1. General route for the synthesis of diaryloxybenezenes

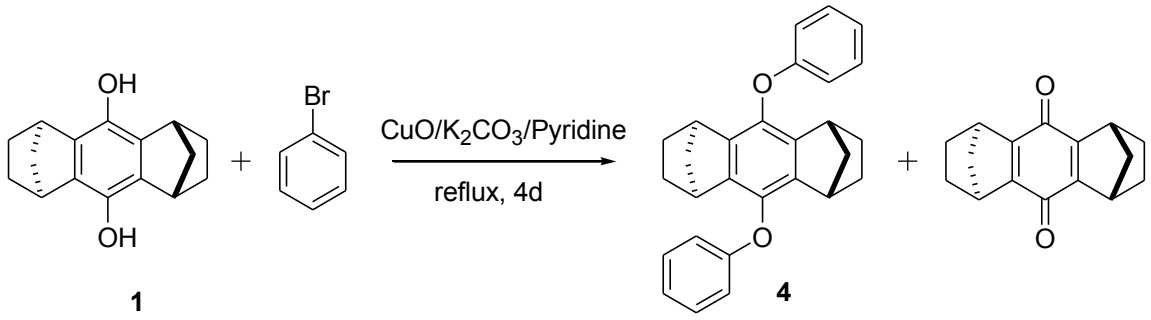

For 5 minutes argon was bubbled through a suspension of hydroquinone (4.0 mmol), arylbromide (12.0 mmol), and anhydrous K_2CO_3 (24 mmol) in pyridine (20 mL). CuO (1.0 g, 12.0 mmol) was then added and the stirring mixture was vigorously refluxed for 4-5 days to yield bis-cycloannulated biaryl ethers as white solids in low yields 10-35%. One of the reasons for the low yields is the competitive oxidation of hydroquinone to corresponding quinone in the reaction conditions employed. It was found that usually 20-45% hydroquinone gets oxidized to quinone.[11]

Figure 3. A series of di-aryloxybenzenes prepared employing the general synthetic strategy.

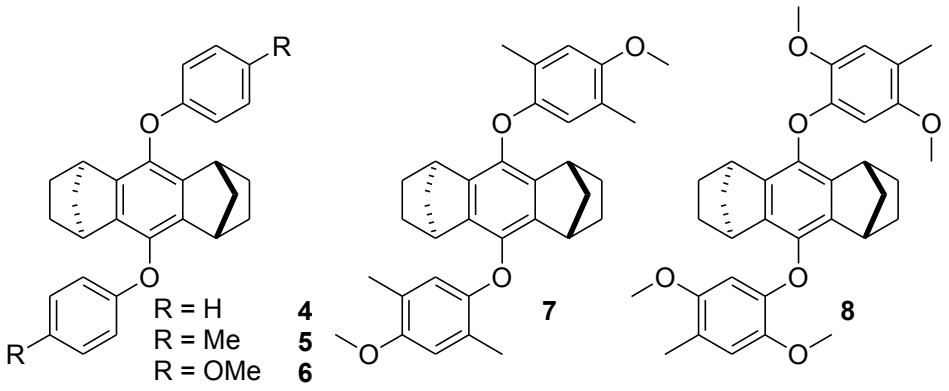

Similar strategy was used to prepare larger biaryl ethers like **10** where hydroquinone **1** was reacted with excess 4-bromo-benzophenone under similar reaction conditions described above to get **9**, which was added to a orange red colored solution obtained by addition of one equivalent of BuLi to 1.2 equivalent diphenylmethane in THF at 0^{o}C. The reaction mixture was allowed to stirr at room temperature for 6h, after workup the crude alcohol was subjected to acid-catalyzed dehydration in toluene using catalytic amount of *p*-toluenesulphonic acid, separating the water formed in the reaction using a Dean-Stark trap, after completion, crude reaction mixture was purified by fractional re-crystallization from a mixture of dichloromethane and methanol to afford **10** as pale yellow colored solid in 66% yield.

Scheme 2. Synthesis route for the preparation of **10**

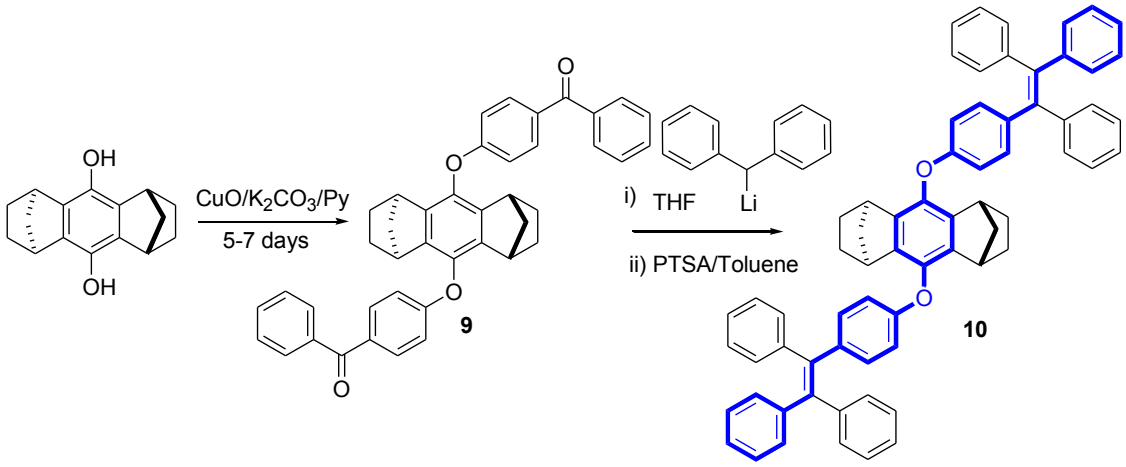

All biaryl ethers, **4-10** were characterized by ^{1}H and ^{13}C NMR spectroscopy, in addition structures of **4**, **5**, **6**, **8** and **9** were further corroborated by X-ray crystallography. For e.g. see Figure 4.

Figure 4. An ORTEP diagram showing the arrangement of **4** in its crystals.

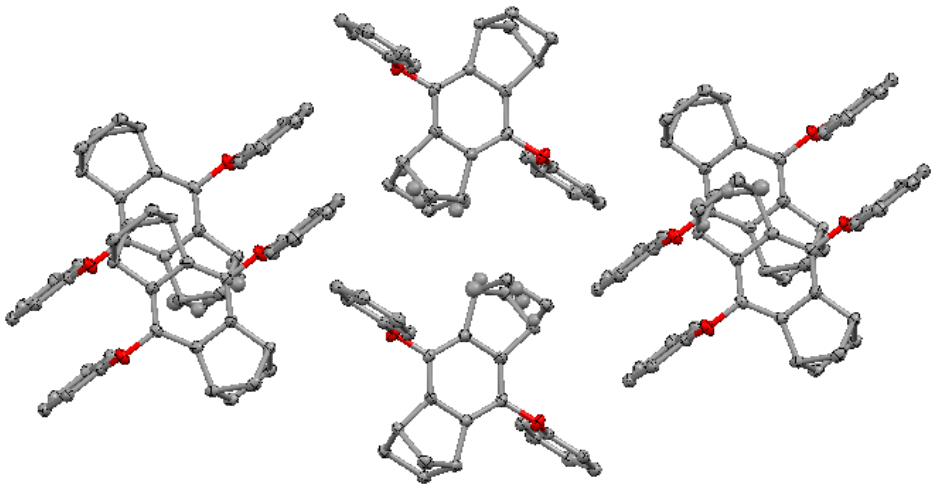

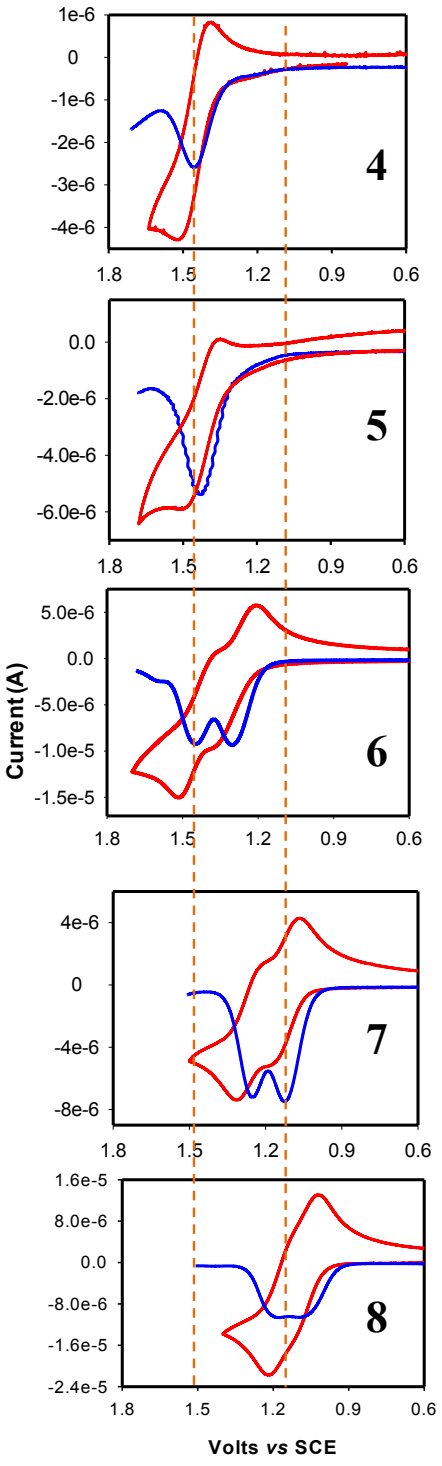

Figure 5. Cyclic voltammograms (red trace) and square waves (blue trace) of 2.5 x 10^{-3} M **4**, **5**, **6**, **7** and **8** in CH_2Cl_2 (containing 0.2 M *n*Bu_4NPF_6 as the supporting electrolyte) at 22 ^{o}C. Cyclic voltammograms measured at a scan rate of ν = 200 mV s^{-1}.

The electron donor strength of **4- 8** was evaluated by electrochemical oxidation at a platinum electrode as a 2.5 x 10^{-3} M solution in dichloromethane containing 0.2 M *n*-Bu_4NPF_6 as the supporting electrolyte. A quantitative evaluation of the CV peaks and peak currents with added ferrocene (as an internal standard, E_{ox} = 0.45 V vs. SCE) revealed that the first wave in the quasi reversible cyclic voltammograms of **4** and **5** correspond to the production of the dication (by transfer of two electron) at E_{ox1} = 1.45, 1.41 (V vs. SCE), while cyclic voltammograms of **6**, **7** and **8** correspond to the production of mono cation (by transfer of one electron) at E_{ox1} = 1.35, 1.17 and 1.06 (V vs. SCE) respectively. The second oxidation in **6**, **7** and **8** (E_{ox2} = 1.49, 1.30 and 1.15 V) occur at relatively higher potentials (see Figure 5), and thus are indicative of the effective electronic coupling amongst aryl groups.[12] Note that the removal of the first electron from **6**, **7** and **8** results in the corresponding cation radicals where a charge is delocalized over two non-cofacial aryl moieties in **6**, **7** and **8**, thereby rendering the ejection of the second electron from both $\mathbf{6}^{+\bullet}$, $\mathbf{7}^{+\bullet}$ and $\mathbf{8}^{+\bullet}$ difficult by roughly ~140, 130 and 90 mV, respectively.

It is interesting to note that cyclic voltammogram of **9** shows one quasi reversible oxidation wave at 1.61 V vs. SCE while **9R** undergoes irreversible oxidation at 1.86 V vs. SCE. Enlarged biarylether **10** and its reference compound **10R** shows first oxidation wave at 1.21 and 1.17 V vs. SCE, while second oxidation wave is at 1.43 and 1.41 V vs. SCE (see Experimental section for the cyclic voltammograms).

Table 1. Table showing various biarylethers and corresponding reference compounds with their oxidation potentials.

Biarylethers	E_{ox1}/E_{ox2} (V vs SCE)	Reference Compds.	E_{ox1}/E_{ox2} (V vs SCE)
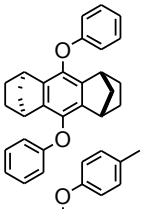 **4**	1.45	 **4R**	1.76
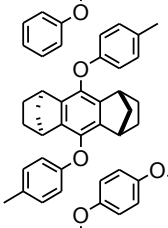 **5**	1.41	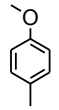 **5R**	1.72
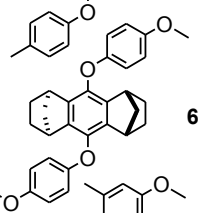 **6**	1.35/1.49	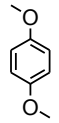 **6R**	1.36
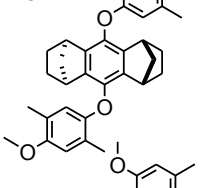 **7**	1.17/1.30	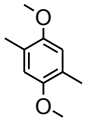 **7R**	1.13
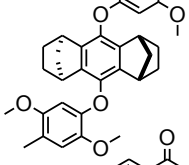 **8**	1.06/1.15	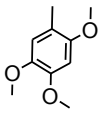 **8R**	0.98
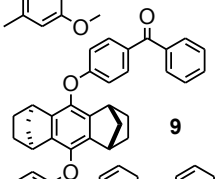 **9**	1.61	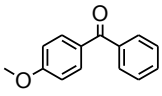 **9R**[a]	1.86
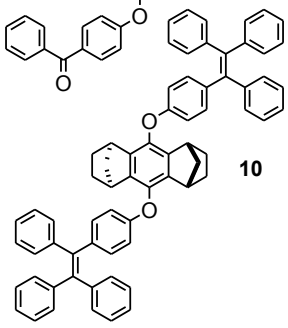 **10**	1.21/1.43	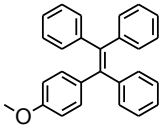 **10R**	1.17/1.41

a= **9R** showed irreversible oxidation wave

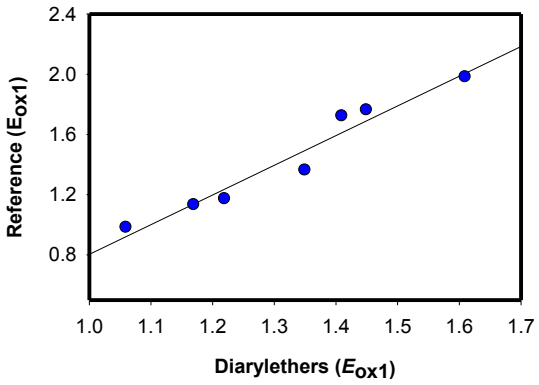

Figure 6. A correlation between E_{ox1} of **4-10** and **4R-10R**[13] in CH_2Cl_2 at 22 °C.

E_{ox1} values of **4-10** and **4R-10R** showed linear correlations which indicate that upon oxid-ation of **1-7** electrons are removed from the aryl groups and not from the biscycloannulated core.

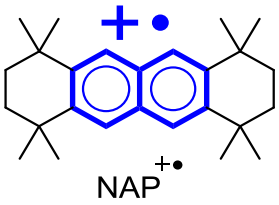

E^{o}_{red} $\quad E_{red} = 1.34$ V (V *vs.* SCE)

The electrochemical reversibility and relatively low oxidation potentials of **7** and **8** allow the generation of their cation radicals in solution using a hindered naphthalene cation radical ($NAP^{+\bullet}$, E_{red} = 1.34 V vs. SCE; λ_{max} = 672, 616, 503, and 396 nm; ε_{672} = 9300 M^{-1} cm^{-1})[14] as stable (aromatic) one-electron oxidants. $\mathbf{4}^{+\bullet}$, $\mathbf{5}^{+\bullet}$ and $\mathbf{6}^{+\bullet}$ were generated by treating **4**, **5** and **6** with one equivalent of NO^{+} $SbCl_6^{-}$[15] respectively

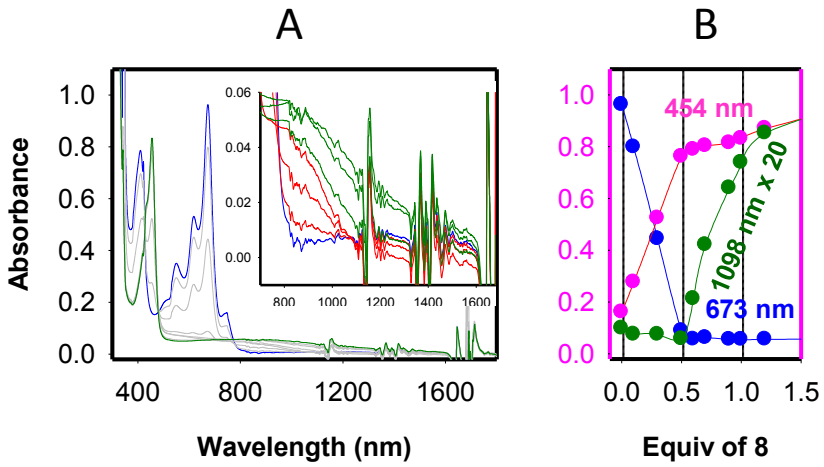

Figure 7. **A**: The spectral changes upon the reduction of 1.07 x 10^{-4} M $NAP^{+\bullet}$ by an incremental addition of sub-stoichiometric amounts of **8** in CH_2Cl_2 at 22 ^{o}C, inset shows the partial zoomed spectrum showing dicationic (red trace) and monocationic (green trace) transitions **B**: A plot of depletion of absorbance of $NAP^{+\bullet}$ (blue squares, at 673 nm) and an increase of the absorbance of $\mathbf{8}^{+\bullet}$ (green circles, at 1098 nm) against the equivalent of added neutral **8**.

Thus, Figure 7A shows the spectral changes attendant upon an incremental addition of sub-stoichiometric amounts of **8** to a solution of $NAP^{+\bullet}$ in dichloromethane at 22 °C. A plot of formation of the $\mathbf{8}^{++}$ (i.e. increase in the absorbance at 454 nm) against the increments of added neutral **8** (see Figure 7B), established that $NAP^{+\bullet}$ was completely consumed after the addition of 0.5 equiv. of **8**; further addition of neutral **8** resulted in the formation of $\mathbf{8}^{+\bullet}$ by the disproportionation of $\mathbf{8}^{++}$. A plot of formation of $\mathbf{8}^{+\bullet}$ (i.e. incr-ease in the absorbance at 1098 nm) against the increments of added neutral **8** shows a band in the Near-IR region[16] at 1098 nm (extending upto 1600 nm) increases only after addition of 0.5 equiv. of **8**.

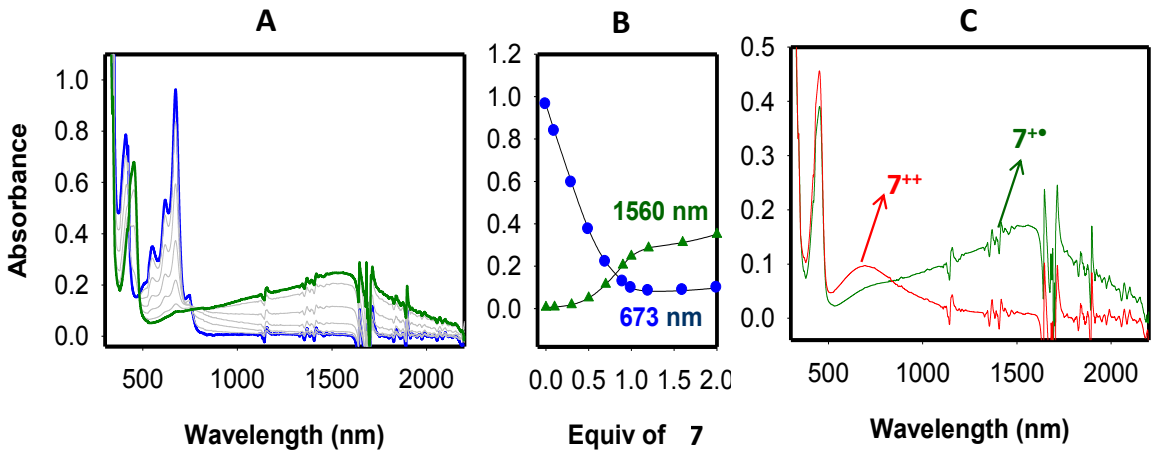

Figure 8. **A**: The spectral changes upon the reduction of 1.07 x 10^{-4} M $NAP^{+\bullet}$ by an incremental addition of sub-stoichiometric amounts of **7** in CH_2Cl_2 at 22 ^oC. **B**: A plot of depletion of absorbance of $NAP^{+\bullet}$ (blue squares, at 673 nm) and an increase of the absorbance of $\mathbf{7}^{+\bullet}$ (green triangles, at 1560 nm) against the equivalent of added neutral **7**. **C**: A qualitative spectra for $\mathbf{7}^{+\bullet}$ and $\mathbf{7}^{++}$, obtained using $NO^+SbCl_6^-$ as an oxidant.

Figure 8A shows the spectral changes attendant upon the reduction of 1.07 x 10^{-4}M $NAP^{+\bullet}$ by an incremental addition of **7** in dichloromethane at 22 ^oC. A plot of formation of $\mathbf{7}^{+\bullet}$ (i.e. increase in the absorbance at 1560 nm) against the increments of **7** established $NAP^{+\bullet}$ was completely consumed by addition of one equivalent of **7**. Moreover, in a separate experiment $\mathbf{7}^{++}$ was generated by treating a solution of **7** with two equivalents of $NO^+ SbCl_6^-$ i.e. Figure 8C. This was further confirmed by the reverse titration i.e. by incremental addition of $NAP^+ SbCl_6^-$ to 1.07 x 10^{-4}M solution of **7**, see Figure 9A. A plot of formation of $\mathbf{7}^{+\bullet}$ (i.e. increase in the absorbance at 1560 nm) against

the added increments of $NAP^{+}SbCl_6^{-}$ (see Figure 9B) established that the NIR band centered at 1560 nm corresponds to the $\mathbf{7}^{+\bullet}$.

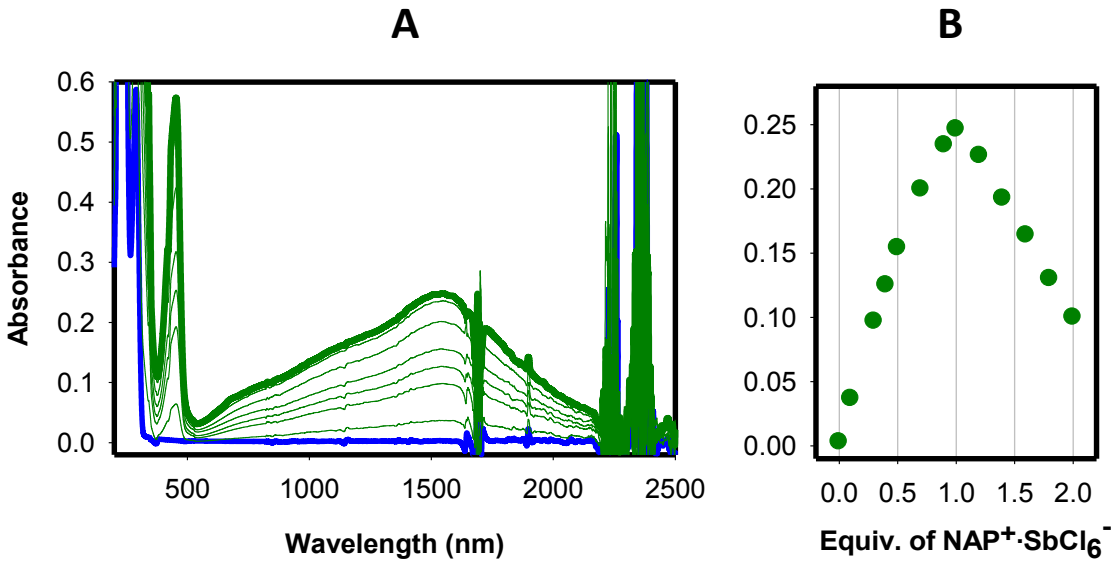

Figure 9. **A**: The spectral changes upon the reduction of 1.07 x 10^{-4} M **7** by an incremental addition of sub-stoichiometric amounts of $NAP^{+\bullet}$ in CH_2Cl_2 at 22 ^{o}C. **B**: A plot of an increase of the absorbance of $\mathbf{7}^{+\bullet}$ (green circles, at 1560 nm) against the equivalent of added $NAP^{+}SbCl_6^{-}$.

Similarly, the cation radicals of donors **4-6** were obtained by the treatment of **4-6** with one equivalent NO^{+} $SbCl_6^{-}$ respectively in CH_2Cl_2 at 22 ^{o}C under argon atmosphere.

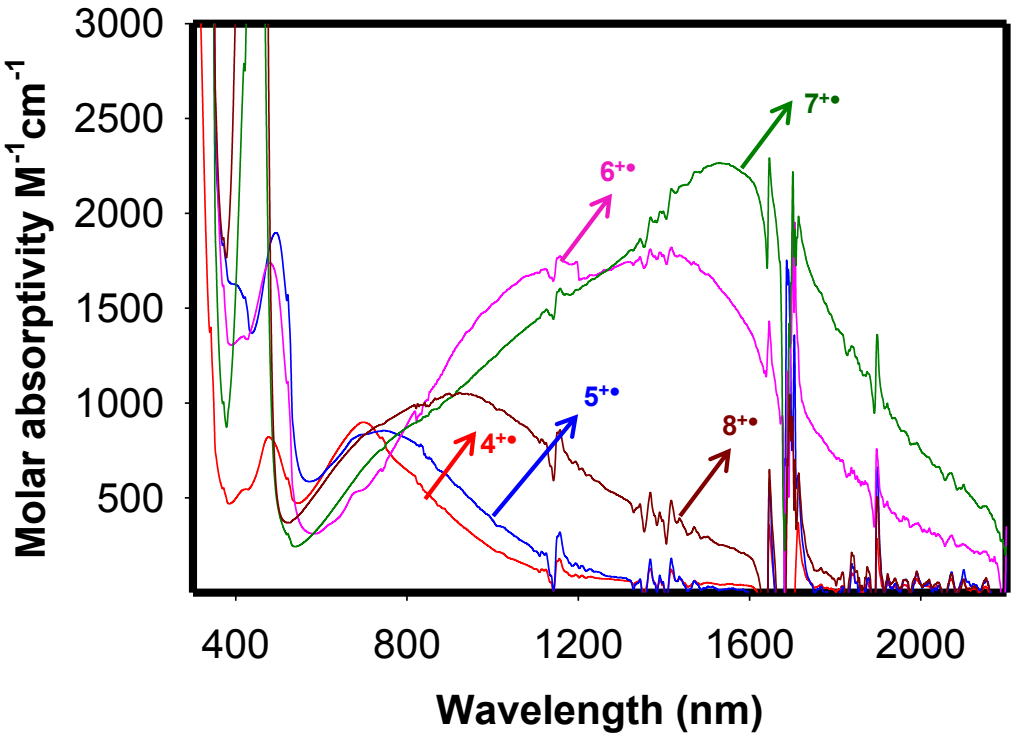

Figure 10. A comparison of the absorption spectras of **4**-**8** cation radicals in CH_2Cl_2 at 22 ^oC.

The observation of reasonable NIR transitions in the absorption spectra of $\mathbf{4}^{+\bullet}$, $\mathbf{5}^{+\bullet}$ and $\mathbf{8}^{+\bullet}$ while $\mathbf{6}^{+\bullet}$ and $\mathbf{7}^{+\bullet}$ showed most intense NIR transitions with bathochromic shift. The cation radicals of donors **4**-**8**, are highly persistent at ambient temperatures and did not show any decomposition during a 12 h period at ~22 °C, as confirmed by UV-vis spectral analysis.

In efforts to crystallize either cation radicals or dications, the single crystals of the $\mathbf{8}^{++}(SbCl_6^-)_2$, suitable for X-ray crystallography, were obtained by a slow diffusion of toluene into the dichloromethane solutions of $\mathbf{8}^{+\bullet}$ $SbCl_6^-$, prepared using equimolar NAP^+ $SbCl_6^-$ as a 1-e^- oxidant, at -10 ^oC during the course of 2 days. Note that the repeated attempts to obtain single crystals of $\mathbf{8}^{+\bullet}$ $SbCl_6^-$, $\mathbf{6}^{+\bullet}$ $SbCl_6^-$ and $\mathbf{7}^{+\bullet}$ $SbCl_6^-$, suitable for X-ray

crystallography, have been thus far unsuccessful. The crystallographic analysis of the highly-colored crystals of $\mathbf{8}^{++}(SbCl_6^-)_2$ revealed the unremarkable arrangement of dicationic **8** and hexachloroantimonate anion.

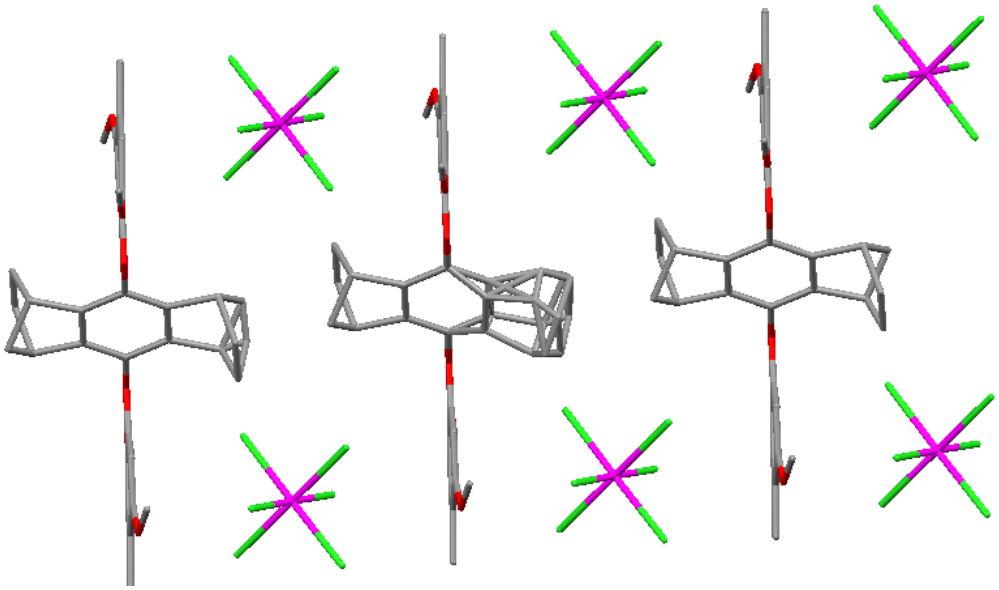

Figure 11. Arrangement of $\mathbf{8}^{++}$ and $SbCl_6^-$ in a single layer, solvent molecules are omitted for clarity.

We have previously shown that the bond length changes upon one and two electron oxidation in the molecule can be accurately predicted using DFT calculations at B3LYP/6-31G* level. On the similar ground DFT calculations were run on **8**, $\mathbf{8}^{+\bullet}$ and $\mathbf{8}^{++}$, indeed the X-ray crystallographic analysis of neutral and dicationic structures of **8** showed same trend predicted by DFT calculations.[17]

Table 2. Experimental and theoretical bond lengths of the neutral and dication of **8** presented in picometers (pm). Numbering scheme for the skeleton of **8** and its HOMO, obtained by DFT calculations at B3LYP/6-31G* level.

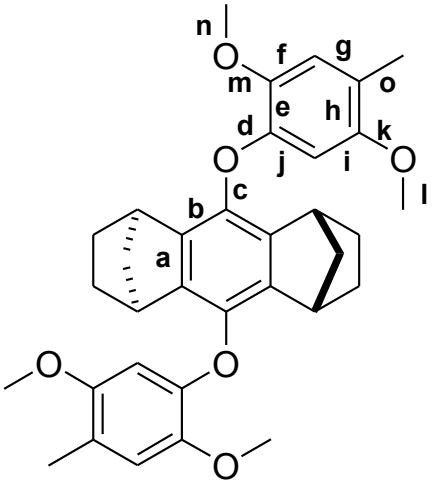

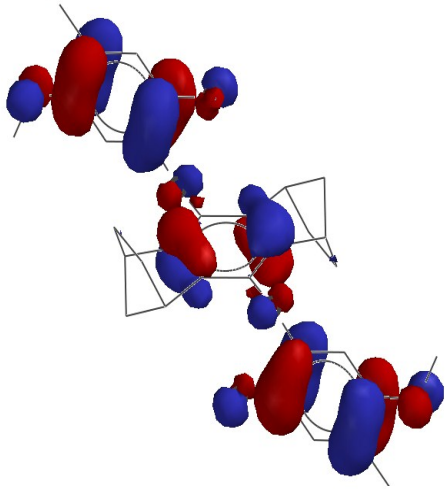

Bond Type	B3LYP/6-31G*			X-Ray Data		
Bond[1]	**8**	**8**$^{++}$	Δ (**8**$^{++}$-**8**)	**8**	**8**$^{++}$	Δ (**8**$^{++}$-**8**)
a	140.7	140.1	-0.6	139.9	140.3	+0.4
b	139.4	140.5	+1.1	141.4	142.1	+0.7
c	138.8	137.7	-1.1	138.5	140.7	+2.2
d	137.8	134.6	-3.2	137.7	134.4	-3.3
e	140.6	144.4	+4.4	139.7	144.5	+4.8
f	139.6	140.6	+1.0	138.8	140.4	-1.6
g	140.0	139.1	-0.9	139.7	136.6	-3.1
h	140.2	144.6	+4.4	139.1	143.9	+4.8
i	140.0	139.8	-0.2	139.2	139.3	+0.1
j	139.4	139.1	-0.3	138.5	136.4	-2.1
k	137.3	133.2	-4.1	137.5	132.4	-5.1

l	141.6	143.6	+2.0	142.6	145.6	+3.0
m	136.9	132.3	-4.6	136.8	130.8	-6.0
n	141.5	144.4	+2.9	142.5	146.0	+3.5
o	150.8	149.7	-1.1	150.5	150.5	0.0
σ	--	--	--	0.5	0.6	--

[1]Average of equivalent bonds.

An inspection of the bond length changes in $\mathbf{8}^{++}$, together with a comparison of its neutral form, suggest that aryl (dimethoxytolyl) groups in $\mathbf{8}^{++}$ are identical (within the experimental precision for various C-C/C-O bond lengths) and thus imply that the cationic charge is evenly distributed over two aryl rings. Furthermore, the bond length changes in the $\mathbf{8}^{++}$, together with a comparison of its neutral form, the structure of which was established by X-ray crystallography, correspond to the predominant contributions from *para*-quinoidal resonance structure **A**, as judged by the significant shortening of bonds labeled '**d**, **g**, **j**, **k**, **m**' and elongation of bonds labeled '**c**, **e**, **h**' and '**i**', along with only marginal shortening of the bonds labeled '**d**' and '**f**', (see Scheme 3 and Table 2). It is also noted that the alternate resonance structures **B-E** does not seem to contribute to the stabilization of the cationic charge in any significant way. Interestingly bonds 'a, b and c' does not undergo major lengthening and shortening as opposed to the changes observed for bis-cycloannulated methyl hydroquinone ether, **2**.

Scheme 3. Resonance structures for the stabilization of cationic charge in $\mathbf{8}^{++}$.

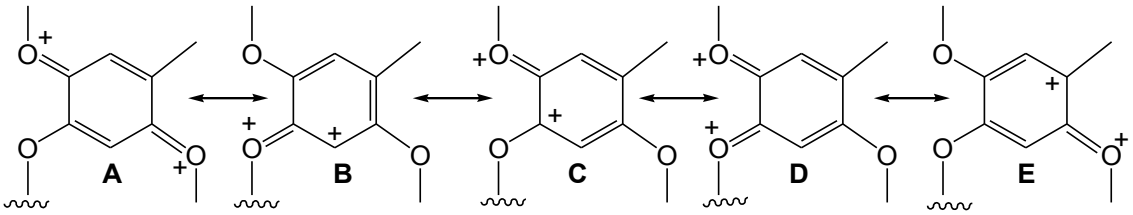

It is noteworthy that the experimental observations of the similar bond length changes in dimethoxytolyl moieties together with a significant shortening of the bonds labeled '**d**, **g**, **j**, **k**, **m**'' in $\mathbf{8}^{++}$ were found to be in reasonable agreement with the calculated values obtained using DFT calculations at the B3LYP/6-31G* level (see Table 2). Agreement of theoretical and experimental data for **8** and $\mathbf{8}^{++}$ advocates the use of DFT calculations at B3LYP/6-31G* level for calculations of bond length changes in neutral as well as mono and dicationic species. Similarly bond length changes in **4**-**7** and their mono and dicationic species were obtained results of which are presented in Table 3-4. It is clear from the Table 3 and 4 that bond **a**, **b** and **c** undergoes minor changes while major bond length changes occur in the aryl rings.

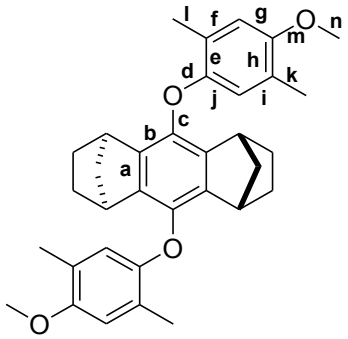

Table 3. Theoretical bond lengths of the neutral, monocation and dication of **7** presented in picometers (pm). Numbering scheme for the skeleton of **7** and its HOMO, obtained by DFT calculations at B3LYP/6-31G* level

Bond Type	**B3LYP/6-31G***				
Bond[1]	**7**	$\mathbf{7}^{+\bullet}$	$\mathbf{7}^{++}$	Δ ($\mathbf{7}^{+\bullet}$-**7**)	Δ ($\mathbf{7}^{++}$-**7**)
a	140.7	140.1	139.6	-0.6	-1.1
b	139.4	140.4	141.4	+1.0	+2.0
c	138.8	137.5	136.0	-1.3	-2.8
d	138.7	137.0	135.5	-1.7	-3.2
e	140.0	141.2	142.8	+1.2	+2.8
f	140.0	139.2	138.4	-0.8	-1.6
g	139.7	140.5	141.3	+0.8	+1.6
h	140.6	142.3	144.1	+1.7	+3.5
i	139.6	138.6	138.0	-1.0	-1.6
j	139.7	140.4	140.9	+0.7	+1.2
k	150.8	150.5	150.1	-0.3	-0.7
l	150.8	150.6	150.2	-0.2	-0.6
m	137.4	134.8	132.4	-2.6	-5.0
n	141.5	143.0	144.5	+1.5	+3.0

[1]Average of equivalent bonds.

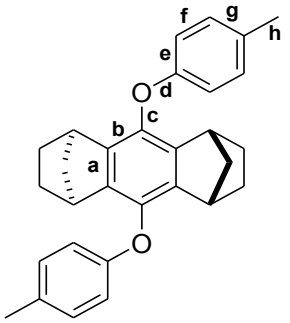

Table 4. Theoretical bond lengths of the neutral, monocation and dication of **6** presented in picometers (pm). Numbering scheme for the skeleton of **6** and its HOMO, obtained by DFT calculations at B3LYP/6-31G* level

Bond Type	**B3LYP/6-31G***				
Bond[1]	**6**	**$6^{+\bullet}$**	**6^{++}**	**$\Delta(6^{+\bullet}\text{-}6)$**	**$\Delta(6^{++}\text{-}6)$**
a	140.7	139.0	138.7	-1.7	-2.0
b	139.4	142.4	143.8	+3.0	+4.4
c	139.0	134.2	133.1	-4.8	-5.9
d	138.0	139.8	137.0	+1.8	-1.0
e	139.7	139.4	140.8	-0.3	+1.1
f	139.5	139.2	138.2	-0.3	-1.3
g	140.1	140.4	141.6	+0.3	+1.5
h	151.2	150.8	149.7	-0.4	-1.5

[1]Average of equivalent bonds.

SUMMARY and CONCLUSIONS

In summary we have demonstrated that bis-cycloannulated hydroquinone arylethers can be easily synthesized from readily available starting materials using Ullmann ether synthesis. These biaryl ethers (**5**-**10**) underwent reversible electrochemical oxidation and formed stable cation radical salts. Appearance of two 1e- oxidation waves for **6**-**8** separated by ~100 mV indicates the effective electronic coupling between two aryl groups. Observance of near-IR transition in the electronic spectrum of **4**-**7** cation radicals and X-ray crystal determination for $\mathbf{8}^{++}$ attest that single charge is localized evenly on terminal aryl groups. Furthermore it is shown that same methodology can be used to get larger molecules such as **10** which can be a potential candidate for functional molecular wire. Efforts are in progress to prepare linear mixed polyaryl ethers which will serve as models for molecular wires.

EXPERIMENTAL

General experimental methods and materials: All reactions were performed under argon atmosphere unless otherwise stated. Copper oxide, potassium carbonate, diphenylmethane, butyllithium, toluene, benzene and anhydrous pyridine were commercially available and were used without further purification. Bis-cycloannulated hydroquinone was synthesized according to the literature procedure (Rathore, R.; Burns, C. L.; Deselnicu, M. I.; Denmark, S. E.; Bui, T. *Org. Syn.* **2005**, *82***,** 1-9). Aryl halides such as bromobenzene, 1-bromo-4-methylbenzene, 1-bromo-4-methoxybenzene and 4-

methoxybenzophenone were commercially available while 1-bromo-4-methoxy-2,5-dimethylbenzene was synthesized from 2,5-dimethylanisole by NBS bromination.

Anhydrous tetrahydrofuran (THF) was prepared by refluxing commercial THF over lithium aluminum hydride under an argon atmosphere for 24 hours followed by distillation under an argon atmosphere. It was stored in a Schlenk flask equipped with a Teflon valve fitted with Viton O-rings. Dichloromethane was repeatedly stirred with fresh aliquots of conc. sulfuric acid (~10 % by volume) until the acid layer remained colorless. After separation, it was washed successively with water, aqueous sodium bicarbonate, water, and aqueous sodium chloride, and dried over anhydrous calcium chloride. The dichloromethane was distilled twice from P_2O_5 under an argon atmosphere and stored in a Schlenk flask equipped with a Teflon valve fitted with Viton O-rings. The hexanes and toluene were distilled from P_2O_5 under an argon atmosphere and then refluxed over calcium hydride (~12 hr). After distillation from CaH_2, the solvents were stored in Schlenk flasks under an argon atmosphere. NMR spectra were recorded on 300 and 400 MHz NMR spectrometers.

Cyclic Voltammetry (CV). The CV cell was of an air-tight design with high vacuum Teflon valves and Viton O-ring seals to allow an inert atmosphere to be maintained without contamination by grease. The working electrode consisted of an adjustable platinum disk embedded in a glass seal to allow periodic polishing (with a fine emery cloth) without changing the surface area (~1 mm^2) significantly. The reference SCE electrode (saturated calomel electrode) and its salt bridge were separated from the catholyte by a sintered glass frit. The counter electrode consisted of platinum gauze that was separated from the working electrode by ~3 mm. The CV measurements were carried

out in a solution of 0.1 to 0.2 M supporting electrolyte (tetra-*n*-butylammonium hexafluorophosphate, TBAH) and the substrate in dry dichloromethane under an argon atmosphere. All the cyclic voltammograms were recorded at a sweep rate of 200 mV sec^{-1}, unless otherwise specified and were IR compensated. The oxidation potentials ($E_{1/2}$) were referenced to SCE, which was calibrated with added (equimolar) ferrocene ($E_{1/2}$ = 0.450 V *vs*. SCE). The $E_{1/2}$ values were calculated by taking the average of anodic and cathodic peak potentials in reversible cyclic voltammograms or directly from square-wave voltammograms in irreversible cyclic voltammograms.

Synthesis of 4-Bromo-2,5-dimethoxytoluene.

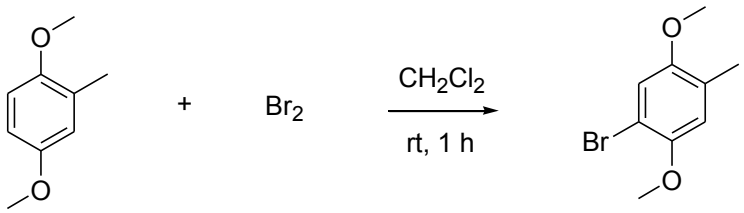

To a solution of 2,5-dimethoxyltoluene (20 g, 132 mmol) in dichloromethane (80 mL), a solution of bromine (23 g, 144 mmol) in dichloromethane (40 mL) was added dropwise over 30 min. After addition was complete the reaction mixture was kept stirring for additional 30 min at room temperature. Then the reaction mixture was washed with 5% aqueous solution of KOH (100 mL), water (100 mL), brine (50 mL), and dried over anhydrous $MgSO_4$. Removal of the solvent in *vacuo* afforded a crude product which was purified by recrystallization from a mixture of dichloromethane and methanol to afford 4-bromo-2,5-dimethoxytoluene as white crystals. Yield: 28.3 g, 92.5%; mp 76-77 ^oC; ^1H NMR ($CDCl_3$) δ: 2.17 (s, 3H), 3.76 (s, 3H), 3.82 (s, 3H), 6.73 (s, 1H), 6.97 (s, 1H); ^{13}C NMR ($CDCl_3$) δ: 16.38, 56.08, 56.95, 108.06, 115.23, 115.39, 126.86, 149.75, 152.22.

^{1}H NMR spectrum of 4-bromo-2,5-dimethoxytoluene

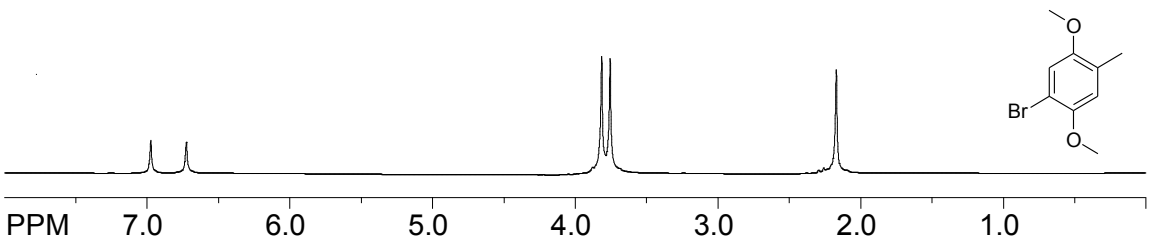

^{13}C NMR spectrum of 4-bromo-2,5-dimethoxytoluene

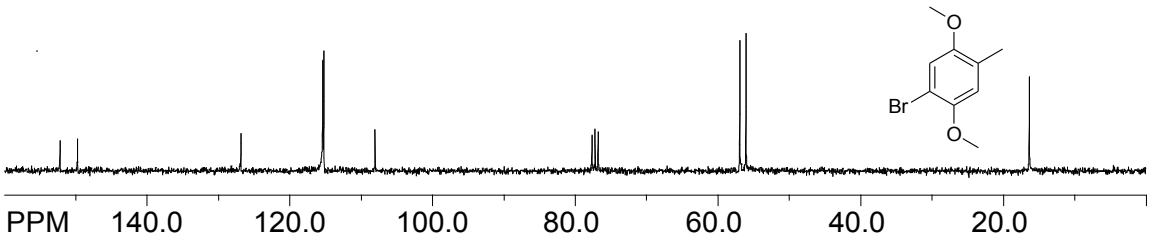

Synthesis of *p*-diaryloxybenzenes: ***General procedure:***

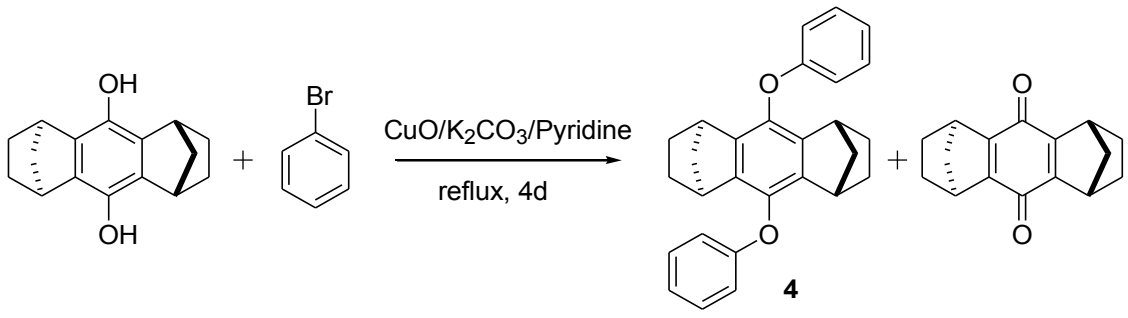

For 5 min. argon was bubbled through a suspension of hydroquinone (1.0 g, 4.1 mmol), bromobenzene (1.9 g, 12.4 mmol), and anhydrous K_2CO_3 (3.45 g, 25 mmol) in 20 mL pyridine. CuO (1.0 g, 12.4 mmol) was then added and the stirring mixture was vigorously refluxed for 4 d. After this time, the reaction was cooled and the solvent was removed

under reduced pressure. The remaining solid was re-suspended in CH_2Cl_2 and run through a short silica gel plug with 100% CH_2Cl_2. Removal of the solvent gave the crude product as a dark brown solid. Column chromatography with 9:1 hexanes: ethyl acetate as mobile phase gave **4** (90 mg, 10%) as a white solid and 0.45 g quinone (Yield is calculated after considering the amount of quinone recovered from the reaction). mp 239-241^{o}C; ^{1}H NMR ($CDCl_3$) 1.06- 1.13 (m, 4H), 1.34 (td, 2H, *J* = *8.7* Hz, 1.5 Hz), 1.61-1.67 (m, 2H), 1.68-1.74 (m, 4H), 3.30 (t, 4H, *J* = 1.7 Hz), 6.86-6.90 (m, 4H), 6.97-7.02 (m, 2H), 7.26-7.32 (m, 4H); ^{13}C NMR ($CDCl_3$) 26.54, 40.82, 49.38, 115.88, 121.62, 129.66, 139.20, 139.59, 159.41. The molecular structure of **4** was also established by X-ray crystallography, see Figure S1

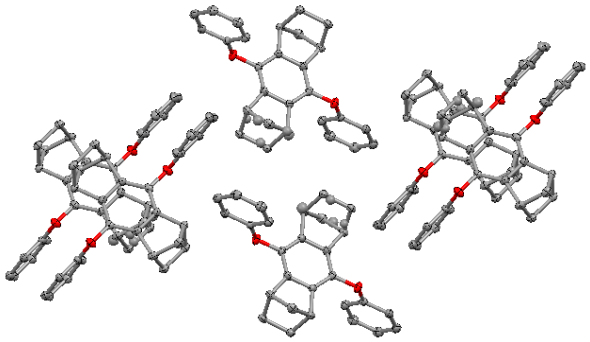

Figure S1. ORTEP diagram of **4**

^{1}H NMR spectra of 4 ($CDCl_3$)

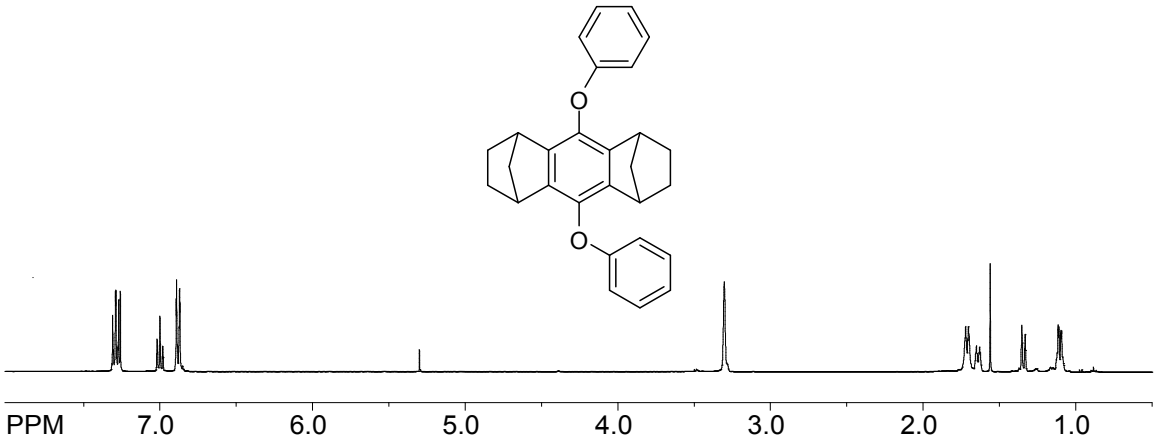

^{13}C NMR spectra of 4 ($CDCl_3$)

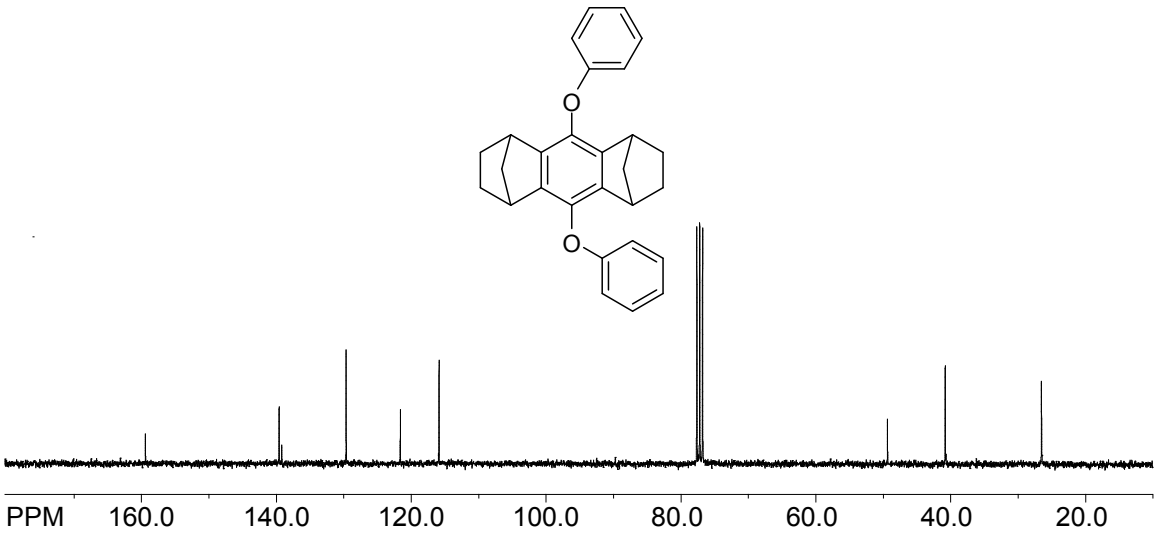

Synthesis of 5: using the general procedure described above hydroquinone (2.0 g, 8.3 mmol), 1-bromo-4-methylbenzene (4.3 g, 25 mmol), K_2CO_3 (6.9 g, 50 mmol) and CuO (2.0 g, 25 mmole) was reacted to give crude product which was purified by silica column chromatography using 9:1 hexane: ethyl acetate as mobile phase to give **5** (150 mg, 7%) as a white solid and quinone (0.73 g) (Yield was calculated after considering the amount of quinone recovered from the reaction). mp 258-260 ^{o}C; ^{1}H NMR ($CDCl_3$) 1.07-1.11 (m, 4H), 1.33 (td, 2H, J = 8.8 Hz, 1.5 Hz), 1.60-1.65 (m, 2H), 1.68-1.74 (m, 4H), 2.31 (s, 6H), 3.30 (t, 4H, J = 1.7 Hz), 6.77 (d, 4H, J = 8.6 Hz), 7.08 (d, 4H, J = 8.6 Hz); ^{13}C NMR ($CDCl_3$) 20.78, 26.59, 40.81, 49.34, 115.63, 130.09, 130.81, 139.32, 139.50, 157.35. The molecular structure of **5** was also established by X-ray crystallography, see Figure S2

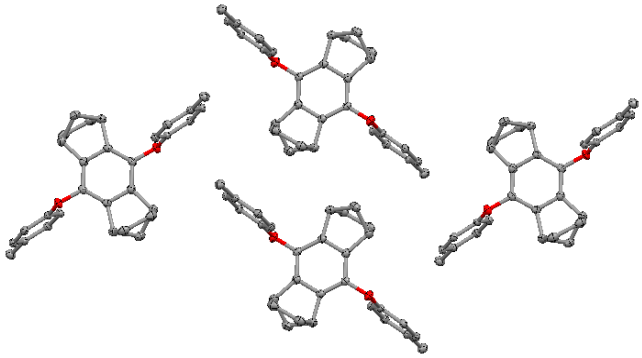

Figure S2. ORTEP diagram of **5**

^{1}H NMR spectra of 5 ($CDCl_3$)

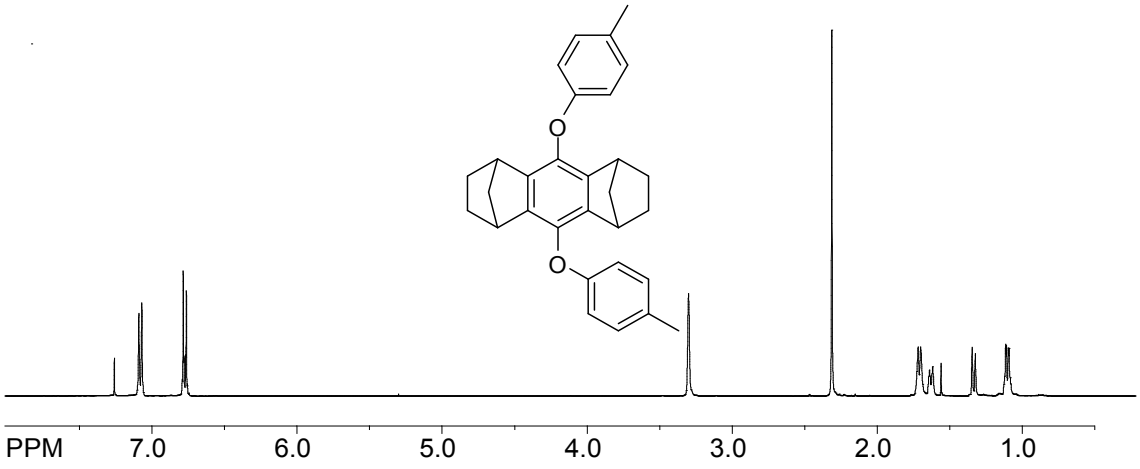

^{13}C NMR spectra of 5 ($CDCl_3$)

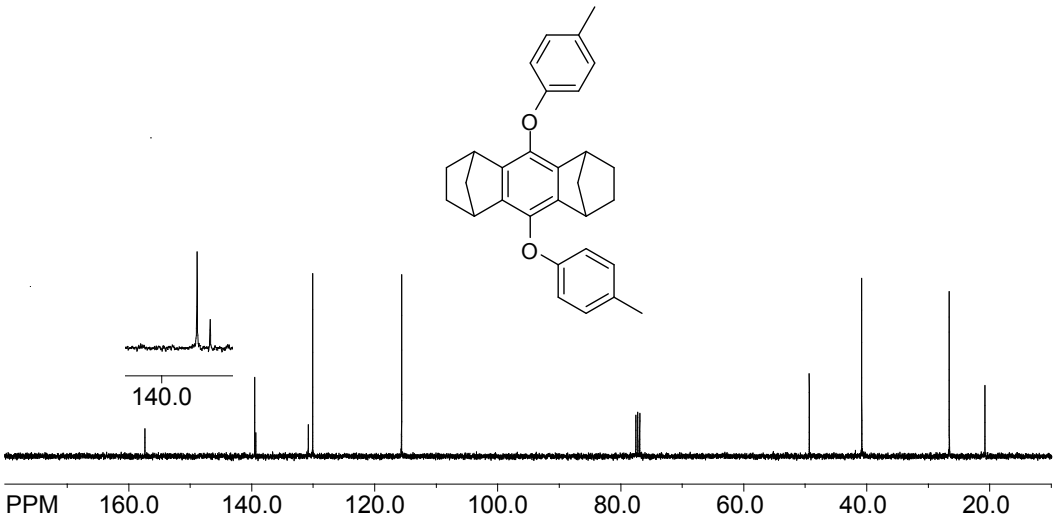

Synthesis of 6: using the general procedure described above hydroquinone (2.0 g, 8.3 mmol), 1-bromo-4-methoxylbenzene (4.6 g, 25 mmol), K_2CO_3 (6.9 g, 50 mmol) and CuO (2.0 g, 25 mmole) was reacted to give crude product which was purified by silica column chromatography using 8:2 hexane : ethyl acetate as mobile phase to give **6** (180 mg, 7%) as a white solid and quinone (0.65 g) (Yield was calculated after considering the amount of quinone recovered from the reaction). mp 208-210 ^{o}C; ^{1}H NMR ($CDCl_3$) 1.02-1.12 (m, 4H), 1.30-1.36 (m, 2H), 1.58-1.74 (m, 6H), 3.29 (s, 4H), 3.78 (s, 6H), 6.82 (s, 8H); ^{13}C NMR ($CDCl_3$) 26.58, 40.82, 49.34, 55.90, 114.73, 116.82, 139.37, 139.76, 153.56, 154.46. The molecular structure of **6** was also established by X-ray crystallography, see Figure S3

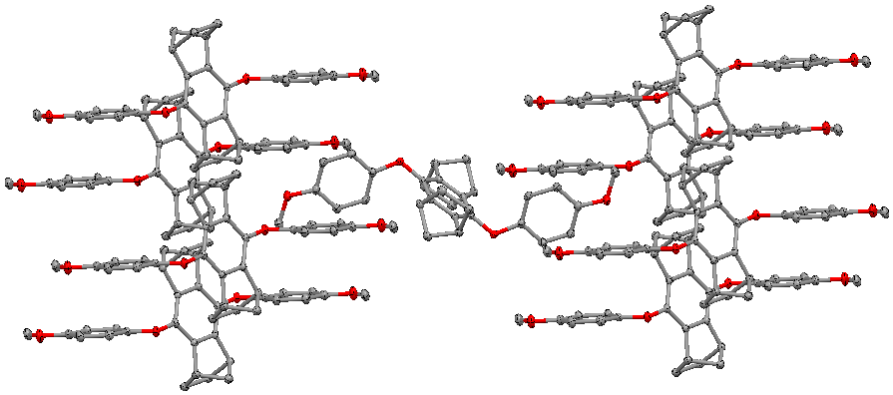

Figure S3. ORTEP diagram of **6**

^{1}H NMR spectra of 6 ($CDCl_3$)

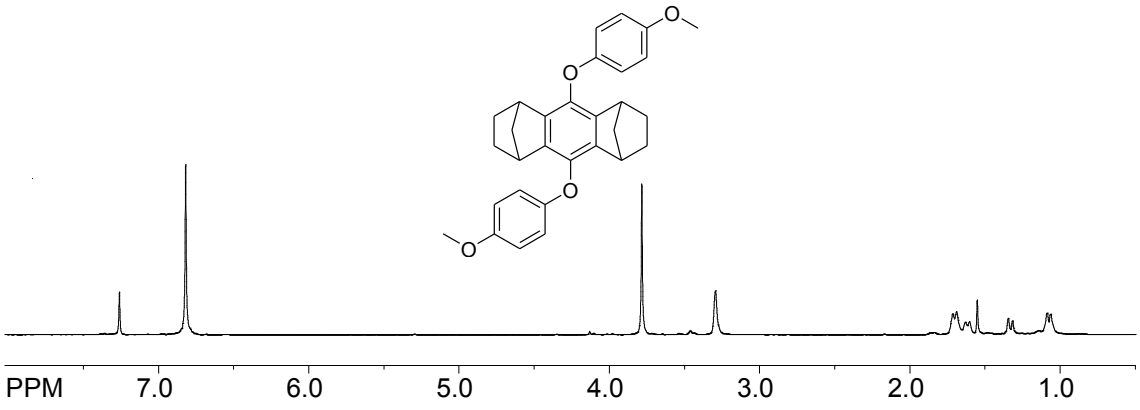

^{13}C NMR spectra of 6 ($CDCl_3$)

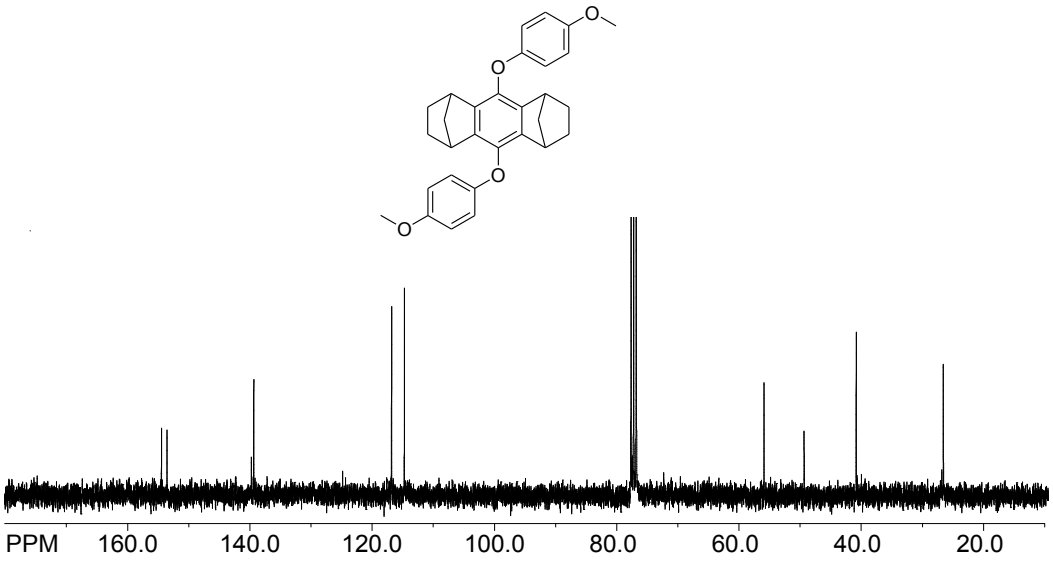

Synthesis of 7: using the general procedure described above hydroquinone (2.0 g, 8.3 mmol), 1-bromo-4-methoxy-2,5-dimethylbenzene (5.4 g, 25 mmol), K_2CO_3 (6.9 g, 50 mmol) and CuO (2.0 g, 25 mmole) was reacted to give crude product which was purified by silica column chromatography using 8:2 hexane: ethyl acetate as mobile phase to give **7** (pure **7** was obtained by recrystallization with dichloromethane and methanol) (520 mg, 18%) as a white solid and quinone (0.64 g) (Yield was calculated after considering the amount of quinone recovered from the reaction). mp 205-207 ^{o}C; ^{1}H NMR ($CDCl_3$) 1.05-1.15 (m, 4H), 1.28-1.36 (m, 2H), 1.60-1.74 (m, 8H), 2.06 (s, 6H), 2.39 (s, 6H), 3.18-3.28 (m, 4H), 3.81 (s, 6H), 6.33 (s, 2H), 6.69 (s, 2H); ^{13}C NMR ($CDCl_3$) 16.10, 16.62, 26.59, 40.77, 49.30, 56.10, 113.15, 117.64, 124.42, 138.78, 140.15, 150.95, 152.29.

^{1}H NMR spectra of 7 ($CDCl_3$)

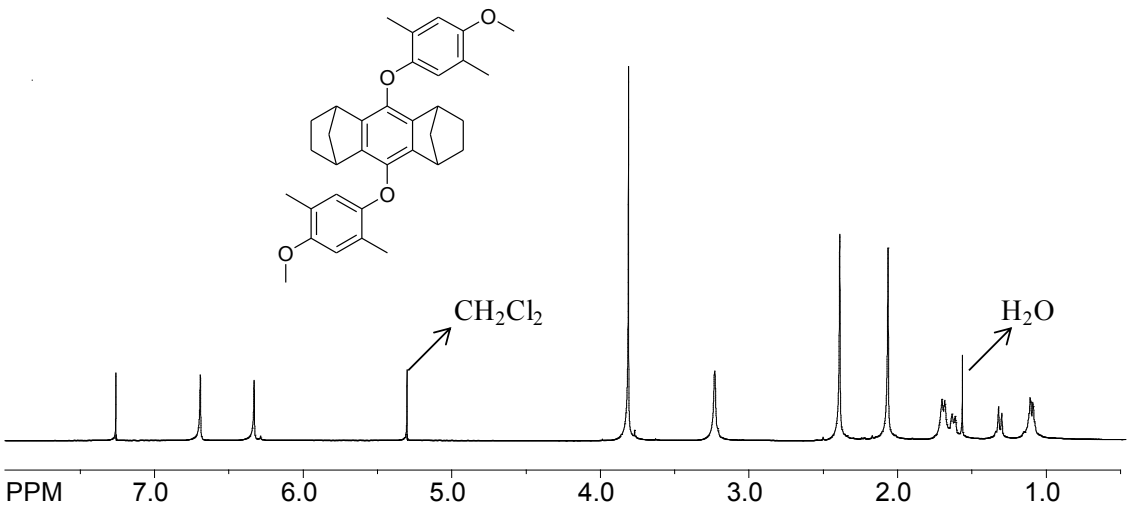

^{13}C NMR spectra of 7 ($CDCl_3$)

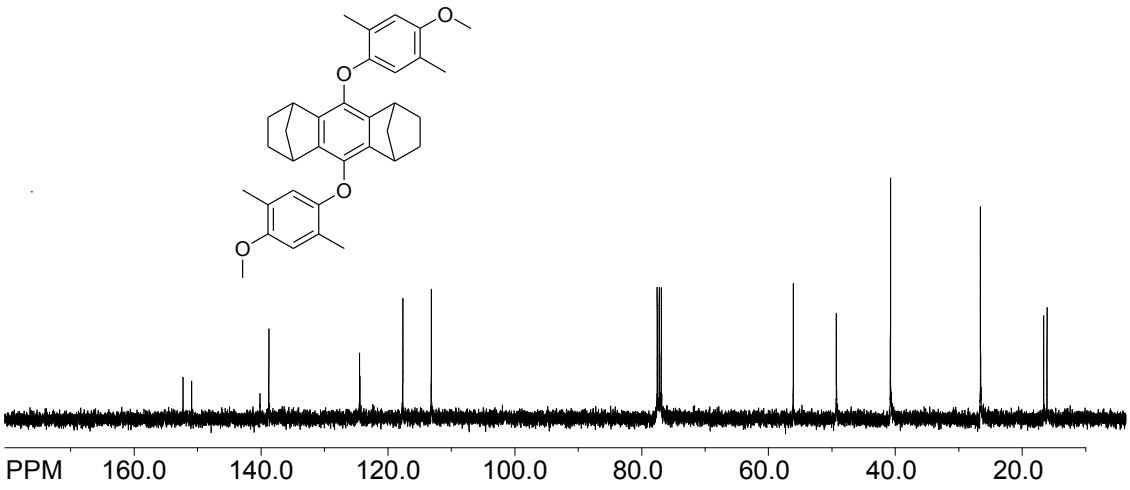

Synthesis of 8: using the general procedure described above hydroquinone (2.0 g, 8.3 mmol), 1-bromo-2,5-dimethoxy-4-methylbenzene (5.75 g, 25 mmol), K_2CO_3 (6.9 g, 50 mmol) and CuO (2.0 g, 25 mmole) was reacted to give crude product which was purified by silica column chromatography using 8:2 hexane: ethyl acetate as mobile phase to give **8** (pure **8** was obtained by recrystallization with dichloromethane and methanol) (520 mg, 18%) (710 mg, 26%) as a white solid and quinone (0.75 g) (Yield was calculated after

considering the amount of quinone recovered from the reaction). mp 184-186 ^{o}C; ^{1}H NMR ($CDCl_3$) 1.06-1.12 (m, 4H), 1.33-1.38 (m, 2H), 1.56-1.62 (m, 2H), 1.68-1.74 (m, 4H), 2.17 (s, 6H), 3.34 (m, 4H), 3.50 (s, 6H), 3.91 (s, 6H), 6.10 (s, 2H), 6.79 (s, 2H); ^{13}C NMR ($CDCl_3$) 15.82, 26.58, 40.82, 49.49, 55.89, 57.33, 100.11, 116.24, 119.10, 139.39, 139.54, 142.61, 147.17, 151.71. The molecular structure of **8** was also established by X-ray crystallography, see Figure S4

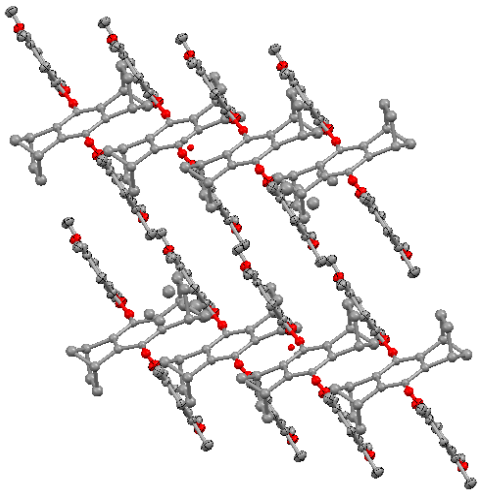

Figure S4. ORTEP diagram of **8**

^{1}H NMR spectra of 8 ($CDCl_3$)

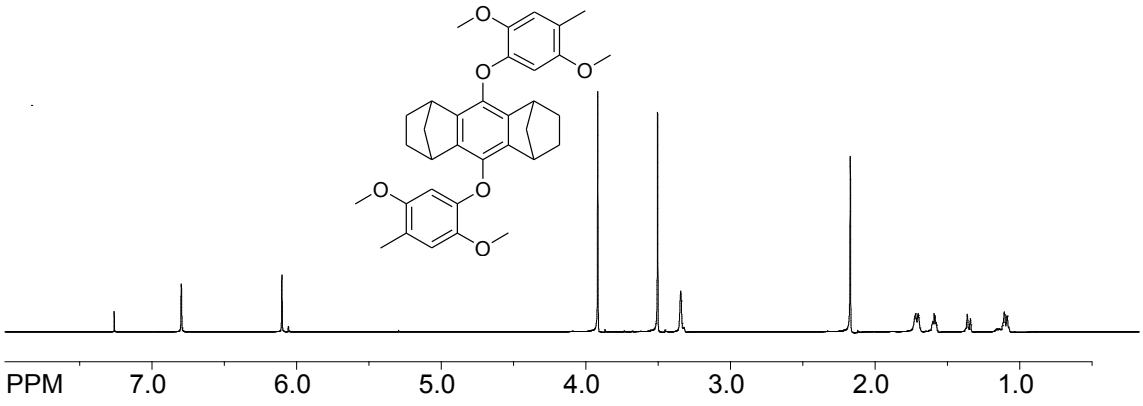

^{13}C NMR spectra of 8 ($CDCl_3$)

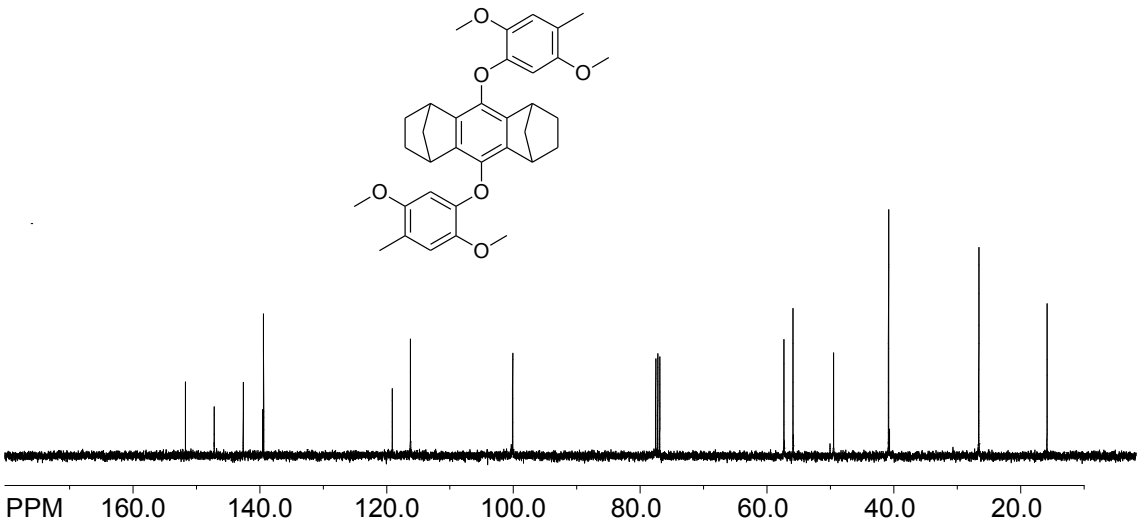

Synthesis of 9: using the general procedure described above hydroquinone (2.0 g, 8.3 mmol), 4-bromobenzophenone (6.50 g, 25 mmol), K_2CO_3 (6.9 g, 50 mmol) and CuO (2.0 g, 25 mmole) was reacted to give crude product which was purified by silica column chromatography using 7:3 hexane: ethyl acetate as mobile phase to give **9** (1.28 g, 32%) as a white solid and quinone (0.43 g) (Yield was calculated after considering the amount of quinone recovered from the reaction). mp 257-259 ^{o}C; ^{1}H NMR ($CDCl_3$) 1.08-1.20 (m, 4H), 1.40 (d, 2H, *J* = 8.5 Hz), 1.64-1.84 (m, 6H), 3.33 (s, 4H), 6.94 (d, 4H, *J* = 8.6 Hz), 7.47 (t, 4H, *J* = 7.5 Hz), 7.57 (t, 2H, *J* = 7.5 Hz), 7.78 (d, 4H, *J* = 7.5 Hz), 7.83 (d, 4H, *J* = 8.6 Hz); ^{13}C NMR ($CDCl_3$) 26.52, 40.85, 49.51, 115.31, 128.44, 129.97, 131.23, 132.23, 132.81, 138.31, 138.89, 139.81, 162.84, 195.72. The molecular structure of **9** was also established by X-ray crystallography, see Figure S5

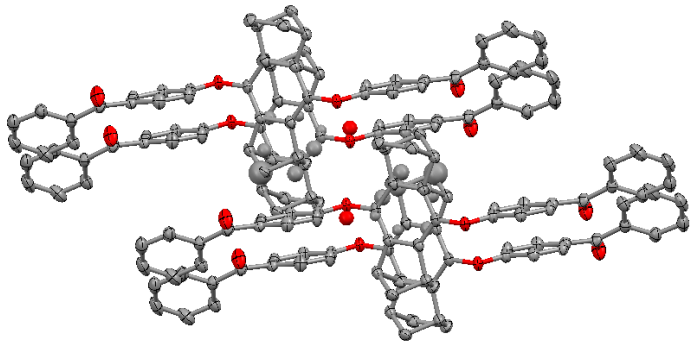

Figure S5. ORTEP diagram of **9**

^{1}H NMR spectra of 9 ($CDCl_3$)

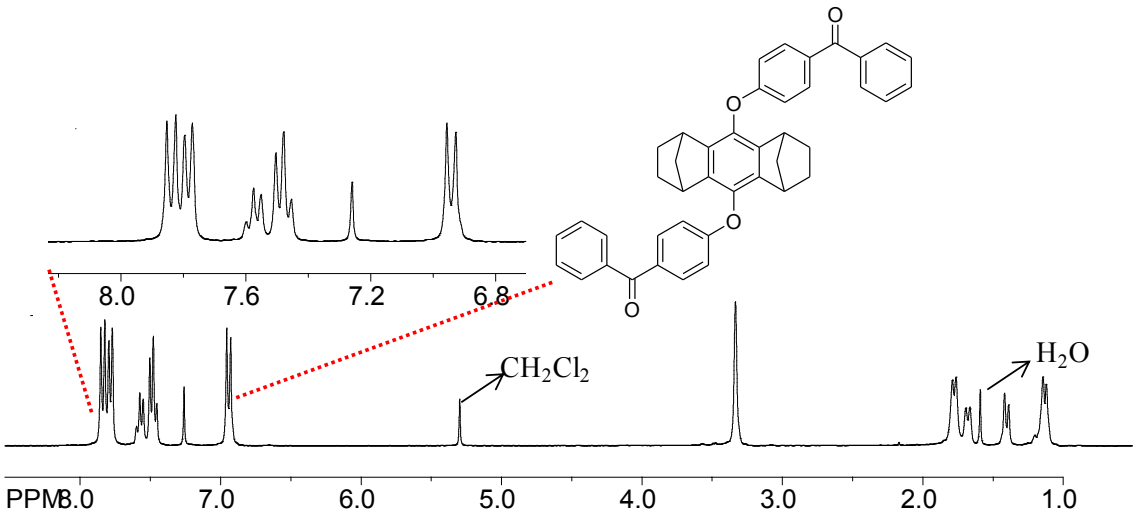

^{13}C NMR spectra of 9 ($CDCl_3$)

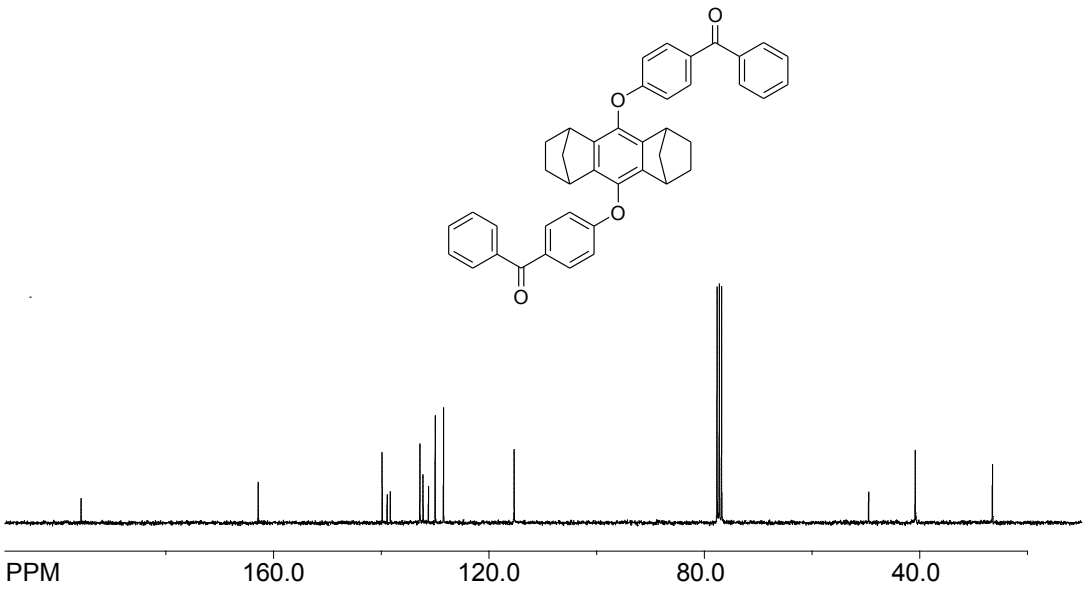

Synthesis of 10:

To a solution of diphenylmethane (1.0 g, 6 mmol) in dry tetrahydrofuran (20 mL) was added 2 mL of a 2.5 M solution of *n*-butyllithium in hexane (10 mmol) at 0 °C under an argon atmosphere. The resulting orange-red solution was stirred for 30 min at that temperature. To this solution was added the benzophenone **9** (0.6 g, 1 mmol) and the reaction mixture was allowed to warm to room temperature with stirring during a 6 h period. The reaction was quenched with addition of an aqueous solution of ammonium chloride, the organic layer was extracted with dichloromethane (3 x 25 mL), and the combined organic layers were washed with a saturated brine solution and dried over anhydrous $MgSO_4$. The solvent was evaporated, and the resulting crude alcohol (containing excess diphenylmethane) was subjected to acid-catalyzed dehydration where, the crude alcohol was dissolved in about 60 mL of toluene in a 100 mL Schlenk flask fitted with a Dean-Stark trap. A catalytic amount of *p*-toluenesulphonic acid (170 mg, 0.9

mmol) was added, and the mixture was refluxed for 3-4 h and cooled to room temperature. The toluene layer was washed with 10% aqueous $NaHCO_3$ solution (2 x 20 mL) and dried over anhydrous magnesium sulfate and evaporated to afford the crude tetraphenylethylene derivative. The crude product was purified by a simple recrystallization from a mixture of dichloromethane and methanol to yield **7** (900 mg 66%) as pale yellow colored solid. mp 317-319 ^{o}C; ^{1}H NMR ($CDCl_3$) 0.9-1.0 (m, 4H), 1.30 (m, 2H), 1.64-1.84 (m, 6H), 3.20 (s, 4H), 6.54 (d, 4H, J = 8.6 Hz), 6.89 (d, 4H, J = 8.6 Hz), 6.96-7.14 (m, 30H); ^{13}C NMR (CD_2Cl_2) 21.75, 36.18, 44.62, 110.94, 121.76, 121.82, 121.91, 123.15, 126.75, 126.78, 126.83, 127.90, 132.73, 134.55, 134.92, 136.03, 136.12, 139.33, 139.42, 139.52, 153.44

^{1}H NMR spectra of 10 ($CDCl_3$)

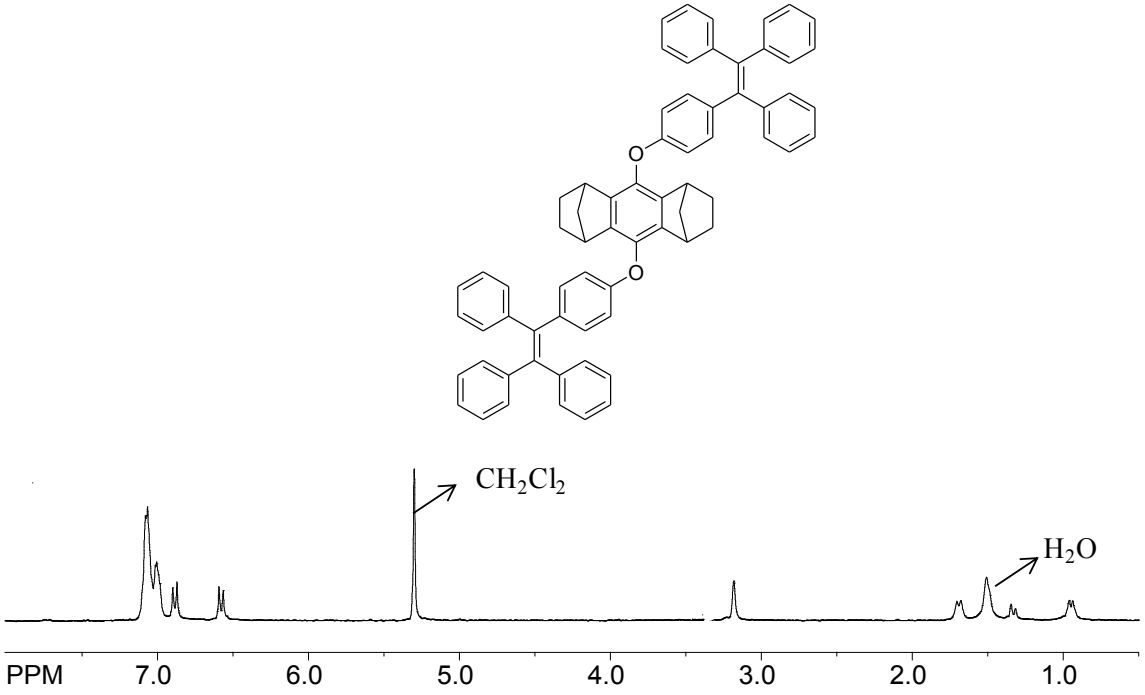

^{13}C NMR spectra of 10 (CD_2Cl_2)

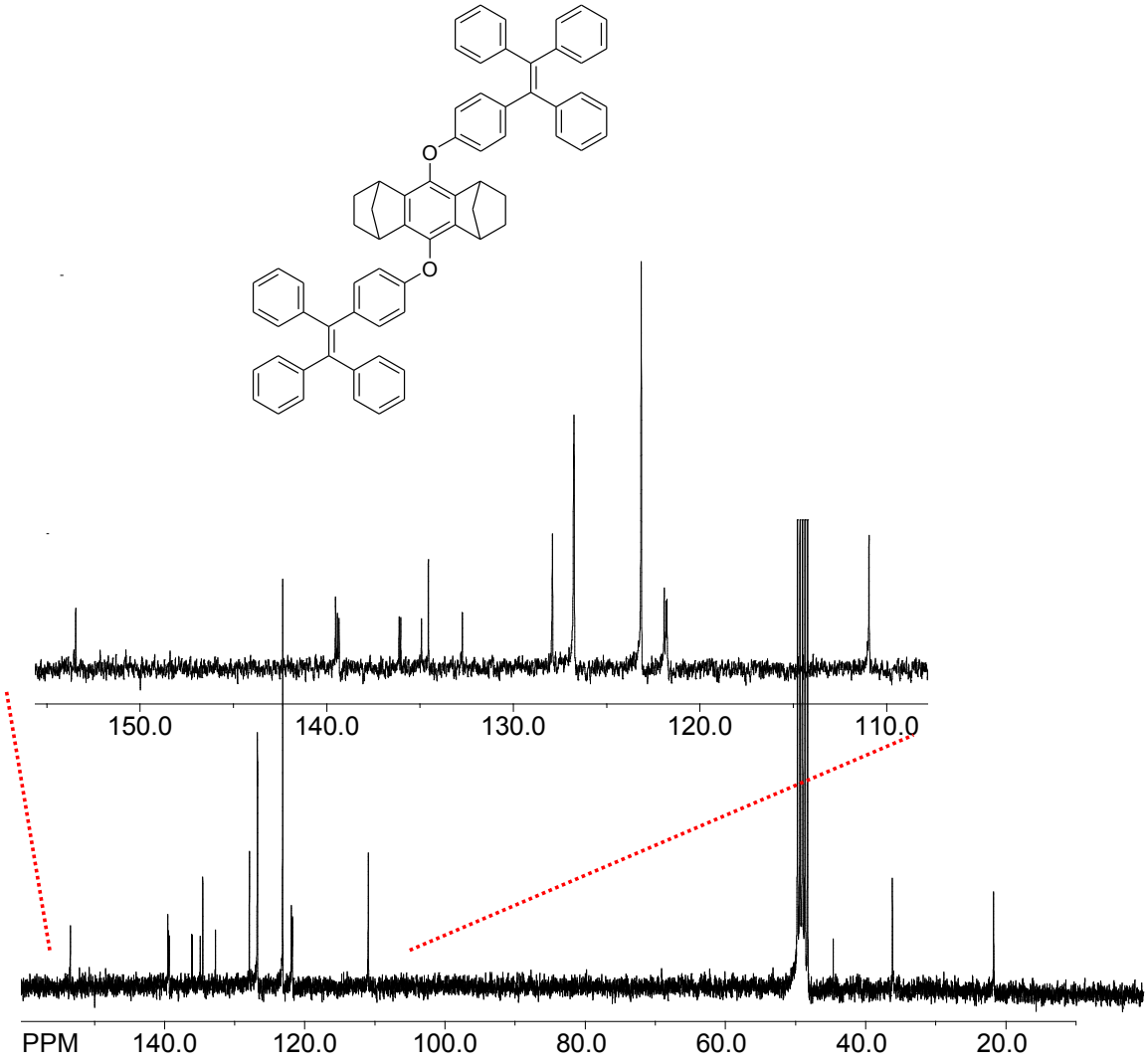

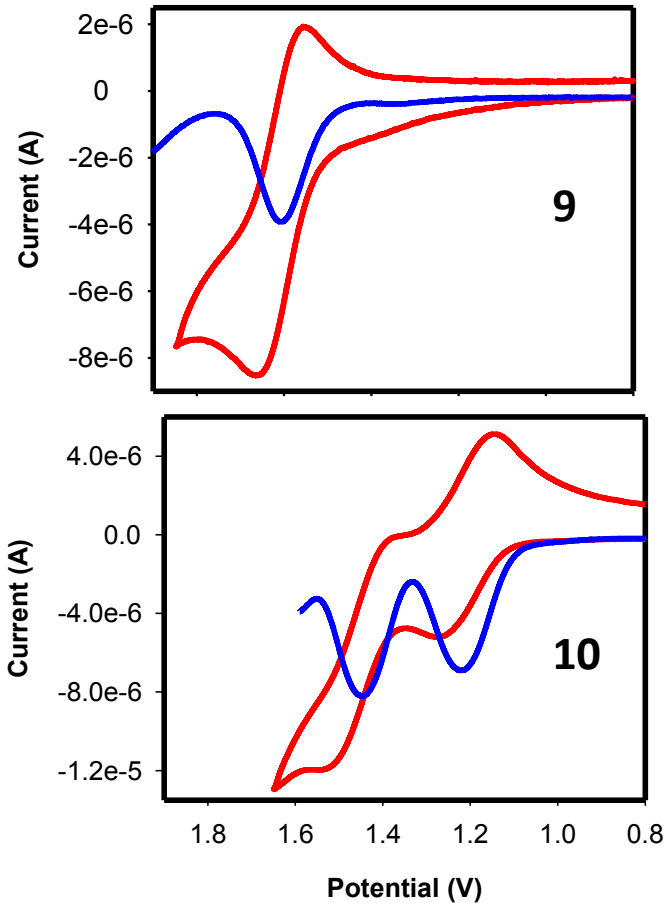

Figure S6. Cyclic voltammograms (red trace) and square waves (blue trace) of 2.5 x 10^{-3} M **9** and **10** in CH_2Cl_2 (containing 0.2 M nBu$_4$NPF$_6$ as the supporting electrolyte) at 22 ^{o}C. Cyclic voltammograms measured at a scan rate of ν = 200 mV s^{-1}.

***Table 5*. Crystal data and structure for structure refinement for raj11oa (8^{++})**

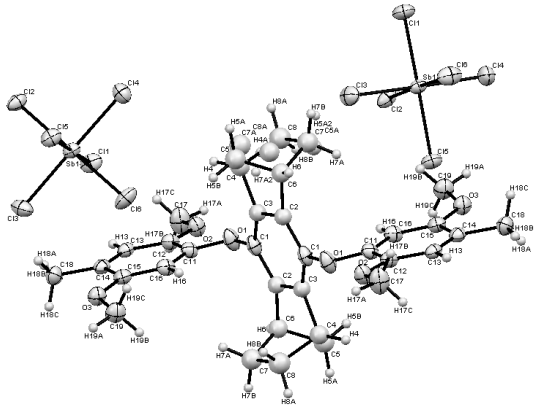

Identification code	raj11oa
Empirical formula	C38 H46 Cl20 O6 Sb2
Formula weight	1551.25
Temperature	100(2) K
Wavelength	1.54178 Å
Crystal system	Monoclinic
Space group	P 21/c
Unit cell dimensions	a = 14.0379(3) Å α= 90°.
	b = 9.7164(2) Å β= 103.160(2)°.
	c = 22.0797(6) Å γ = 90°.
Volume	2932.53(12) $Å^3$
Z	2
Density (calculated)	1.757 Mg/m^3
Absorption coefficient	16.032 mm^{-1}
F(000)	1528
Crystal size	0.32 x 0.19 x 0.08 mm^3
Theta range for data collection	3.23 to 67.52°.
Index ranges	-16<=h<=16, 0<=k<=11, 0<=l<=26
Reflections collected	23595
Independent reflections	5120 [R(int) = 0.0245]
Completeness to theta = 67.52°	96.6 %
Absorption correction	Numerical
Max. and min. transmission	0.3603 and 0.0795
Refinement method	Full-matrix least-squares on F^2
Data / restraints / parameters	5120 / 23 / 332
Goodness-of-fit on F^2	1.061
Final R indices [I>2sigma(I)]	R1 = 0.0400, wR2 = 0.0957
R indices (all data)	R1 = 0.0428, wR2 = 0.0971
Largest diff. peak and hole	1.206 and -1.236 $e.Å^{-3}$

Table 6. **Crystal data and structure for structure refinement for raj11a (4)**

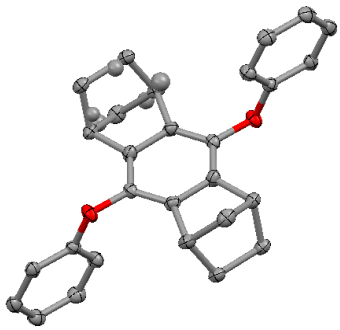

Identification code	raj11a	
Empirical formula	C28 H26 O2	
Formula weight	394.49	
Temperature	100(2) K	
Wavelength	0.71073 Å	
Crystal system	Monoclinic	
Space group	P 21/n	
Unit cell dimensions	a = 5.8179(8) Å	α= 90°.
	b = 19.246(3) Å	β= 99.982(2)°.
	c = 9.1936(12) Å	γ = 90°.
Volume	1013.8(2) $Å^3$	
Z	2	
Density (calculated)	1.292 Mg/m^3	
Absorption coefficient	0.080 mm^{-1}	
F(000)	420	
Crystal size	0.45 x 0.11 x 0.10 mm^3	
Theta range for data collection	2.12 to 31.82°.	
Index ranges	-8<=h<=8, 0<=k<=28, 0<=l<=13	
Reflections collected	16424	
Independent reflections	3335 [R(int) = 0.0454]	
Completeness to theta = 31.82°	98.8 %	
Absorption correction	Semi-empirical from equivalents	
Max. and min. transmission	0.9921 and 0.9651	
Refinement method	Full-matrix least-squares on F^2	
Data / restraints / parameters	3335 / 0 / 157	
Goodness-of-fit on F^2	1.045	
Final R indices [I>2sigma(I)]	R1 = 0.0517, wR2 = 0.1262	
R indices (all data)	R1 = 0.0762, wR2 = 0.1371	
Largest diff. peak and hole	0.320 and -0.250 $e.Å^{-3}$	

Table 7. **Crystal data and structure for structure refinement for raj11n (5)**

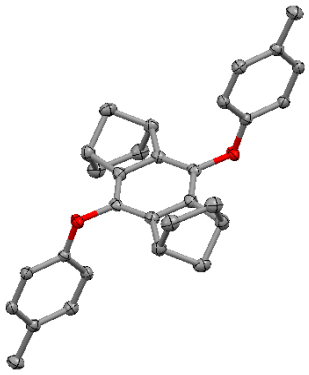

Identification code	raj11n	
Empirical formula	C30 H30 O2	
Formula weight	422.54	
Temperature	100(2) K	
Wavelength	1.54178 Å	
Crystal system	Monoclinic	
Space group	P 21/c	
Unit cell dimensions	a = 5.96450(10) Å	α= 90°.
	b = 21.4327(4) Å	β= 98.4960(10)°.
	c = 8.68680(10) Å	γ = 90°.
Volume	1098.29(3) $Å^3$	
Z	2	
Density (calculated)	1.278 Mg/m^3	
Absorption coefficient	0.605 mm^{-1}	
F(000)	452	
Crystal size	0.25 x 0.10 x 0.08 mm^3	
Theta range for data collection	4.13 to 67.57°.	
Index ranges	-7<=h<=7, 0<=k<=24, 0<=l<=10	
Reflections collected	9039	
Independent reflections	1944 [R(int) = 0.0168]	
Completeness to theta = 67.57°	98.0 %	
Absorption correction	Semi-empirical from equivalents	
Max. and min. transmission	0.9532 and 0.8634	
Refinement method	Full-matrix least-squares on F^2	
Data / restraints / parameters	1944 / 0 / 206	
Goodness-of-fit on F^2	1.006	
Final R indices [I>2sigma(I)]	R1 = 0.0406, wR2 = 0.1051	
R indices (all data)	R1 = 0.0443, wR2 = 0.1079	
Extinction coefficient	0.0006(2)	
Largest diff. peak and hole	0.391 and -0.230 e.$Å^{-3}$	

***Table 8*. Crystal data and structure for structure refinement for raj11p (6)**

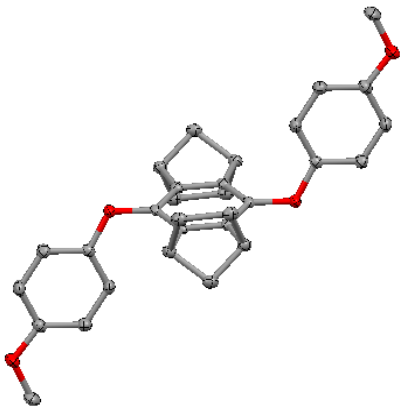

Identification code	raj11p	
Empirical formula	C30 H30 O4	
Formula weight	454.54	
Temperature	100(2) K	
Wavelength	1.54178 Å	
Crystal system	Monoclinic	
Space group	P 21/n	
Unit cell dimensions	a = 5.88530(10) Å	α= 90°.
	b = 8.43510(10) Å	β= 96.8810(10)°.
	c = 23.3180(3) Å	γ = 90°.
Volume	1149.24(3) $Å^3$	
Z	2	
Density (calculated)	1.314 Mg/m^3	
Absorption coefficient	0.684 mm^{-1}	
F(000)	484	
Crystal size	0.40 x 0.16 x 0.05 mm^3	
Theta range for data collection	3.82 to 67.96°.	
Index ranges	-6<=h<=6, 0<=k<=10, 0<=l<=27	
Reflections collected	9574	
Independent reflections	2043 [R(int) = 0.0162]	
Completeness to theta = 67.96°	98.7 %	
Absorption correction	Semi-empirical from equivalents	
Max. and min. transmission	0.9666 and 0.7714	
Refinement method	Full-matrix least-squares on F^2	
Data / restraints / parameters	2043 / 0 / 215	
Goodness-of-fit on F^2	1.012	
Final R indices [I>2sigma(I)]	R1 = 0.0350, wR2 = 0.0922	
R indices (all data)	R1 = 0.0364, wR2 = 0.0932	
Extinction coefficient	0.0013(4)	
Largest diff. peak and hole	0.247 and -0.194 $e.Å^{-3}$	

***Table 9*. Crystal data and structure for structure refinement for raj11k (8)**

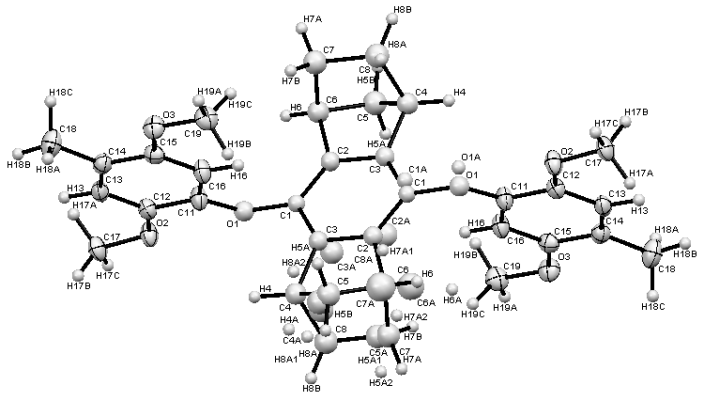

Identification code	raj11k	
Empirical formula	C34 H38 O6	
Formula weight	542.64	
Temperature	100(2) K	
Wavelength	1.54178 Å	
Crystal system	Triclinic	
Space group	P -1	
Unit cell dimensions	a = 6.4154(2) Å	α= 69.307(2)°.
	b = 10.9430(3) Å	β= 76.871(2)°.
	c = 11.0037(3) Å	γ = 81.8590(10)°.
Volume	702.18(3) Å^3	
Z	1	
Density (calculated)	1.283 Mg/m^3	
Absorption coefficient	0.699 mm^{-1}	
F(000)	290	
Crystal size	0.65 x 0.35 x 0.25 mm^3	
Theta range for data collection	4.33 to 67.60°.	
Index ranges	-7<=h<=7, -11<=k<=12, 0<=l<=13	
Reflections collected	5746	
Independent reflections	2376 [R(int) = 0.0185]	
Completeness to theta = 67.60°	98.4 %	
Absorption correction	Semi-empirical from equivalents	
Max. and min. transmission	0.8447 and 0.6595	
Refinement method	Full-matrix least-squares on F^2	
Data / restraints / parameters	2376 / 24 / 218	
Goodness-of-fit on F^2	1.012	
Final R indices [I>2sigma(I)]	R1 = 0.0514, wR2 = 0.1283	
R indices (all data)	R1 = 0.0542, wR2 = 0.1306	
Extinction coefficient	0.0067(10)	
Largest diff. peak and hole	0.409 and -0.319 e.Å^{-3}	

***Table 10*. Crystal data and structure for structure refinement for raj11q (9)**

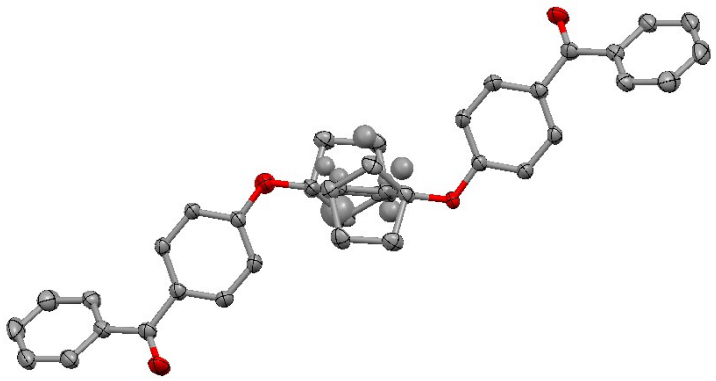

Identification code	raj11q	
Empirical formula	C42 H34 O4	
Formula weight	602.69	
Temperature	100(2) K	
Wavelength	1.54178 Å	
Crystal system	Triclinic	
Space group	P -1	
Unit cell dimensions	a = 6.0402(2) Å	α= 99.075(2)°.
	b = 8.7385(3) Å	β= 92.716(2)°.
	c = 15.4340(6) Å	γ = 107.290(2)°.
Volume	764.25(5) $Å^3$	
Z	1	
Density (calculated)	1.310 Mg/m^3	
Absorption coefficient	0.656 mm^{-1}	
F(000)	318	
Crystal size	0.36 x 0.10 x 0.08 mm^3	
Theta range for data collection	2.91 to 66.90°.	
Index ranges	-7<=h<=7, -10<=k<=10, 0<=l<=17	
Reflections collected	5772	
Independent reflections	2533 [R(int) = 0.0171]	
Completeness to theta = 66.90°	98.1 %	
Absorption correction	Semi-empirical from equivalents	
Max. and min. transmission	0.9494 and 0.7981	
Refinement method	Full-matrix least-squares on F^2	
Data / restraints / parameters	2533 / 24 / 245	
Goodness-of-fit on F^2	1.003	
Final R indices [I>2sigma(I)]	R1 = 0.0504, wR2 = 0.1289	
R indices (all data)	R1 = 0.0586, wR2 = 0.1341	
Largest diff. peak and hole	0.245 and -0.240 $e.Å^{-3}$	

CHAPTER 3

Sequential Oxidative Transformation of Tetraarylethylenes to 9,10-Diaryl-phenanthrenes and Dibenzo[g,p]-chrysenes using DDQ as an Oxidant

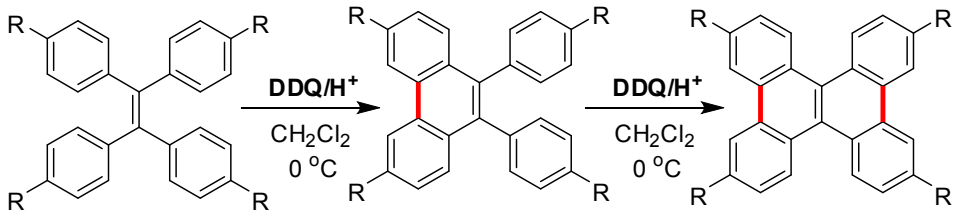

Abstract: Readily-available tetraarylethylenes can be sequentially transformed into 9,10-diarylphenanthrenes and dibenzochrysenes using one and two equivalents of DDQ, respectively, in dichloromethane containing methanesulfonic acid, in excellent yields. The efficient access to substituted dibenzochrysenes from tetraarylethylenes further establishes the versatility of this procedure over the existing multi-step syntheses of dibenzochrysenes. Moreover, the ready regeneration of DDQ from easily recovered reduced DDQ-H_2 continues to advance the use of DDQ/H^+ for the oxidative C-C bond formation reactions.

INTRODUCTION

The design and synthesis of polycyclic aromatic hydrocarbons (PAHs) for use as functional materials in electronic and optoelectronic devices continues to grow with an unabated pace owing to their potential applications in the ever evolving areas of molecular electronics and nanotechnology.[1-2] Of these, dibenzochrysene, a twisted polycyclic aromatic hydrocarbon and its derivatives have been explored by Swager and coworkers[3] and others[4] for the preparation of sensors, non-linear optical and liquid-crystalline materials, etc. Unfortunately, however the access to various substituted dibenzochrysenes as well as the unsubstituted parent dibenzochrysene (DBC) requires multi-step syntheses.[3-5]

In principle, various dibenzochrysenes should be accessible via a pair of oxidative C-C bond formations in readily available symmetrical (via McMurry coupling)[6] as well as unsymmetrical[7] (via a recently developed procedure from our laboratory) tetraarylethylenes (TAE) using oxidants similar to those employed for the Scholl reaction.[8] Unfortunately, such oxidative transformations of tetraarylethylenes (TAE) to dibenzochrysenes (DBC) are rarely employed,[9] i.e. Scheme 1.

In this context, it is noteworthy that Olah and coworkers[10] have shown that a treatment of tetraarylpinacols with a superacid (CF_3SO_3H) affords 9,10-diarylphenanthrenes (DAP) via a dicationic inter-mediate TAE^{+2} (Scheme 1). Interestingly, it is also well-known[11] that the same dicationic intermediate (i.e. TAE^{+2}) can also be accessed from tetraarylethylenes via two successive 1-e^- oxidations (i.e. Scheme 1).

Scheme 1. Sequential oxidative transformation of TAE to DAP and DBC

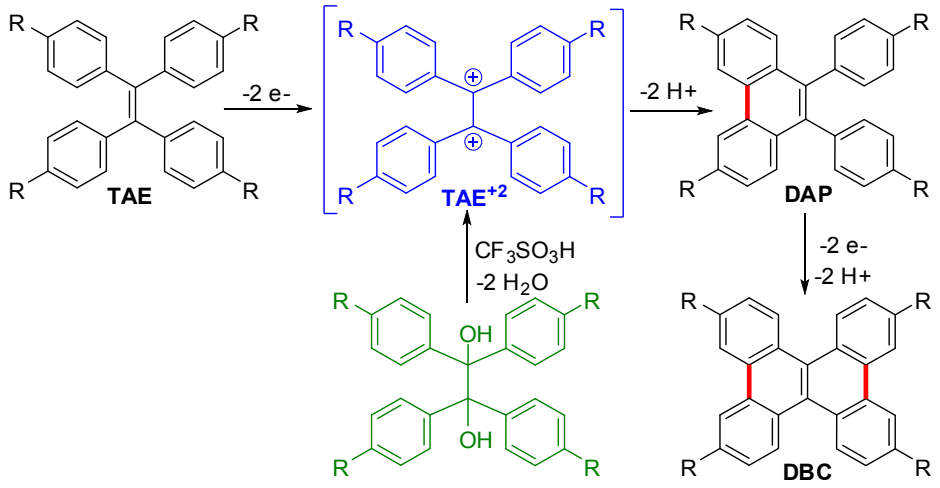

Accordingly, our initial attempts to transform parent tetraphenylethylene to either 9,10-diphenylphenanthrene or dibenzochrysene using $FeCl_3$ (an extensively utilized oxidant for the oxidative C-C bond forming reactions),[8] gave a complex mixture of products.[12] We recently demonstrated[13] that DDQ/H^+ system, which oxidizes a variety of aromatic electron donors with oxidation potentials as high as ~1.6 V vs. SCE to their cation radicals, can be used for an efficient oxidative C-C bond forming reactions, e.g. see Scheme 2.

Scheme 2. Oxidative transformation of a o-Terphenyl to the corresponding Triphenylene Using DDQ as Oxidant

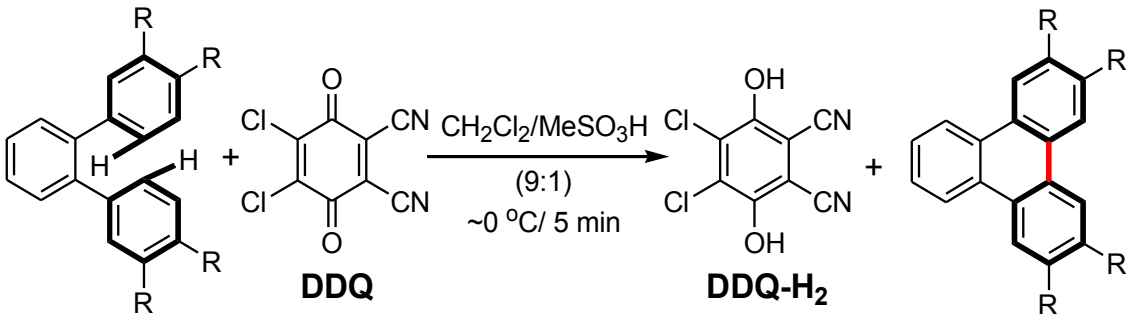

Herein, we now report that the same DDQ/H^+ system (i.e. Scheme 2) can also be employed for the sequential transformations of a variety of symmetrical and unsymmetrical tetraarylethylenes to corresponding 9,10-diarylphenanthrenes (DAP) using 1 equiv of DDQ or to dibenzochrysenes (DBC) using 2 equiv of DDQ in excellent yields. The preliminary details of these findings including the involvement of the tetraarylethylene cation radicals as intermediates in a rapid conversion of TAE to DAP, as well as a relatively slow transformation of DAP to DBC are discussed in the context of electron transfer mechanism as follows.

RESULTS and DISCUSSION

Thus, a 0.1 M solution of tetraphenylethylene (**1a**) in a 9:1 mixture of dichloromethane and methanesulfonic acid (10 mL) was reacted with 1 equivalent of DDQ at ~0 ^{o}C, under an argon atmosphere, to afford a blue-violet solution[14] which turned brown during the course of 30 min. The resulting brown mixture was quenched by an addition of saturated aqueous sodium bicarbonate solution (20 mL). The dichloromethane layer was separated and washed with saturated brine solution (2 x 10 mL), dried over anhydrous magnesium sulfate and evaporated to afford corresponding 9,10-diphenylphenanthrene (**1b**) in quantitative yield (i.e. Scheme 3).

Scheme 3. Oxidative transformation of a **1a** to **1b** using DDQ as oxidant.

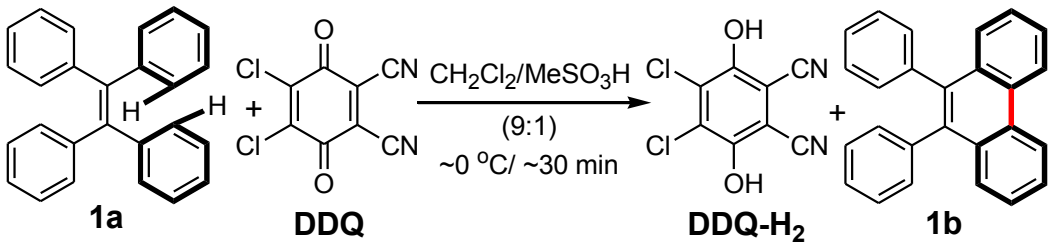

It is important to note that the reduced hydroquinone (DDQ-H_2) in Scheme 3 readily dissolves into the aqueous sodium bicarbonate layer and can be recovered quantitatively by acidification (using aqueous hydrochloric acid, 10%) followed by extraction with diethyl ether. Furthermore, DDQ can be regenerated from DDQ-H_2 by a simple oxidation using either conc. nitric acid or N_2O_4.[15]

A series of TAE **1a**-**8a** (with oxidation potentials varying from ~1.1 to ~1.5 V vs. SCE) were converted to the corresponding DAP **2b**-**8b** in good to excellent yields when subjected to the oxidative cyclodehydrogenation reaction according to the reaction conditions depicted in Scheme 3 (see Table 1). It is noteworthy that the reaction time for the conversion of TAEs to DAPs increased from ~30 min to 24 h with the increasing oxidation potentials of TAEs (see Table 1). The most electron-poor tetrabromo derivative **8a** (E_{ox} = 1.51 V), amongst the TAEs in the Table 1, underwent only partial conversion (56%) to **8b** in 96 h.

Table 1. Oxidative transformation of TAE's to DAPs using DDQ/H^+ oxidant system in dichloromethane at 0 ^oC.

reactant	E_{ox1}/E_{ox2} (V vs SCE)	products	time (h)	% yield[a]
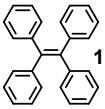 **1a**	1.36/1.67	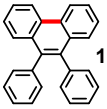 **1b**	~0.5	99
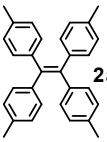 **2a**	1.11/1.39	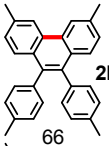 **2b** 66 : 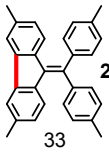 **2c** 33	~0.5	97
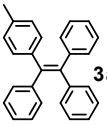 **3a**	1.29/1.57	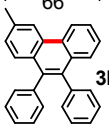 **3b**	~0.5	97
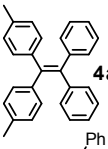 **4a**	1.23/1.53	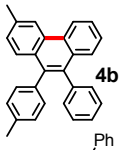 **4b**	~0.5	97
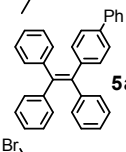 **5a**	1.31/1.57	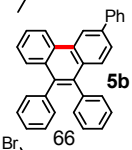 **5b** 66 : 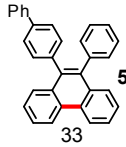 **5c** 33	~0.5	99
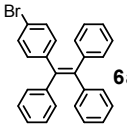 **6a**	1.40/1.69	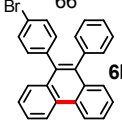 **6b**	10.0	99
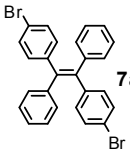 **7a**[b]	1.44/1.69	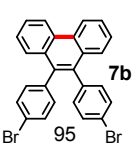 **7b** 95 : 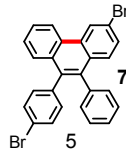 **7c** 5	24.0	98
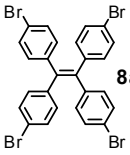 **8a**	1.51/1.71	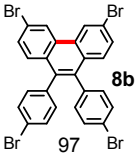 **8b** 97 : 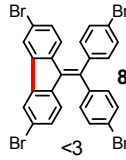 **8c** <3	96.0	99[c]
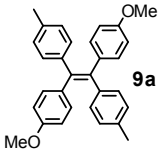 **9a**	0.89/1.02	no reaction	24.0	0
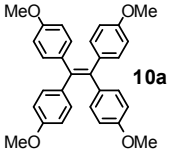 **10a**	0.79/0.91	no reaction	24.0	0

[a]The yields refer to both b and c products in cases of entries **2**, **5**, **7,** and **8**. [b]*cis*-1,2-bis(4-bromophenyl)-1,2-diphenylethylene also gave an identical mixture of products (i.e. **7b** and **7c**). [c]Yiled is based on conversion (56%) and recoverd **8a** (44%).

The structures of various DAPs in Table 1 were established by $^{1}H/^{13}C$ NMR spectroscopy and further confirmed by X-ray crystallography. Diarylmethylidene-fluorene **2c** and **8c** were synthesized by independent route and characterized by $^{1}H/^{13}C$ NMR spectroscopy and X-ray crystallography (see Experimental section).

The symmetrical tetraarylethylenes both with electron-donating (**2a**) and electron withdrawing substituents (**8a**) also produced minor amounts of diarylmethylidene-fluorene **2c** and **8c**, respectively, together with the expected **2b** and **8b** as major products (Table 1).[16a] The unsymmetrical tetraarylethylenes **3a**, **5a**, **6a** and **7a**,[16b] on the other hand, underwent regioselective conversion to the corresponding 9,10-diarylphenan-threnes where the oxidative C-C bond formation occurred between the relatively electron-rich aryl rings (see Table 1).

Interestingly, the most electron-rich 1,2-dianisyl-1,2-ditolylethylene[11] (**9a**, E_{ox1} = 0.89 V) and tetraanisyl-ethylene[11] (**10a**, E_{ox1} = 0.79 V) produced intensely colored solutions when treated with DDQ and methanesulfonic acid according to the Scheme 3. The quenching of the resulting reaction mixtures, after 24 h, using aqueous sodium bicarbonate, afforded a quantitative recovery of the starting TAEs **9a** and **10a**. A photo-spectrometric analyses in Figure 1 of the highly-colored reaction mixtures of **9a** and **10a**, prior to aqueous work-up, produced characteristic absorption spectra which were readily assigned to the corresponding dications of the TAEs (i.e. $\mathbf{9a}^{+2}$ and $\mathbf{10a}^{+2}$) by comparison with the reported spectra of $\mathbf{9a}^{+2}$ and $\mathbf{10a}^{+2}$.[11]

Figure 1. UV-vis absorption spectra of dicationic **10a** (blue) and **9a** (red) dications formed qunatitatively from the reactions of the corresponding **TAEs** with one equivalent of DDQ in $CH_2Cl_2/MeSO_3H$ at 22 ^oC.

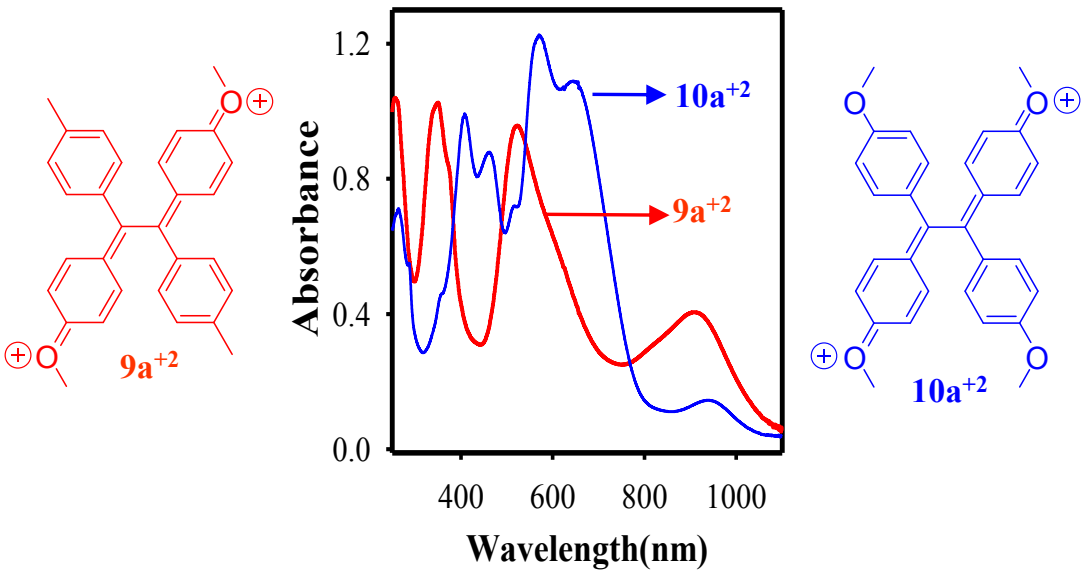

As such, the singular lack of formation of DAPs from tetraarylethylenes **9a** and **10a** is not surprising in the light of the fact that they form rather stable dications (i.e. **9a**$^{+2}$ and **10a**$^{+2}$) owing to the effective quinoidal delocalization of a pair of cationic charges, i.e. (Figure 1). Moreover, the high stability of the dicationic **9a**$^{+2}$ and **10a**$^{+2}$ was further demonstrated by their isolation and structural characterization by X-ray crystallography.[11]

Surprisingly, the oxidative transformations of various TAEs to DAPs using one equiv of DDQ, according to Scheme 3, did not show any indication of the formation of corresponding dibenzochrysenes. However, a reaction of isolated 9,10-diphenylphenanthrene (**1b**) with DDQ/H^+ for an extended period at 22 ^oC showed a partial conversion of **1b** to dibenzochrysene (**1d**), i.e. Scheme 4.

Scheme 4. Oxidative transformation of a **1b** to **1d** using DDQ as oxidant.

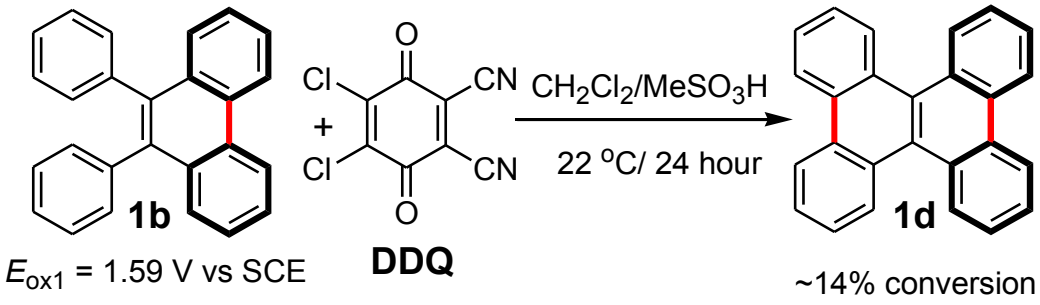

As noted above, the reaction times for the oxidative conversion of various **TAEs** to the corresponding **DAPs** increased with increasing oxidation potentials of **TAEs** and therefore, the slow reactivity of **1b** towards DDQ/H^+ oxidation system suggested that its oxidation potential must be relatively high as compared to tetraphenylethylene. Indeed, a cyclic voltammetric analysis of **1b** showed that its oxidation potential (E_{ox1} = 1.59 V vs SCE) was ~230 mV higher than the tetraphenylethylene (E_{ox1} = 1.36 V vs SCE) and was comparable to tetrakis(4-bromophenylethylene (E_{ox1} = 1.51 V vs SCE) whose (partial) oxidative conversion to corresponding DAP required 96 h (see Table 1).

Encouraged by the partial oxidative conversion of **1b** to dibenzochrysene (**1d**) in Scheme 4, we subjected various isolated **DAPs** to reaction with DDQ/H^+, according to Scheme 4, and found that they can be transformed to the corresponding dibenzochrysenes with excellent to moderate conversions depending on their redox potentials (see Table 2).

Table 2 shows that DAP **2b** with lowest oxidation potential (i.e. E_{ox1} = 1.37 V) undergoes an efficient and quantitative conversion to the corresponding tetramethyl-dibenzochrysene **2d** while electron-poor bromo-substituted DAPs **6b**, **7b** and **8b** with E_{ox1} values ≥1.64 V, expectedly, do not react under these conditions.[17]

Synthesis of various substituted dibenzochrysenes in Table 2 can also be accomplished directly from tetraarylethylene using 2 equiv of DDQ under otherwise identical conditions listed in Scheme 4 (see Scheme 5). A one-pot sequential oxidative transformation of **2a** to **2d** was also carried out and it showed that a ~2:1 mixture of **2b** and diarylmethylidenefluorene **2c** formed after the addition of the first equivalent of DDQ and was cleanly transformed into a single dibenzochrysene **2d** upon addition of a second equivalent of DDQ, i.e. Scheme 5.[18]

Scheme 5. Sequential oxidative transformation of TAE **2a** to DAP **2b** and DBC **2d** using 1 and 2 equiv of DDQ, respectively

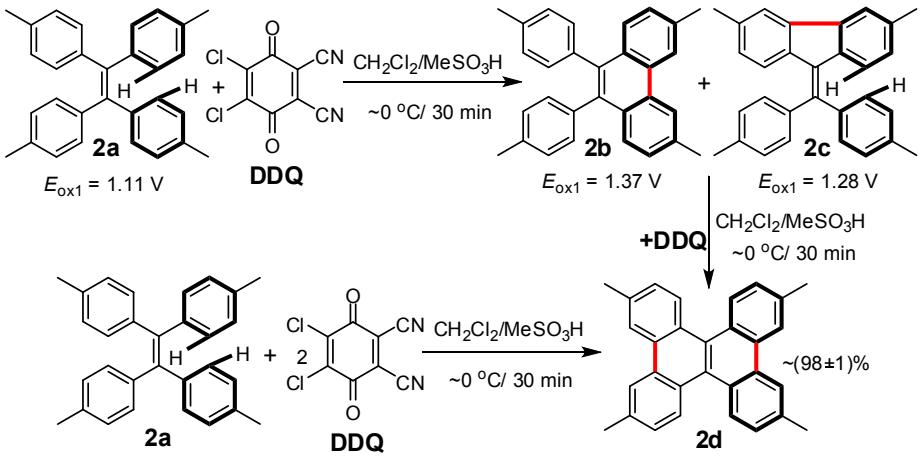

Table 2. Oxidative transformation of DAPs to DBCs using DDQ/H^+ oxidant system in dichloromethane at 22 °C.

reactant	E_{ox1}/E_{ox2} (V vs SCE)[b]	product	time (h)	%conversion (%yield)[a]
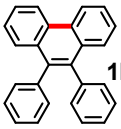 **1b**	1.59/>2.0	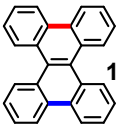 **1d**	24.0	14 (98)
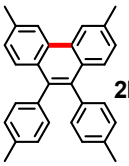 **2b**	1.37/~1.7	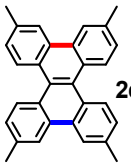 **2d**	0.5	100 (98)[b]
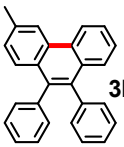 **3b**	1.53/~1.9	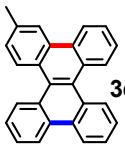 **3d**	9.0	100 (76)
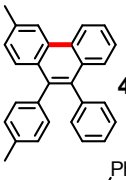 **4b**	1.46/~1.8	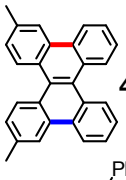 **4d**	1.0	100 (94)
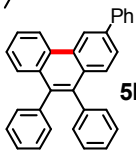 **5b**	1.48/~1.8	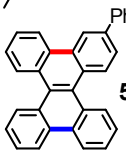 **5d**	6.0	100 (80)[c]
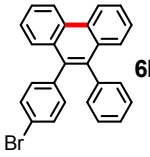 **6b**	1.64/>2.0	no reaction	24.0	--
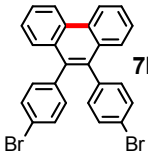 **7b**	1.66/>2.0	no reaction	24.0	--
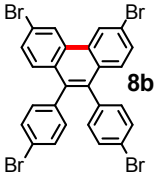 **8b**	1.80/>2.0	no reaction	96.0	--

[a]Conversion percentages were determined by ^{1}H NMR spectroscopy and yields refer to the isolated dibenzochrysenes based on recovered DAPs. [b]The E_{ox1} and E_{ox2} values were determined by cyclic voltammetry in CH_2Cl_2 containing 0.1 M nBu$_4$PF$_6$ at a scan rate of 200 mV s^{-1}. [c]An isomeric mxiture of **5b**/**5c** was used.

Similarly, tetraarylethylene **3a**, **4a** and **5a** were converted to the corresponding dibenzochrysenes **3d**, **4d** and **5d**, respectively, in yields comparable to those in Table 2, using 2 equiv of DDQ in a one-pot procedure. Note that bromo-substituted TAEs (i.e. **6a**, **7a**, and **8a**) even with excess DDQ (3-5 equiv) afforded only the DAP derivatives (see table 1 and 2).

The observation of selective oxidative transformation of various TAEs to DAPs without the contamination from DBCs with one equivalent of DDQ warrants further explanation, especially in the light of the fact that the conversion of the TAE **2a** to DAP **2b** or DAP **2b** to DBC **2d**, under identical conditions, occur on a similar time scale (e.g. see Scheme 5). As such, the explanation for this remarkable selectivity may lie in the fact that both the oxidative transformations (i.e. TAE→DAP and DAP→DBC) proceed via an electron transfer mechanism.

As noted above the oxidation potentials of DAPs are considerably higher than TAEs and therefore in the presence of TAE, concentration of DAP cation radical is expected to be insignificant. For example, based on the oxidation potential difference of 260 mV between **2a** and **2b**, one can easily estimate that even in a 1:1 mixture of $\mathbf{2a}^{+\bullet}$ and **2b**, the concentration of $\mathbf{2b}^{+\bullet}$ will be negligible (see eq 1).[11] Therefore the oxidative transformation of **2b** to corresponding dibenzochrysene **2d** via a cation radical mechanism will not occur while **2a** is present in the reaction mixture.

$$\mathbf{2a}^{+\bullet} + \mathbf{2b} \underset{\Delta G = +230 \text{ mV or } 6.24 \text{ kcal/mol}}{\overset{K = 2.8 \times 10^{-5}}{\rightleftharpoons}} \mathbf{2a} + \mathbf{2b}^{+\bullet} \qquad \text{(eq 1)}$$

SUMMARY and CONCLUSIONS

In summary, we have shown that substituted 9,10-diarylphenanthrenes and dibenzochrysenes can be easily accessed from readily-available symmetrical and unsymmetrical tetraarylethylenes by sequential oxidative transformation using one and two equiv of DDQ, respectively, in dichloromethane in the presence of methanesulfonic acid. The selective formation of 9,10-diarylphenanthrenes, without the contamination form dibenzochrysenes, with one equivalent of DDQ strongly suggests that these sequential oxidative transformations proceed via paramagnetic cation radicals as reactive intermediates. The detailed mechanisms of these oxidative transformations of tetraaryl-ethylenes to 9,10-diaryl-phenanthrenes and dibenzochrysenes are currently under investigation.

EXPERIMENTAL

General experimental methods and materials: All reactions were performed under argon atmosphere unless otherwise stated. DDQ, anhydrous ferric chloride and anhydrous ether were commercially available and were used without further purification. Tetraarylethylenes (TAEs) **1a**,[7] **3a-6a**,[7] **7a**,[19] **8a**,[20] and **9a**[10] and **10a**[10] were prepared according to the literature procedures.

Anhydrous tetrahydrofuran (THF) was prepared by refluxing commercial THF over lithium aluminum hydride under an argon atmosphere for 24 hours followed by distillation under an argon atmosphere. It was stored in a Schlenk flask equipped with a

Teflon valve fitted with Viton O-rings. Dichloromethane was repeatedly stirred with fresh aliquots of conc. sulfuric acid (~10 % by volume) until the acid layer remained colorless. After separation, it was washed successively with water, aqueous sodium bicarbonate, water, and aqueous sodium chloride, and dried over anhydrous calcium chloride. The dichloromethane was distilled twice from P_2O_5 under an argon atmosphere and stored in a Schlenk flask equipped with a Teflon valve fitted with Viton O-rings. The hexanes and toluene were distilled from P_2O_5 under an argon atmosphere and then refluxed over calcium hydride (~12 hr). After distillation from CaH_2, the solvents were stored in Schlenk flasks under an argon atmosphere. NMR spectra were recorded on 300 and 400 MHz NMR spectrometers.

Cyclic Voltammetry (CV). The CV cell was of an air-tight design with high vacuum Teflon valves and Viton O-ring seals to allow an inert atmosphere to be maintained without contamination by grease. The working electrode consisted of an adjustable platinum disk embedded in a glass seal to allow periodic polishing (with a fine emery cloth) without changing the surface area (~1 mm^2) significantly. The reference SCE electrode (saturated calomel electrode) and its salt bridge were separated from the catholyte by a sintered glass frit. The counter electrode consisted of platinum gauze that was separated from the working electrode by ~3 mm. The CV measurements were carried out in a solution of 0.1 to 0.2 M supporting electrolyte (tetra-*n*-butylammonium hexafluorophosphate, TBAH) and the substrate in dry dichloromethane under an argon atmosphere. All the cyclic voltammograms were recorded at a sweep rate of 200 mV sec^{-1}, unless otherwise specified and were IR compensated. The oxidation potentials ($E_{1/2}$) were referenced to SCE, which was calibrated with added (equimolar) ferrocene ($E_{1/2}$ =

0.450 V *vs*. SCE). The $E_{1/2}$ values were calculated by taking the average of anodic and cathodic peak potentials in reversible cyclic voltammograms or directly from square-wave voltammograms in irreversible cyclic voltammograms.

Synthesis of Tetratolylethylene (2a).

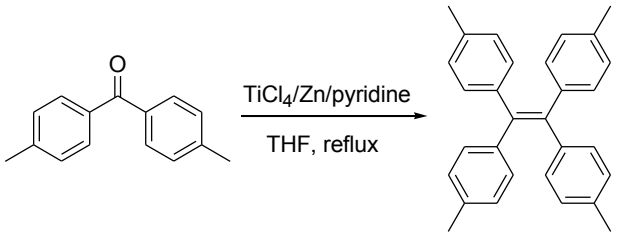

To a chilled (-10 ^{o}C) Schlenk flask containing anhydrous tetrahydrofuran (25 mL) was added $TiCl_4$ (1.2 mL, ~11 mmol) dropwise with the aid of a dropping funnel under an argon atmosphere. To this mixture was then added Zn dust (1.0 g, 15.3 mmol) and dry pyridine (0.05 mL, 0.6 mmol) and a black suspension thus obtained was warmed to room temperature and refluxed for an additional 2 h. A solution of the 4,4'-dimethylbenzophenone (1.05 g, 5 mmol) in THF (20 mL) was added dropwise to the above mixture during a course of 15 min while refluxing, and the resulting mixture was refluxed for an additional 12 h. The reaction mixture was cooled to room temperature and quenched with 10% aqueous K_2CO_3 (25 mL). The organic layer was separated, and the aqueous suspension was extracted with dichloromethane (3 × 25 mL). The combined organic extracts were dried over anhydrous $MgSO_4$, filtered and evaporated to afford a solid which was purified by flash chromatography on silica gel using a 1:9 mixture of ethyl acetate/hexanes to afford pure **2a** (0.63 g, 65%) as a white crystalline solid. mp 150-151 ^{o}C (lit[7] mp 150-152 ^{o}C) ; ^{1}H NMR ($CDCl_3$) δ: 2.26 (s, 12H), 6.90 (s, 16H); ^{13}C NMR δ: 21.41, 128.50, 131.42, 135.86, 140.00, 141.53.

^{1}H NMR spectrum of tetratolylethylene (2a)

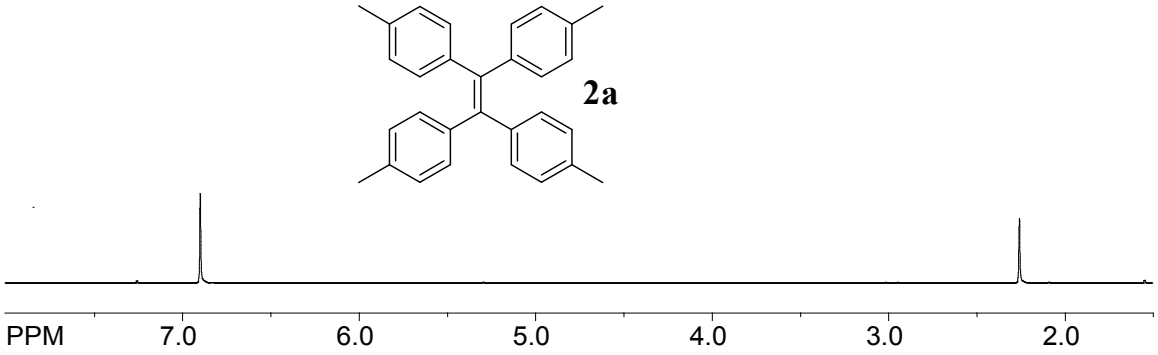

^{13}C NMR spectrum of tetratolylethylene (2a)

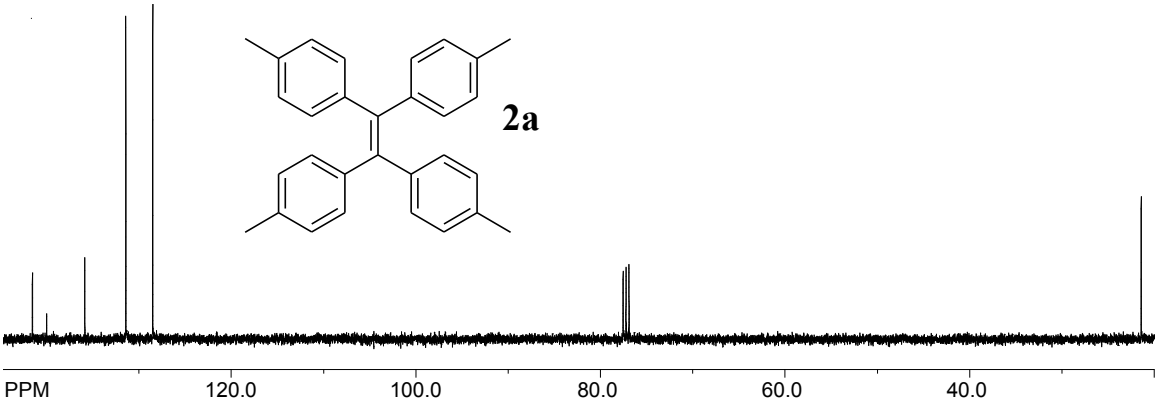

Oxidative Transformation of Tetraarylethylenes to Diarylphenanthrenes Using DDQ/H^{+}.

9,10-Diphenylphenanthrene (1b). General procedure: For example, tetraphenylethylene (33 mg 0.1 mmol) was dissolved in dry dichloromethane (9 mL) and cooled to ~0 ^{o}C. To this solution, methanesulfonic acid (1 mL) and solid DDQ (23 mg, 0.1 mmol) were added and the resulting highly colored mixture was stirred. After 30 min, the resulting reaction mixture was quenched by pouring onto saturated aqueous $NaHCO_3$ (20 mL). The organic layer was separated and the aqueous layer was extracted with dichloromethane (2 x 10

mL). Combined organic layers were washed with water and brine, dried over anhydrous $MgSO_4$ and evaporated under vacuum to afford 9,10-diphenylphenanthrene (**1b**) which was purified by filtration through a short pad of silica gel using 1:9 mixture of ethylacetate and hexanes to afford pure DAP **1b.** Yield: 99%, mp 237-239 ^{o}C (lit[10] 237-238 ^{o}C); ^{1}H NMR δ: 7.13-7.25 (m, 5H), 7.48 (t, 1H, J = 7.3 Hz), 7.56 (d, 1H, J = 7.3 Hz), 7.66 (t, 1H, J = 7.3 Hz), 8.82 (d, 1H, J = 7.3 Hz); ^{13}C NMR δ: 122.69, 126.60, 126.67, 126.82, 127.78, 128.04, 130.16, 131.23, 132.07, 137.39, 139.74.

^{1}H NMR spectrum of 9,10-diphenylphenanthrene (1b).

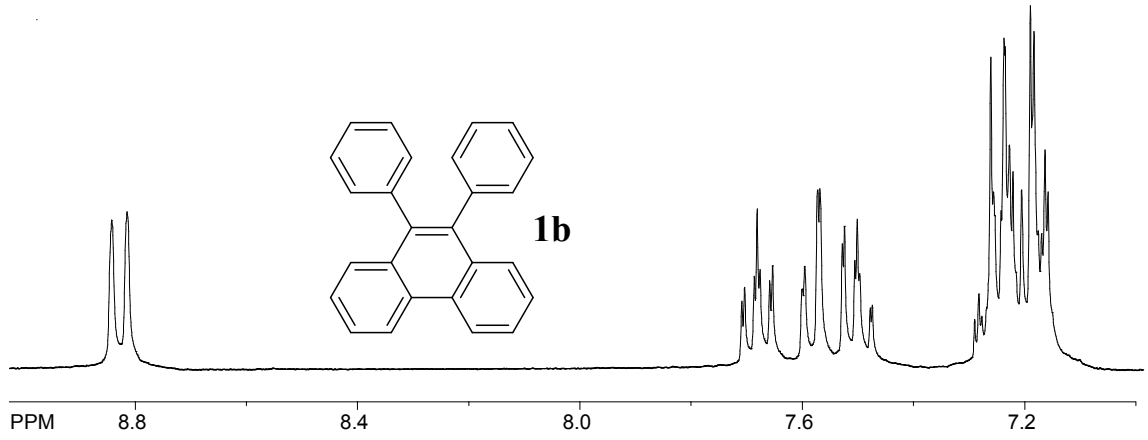

^{13}C NMR spectrum of 9,10-diphenylphenanthrene (1b).

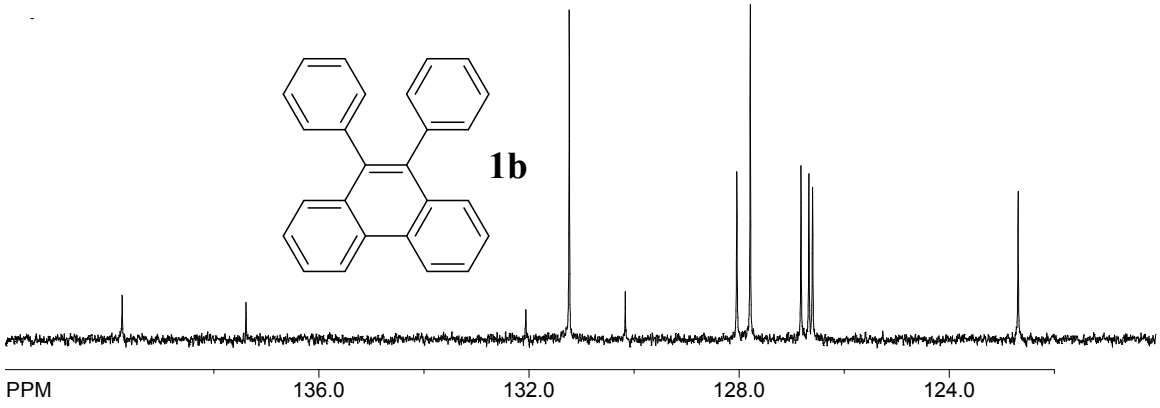

9,10-Di-*p*-tolyl-3,6-dimethylphenanthrene (2b). Using the general procedure described above, tetratolylethylene (**2a**) was reacted with 1 equiv DDQ to afford a 2:1 mixture of DAP **2b** and diarylethylidinefluorene **2c** in quantitative yield, as established by ^{1}H NMR spectroscopy. A pure sample of DAP **2b** was obtained by a fractional crystallization of **2b**/**2c** mixture from a 1:1 dichloromethane and acetonitrile mixture and structure of **2b** was further established by X-ray crystallography, see Figure 2. **2c** was not only selectively crystallized from **2b**/**2c** mixture but also synthesized independently from 3,6-dimethylfluorenone, which was obtained from intra-molecular heck coupling of 2-bromo-4,4'-dimethylbenzophenone. Identity of **2c** was further corroborated by X-ray crystallography, see Figure 3. The spectral data for **2b** and **2c** are summarized below:

2b: mp 256-258 ^{o}C (lit[10] mp 256-258 ^{o}C); ^{1}H NMR δ: 2.34 (s, 6H), 2.64 (s, 6H), 7.06 (m, 8H), 7.30 (dd, 2H, J = 8.6, 1.6 Hz), 7.46 (d, 2H, J = 8.6 Hz), 8.59 (s, 2H); ^{13}C NMR δ: 21.46, 22.15, 122.38, 127.88, 128.26, 128.44, 129.89, 130.42, 131.11, 135.78, 135.84, 136.27, 137.07. **2c:** ^{1}H NMR δ**:** 2.38 (s, 6H), 2.42 (s, 6H), 6.60 (d, 2H, J = 8.0 Hz), 6.76 (d, 2H, J = 8.0 Hz), 7.19 (d, 4H, J = 8.0 Hz), 7.25 (d, 4H, J = 8.0 Hz), 7.50 (s, 2H); ^{13}C NMR 21.62, 21.75, 119.85, 124.72, 127.36, 129.54, 130.12, 133.68, 136.98, 137.40, 138.02, 140.62, 140.75, 144.08

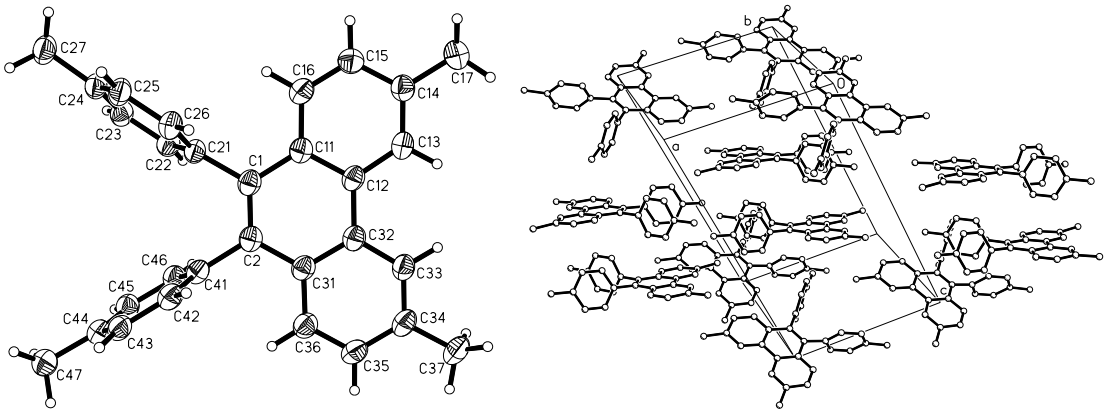

Figure 2. ORTEP diagram of **2b** (left) and its packing diagram showing that molecules of **2b** are arranged in edge to face dimers.

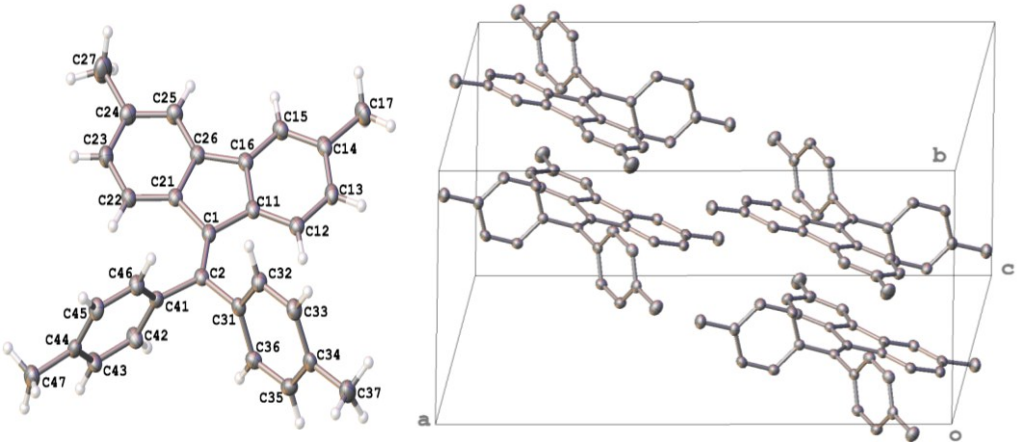

Figure 3. ORTEP diagram of **2c** (left) and its packing diagram showing that molecules of **2c** are stacked along b in an “edge-to-face” fashion

^{1}H NMR spectrum of 2b.

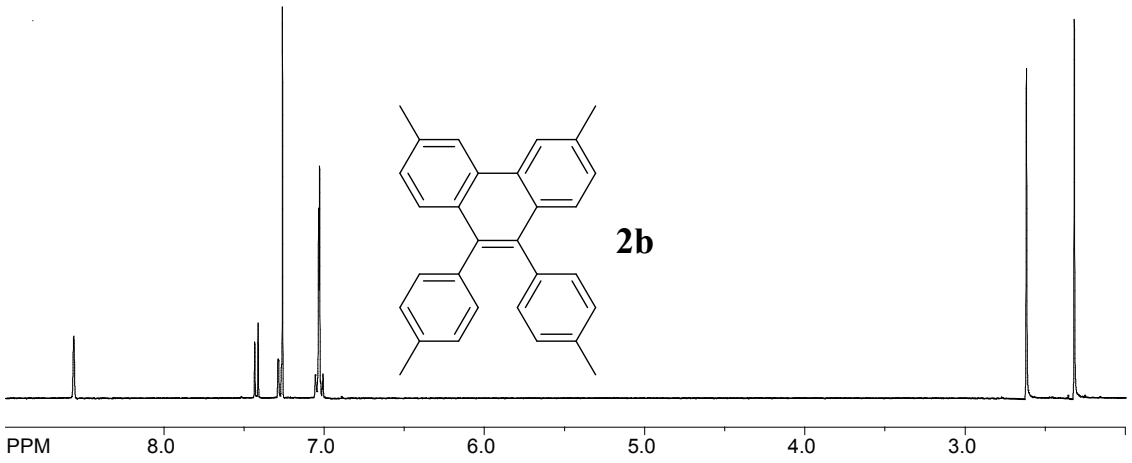

^{13}C NMR spectrum of 2b.

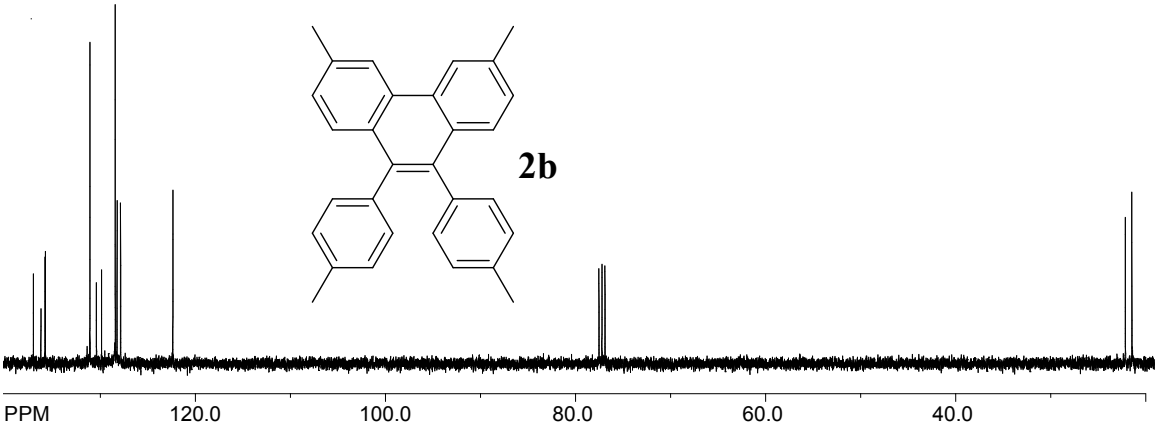

Independent synthesis of 2c:

Synthesis of 2-bromo-4,4'-dimethylbenzophenone

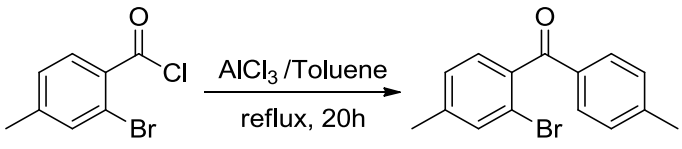

Under an argon atmosphere, 2-bromo-4-methyl-Benzoylchloride (2.71 g, 11.60 mmol) was dissolved into 40 mL toluene and subsequently cooled to 0^{o}C. Powdered $AlCl_3$ (3.86 g, 29 mmol) was then added in small portions with vigorous stirring for 30 mins at 0^{o}C.It

was subsequently allowed to warm to room temperature and then refluxed for 20h. The reaction mixture was poured over crushed ice, extracted with dichloromethane and dried (magnesium sulfate). The solvent was evaporated under vacuum to give the crude product, which was purified by chromatography over silica gel using hexane/ethyl acetate as eluents to afford 2-bromo-4,4'-dimethylbenzophenone (3.0 g, yield 90%).[1]H NMR ($CDCl_3$) δ: 2.40 (s, 3H), 2.42 (s, 3H), 7.15-7.22 (m, 2H), 7.25 (d, 2H, J = 8.0 Hz), 7.47 (s, 1H), 7.71 (d, 2H, J = 8.0 Hz); [13]C NMR δ: 21.24, 21.96, 119.65, 128.04, 129.15, 129.46, 130.55, 133.77, 134.08, 138.08, 141.82, 144.76, 195.85.

[1]H NMR spectrum of 2-bromo-4,4'-dimethylbenzophenone

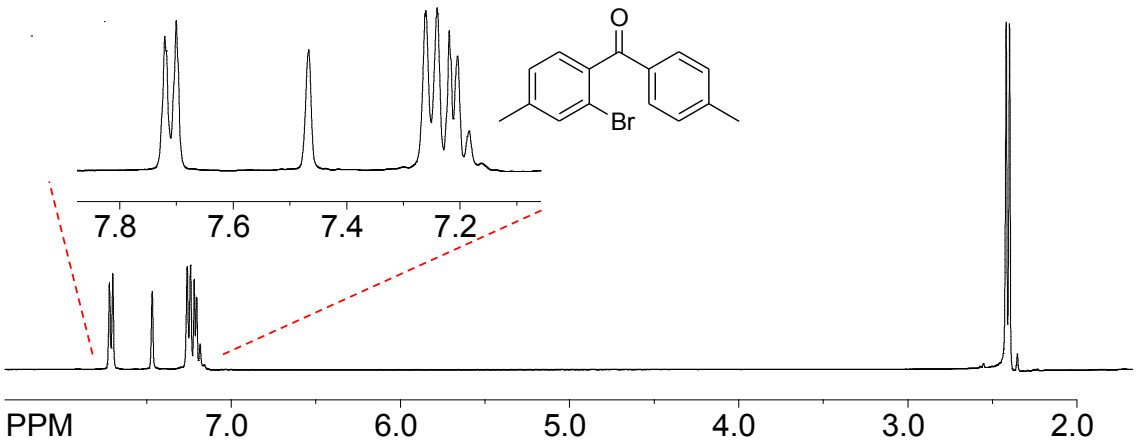

[13]C NMR spectrum of 2-bromo-4,4'-dimethylbenzophenone

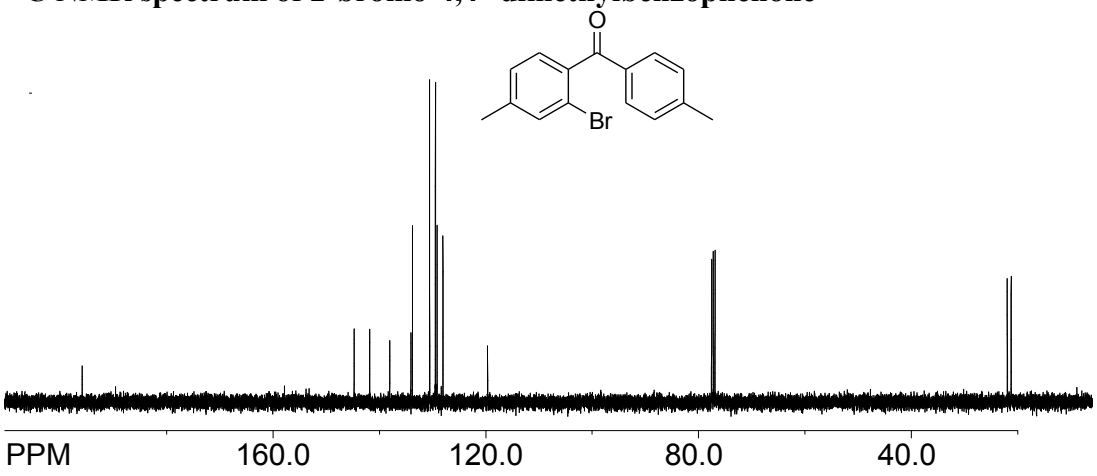

Synthesis of 3,6-dimethylfluorenone

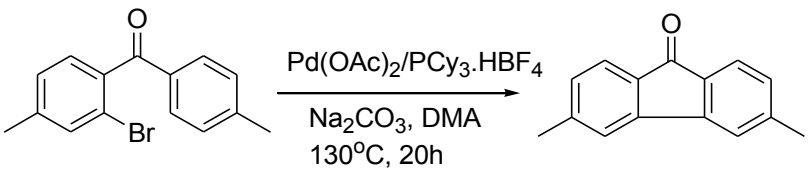

Under an argon atmosphere, to a stirred solution of 2-bromo-4,4'-dimethylbenzophenone (3.6 g, 12.44 mmol) in 30 ml dimethylacetamide were successively added $Pd(OAc)_2$ (28 mg, 0.12 mmol), $PCy_3 \cdot HBF_4$ (91 mg, 0.25 mmol), and Na_2CO_3 (3.1 g, 22.39 mmol) at room temperature, and the mixture was heated at 130°C for 20h. The mixture was filtered through a short pad of SiO_2 with hexane/EtOAc (1:1), and the filtrate was purified by column chromatography over SiO_2 with hexane/EtOAc to give 3,6-dimethylfluorenone (1.35 g, 54% yield) as a yellow solid. mp 112-114 °C; ^{1}H NMR ($CDCl_3$) δ: 2.42 (s, 6H), 7.07 (d, 2H, J = 7.50 Hz), 7.28 (s, 2H), 7.52 (d, 2H, J = 7.50 Hz) ; ^{13}C NMR δ: 22.28, 121.17, 124.21, 129.57, 132.49, 144.79, 145.60, 193.52.

^{1}H NMR spectrum of 3,6-dimethylfluorenone

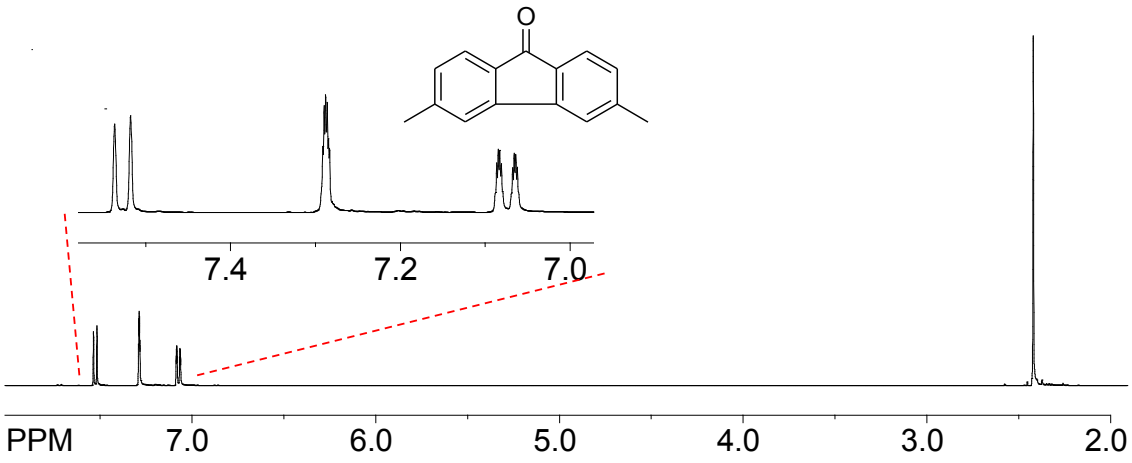

^{13}C NMR spectrum of 3,6-dimethylfluorenone

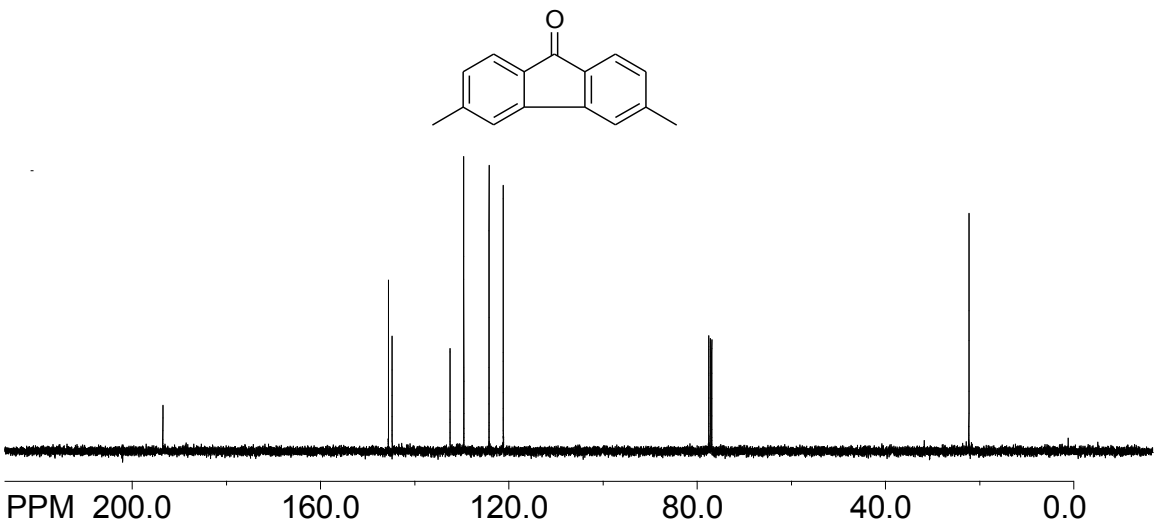

Synthesis of 9,9-(dibromomethylene)-3,6-dimethyl-9H-fluorene

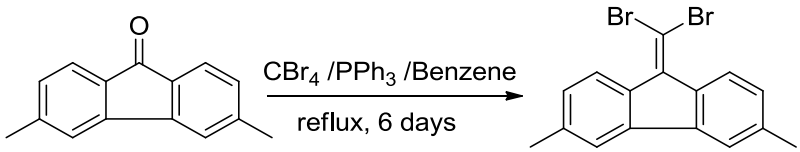

An oven-dried 100-mL schlenk flask was charged with 3,6-dimethylfluorenone (0.2 g, 0.96 mmol), carbon tetrabromide (0.57 g, 1.73 mmol), and a magnetic stirring bar. The flask was purged with argon gas, 50 mL of anhydrous benzene was added, and the mixture was stirred for 5 min. Triphenyl phosphine (0.90 g, 3.45 mmol) was then added. The reaction mixture was heated to reflux for 6 days with vigorous stirring. After cooling, the reaction mixture was diluted with water and extracted with dichloromethane (3 x 50 ml), combined organic layers were then washed with water (3x100 ml), dried over magnesium sulfate, evaporated under vacuum to get crude mixture which was purified by silica gel column chromatography using hexanes as an eluent to afford 90 mg of 3,6-dimethylfluorenone and 9,9-(dibromomethylene)-3,6-dimethyl-9H-fluorene as pale

yellow solid (0.16 g, yield 84%). mp 102-104 ^{o}C; ^{1}H NMR ($CDCl_3$) δ: 2.41 (s, 6H), 7.09 (d, 2H, J = 8.10 Hz), 7.45 (s, 2H), 8.44 (d, 2H, J = 8.1 Hz) ; ^{13}C NMR δ: 21.85, 88.69, 120.29, 125.89, 128.18, 136.08, 139.39, 139.63, 140.82.

^{1}H NMR spectrum of 9,9-(dibromomethylene)-3,6-dimethyl-9H-fluorene

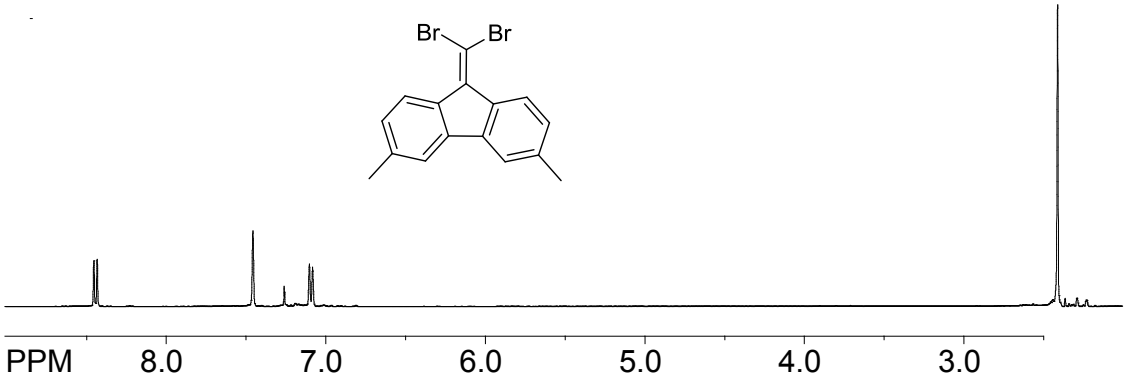

^{13}C NMR spectrum of 9,9-(dibromomethylene)-3,6-dimethyl-9H-fluorene

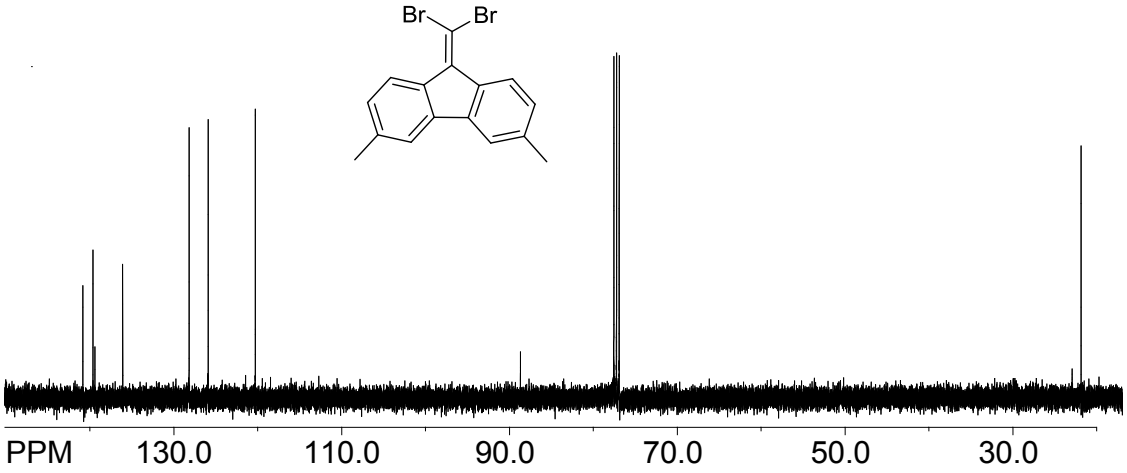

Synthesis of 2c

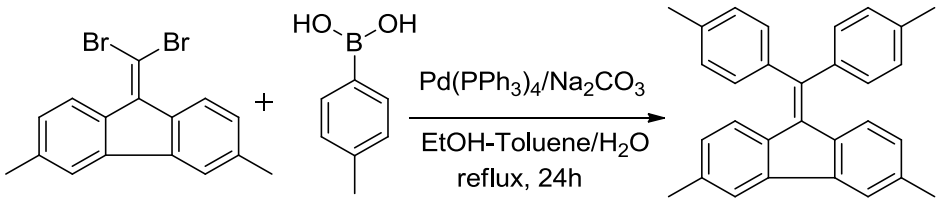

To a degassed solution of 9,9-(dibromomethylene)-3,6-dimethyl-9H-fluorene (0.13 g, 0.36 mmol), 4-methyl-benzeneboronic acid (0.12 g, 0.89 mmol), Pd $(PPh_3)_4$ (9 mg, 2.5 mol%) in dry toluene (25 mL) and ethanol (7 mL) taken in a Schlenk flask, was added a degassed solution of potassium carbonate (2 M, 12.5 mL) using a syringe. The resulting mixture was refluxed for 24 hours under complete exclusion of light. The reaction mixture was then cooled to room temperature, poured into 5 % aqueous HCl (50 mL), and extracted with dichloromethane (3 x 30 mL). The combined extracts were washed with water (50 mL) and brine (50 mL) and dried over anhydrous $MgSO_4$. Removal of the solvent in *vacuo* afforded a crude product that was purified using column chromate-graphy on silica gel with ethyl acetate and hexanes (1:19) as eluent to afford **2c** as a white solid (0.11g, yield 80%). mp 228-230 ^oC; ^1H NMR ($CDCl_3$) δ: 2.38 (s, 6H), 2.42 (s, 6H), 6.60 (d, 2H, J = 8.0 Hz), 6.76 (d, 2H, J = 8.0 Hz), 7.19 (d, 4H, J = 8.0 Hz), 7.25 (d, 4H, J = 8.0 Hz), 7.50 (s, 2H); ^{13}C NMR δ: 21.62, 21.75, 119.85, 124.72, 127.36, 129.54, 130.12, 133.68, 136.98, 137.40, 138.02, 140.62, 140.75, 144.08.

^1H NMR spectrum of 2c.

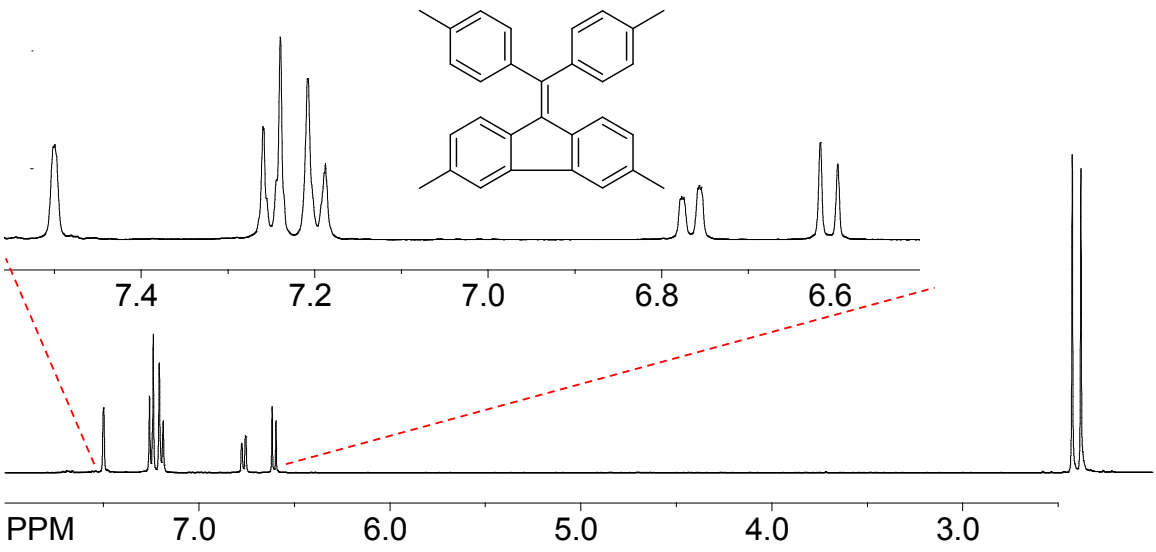

^{13} C NMR spectrum of 2c.

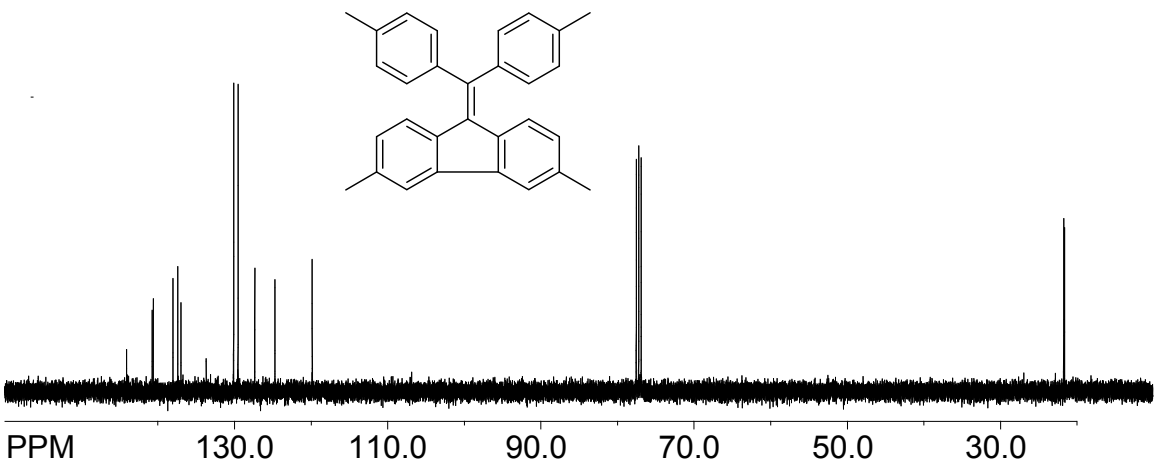

9,10-Diphenyl-3-methylphenanthrene (3b). Using the general procedure described above, p-tolyl-triphenylethylene (**3a**) was reacted with 1 equiv DDQ to afford 9,10-diphenyl-3-methyl-phenanthrene (**3b**) as a single product. It was further purified by filtration through a short pad of silica gel using 1:9 mixture of ethyl acetate and hexanes to afford pure **3b.** Yield: 97%, mp 208-210 ^{0}C; ^{1}H NMR δ: 2.62 (s, 3H), 7.12-7.25 (m, 10H), 7.31 (d, 1H, *J* = 8.0 Hz), 7.43-7.49 (m, 2H), 7.56 (d, 1H, *J* = 8.0 Hz), 7.63 (t, 1H, *J* = 8.0 Hz), 8.79 (d, 1H, *J* = 8.0 Hz); ^{13}C NMR δ: 122.48, 122.66, 126.37, 126.59, 126.68, 127.75, 127.92, 127.97, 128.51, 129.89, 129.98, 130.22, 131.22, 131.32, 132.20, 136.31, 136.41, 137.27, 139.55, 139.9.

^{1}H NMR spectrum of 3b.

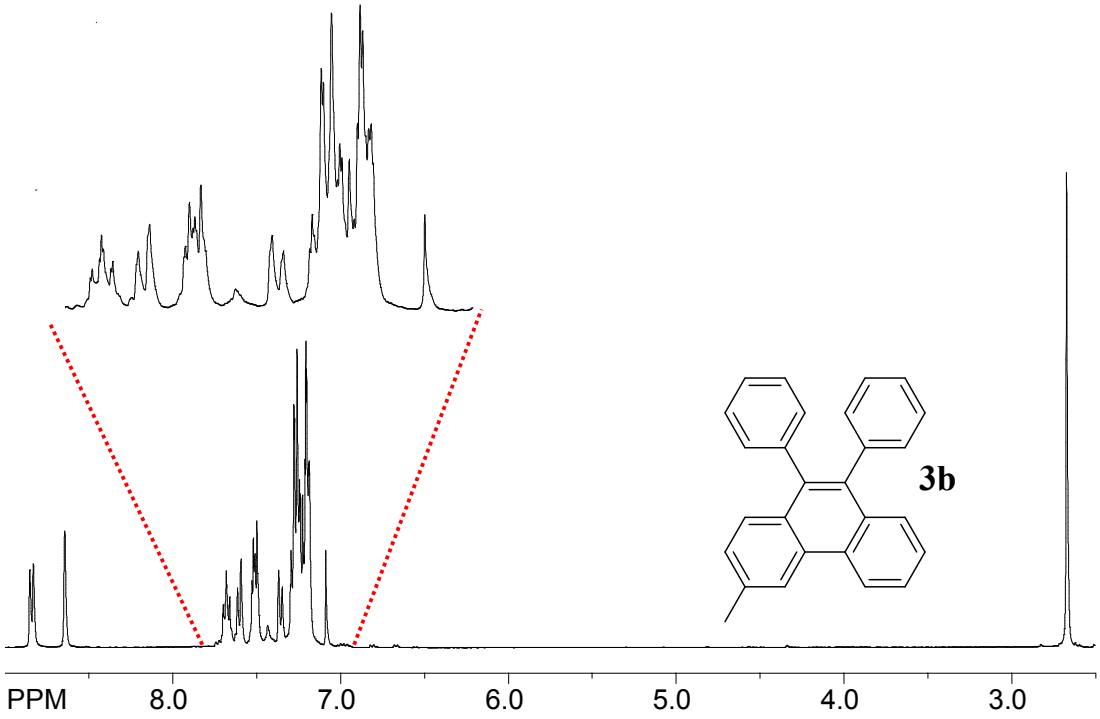

^{13}C NMR spectrum of 3b.

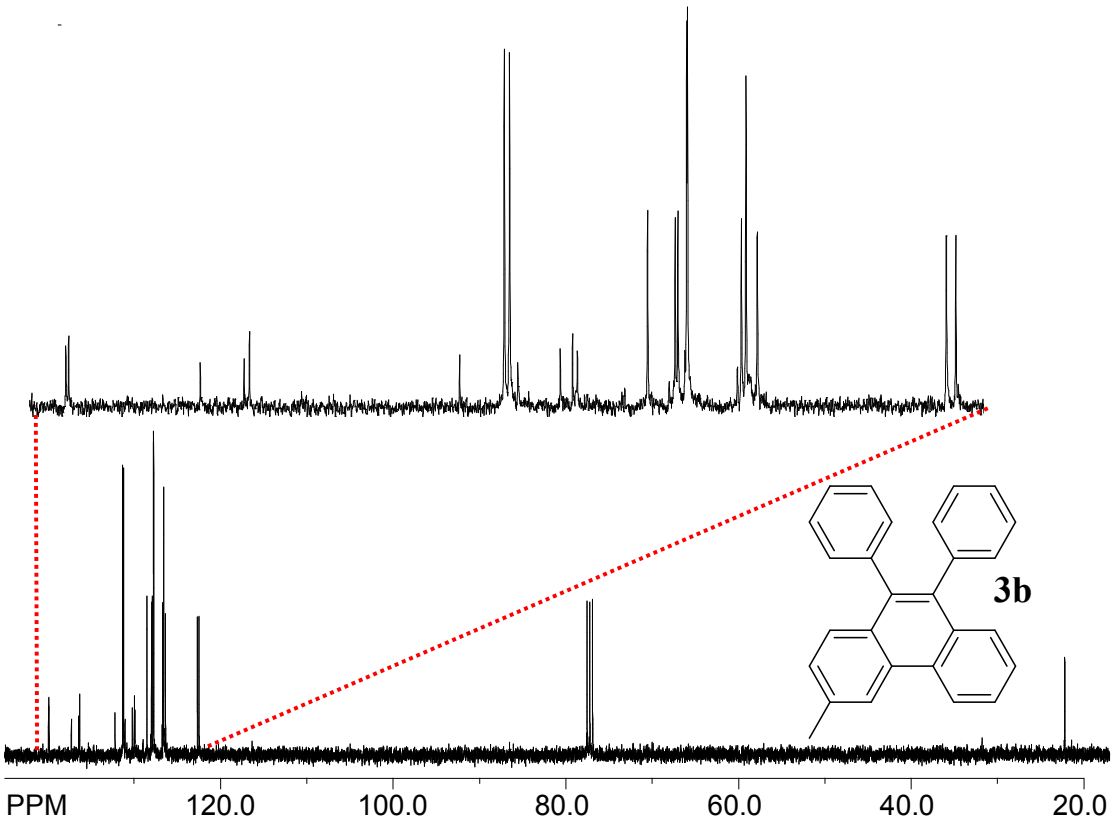

9-Phenyl-10-*p*-tolyl-3-methylphenanthrene (4b). Using the general procedure described above, 1,1-di-p-tolyl-2,2-diphenylethylene (**4a**) was reacted with 1 equiv DDQ to afford **4b** as a single product. It was further purified by filtration through a short pad of silica gel using 1:9 mixture of ethyl acetate and hexanes to afford pure **4b.** Yield: 97%, mp 168-170 ^{0}C; ^{1}H NMR δ: 2.39 (s, 3H), 2.71 (s, 3H), 7.12 (s, 4H), 7.22-7.37 (m, 5H), 7.39 (d, 1H, *J* = 8.5 Hz), 7.52-7.59 (m, 2H), 7.62 (d, 1H, *J* = 8.5 Hz), 7.71 (t, 1H, *J* = 8.5 Hz), 8.67 (s, 1H), 8.87 (d, 1H, *J* = 8.5 Hz); ^{13}C NMR δ: 21.44, 22.19, 122.45, 122.64, 126.26, 126.50, 126.62, 127.75, 127.82, 127.93, 127.98, 128.45, 129.63,129.83, 130.09, 130.23, 131.04, 131.32, 132.27, 135.96, 136.21, 136.39, 136.80, 137.26, 140.03. The molecular structure of **4b** was also established by X-ray crystallography, see Figure 4.

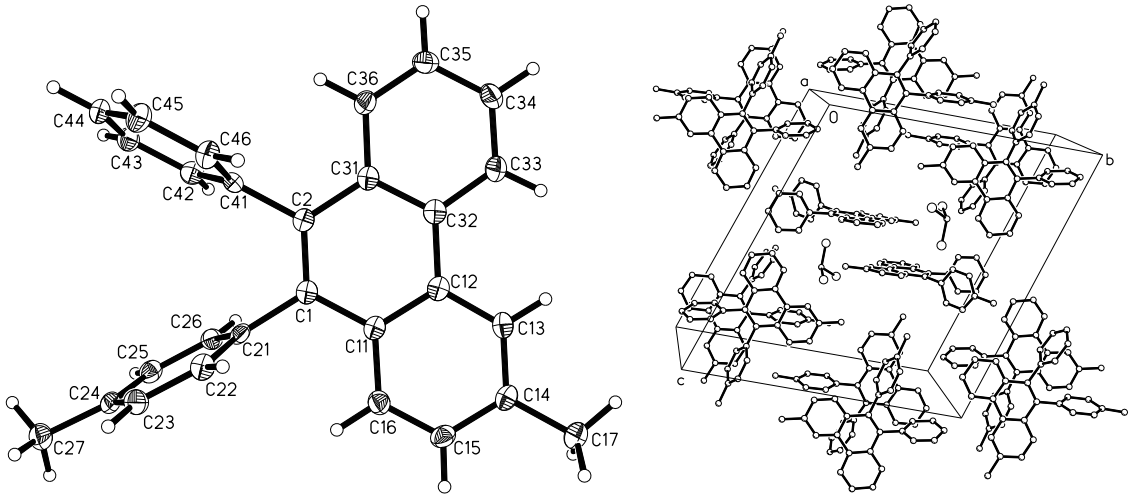

Figure 4. ORTEP diagram of **4b** (left) and its packing diagram showing that molecules of **4b** form alternating edge-to-face "columns" along X-axis.

^{1}H NMR spectrum of 4b.

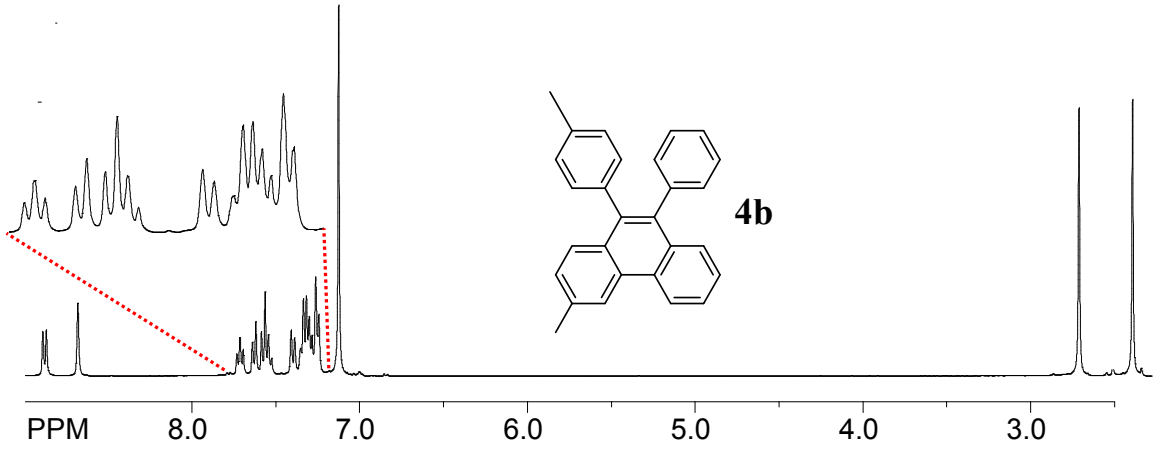

^{13}C NMR spectrum of 4b.

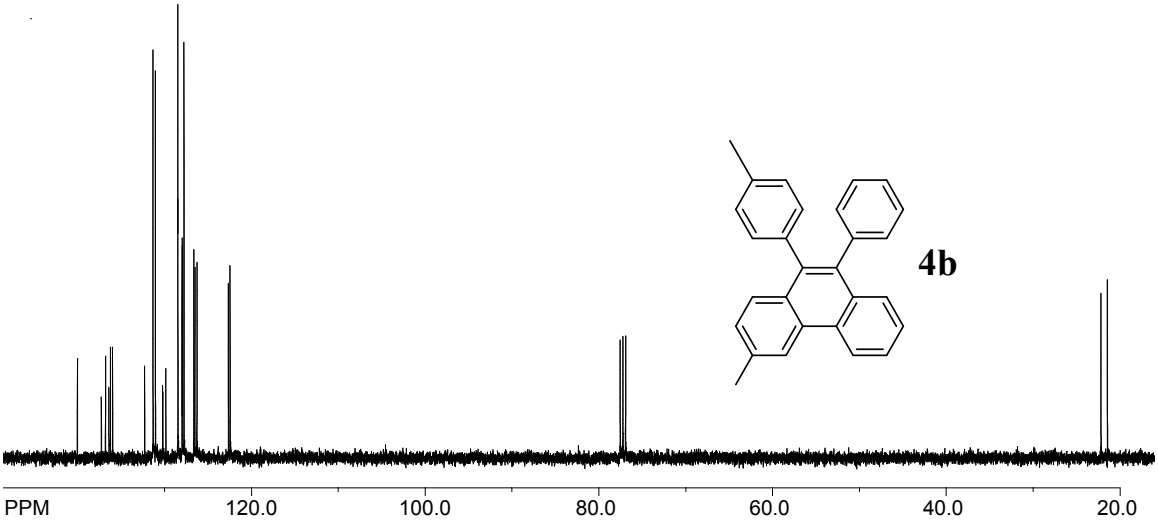

9,10-Diphenyl-3-phenylphenanthrene (5b) and 9-(4-phenylphenyl)-10-phenylphenanthrene (5c). Using the general procedure described above, (4-phenylphenyl)triphenylethylene (**5a**) was reacted with 1 equiv DDQ to afford a isomeric mixture of **5b** and **5c** in 2:1 ratio, which was separated by fractional crystallization. Yield of isomeric mixture: 99%,

5b m.pt 220-222^{o}C, ^{1}H NMR δ: 7.15- 7.30 (m, 9H), 7.42 (t, 1H, *J* = 7.8 Hz), 7.50-7.76 (m, 8H), 7.80 (d, 2H, *J* = 7.8 Hz), 8.90 (d, 1H, *J* = 8.6 Hz), 9.01 (s, 1H); ^{13}C NMR δ:

121.17, 126.17, 126.65, 126.71, 126.72, 126.97, 127.12, 127.13, 127.80, 127.82, 127.84,128.17, 128.57, 128.92, 129.14, 129.15, 130.29, 130.46, 131.25, 131.26, 132.37, 137.20, 137.50, 139.33, 139.72, 141.61. **5c** m.pt 234-236^{o}C, ^{1}H NMR δ: 7.14-7.28 (m, 7H), 7.32 (t, 1H, *J* = 7.4 Hz), 7.42 (t, 2H, *J* = 8.0 Hz), 7.46-7.54 (m, 4H), 7.55-7.63 (t, 3H, *J* = 7.8 Hz), 7.63-7.71 (m, 3H), 8.82 (d, 2H, *J* = 8.3 Hz); ^{13}C NMR δ: 122.70, 122.73, 126.39, 126.64, 126.74, 126.84, 126.87, 127.14, 127.39, 127.87, 128.04, 128.07, 128.93, 130.20, 130.22, 131.23, 131.69, 132.06, 132.08, 137.03, 137.50, 138.83, 139.12, 139.70, 140.94.

^{1}H NMR spectrum of 5b.

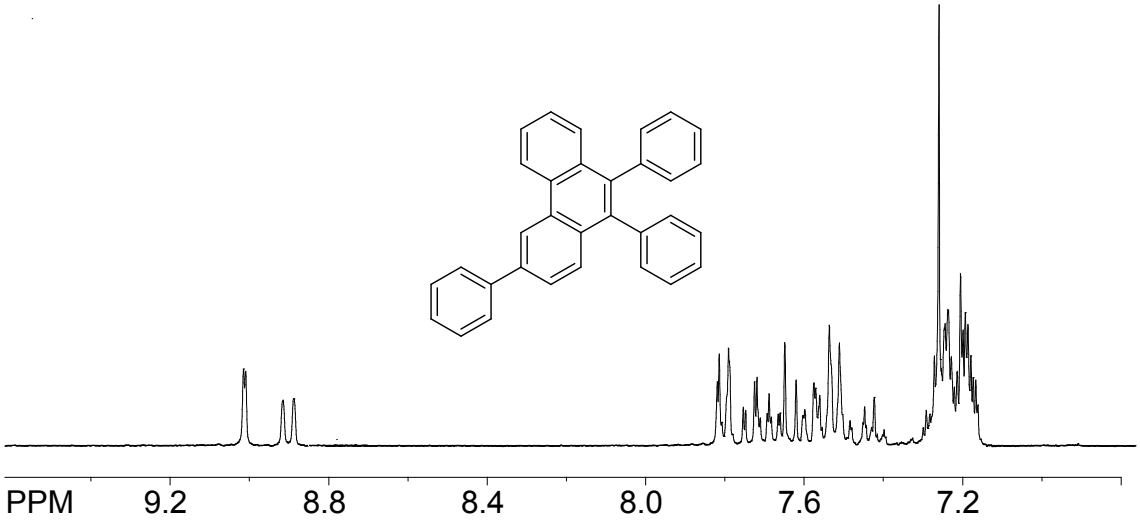

^{13}C NMR spectrum of 5b.

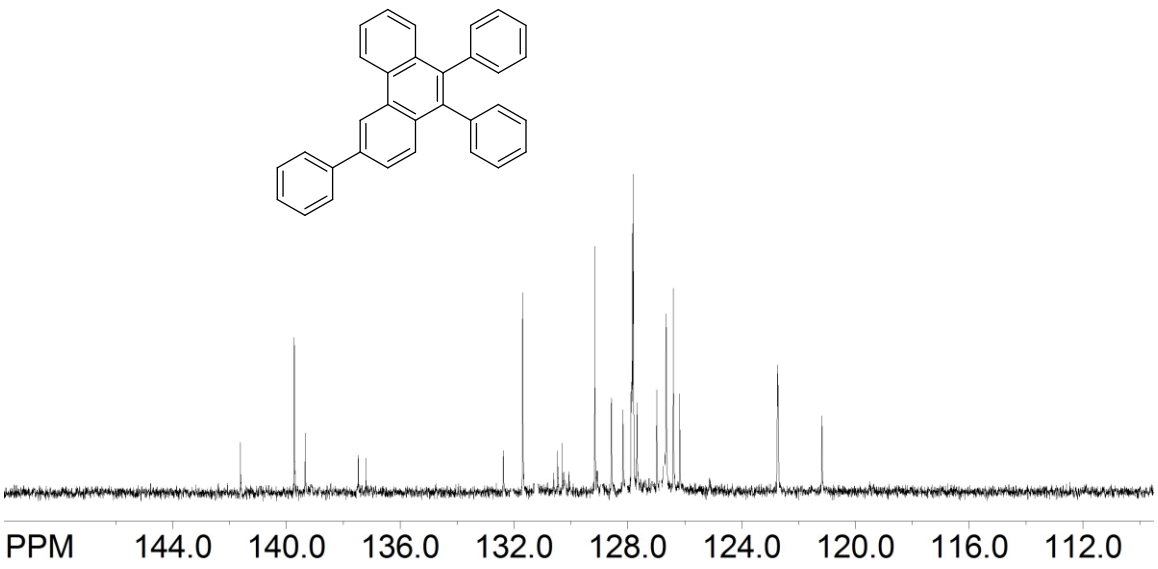

^{1}H NMR spectrum of 5c.

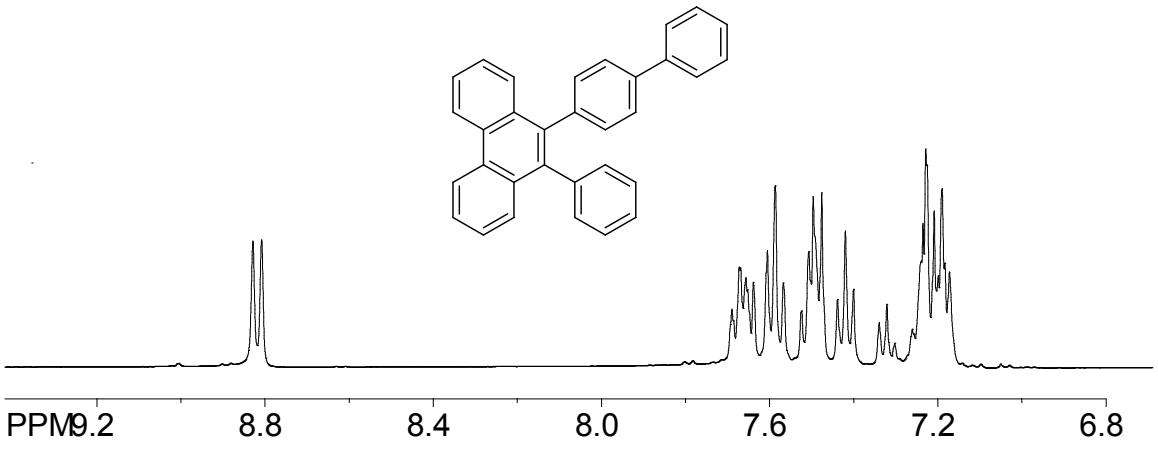

^{13}C NMR spectrum of 5c.

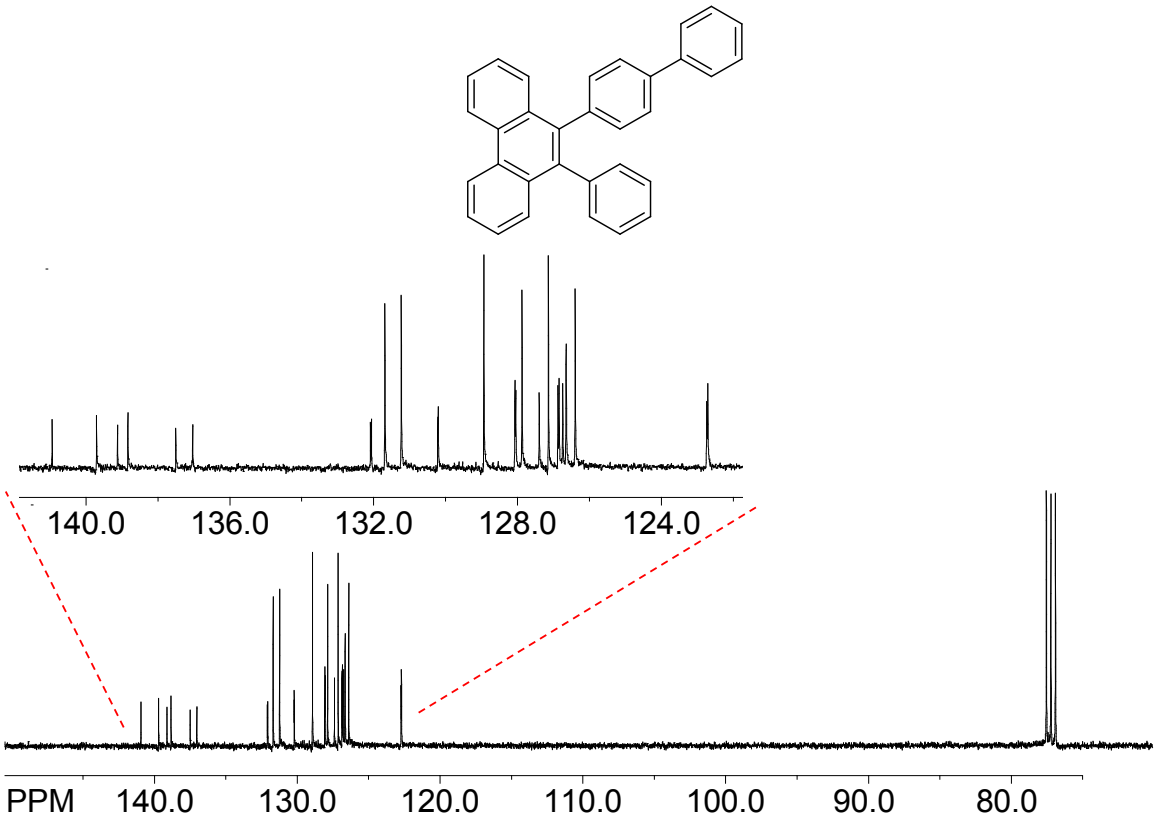

9-(4-Bromophenyl)-10-phenylphenanthrene (6b). Using the general procedure described above, (4-bromophenyl)-triphenylethylene (**6a**) was reacted with 1 equiv DDQ to afford **6b** as a single product. It was further purified by filtration through a short pad of silica gel using 1:9 mixture of ethyl acetate and hexanes to afford pure **6b.** Yield: 99%, mp 244-246 ^{o}C; ^{1}H NMR δ: 7.02-7.06 (m, 2H), 7.12-7.16 (m, 2H), 7.22-7.30 (m, 3H), 7.36-7.40 (m, 2H), 7.47-7.56 (m, 4H), 7.65-7.71 (m, 2H), 8.80 (d, 2H, J = 8.3 Hz); ^{13}C NMR δ: 120.87, 122.70, 122.80, 126.76, 126.83, 126.93, 126.94, 126.96, 127.70, 128.01, 128.08, 130.20, 130.24, 131.04, 131.10, 131.69, 131.93, 132.93, 136.02, 137.59, 138.76, 139.41.

^{1}H NMR spectrum of 6b.

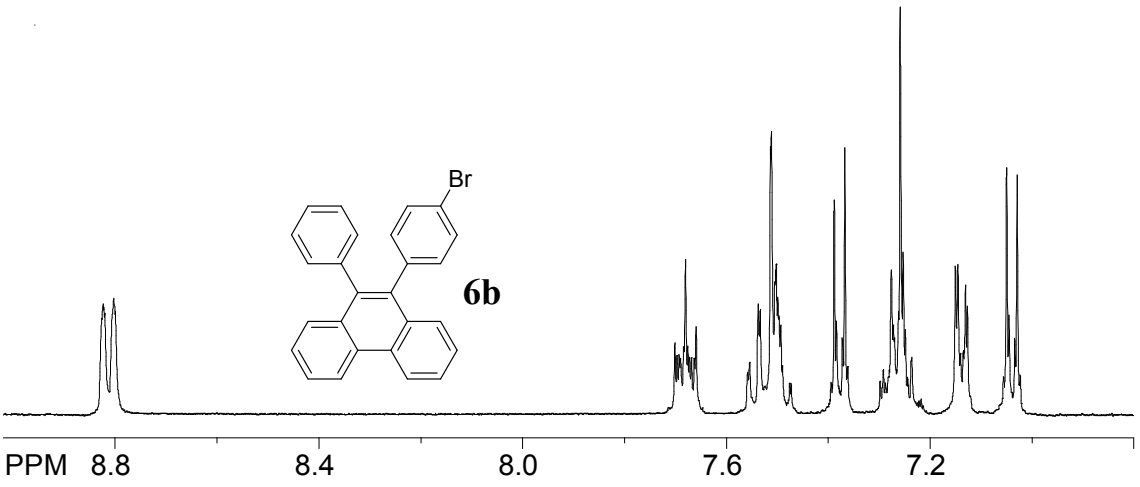

^{13}C NMR spectrum of 6b.

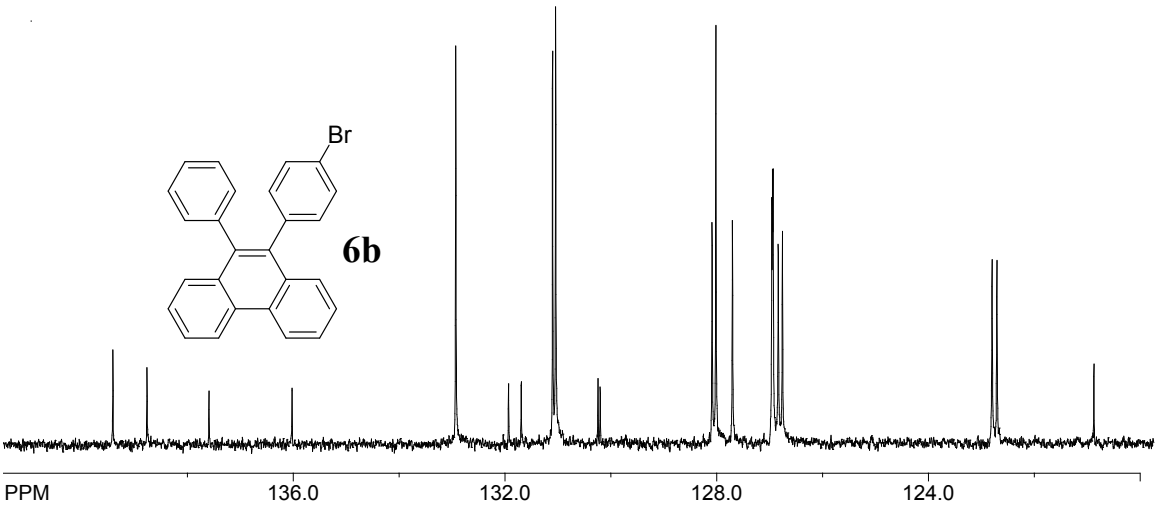

9,10-Bis-(4-bromophenyl)phenanthrene (7b) and 9-(4-bromophenyl)-10-pheny-l-3-bromophenanthrene (7c). Using the general procedure described above, reactions of both cis- and trans-1,2-bis(4-bromophenyl)-1,2-diphenylethlyene (**7a**) with 1 equiv DDQ afforded 9,10-bis-(4-bromophenyl)phenanthrene (**7b**), contaminated with ~5% of isomeric phenanthrene **7c**, as established by ^{1}H NMR spectroscopy of the mixture. Yield

of mixture of **7b** and **7c**: 98%. A small fraction of pure **7b** was obtained by fractional crystallization from a mixture of dichloromethane and methanol and its structure was established by X-ray crystallography, see Figure 5. **7b**: mp 266-268 ^{o}C; ^{1}H NMR δ: 7.00-7.06 (m, 4H), 7.39-7.44 (m, 4H), 7.47-7.55 (m, 4H), 7.66-7.72 (m, 2H), 8.81 (d, 2H, *J* = 8.2 Hz); ^{13}C NMR δ: 121.18, 122.82, 127.00, 127.08, 127.75, 130.27, 131.26, 131.29, 131.57, 132.78, 136.22, 138.42 **7c:** ^{1}H NMR δ : 7.00-7.05 (m, 2H), 7.08-7.13 (m, 2H), 7.24-7.30 (m, 3H), 7.38 (t, 3H, *J* = 8.6Hz), 7.50-7.58 (m, 3H), 7.66-7.72 (m, 1H, *J* = 7.6, 2.3 Hz), 8.71 (d, 1H, *J* = 8.3 Hz), 8.91 (d, 1H, *J* = 2.3 Hz); ^{13}C NMR δ: 120.05, 120.41, 121.86, 124.52, 126.08, 126.17, 126.61, 126.80, 127.13, 128.14, 128.79, 129.02, 129.59, 130.00, 130.11, 130.32, 130.79, 131.03, 131.78, 136.19, 137.39, 137.87 .

^{1}H NMR spectrum of pure 7b.

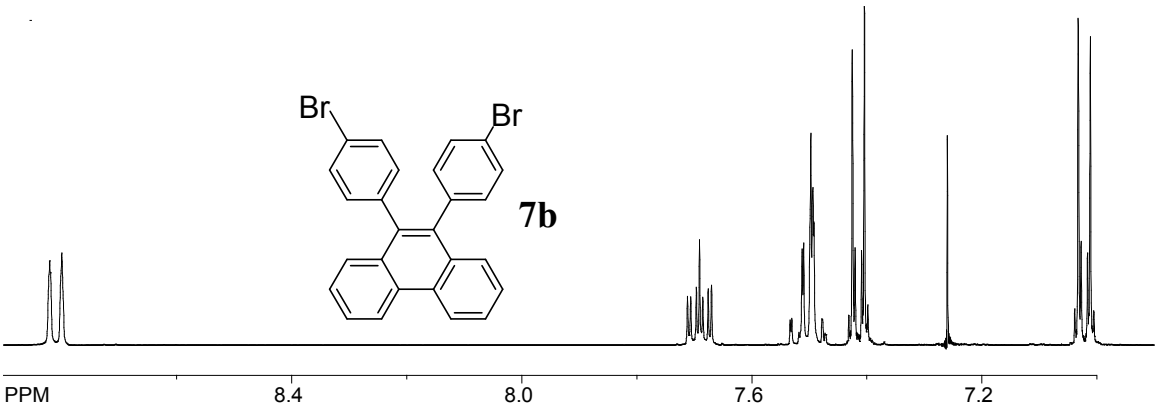

^{13}C NMR spectrum of pure 7b.

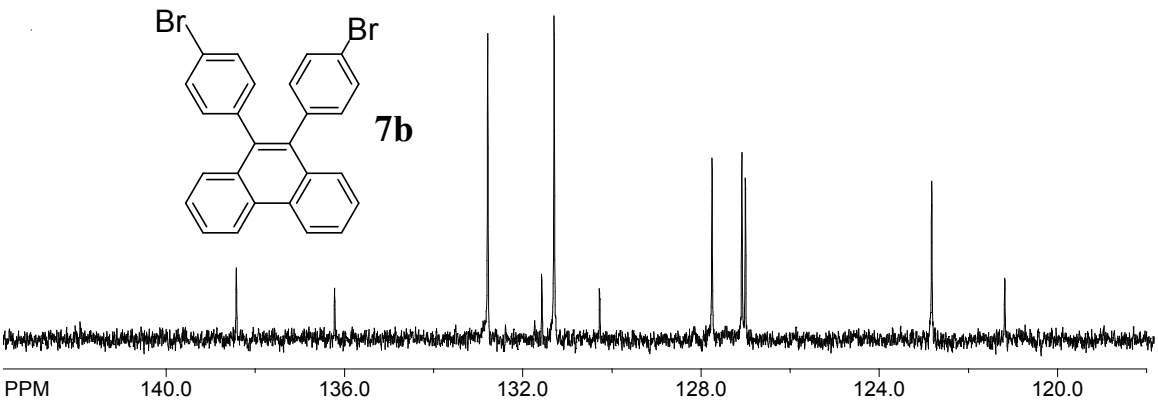

^{1}H NMR spectrum of 7c.

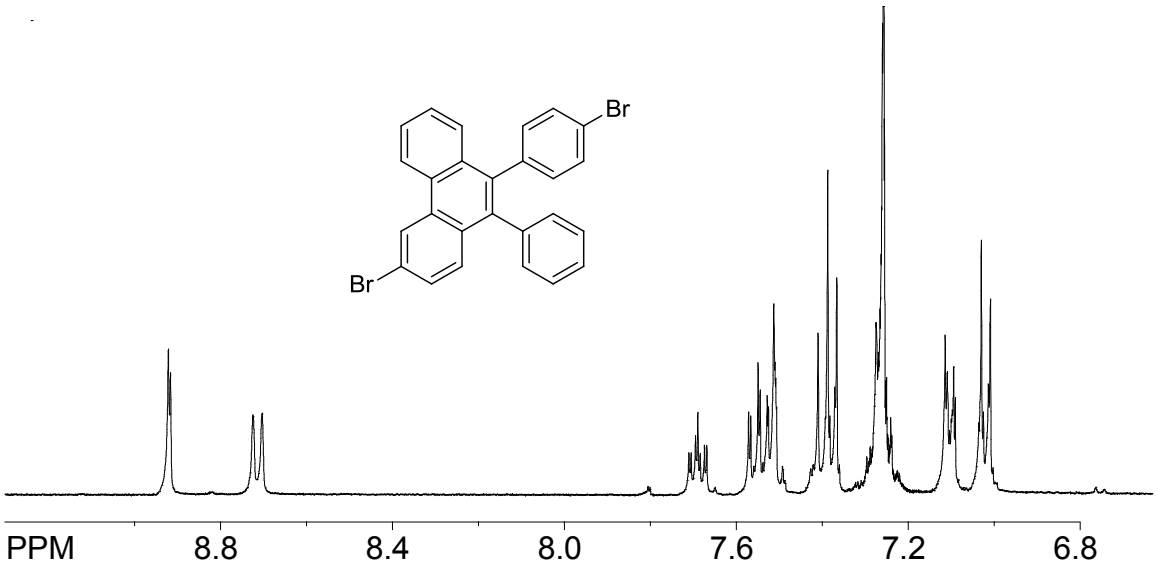

^{13}C NMR spectrum of pure 7c.

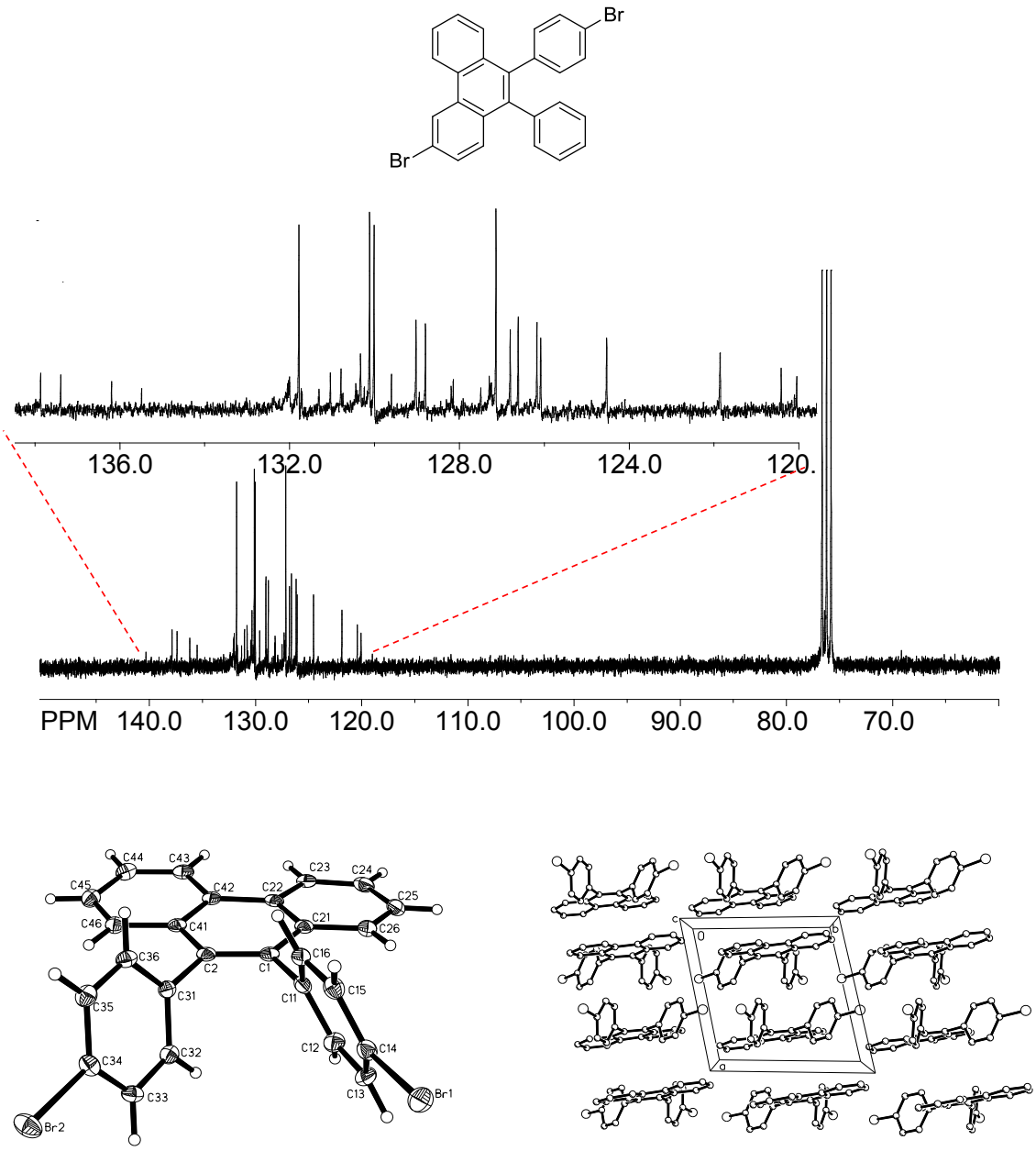

Figure 5. ORTEP diagram of **7b** (left) showing that bromophenyl groups are symmetrically rotated by 70 deg relative to the plane of phenanthrene ring and (right) its packing diagram is built of "stacks" of anti-parallel molecules of **7b** where bromophenyl groups make edge-to-face contacts with neighboring phenanthrene units.

9,10-Bis-(4-bromophenyl)-3,6-dibromophenanthrene (8b) and 9-[bis-(4-bromophenyl) methylidine-3,6-dibromofluorene (8c). Using the general procedure described above, reactions of tetrakis(4-bromophenyl)ethylene (**8a**) with 1 equiv DDQ afforded **8b**, contaminated with ~3% of isomeric methylidinefluorene **8c**, as established by ^{1}H NMR spectroscopy of the mixture. Yield of mixture of **8b** and **8c**: 99%. Pure **8b** was obtained by fractional crystallization from a mixture of dichloromethane and methanol and its structure was established by X-ray crystallography, see Figure 6. Identity of **8c** was established by independent synthesis and X-ray crystallography, see Figure 7. Spectral data of **8b** and **8c** are summarized below

8b: mp 300-302 ^{o}C; ^{1}H NMR δ : 6.97 (d, 2H, *J* = 8.2 Hz), 7.34(d, 1H, *J* = 8.8 Hz), 7.41 (d, 2H, *J* = 8.2 Hz), 7.60 (dd, 1H, *J* = 8.8 Hz, *J* = 1.9 Hz), 8.81(d, 1H, *J* = 1.9 Hz); ^{13}C NMR δ: 121.63, 121.93, 125.68, 129.52, 130.58, 130.67, 130.87, 131.51, 132.53, 136.30, 137.50. **8c:** mp 242-244 ^{o}C; ^{1}H NMR δ: 6.56 (d, 2H, *J* = 8.5 Hz), 7.12 (dd, 2H, *J* = 8.5 Hz, 1.9 Hz), 7.18 (d, 4H, *J* = 8.5 Hz), 7.55 (d, 4H, *J* = 8.5 Hz), 7.78 (d, 2H, *J* = 1.9 Hz) ; ^{13}C NMR δ: 120.53, 121.06, 121.59, 124.23, 128.26, 129.80, 130.50, 131.64, 135.27, 138.91, 139.27, 142.02.

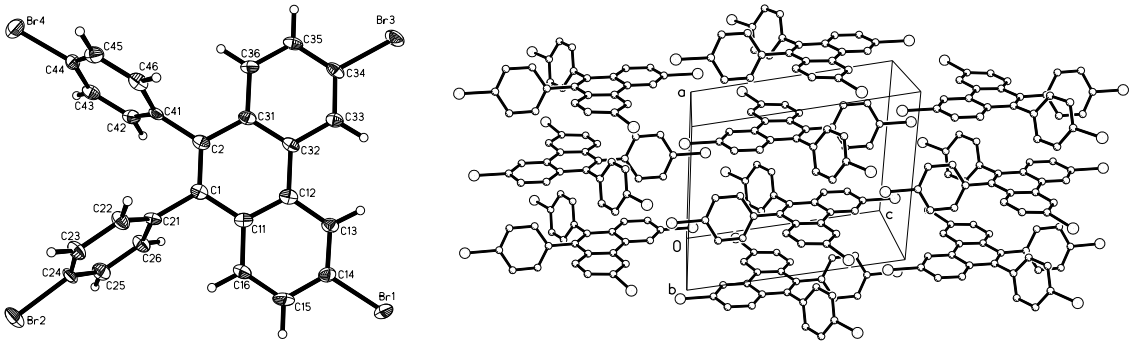

Figure 6. ORTEP diagram of **8b** (left) showing that bromophenyl groups are rotated by 69 and 71 deg relative to the plane of phenanthrene ring and (right) its packing diagram.

^{1}H NMR spectrum of pure 8b.

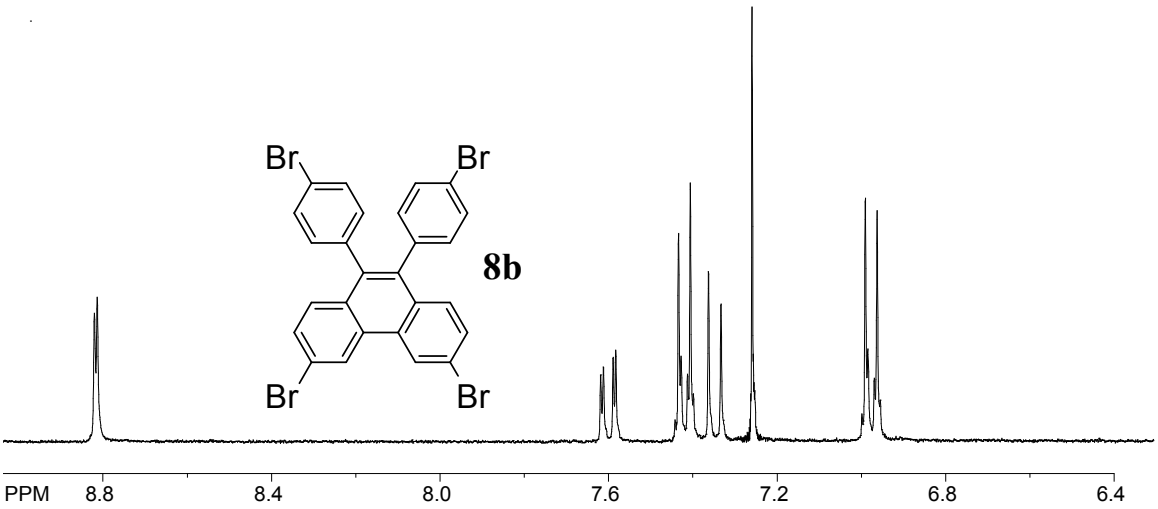

^{13}C NMR spectrum of pure 8b.

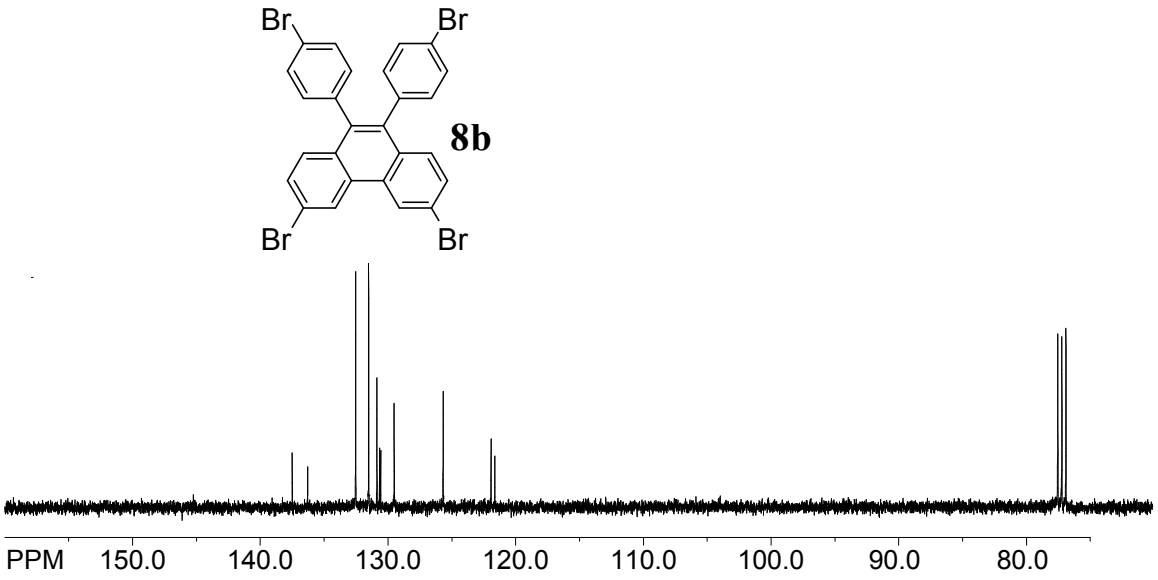

Independent synthesis of 8c

Synthesis of 3,6-dibromophenantrenequinone

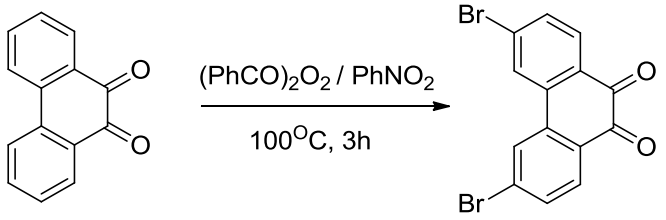

First, 2.34 g (11.23 mmol) of phenantrenequinone and 0.2 g of benzoyl peroxide were dissolved in 15 ml of freshly distilled nitrobenzene and 6.5 g (40.63 mmol) of Br_2 was added to the mixture dropwise, then the reaction mixture was exposed to the light of Hg (120W) lamp and heated to 100 ^oC for 3h. After evolution of HBr had stopped the reaction mixture was cooled to room temperature. Brown precipitate was filtered off and washed with methanol. The product was recrystallized from nitrobenzene to give golden needles (3.0 g). Yield 73%, mp 284-286 ^oC (Fomina, N.; Hogen-Esch, T.E. *Macromolecules* **2008**, *41*, 3765-3768, mp 284-289 ^oC); ^1H NMR ($CDCl_3$) δ: 7.67 (dd, 2H, *J* = 8.34 Hz, 1.8Hz), 8.07 (d, 2H, *J* = 8.34 Hz), 8.12 (d, 1H, *J* = 1.8Hz) ; ^{13}C NMR δ: 127.60, 130.05, 132.31, 132.33, 133.64, 136.14, 179.06

^1H NMR spectrum of 3,6-dibromophenantrenequinone

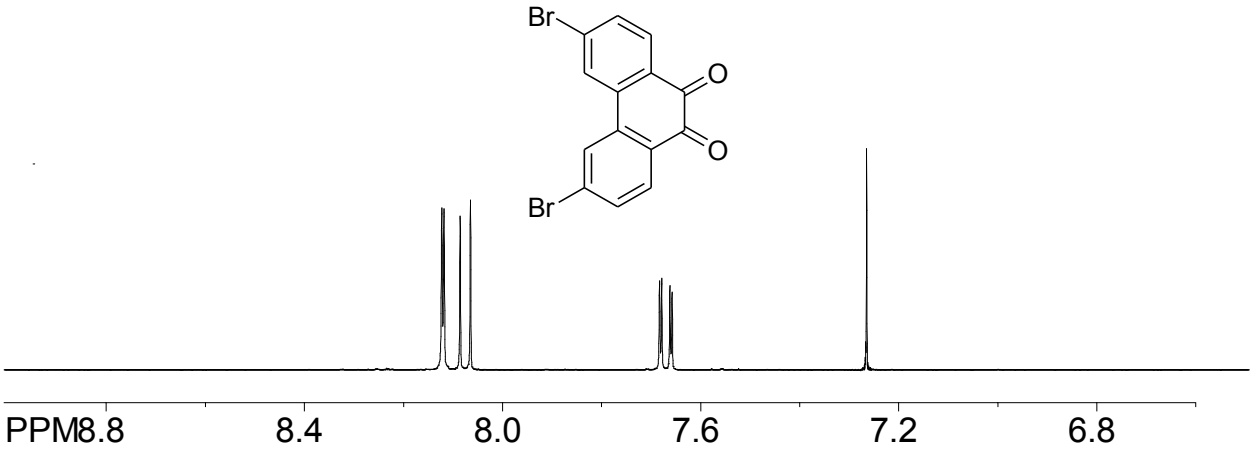

^{13}C NMR spectrum of 3,6-dibromophenantrenequinone

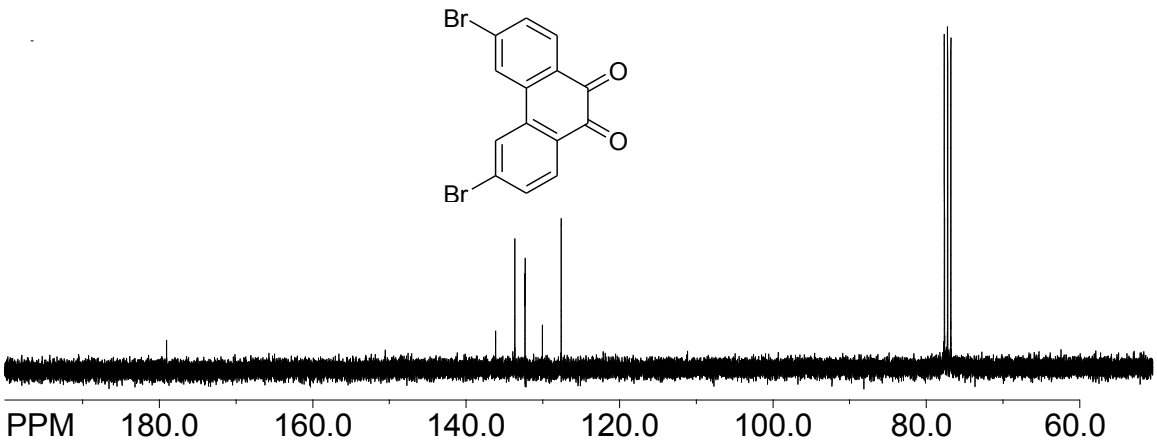

Synthesis of 3,6-dibromfluorenone

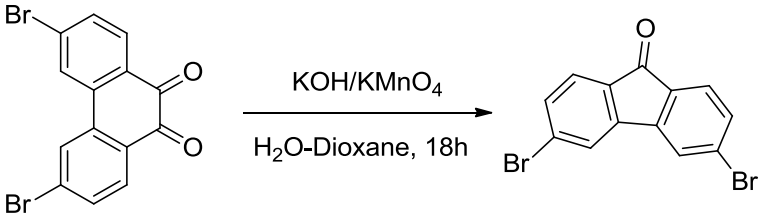

First, 2.5 g (6.83 mmol) of 3,6-dibromophenanthrenequinone were stirred with 3.67 g (65.57 mmol) of KOH in 25 ml H_2O/dioxane (1:1) for 18 h under reflux. Then 3 portions of $KMnO_4$ (1.38 g each) were added to the refluxing reaction mixture with 8 h periods between the additions. At the end of 24 h reaction mixture was cooled to room temperature, filtered, and the solid material was transferred to Soxhlet extractor and extracted with toluene for 3 days. Yellow crystals of pure product (1.61 g) were isolated with 70% yield. mp 322-324 ^{o}C (Fomina, N.; Hogen-Esch, T.E. *Macromolecules* **2008**, *41*, 3765-3768, mp 325-327 ^{o}C); ^{1}H NMR (DMSO) δ: 7.57 (d, 2H, J = 7.9 Hz), 7.63 (dd, 2H, J = 7.9 Hz, 1.6 Hz), 8.20 (d, 2H, J = 1.6 Hz). ^{13}C NMR was found to be similar as

reported before in the literature. (Fomina, N.; Hogen-Esch, T.E. *Macromolecules* **2008**, *41*, 3765-3768)

^{1}H NMR spectrum of 3,6-dibromfluorenone

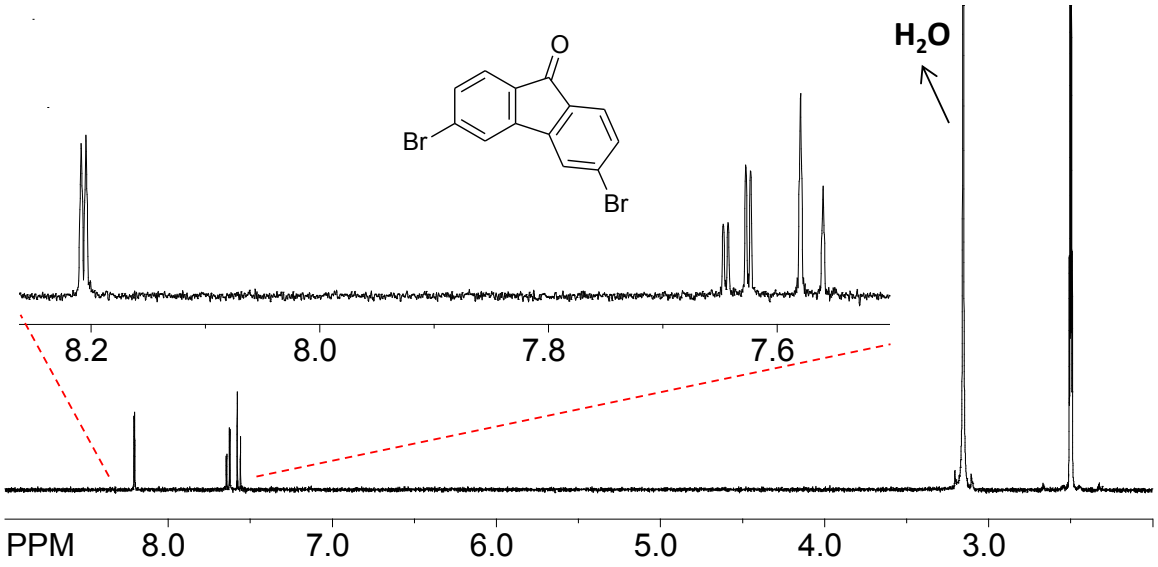

Synthesis of 8c

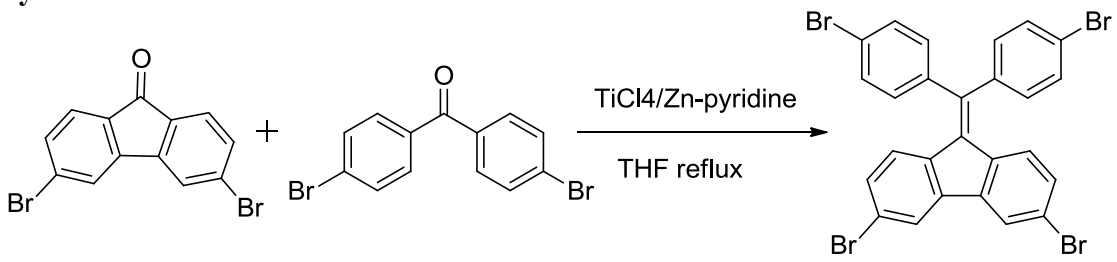

To a chilled (-10 ^{o}C) Schlenk flask containing anhydrous tetrahydrofuran (25 mL) was added $TiCl_4$ (1.0 mL, ~9 mmol) dropwise with the aid of a dropping funnel under an argon atmosphere. To this mixture was then added Zn dust (1.15 g, ~18 mmol) and dry pyridine (0.05 mL, 0.6 mmol) and a black suspension thus obtained was warmed to room temperature and refluxed for an additional 2 h. A solution of the 4,4'-

dibromobenzophenone (1.60 g, 4.7 mmol) and 3,6-dibromfluorenone (0.2g, 0.6 mmol) in THF (20 mL) was added dropwise to the above mixture during a course of 15 min while refluxing, and the resulting mixture was refluxed for an additional 12 h. The reaction mixture was cooled to room temperature and quenched with 10% aqueous K_2CO_3 (25 mL). The organic layer was separated, and the aqueous suspension was extracted with diethylether (3 × 25 mL). The combined organic extracts were dried over anhydrous $MgSO_4$, filtered and evaporated to afford a solid which was purified by flash chromatography on silica gel using mixture of ethyl acetate/hexanes to afford pure **8c** (0.052 g, 14%) as a white crystalline solid. mp 242-244 ^{o}C; ^{1}H NMR ($CDCl_3$) δ: 6.56 (d, 2H, J = 8.5 Hz), 7.12 (dd, 2H, *J* = 8.5 Hz, 1.9 Hz), 7.18 (d, 4H, *J* = 8.5 Hz), 7.55 (d, 4H, *J* = 8.5 Hz), 7.78 (d, 2H, *J* = 1.9 Hz) ; ^{13}C NMR δ: 120.53, 121.06, 121.59, 124.23, 128.26, 129.80, 130.50, 131.64, 135.27, 138.91, 139.27, 142.02.

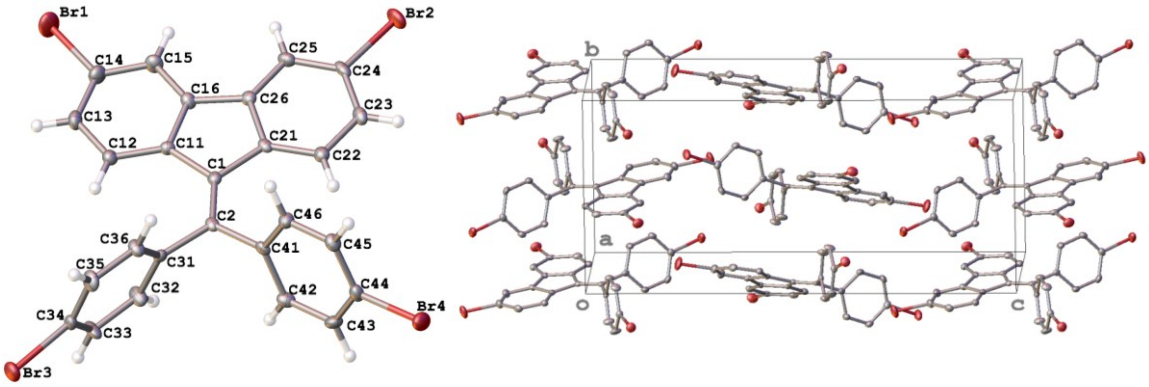

Figure 7. ORTEP diagram of **8c** (left) showing that 4-methyl-phenyl groups make dihedral angles of 76.3 and 78.8° with the central double bond, (right) The molecules are stacked along b in an edge-to face fashion

^{1}H NMR spectrum of 8c.

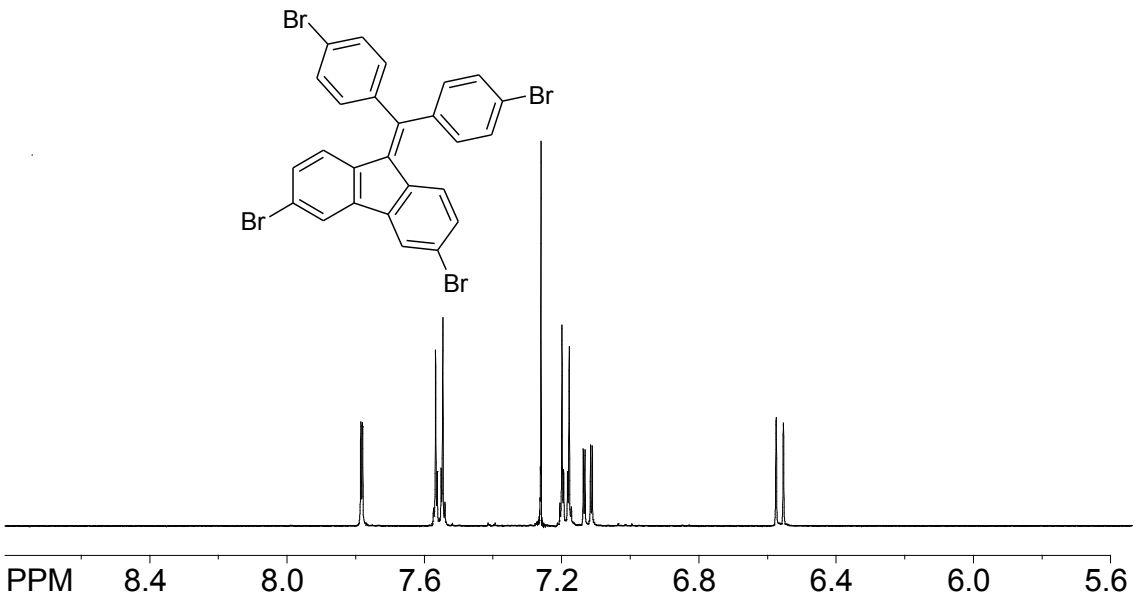

^{13}C NMR spectrum of 8c.

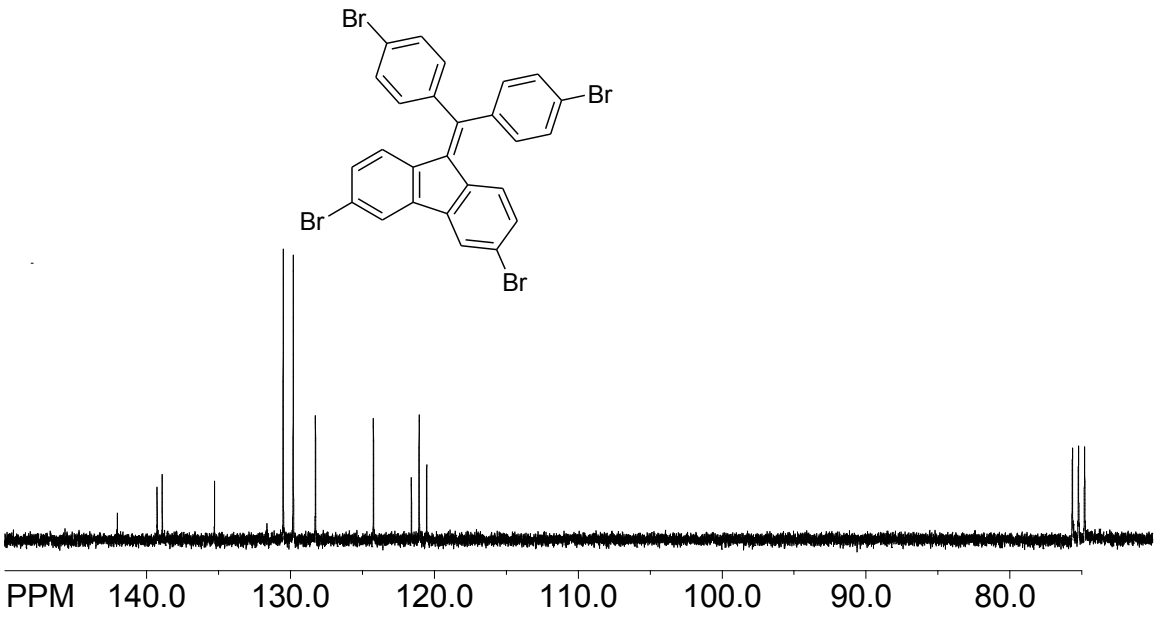

Oxidative Transformation of Diarylphenanthrenes or Tetraarylethylenes to Dibenzochrysenes Using DDQ/H^+. A reaction of isolated DAPs with one equiv. of DDQ or the corresponding TAE with two equiv of DDQ afforded almost identical yields of the corresponding dibenzochrysene and a general procedure for the preparation of dibenzochrysenes is described using tetratolylethylene as follows.

Dibenzochrysene (2d). General procedure: For example, tetratolylethylene (39 mg ~0.1 mmol) was dissolved in dry dichloromethane (9 mL) and cooled to ~0 ^oC. To this solution, methanesulfonic acid (1 mL) and solid DDQ (26 mg, 0.2 mmol) were added and the resulting highly colored mixture was stirred. After 30 min, the resulting reaction mixture was quenched by pouring onto saturated aqueous $NaHCO_3$ (20 mL). The organic layer was separated and the aqueous layer was extracted with dichloromethane (2 x 20 mL). Combined organic layers were washed with water and brine, dried over anhydrous $MgSO_4$ and evaporated under vacuum to afford DBC **2d** which was purified by filtration through a short pad of silica gel using 1:9 mixture of ethyl acetate and hexanes to afford pure DBC **2d.** Yield: 98%, mp 250-252 ^oC; ^{1}HNMR δ : 2.64 (s, 3H), 7.43 (dd, 3H, J = 8.43 Hz, 1.4 Hz), 8.47 (s, 3H), 8.56 (d, 3H, J = 8.4 Hz); ^{13}CNMR δ : 22.03, 123.64, 126.62, 127.50, 128.03, 128.94, 130.76, 136.02

^{1}H NMR spectrum of 2d.

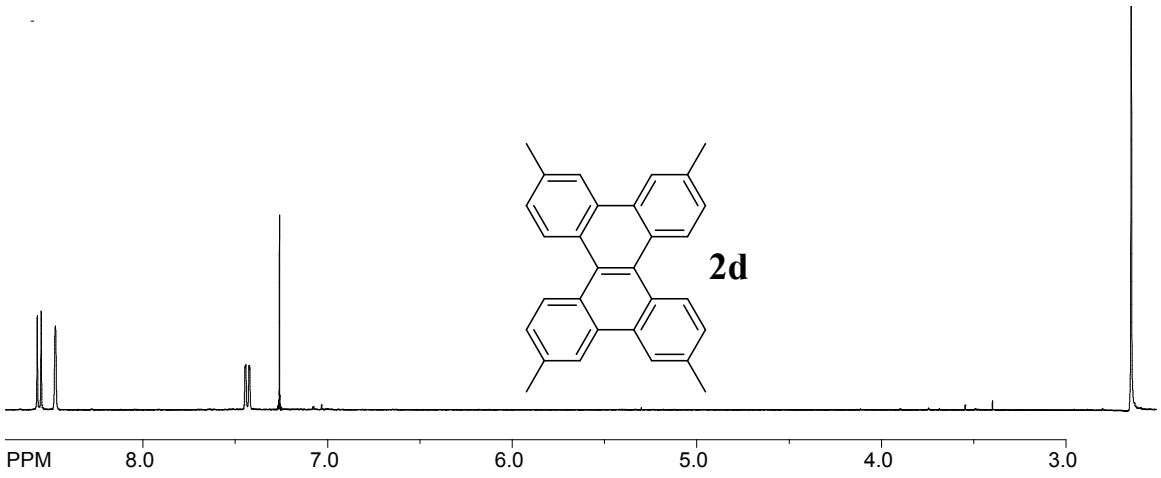

^{13}C NMR spectrum of 2d.

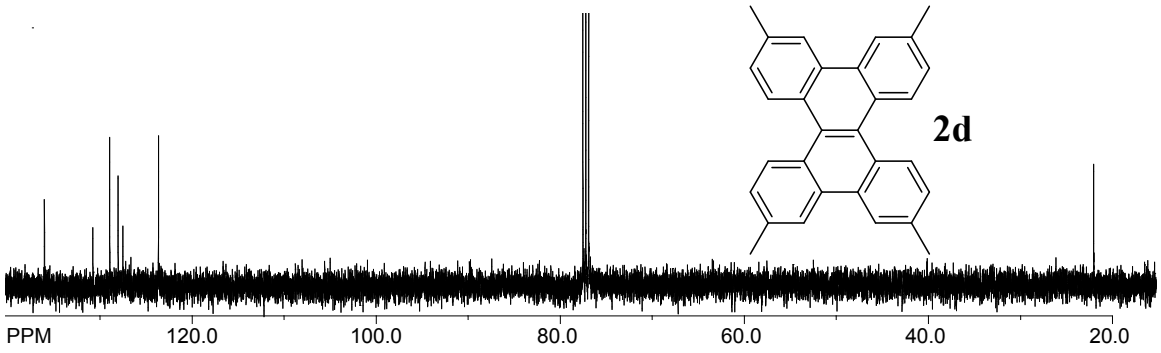

Using the general procedure described above, various tetraarylethylenes (TAEs) or isolated DAPs in Table 1 were subjected to oxidative C-C bond formation using DDQ/H^{+} to afford dibenzochrysenes in good to excellent yields (see Table 2in the text) and their spectral data are summarized below.

1d: Yield: 98% (based on the recovered **1b**, 86%); mp 216- 218 ^{o}C (lit[6] 216- 218 ^{o}C); ^{1}H NMR δ: 7.56-7.72 (m, 8H), 8.67-8.75 (m, 8H); ^{13}C NMR δ: 123.80, 126.77, 127.69, 129.10, 129.42, 130.71, 131.06.

^{1}H NMR spectrum of 1d.

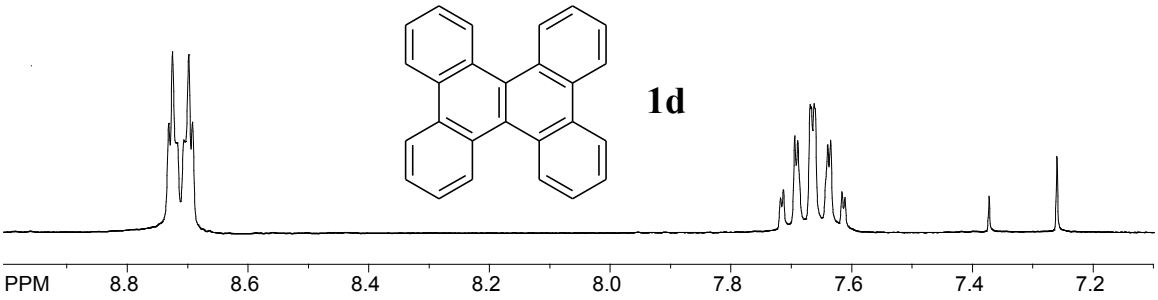

^{13}C NMR spectrum of 1d.

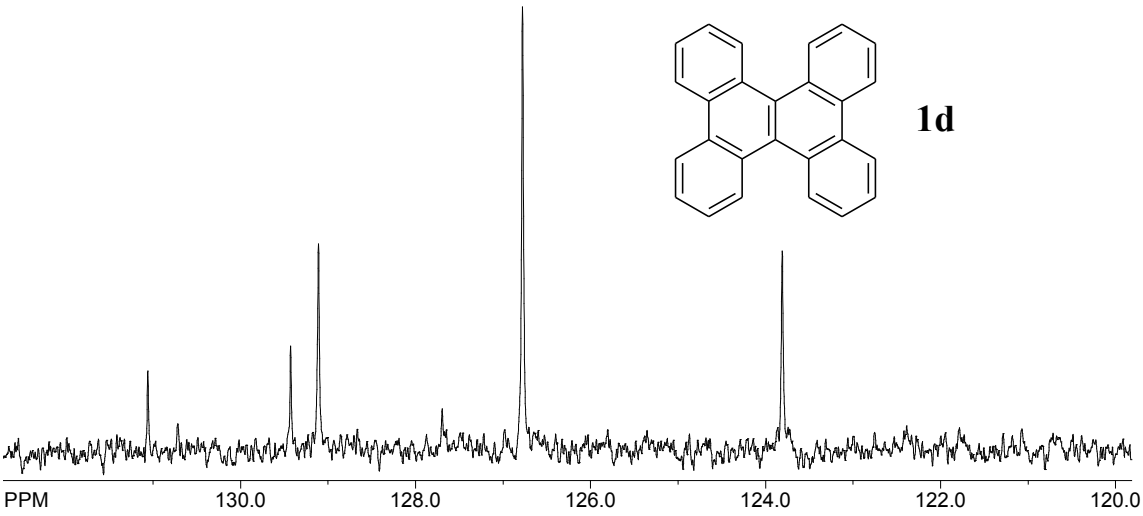

3d: Yield: 76%; mp 206- 208 ^{o}C; ^{1}H NMR: 2.65 (s, 3H), 7.46 (dd, 1H, *J* = 8.6 Hz, 1.6 Hz), 7.59-7.71 (m, 6H), 8.49(s, 1H), 8.58(d, 1H, *J* = 8.4 Hz), 8.67-8.73(m, 6H); ^{13}C NMR: 22.06, 123.73, 123.76, 126.53, 126.61, 126.67, 126.70, 127.05, 127.24, 127.76, 128.28, 128.99, 129.01, 129.07, 129.12, 129.44, 129.49, 129.51, 130.85, 130.87, 131.01, 131.11, 136.53.

^{1}H NMR spectrum of 3d.

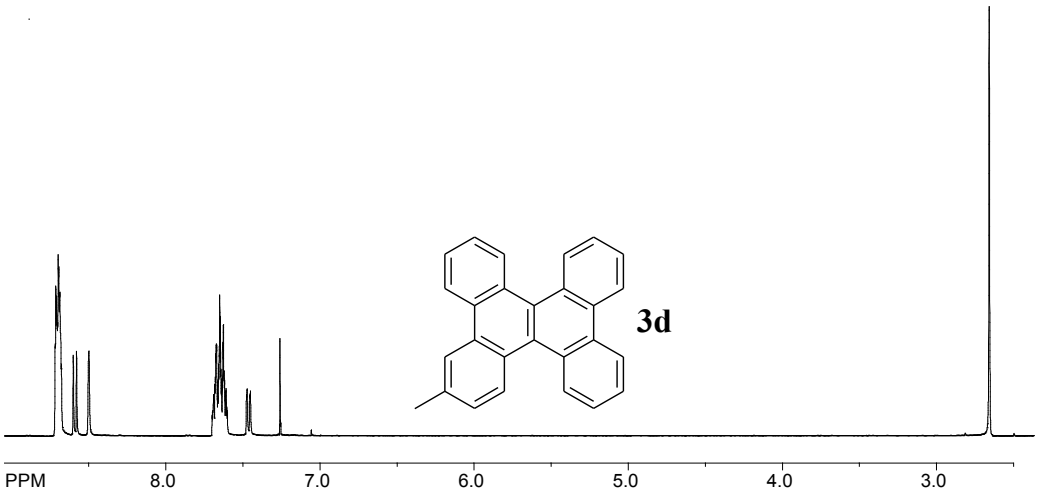

^{13}C NMR spectrum of 3d.

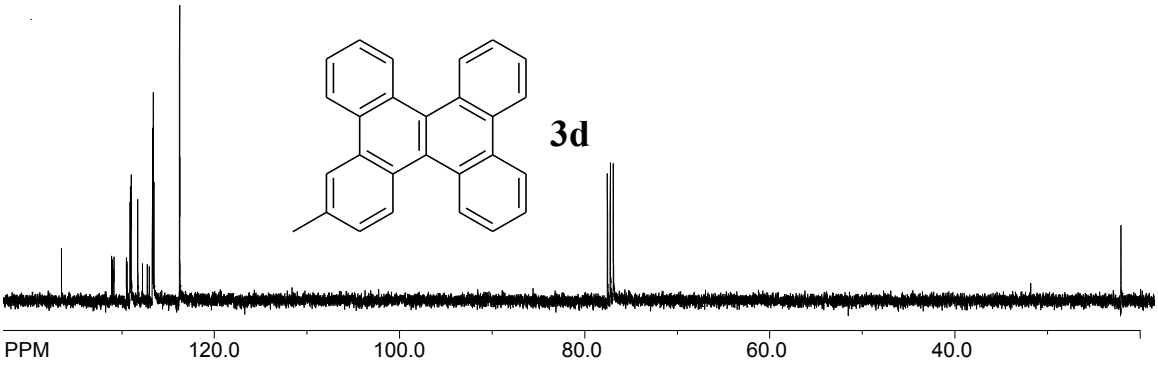

4d: Yield: 94%, mp 320- 322 ^{o}C; ^{1}H NMR δ: 2.65 (s, 6H), 7.45 (dd, 2H, *J* = 8.4 Hz, 1.4 Hz), 7.59-7.68 (m, 4H), 8.49 (s, 2H), 8.57 (d, 2H, *J* = 8.4 Hz), 8.69 (td, 4H, *J* = 8.0 Hz, 1.5 Hz); ^{13}C NMR δ: 22.05, 123.69, 123.72, 126.37, 126.43, 126.55, 127.27, 127.83, 128.19, 128.96, 129.03, 129.60, 130.69, 131.08, 136.40.

^{1}H NMR spectrum of 4d.

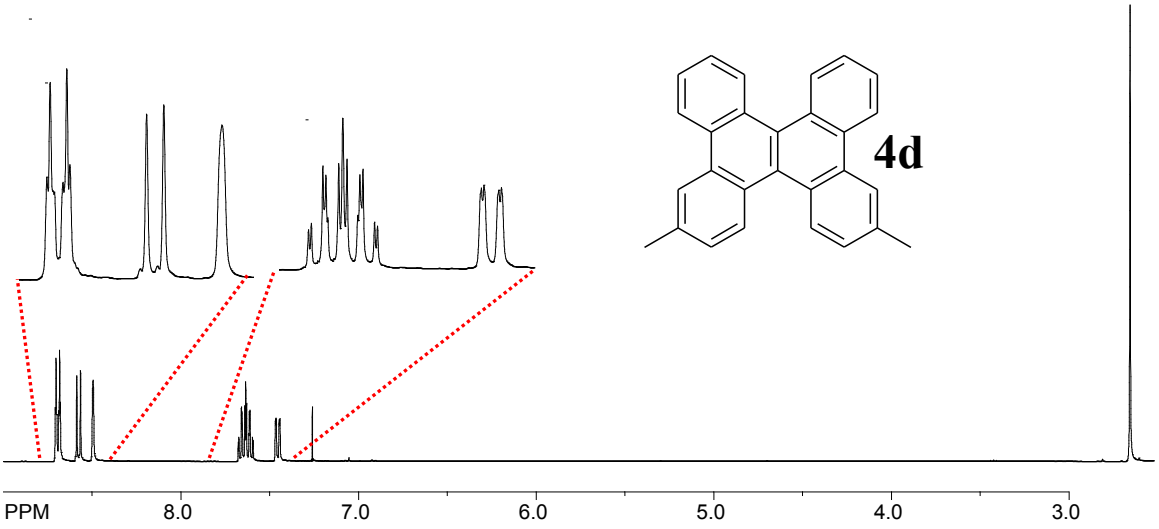

^{13}C NMR spectrum of 4d.

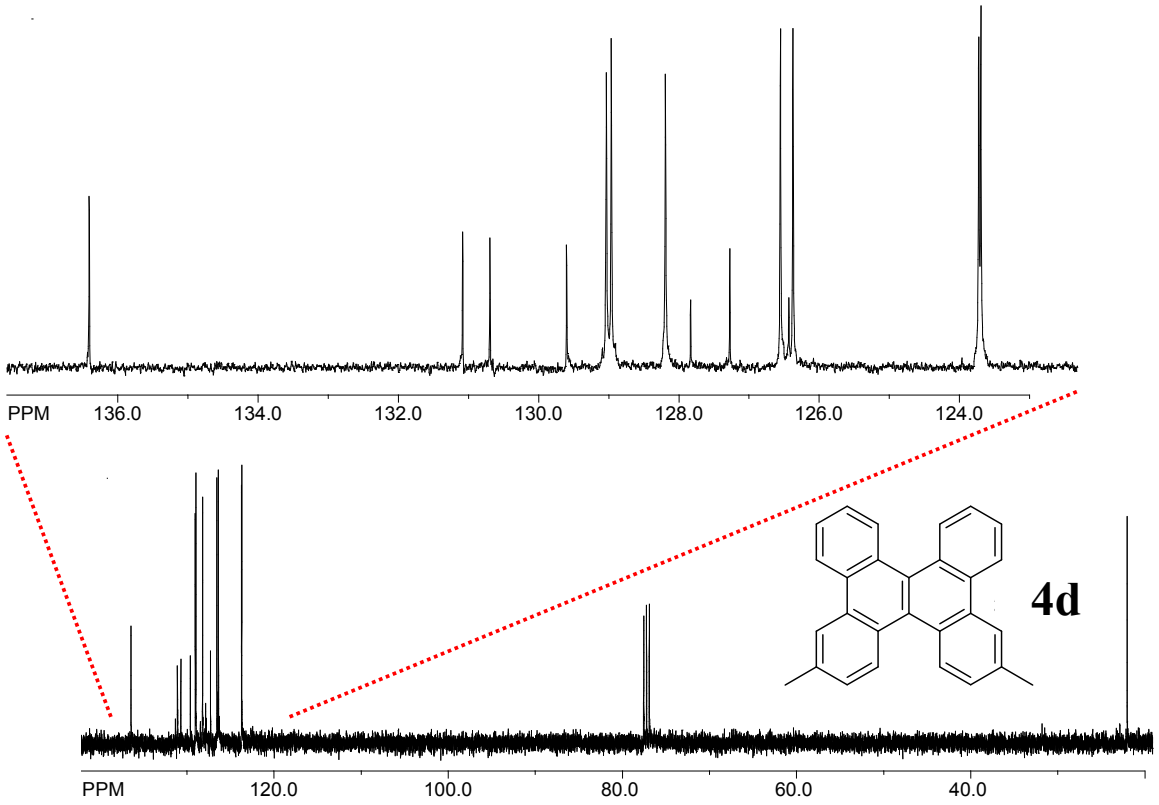

5d: Yield: 80%; mp 238- 340 ^{o}C; ^{1}H NMR δ: 7.44 (tt, 1H, *J* = 7.4 Hz, 1.3 Hz), 7.56 (t, 2H, *J* = 7.9 Hz), 7.62-7.73 (m, 6H), 7.83-7.90 (m, 3H), 8.69-8.74 (m, 5H), 8.76 (d, 1H, *J*

= 8.6 Hz), 8.79 (dd, 1H, *J* = 8.4 Hz, 1.4 Hz), 8.91 (d, 1H, *J* = 1.9 Hz); ^{13}C NMR δ: 122.15, 123.82, 125.91, 126.80, 126.82, 126.86, 126.89, 126.91, 127.56, 127.65, 127.75, 127.78, 127.80, 127.81, 128.54, 129.07, 129.15, 129.19, 129.23, 129.38, 129.42, 129.60, 129.66, 131.05, 131.08, 131.12, 131.34, 139.34, 141.28.

^{1}H NMR spectrum of 5d.

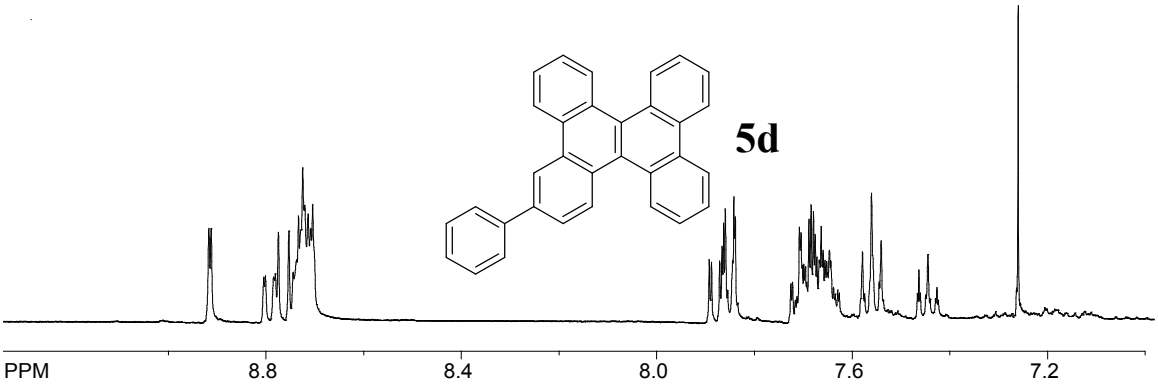

^{13}C NMR spectrum of 5d.

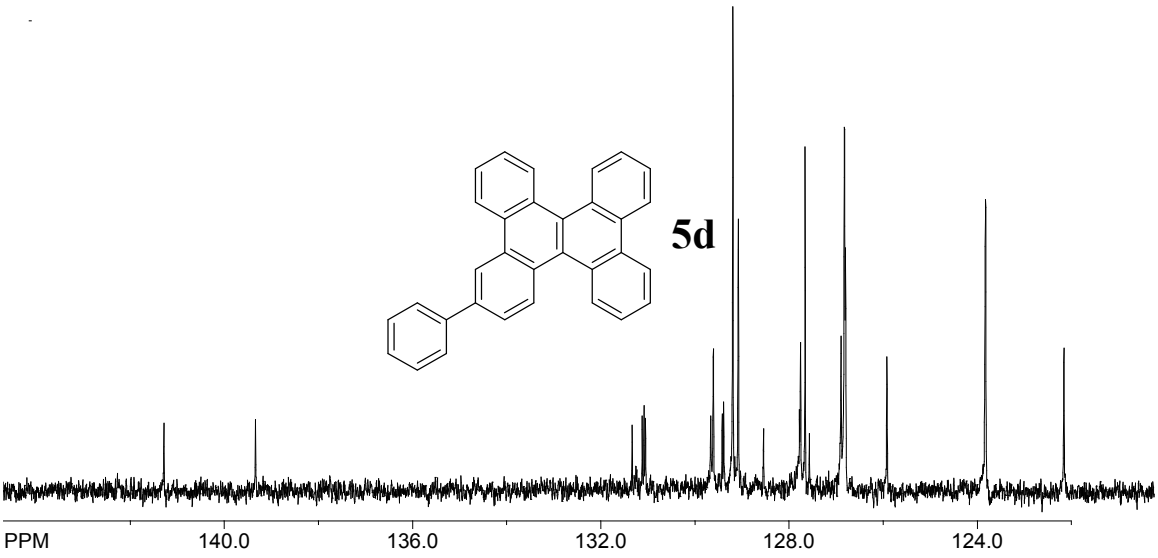

Table 3. **Crystal data and structure for structure refinement for raj15y (2b)**

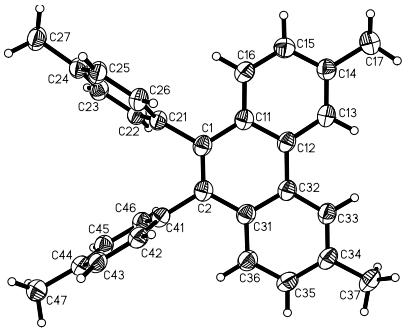

Identification code	raj15y	
Empirical formula	C30 H26	
Formula weight	386.51	
Temperature	100(2) K	
Wavelength	1.54178 Å	
Crystal system	Monoclinic	
Space group	P 21/n	
Unit cell dimensions	a = 10.9572(11) Å	α= 90°.
	b = 10.3404(12) Å	β= 104.931(6)°.
	c = 19.780(2) Å	γ = 90°.
Volume	2165.4(4) $Å^3$	
Z	4	
Density (calculated)	1.186 Mg/m^3	
Absorption coefficient	0.501 mm^{-1}	
F(000)	824	
Crystal size	0.38 x 0.08 x 0.04 mm^3	
Theta range for data collection	4.22 to 67.64°.	
Index ranges	-13<=h<=12, 0<=k<=11, 0<=l<=22	
Reflections collected	17345	
Independent reflections	3718 [R(int) = 0.0724]	
Completeness to theta = 67.64°	98.1 %	
Absorption correction	Semi-empirical from equivalents	
Max. and min. transmission	0.9802 and 0.8323	
Refinement method	Full-matrix least-squares on F^2	
Data / restraints / parameters	3718 / 0 / 276	
Goodness-of-fit on F^2	0.998	
Final R indices [I>2sigma(I)]	R1 = 0.0550, wR2 = 0.1302	
R indices (all data)	R1 = 0.0938, wR2 = 0.1506	
Extinction coefficient	0.0017(3)	
Largest diff. peak and hole	0.246 and -0.177 $e.Å^{-3}$	

Table 4. **Crystal data and structure for structure refinement for raj19l (2c)**

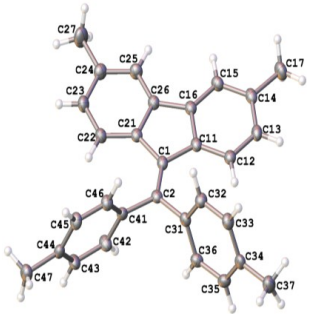

Identification code	raj19l
Empirical formula	$C_{30}H_{26}$
Formula weight	386.51
Temperature / K	100.0
Crystal system	monoclinic
Space group	C2/c
a / Å, b / Å, c / Å	20.3854(4), 10.05033(19), 21.6071(5)
α/°, β/°, γ/°	90.00, 97.210(2), 90.00
Volume / $Å^3$	4391.87(17)
Z	8
ρ_{calc} / mg mm^{-3}	1.169
μ / mm^{-1}	0.494
F(000)	1648
Crystal size / mm^3	0.09 × 0.04 × 0.02
Theta range for data collection	4.12 to 70.73°
Index ranges	$-24 \le h \le 24$, $-12 \le k \le 12$, $-26 \le l \le 17$
Reflections collected	14666
Independent reflections	4130[R(int) = 0.0415]
Data/restraints/parameters	4130/0/275
Goodness-of-fit on F^2	1.008
Final R indexes [I>2σ (I)]	R_1 = 0.0394, wR_2 = 0.0989
Final R indexes [all data]	R_1 = 0.0544, wR_2 = 0.1052
Largest diff. peak/hole / e $Å^{-3}$	0.217/-0.183

Table 5. **Crystal data and structure refinement for raj16c (4b)**

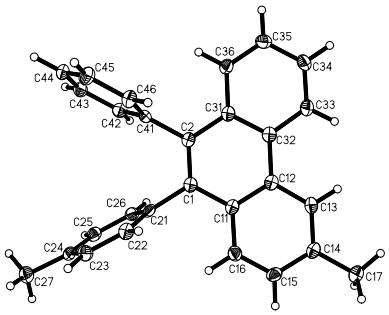

Identification code	raj16c	
Empirical formula	C28.33 H22.33 Cl	
Formula weight	398.25	
Temperature	100(2) K	
Wavelength	1.54178 Å	
Crystal system	Triclinic	
Space group	P -1	
Unit cell dimensions	a = 9.8526(2) Å	α= 108.7570(10)°.
	b = 18.1426(3) Å	β= 100.3990(10)°.
	c = 19.4664(3) Å	γ = 100.0760(10)°.
Volume	3137.68(10) $Å^3$	
Z	6	
Density (calculated)	1.265 Mg/m^3	
Absorption coefficient	1.683 mm^{-1}	
F(000)	1256	
Crystal size	0.42 x 0.10 x 0.07 mm^3	
Theta range for data collection	2.66 to 67.81°.	
Index ranges	-10<=h<=10, -21<=k<=20, 0<=l<=22	
Reflections collected	25938	
Independent reflections	10672 [R(int) = 0.0214]	
Completeness to theta = 67.81°	98.8 %	
Absorption correction	Semi-empirical from equivalents	
Max. and min. transmission	0.8913 and 0.5383	
Refinement method	Full-matrix least-squares on F^2	
Data / restraints / parameters	10672 / 0 / 799	
Goodness-of-fit on F^2	1.020	
Final R indices [I>2sigma(I)]	R1 = 0.0371, wR2 = 0.0960	
R indices (all data)	R1 = 0.0462, wR2 = 0.1005	
Largest diff. peak and hole	0.257 and -0.345 e.$Å^{-3}$	

Table 6. Crystal data and structure for raj16ha (7b)

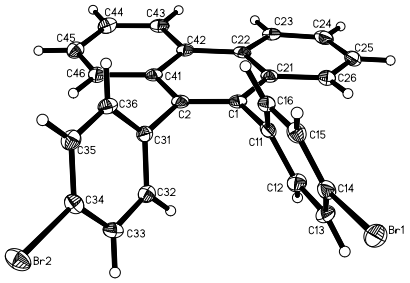

Identification code	raj16ha	
Empirical formula	C26 H16 Br2	
Formula weight	488.21	
Temperature	100(2) K	
Wavelength	1.54178 Å	
Crystal system	Triclinic	
Space group	P -1	
Unit cell dimensions	a = 9.6702(2) Å	α= 79.5680(10)°.
	b = 9.6964(2) Å	β= 77.8540(10)°.
	c = 11.0895(2) Å	γ = 76.2330(10)°.
Volume	977.90(3) $Å^3$	
Z	2	
Density (calculated)	1.658 Mg/m^3	
Absorption coefficient	5.307 mm^{-1}	
F(000)	484	
Crystal size	0.58 x 0.25 x 0.20 mm^3	
Theta range for data collection	4.12 to 67.86°.	
Index ranges	-10<=h<=11, -10<=k<=11, 0<=l<=13	
Reflections collected	8064	
Independent reflections	3317 [R(int) = 0.0190]	
Completeness to theta = 67.86°	98.1 %	
Absorption correction	Numerical	
Max. and min. transmission	0.4197 and 0.1491	
Refinement method	Full-matrix least-squares on F^2	
Data / restraints / parameters	3317 / 0 / 254	
Goodness-of-fit on F^2	1.002	
Final R indices [I>2sigma(I)]	R1 = 0.0234, wR2 = 0.0625	
R indices (all data)	R1 = 0.0238, wR2 = 0.0628	
Extinction coefficient	0.00261(18)	
Largest diff. peak and hole	0.413 and -0.281 $e.Å^{-3}$	

Table 7. **Crystal data and structure refinement for raj15t5 (8b)**

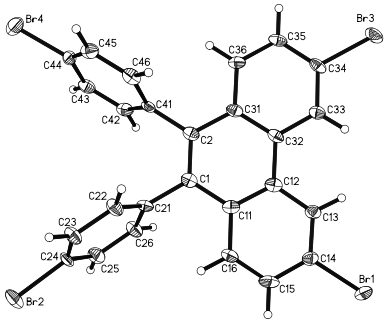

Identification code	raj15t5	
Empirical formula	C26 H14 Br4	
Formula weight	646.01	
Temperature	100(2) K	
Wavelength	1.54178 Å	
Crystal system	Triclinic	
Space group	P -1	
Unit cell dimensions	a = 9.5315(6) Å	α= 81.715(2)°.
	b = 10.4853(5) Å	β= 76.668(3)°.
	c = 11.9199(6) Å	γ = 79.787(3)°.
Volume	1134.17(11) $Å^3$	
Z	2	
Density (calculated)	1.892 Mg/m^3	
Absorption coefficient	8.737 mm^{-1}	
F(000)	620	
Crystal size	0.48 x 0.12 x 0.06 mm^3	
Theta range for data collection	3.83 to 67.41°.	
Index ranges	-10<=h<=10, -12<=k<=12, 0<=l<=14	
Reflections collected	12663	
Independent reflections	3774 [R(int) = 0.0485]	
Completeness to theta = 67.41°	98.2 %	
Absorption correction	Semi-empirical from equivalents	
Max. and min. transmission	0.6222 and 0.1022	
Refinement method	Full-matrix least-squares on F^2	
Data / restraints / parameters	3774 / 0 / 272	
Goodness-of-fit on F^2	1.127	
Final R indices [I>2sigma(I)]	R1 = 0.0407, wR2 = 0.1173	
R indices (all data)	R1 = 0.0422, wR2 = 0.1195	
Largest diff. peak and hole	0.997 and -0.698 $e.Å^{-3}$	

Table 8. **Crystal data and structure refinement for raj19e (8c)**

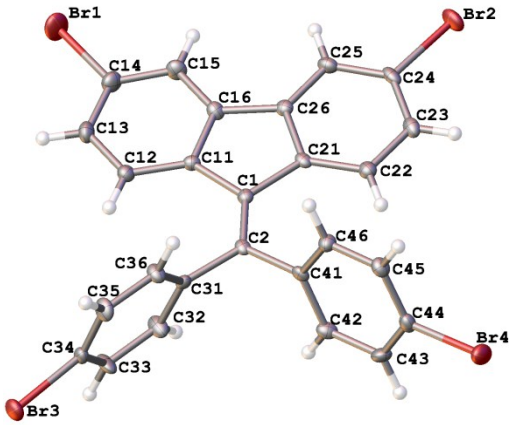

Identification code	raj19e
Empirical formula	$C_{26}H_{14}Br_4$
Formula weight	646.01
Temperature / K	100
Crystal system	Monoclinic
Space group	C2/c
a / Å, b / Å, c / Å	20.7871(3), 9.92103(17), 22.1583(3)
α/°, β/°, γ/°	90.00, 97.5244(14), 90.00
Volume / $Å^3$	4530.34(12)
Z	8
ρ_{calc} / mg mm^{-3}	1.894
μ / mm^{-1}	7.118
F(000)	2480
Crystal size / mm^3	0.3544 × 0.1255 × 0.0254
Theta range for data collection	3.50 to 32.84°
Index ranges	$-31 \le h \le 31$, $-14 \le k \le 14$, $-33 \le l \le 33$
Reflections collected	42334
Independent reflections	7976[R(int) = 0.0854]
Data/restraints/parameters	7976/0/271
Goodness-of-fit on F^2	1.076
Final R indexes [I>2σ (I)]	R_1 = 0.0544, wR_2 = 0.0886
Final R indexes [all data]	R_1 = 0.1101, wR_2 = 0.1034
Largest diff. peak/hole / e $Å^{-3}$	1.127/-0.825

CHAPTER 4

Synthesis and Photophysical Properties of Highly Soluble hexa-*peri*-hexabenzocoronenes (HBC)

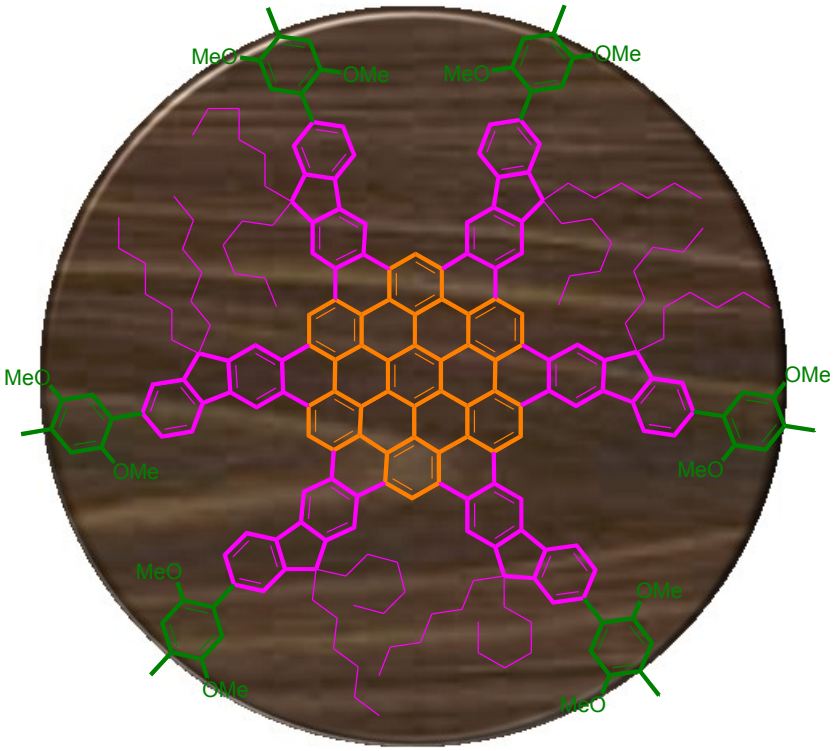

Abstract: Synthesis of a highly soluble hexa-*peri*-hexabenzocoronene (HBC) based polycyclic aromatic hydrocarbon (PAH) is described. Deployment of fluorenes at the periphery of the HBC core not only imparts solubility to the structure, but also allows the new PAHs to be functionalized further to make bigger PAHs or attach electroactive groups in order to study the intramolecular charge transport phenomena.

INTRODUCTION

A large number of polycyclic aromatic hydrocarbons (PAHs) with diverse shapes and lengths have been recognized as potential candidates for their use in thin film electronic devices like organic light emitting diodes (OLEDs), field effect transistors (FETs) and solar cells.[1] Of these, graphitic PAHs especially, those based on hexa-*peri*-hexabenzocoronenes (HBCs), continue to receive tremendous attention[2,3] due to their large flat π-conjugated aromatic core which endows the ability to self organize into columnar superstructures and provides high charge carrier mobility.[4]

Thus, attempts have been made to extend the HBC core and prepare larger PAHs for three important reasons: 1) a larger aromatic core can lead to better charge carrier mobility. 2) In light of the liquid crystalline properties, PAHs with smaller disc (mesogen) size tend to tilt against the columnar axis. Therefore, use of larger mesogens will reduce the tendency to tilt against the columnar axis and give increased columnar stability and order, which will also help to enhance charge carrier mobility. 3) Increasing the size of the aromatic core will lead to larger chromophores that can absorb over a broader range of the electromagnetic spectrum and increase the molar extinction coefficient - a highly desired quality for photovoltaic devices.[5]

However, the efforts to extend the size of the HBC core have largely been unsuccessful. Although the parent HBC is readily synthesized by oxidative cyclodehydrogenation of the readily available hexaphenylbenzene, the resulting HBC is completely insoluble in common organic solvents due to the formation of large

aggregates in solution.[2] This in turn leads to highly broadened signals in ^{1}H and ^{13}C NMR spectra to the extent that they cannot be characterized without resorting to variable temperature NMR spectroscopy at very high temperatures. Preparation of a soluble HBC derivative thus necessitates the installation of bulky or long alkyl side chains at the vertices of the HBC core which unfortunately requires multi step synthesis of the precursors.[2] However, the incorporation of these side chains obliterates the chances of growing the HBC further to larger flat π conjugated core.

Our recent success in effective utilization of fluorene backbone to prepare a variety of planar, soluble PAHs prompted us to design a strategy to prepare a HBC derivative such that flourene units are an integral part of HBC.

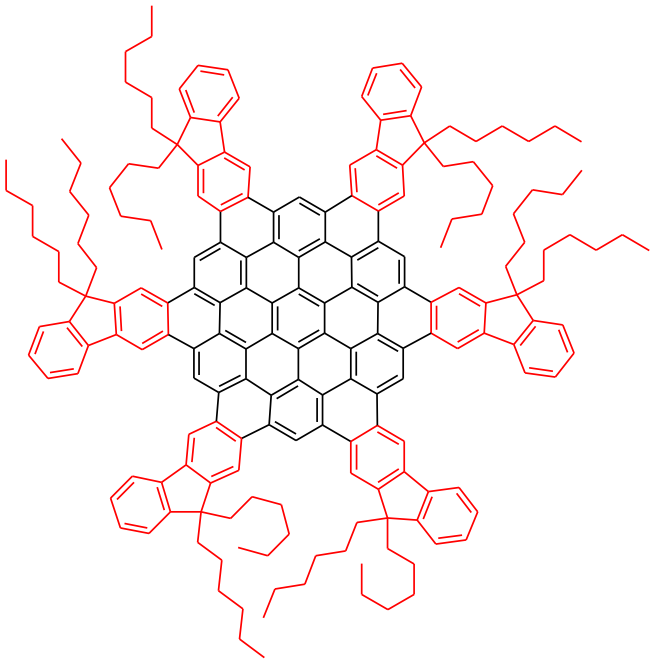

Figure 1. Proposed HBC derivative having peripheral fluorenes

It should be noted that fluorene—a tricyclic aromatic hydrocarbon has been extensively utilized for the preparation of a variety of electro-active materials[6] including the preparation of cofacially stacked polyfluorenes[7] (Figure 2).

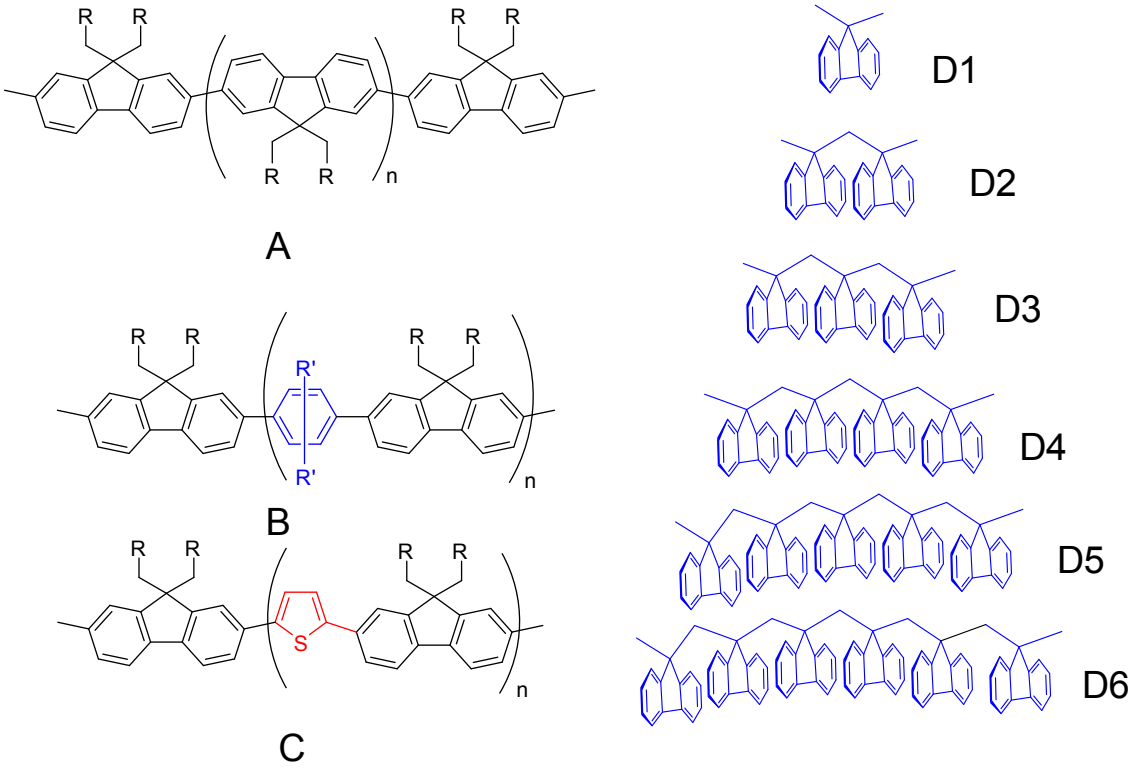

Figure 2. Representative examples of electro-active materials obtained using fluorene framework.[6,7]

The unique molecular structure of fluorene provides a platform for the attachment of groups at C_2/C_7 by palladium-catalyzed coupling reactions (generally for the preparation of linear polyfluorene molecular wires (i.e. Structures **A-C** in Figure 2)[6] and at C_9 by nucleophilic substitution reactions for imparting solubility in various polyfluorene derivatives as well as the synthesis of cofacially stacked polyfluorenes[7] (i.e. Structures **D1-D6** in Figure 2). Recently, C_3/C_6 positions of fluorene framework have

also largely been exploited by our group for oxidative cyclization using Scholl reaction to prepare a variety of large PAHs.

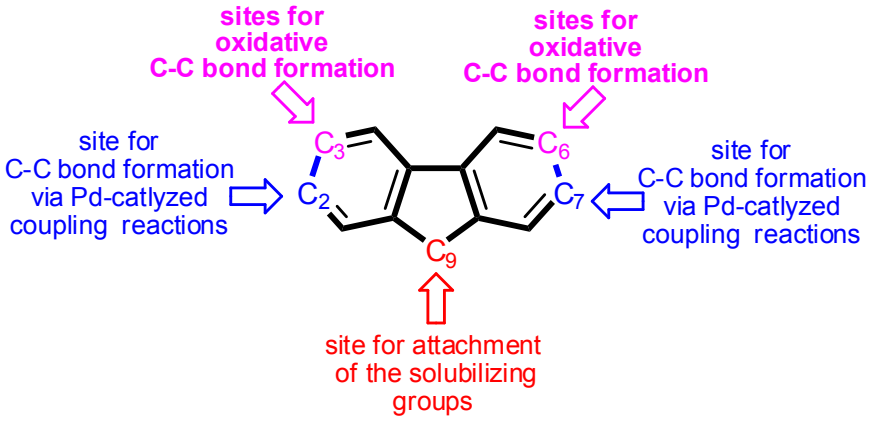

Figure 3. Showing various reactive sites onto the basic fluorene framework.

As such, the incorporation of fluorene units is envisioned to serve two functions. First, the alkyl substituents at the C_9 position of the original flourene shall make the resulting product soluble in common organic solvents, and second, one can extend the HBC core further by functionalizing the original C_2 position of these fluorenes. Availability of these soluble HBCs will not only allow the effective exploration of their optoelectronic properties in solution but ready processability of these materials will also spur interest of others for potential usage in the devices.

Accordingly, herein we describe a synthetic methodology that involves the buildup of a fluorene substituted hexaphenylbenzene, which upon cyclization leads to planar fluorenated HBC derivative (**FHBC**). Preparation of soluble **FHBC** readily allowed us to explore its optoelectronic properties in solution. Further extension of **FHBC** was achieved by appending electro active aryl groups to the peripheral fluorenes.

RESULT and DISCUSSION

The synthesis of **FHBC** starts with a Sonogashira coupling of phenyl acetylene with commercially available 1,3-dibromo-5-iodo-benzene (**1**) leading to **2** in excellent yield. A subsequent two fold Suzuki coupling[8] of **2** with 9,9-dihexylfluorene-2-boronic acid (prepared from 9,9-dihexyl-2-bromofluorene using standard boronic acid synthesis) afforded the unsymmetrical acetylene (**4**) in good yield. Cobalt (0) catalyzed trimerization of **4** gave a mixture of the two possible isomers **5a** and **5b,** in quantitative yield (Scheme 1)

Scheme 1. Synthesis of a mixture containing **5a** and **5b** from **1** employing Sonogashira coupling, Suzuki coupling, and dicobaltoctacarbonyl mediated cyclotrimerization.

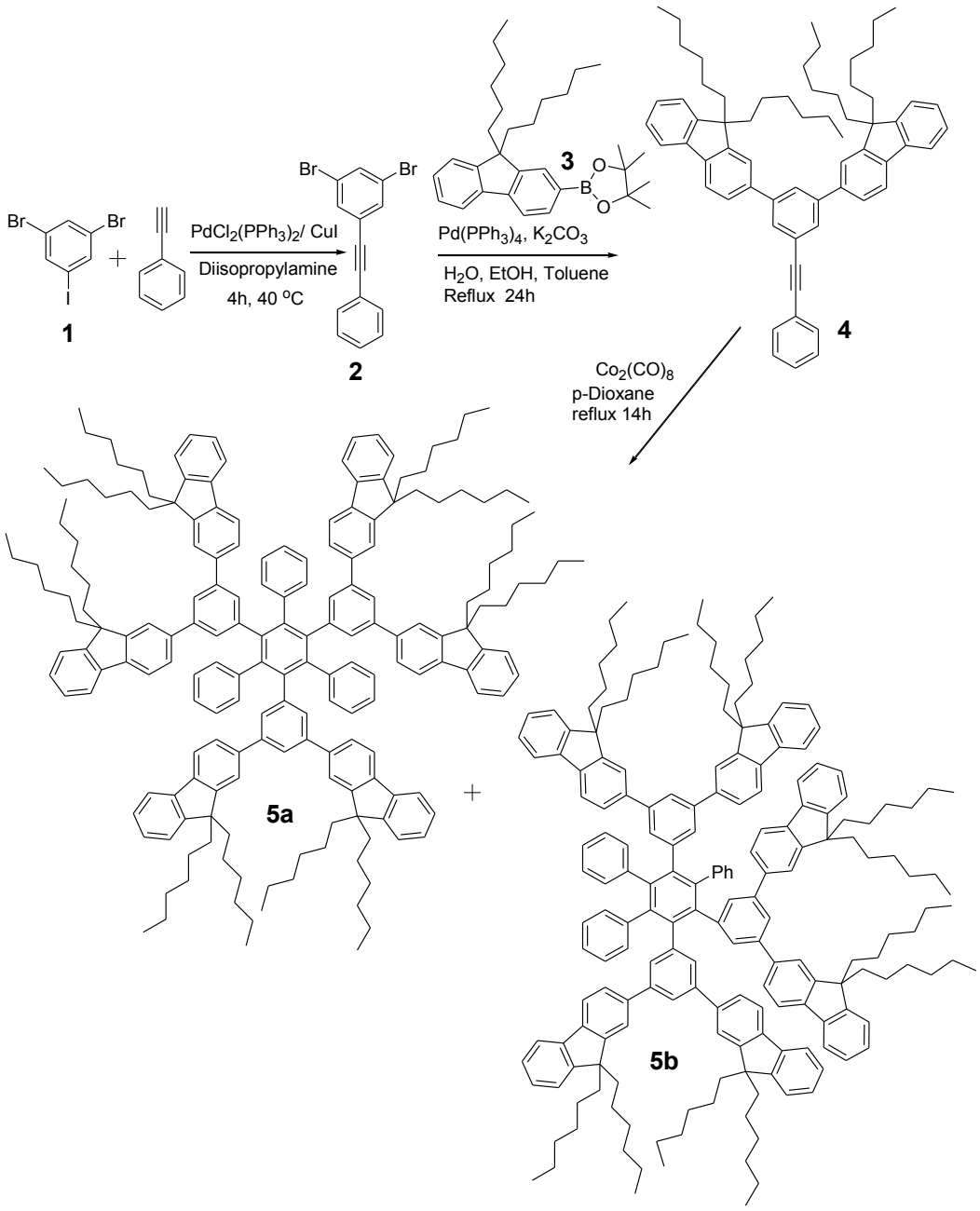

Unfortunately, the NMR spectroscopy was not of much help in deciphering the ratio of **5a**: **5b**. The attempts to separate **5a** and **5b** by column chromatography also failed owing to the similar R_f of the two isomers possibly due to the presence of long alkyl groups which also did not allow their easy crystallization. Thus, in order to determine the ratio of **5a** and **5b** in the trimerized mixture, we resorted to Scheme 2, in which we

replaced the hexyl groups at C_9 position of original fluorene by smaller ethyl groups. Hence, a twofold Suzuki coupling of **2** with 9,9-diethylfluorene-2-boronic acid (prepared from 9,9-diethyl-2-bromofluorene using standard boronic acid synthesis) afforded the unsymmetrical acetylene (**7**) in good yield. A subsequent cobalt(0) catalyzed trimerization of 7 gave a mixture of the two possible isomers **8a** and **8b,** in quantitative yield. The resulting product was recrystallized using dichloromethane and methanol (4:1) to afford pure **8a** which was characterized by ^1H and ^{13}C NMR spectroscopy and the structure was further confirmed by X-ray crystallography (see Figure 4). The successful characterization of **8a**, then allowed as to decipher the ratio **8a** and **8b** in the original product by analyzing the ^1H NMR spectra of the product mixture. A careful integration of the peaks of **8a** and **8b** allowed us to establish the ratio of **8a** and **8b** as 1: 2. The symmetrical isomer **8a** was then subjected to $FeCl_3$ catalyzed Scholl reaction[9] to give orange-red colored insoluble mass showing very broad peaks in the ^1H NMR spectrum possibly belonging to HBC derivative.

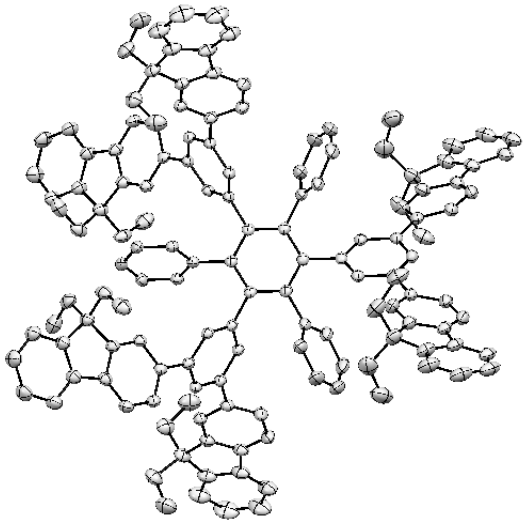

Figure 4. An ORTEP diagram of **8a** (hydrogens removed for the clarity)

Scheme 2. Synthesis of a mixture containing **8a** and **8b** from **2** employing Suzuki coupling and dicobaltoctacarbonyl mediated cyclcotrimerization.

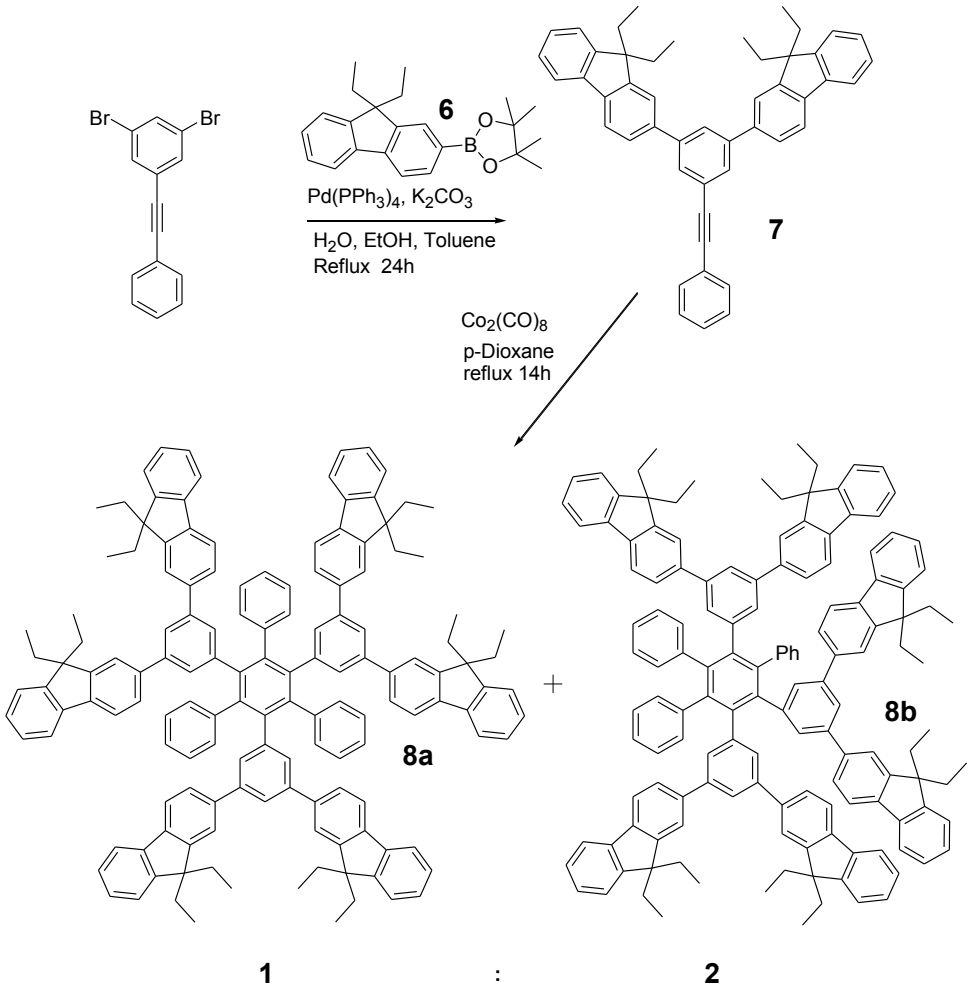

Next, we subjected the mixture of two isomers **5a** and **5b,** to $FeCl_3$ catalyzed cyclization to afford a deep red colored mixture containing **FHBC** and the cyclization products of the unsymmetrical isomer **5b** (Scheme 3). The resulting product mixture was then purified by column chromatography to afford red-orange colored **FHBC** in 28 %

yield in addition to 72 % of the unidentifiable deep red colored solid possibly arising from the cyclization of **5b**.

Scheme 3. Oxidation of a mixture containing **5a** and **5b** to **FHBC** using Ferric chloride as an oxidant.

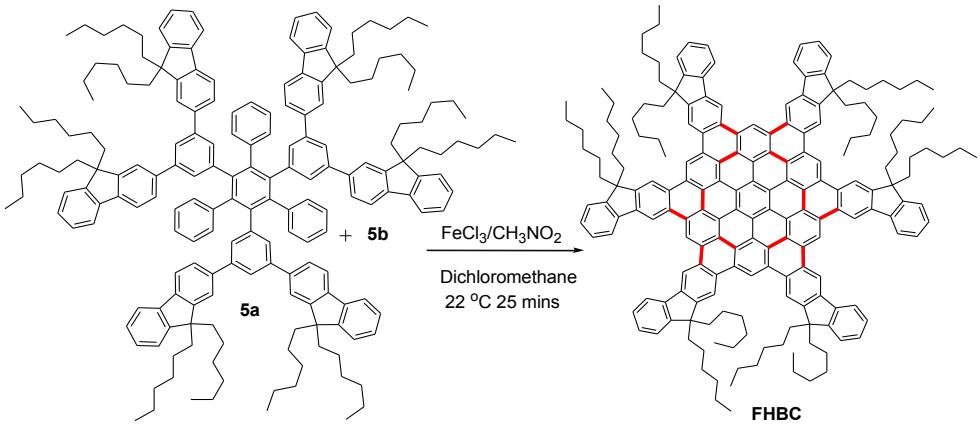

As expected, **FHBC** was highly soluble in most organic solvents including hexane, dichloromethane, chloroform, tetrahydrofuran, toluene and benzene. The high solubility of **FHBC** allowed its easy characterization by ^{1}H and ^{13}C NMR spectroscopy (Figure 5). MALDI-TOF mass spectrum showed molecular ion peak at m/z =2506 (see Experimental section)

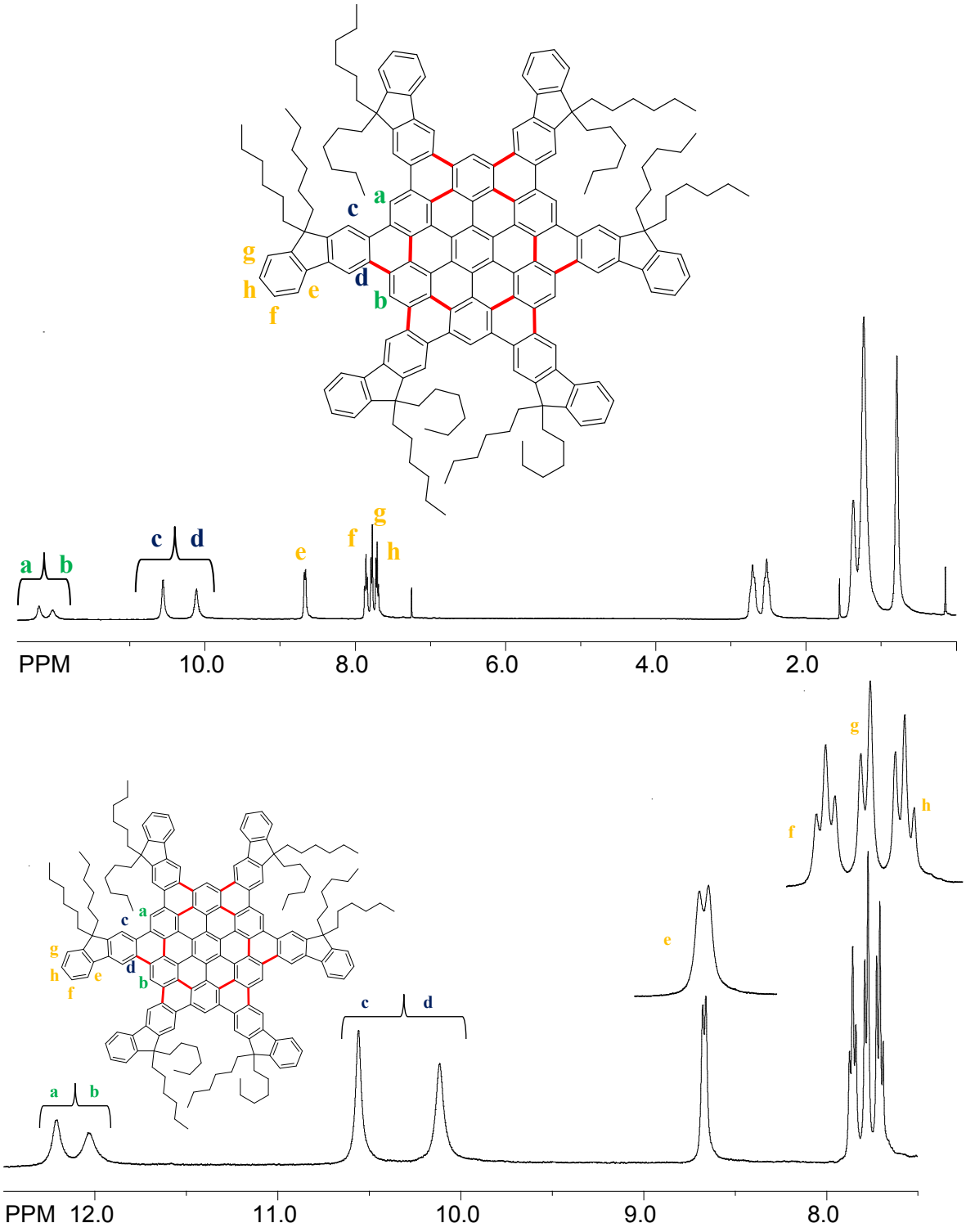

Figure 5. (Top) ^{1}H NMR spectra of **FHBC** at 22 ^{o}C in $CDCl_3$ (Bottom) partial ^{1}H NMR spectra of **FHBC** showing aromatic signals.

The low atom economy of the whole synthetic process, particularly the trimerization step where 66 % of the product is the undesired unsymmetrical isomer, compelled us to look for a more efficient synthetic pathway. In order to eliminate the possibility of undesired unsymmetrical product resulting from the trimerization of unsymmetrical alkyne (like **4** or **7**), we then resorted to the preparation of a symmetrical alkyne. The new synthetic scheme (scheme 4) starts with Sonogashira coupling of 1-bromo-3-iodo-benzene (**10**) with phenyl acetylene to give the symmetrical alkyne **11** in excellent yield. Suzuki coupling of 9,9-dihexylfluorene-2-boronicacid (**3**) with **11** afforded **12** in good yield. Cobalt(0) catalyzed trimerization of **12** afforded **13** in quantitative yield. The cyclization of **13** to prepare FHBC, was attempted using both Ferric chloride and DDQ/$H^{+\cdot}$ Unfortunately, the oxidative cyclodehydrogenation of **13** gave an intractable mixture of products in both of the above-mentioned cases, probably due to numerous cyclodehydrogenation routes possible for **13**.

Scheme 4. Attempted synthesis of **FHBC** using symmetrical alkyne **12**

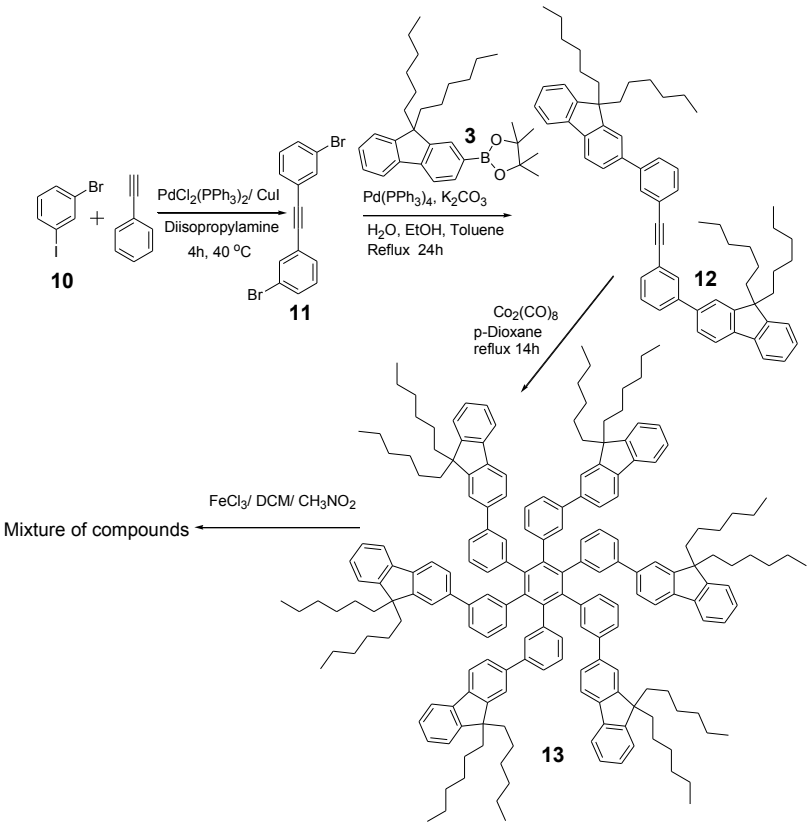

High solubility of **FHBC** in commonly employed organic solvents allowed us to investigate its optoelectronic properties.

Electrochemistry The electron donor strength of **FHBC** was evaluated by electrochemical oxidation at a platinum electrode as a 6.3 x 10^{-4} M solution of FHBC in dichloromethane containing 0.2 M *n*-Bu_4NPF_6 as the supporting electrolyte. The cyclic voltammograms of **FHBC**, when terminated before the start of the fifth oxidation event, showed three reversible oxidation waves (Figure 6), which consistently met the reversibility criteria at various scan rates of 200-500 mV/s, as they all showed cathodic/anodic peak current ratios of i_a/i_c=1.0 (theoretical) as well as the differences between anodic and cathodic peak potentials of E_{pa}-E_{pc} ~ 70 mV at 22 ^oC. The reversible oxidation potentials of **FHBC** were calibrated with ferrocene as internal standard (E_{ox} =

0.45 V *vs* SCE) and were found to be 0.85, 1.21, 1.46 and 1.64 volt corresponding to the formation of mono, di, tri and tetracation respectively. It is noted that the fourth oxidation wave in the cyclic voltammogram of **FHBC** displays a quasi-reversible oxidation wave (E_{ox4} = 1.64 V).

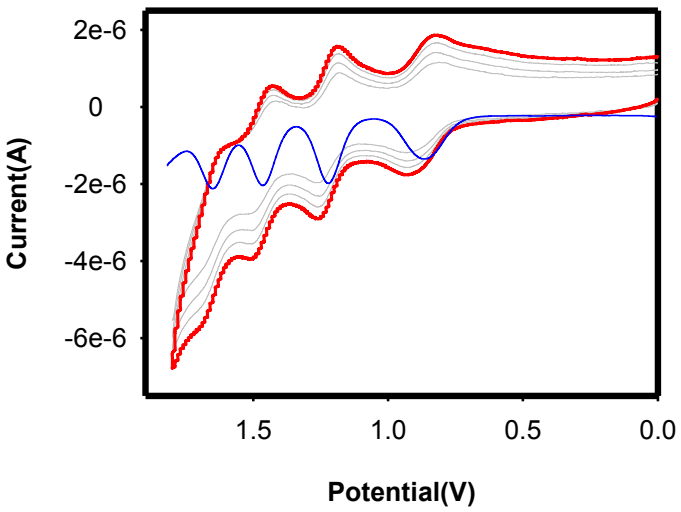

Figure 6. Cyclic voltammograms of 6.3 x 10^{-4} M **FHBC** at scan rates of 200-500 mV/s (gray traces for 200-400 mV/s and the red trace for 500 mV/s) and square wave (blue trace) in CH_2Cl_2 containing 0.2 M *n*-Bu_4NPF_6 at a scan rate of 200 mV/s at 22 °C.

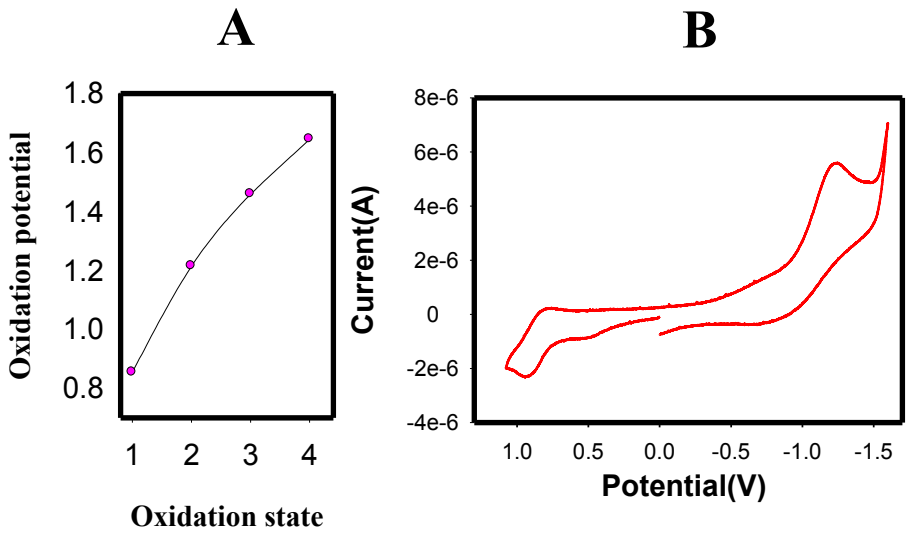

Figure 7. (A) Plot of oxidation potentials of **FHBC** against the oxidation states. (B) Cyclic voltammograms (red trace) of 6.3 x 10^{-4} M **FHBC** in CH_2Cl_2 containing 0.2 M *n*-Bu_4NPF_6 at a scan rate of 200 mV/s showing oxidation and reduction waves.

FHBC was found have a band gap of 1.46 eV. The band gap was calculated based on the onset of oxidation and reduction waves by using the equation:

$$\mathbf{E_g^{CV} = E_{ox1} - E_{red1}}$$

where, E_{ox1} and E_{red1} are onset potentials.

The low oxidation potential and electrochemical reversibility of **FHBC**, permitted ready oxidation to the corresponding cation radical using either a hydroquinone ether cation radical (**CRET**$^{+\bullet}$ $SbCl_6^-$; E_{red} = 1.11 V vs. SCE)[10], magic blue (**MB**$^{+\bullet}$ $SbCl_6^-$; E_{red} = 1.15 V vs. SCE)[11] or hindered naphthalene cation radical (**NAP**$^{+\bullet}$ $SbCl_6^-$; E_{red} = 1.34 V vs. SCE)[12] as oxidants.

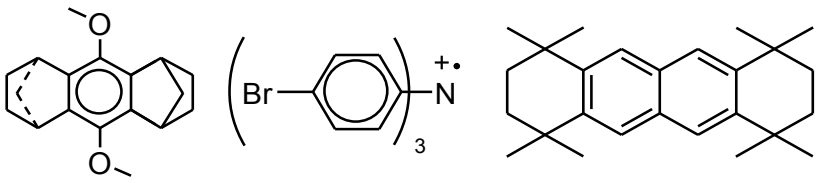

CRET$^{+\bullet}$ **MB**$^{+\bullet}$ **NAP** $^{+\bullet}$

E^{o}_{red} 1.11 1.15 1.34 (V *vs.* SCE)

Figure 8A shows the spectral changes attendant upon the reduction of blue-colored **MB**$^{+\bullet}$ (λ_{max} = 728 nm, log ε_{728} = 4.45) by incremental addition of sub-stoichiometric amounts of **FHBC** in dichloromethane at 22 °C. The presence two isosbestic points at 685 nm and 790 nm indicates the uncluttered nature of electron transfer from **FHBC** to **MB**$^{+\bullet}$ without decomposition of **FHBC**$^{+\bullet}$. Furthermore, a plot of formation of **FHBC**$^{+\bullet}$ (i.e. an increase in the absorbance at 1400 nm against the increments of added **FHBC** (Figure 8B) , established that **MB**$^{+\bullet}$ was completely consumed after the addition of 1 equiv of **FHBC**; and the resulting highly intense and structured absorption band of **FHBC**$^{+\bullet}$ in near IR region (ε_{1418} = 43,200 $M^{-1}cm^{-1}$; ε_{1261} = 30,437 $M^{-1}cm^{-1}$) and in the visible region (ε_{460} = 152,000 $M^{-1}cm^{-1}$; ε_{528} = 75,000 $M^{-1}cm^{-1}$ and ε_{664} = 55,700 $M^{-1}cm^{-1}$) showed a marginal increase upon further addition of neutral **FHBC**.

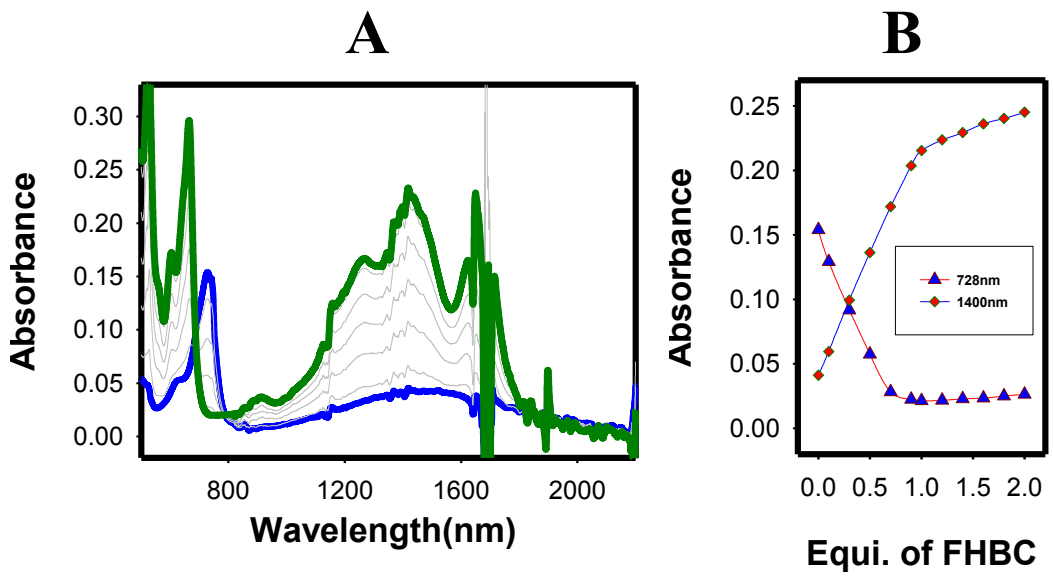

Figure 8. (**A**) The spectral changes observed upon the reduction of 5.5 x 10^{-6} M $\mathbf{MB}^{+\bullet}$ by an incremental addition of substoichiometric amounts of **FHBC** in CH_2Cl_2 at 22 ^{o}C. (**B**) A plot of depletion of absorbance of $\mathbf{MB}^{+\bullet}$ (blue triangles, at 728 nm) and an increase of the absorbance of $\mathbf{FHBC}^{+\bullet}$ (red rectangles, at 1400 nm) against the equivalents of added neutral **FHBC**.

Absorption/emission spectroscopy of FHBC The UV-vis and fluorescence spectrum of **FHBC** (6.4 x 10^{-4} M) was recorded in dichloromethane at 22 ^{o}C. Increments of **FHBC**, added to a dichloromethane solution showed linear concentration dependence with no observable shift (see Figure 9A and B).

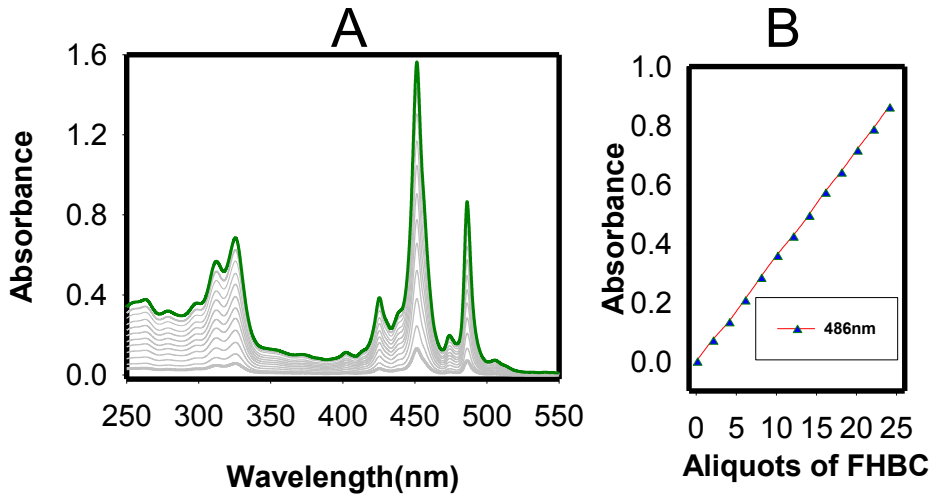

Figure 9. (**A**) The spectral changes observed upon addition of 6.4 x 10^{-4} M **FHBC** in CH_2Cl_2 at 22 ^{o}C. (**B**) A plot of increase in absorbance of **FHBC** at 486 nm obtained upon incremental additions of **FHBC** to 3 mL dichloromethane.

Excitation of **FHBC** at 451 nm (λ_{max}) gave a structured emission in the region from 550 nm to 660 nm with sharp emission peak at 583 nm while the excitation at 325 nm gave same structured emission in addition to very weak emission at 340 - 450 nm (see Figure 10A and 10B).

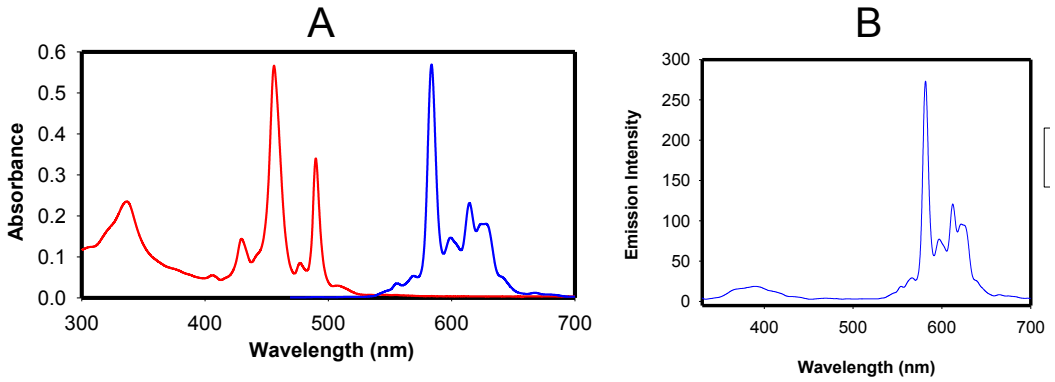

Figure 10. (A) Absorption (blue trace) and emission (pink trace) spectra of **FHBC** obtained upon excitation at 451 nm in dichloromethane at 22 °C. (B) Emission spectra of FHBC obtained upon excitation at 325 nm.

Next, we attempted to extend the size of the aromatic core further with the conjecture that the six peripheral fluorenes can be functionalized at their original C_7 position. Unfortunately, a six-fold bromination of **FHBC** using bromine in dichloromethane, led to a complex mixture of products.

Scheme 5. Unsuccessful bromination of **FHBC** to prepare **FHBC-Br$_6$**

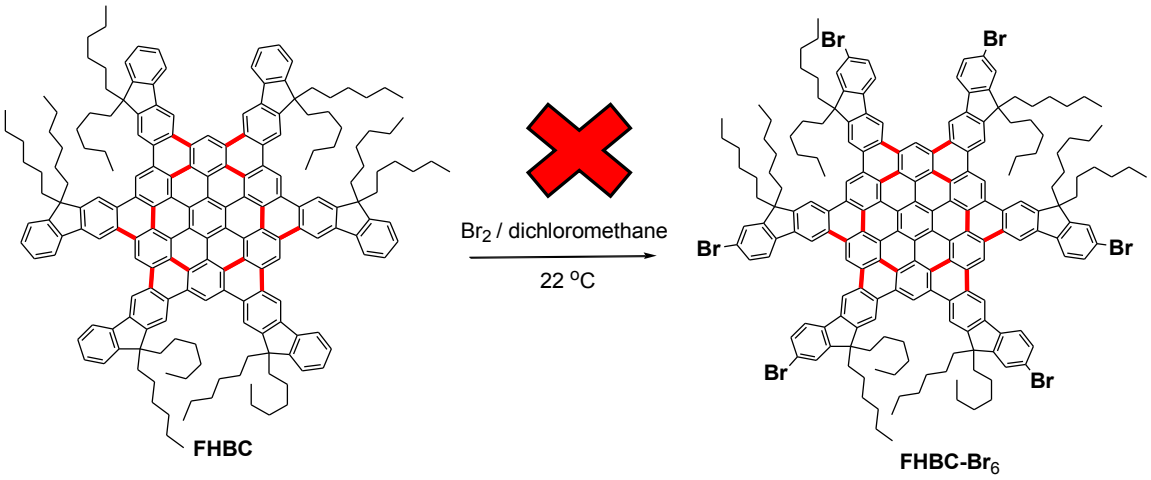

To understand the observation, we examined the HOMO of **FHBC** using DFT calculations at B3LYP level (Figure 11). The even distribution of HOMO along the core and its complete absence at the peripheral aryl rings of the fluorenes, thus explains our failure to brominate the periphery of FHBC at the desired C_7 position of the original fluorenes.

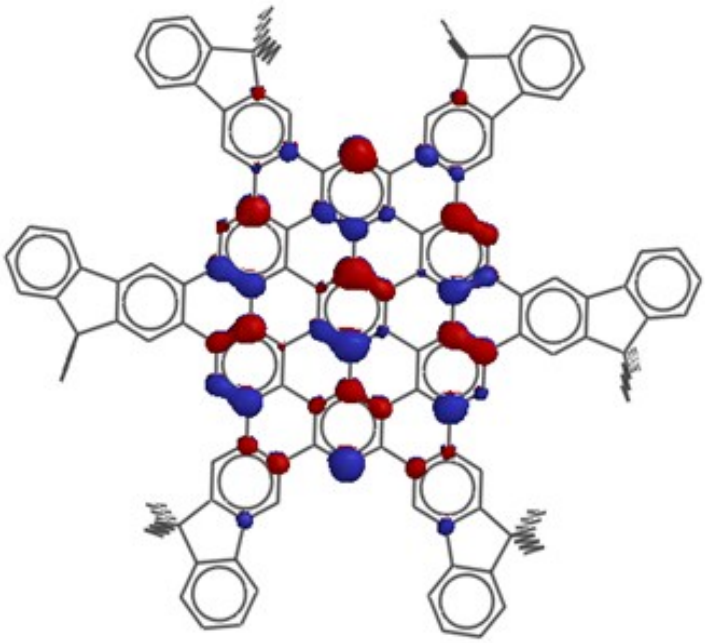

Figure 11. Showing evenly delocalized highest occupied molecular orbital (HOMO) of **FHBC**.

Thus, we decided to rollback one step and brominate the **FHBC** precursor, i.e. the unseparated mixture of **5a** and **5b**. A careful treatment of the above mixture in dichloromethane with 6 equivalents of bromine in the presence of catalytic amount of iodine, afforded the hexabrominated mixture of isomers **9a** and **9b** resulting from **5a** and **5b**, respectively, in quantitative yield. Our repeated attempts to separate the mixture of **9a** and **9b**, however, did not met success. Therefore, we subjected the above mixture of **9a** and **9b** to ferric chloride mediated cyclization to yield the dark red crude product, a column chromatography of which afforded **FHBC-Br$_6$** was in 20 % yield as a dark red solid (Scheme 6).

Scheme 6. Synthesis of **FHBC-Br$_6$** from a mixture containing **5a** and **5b** employing bromination followed by Ferric chloride mediated oxidative cyclodehydrogeantion.

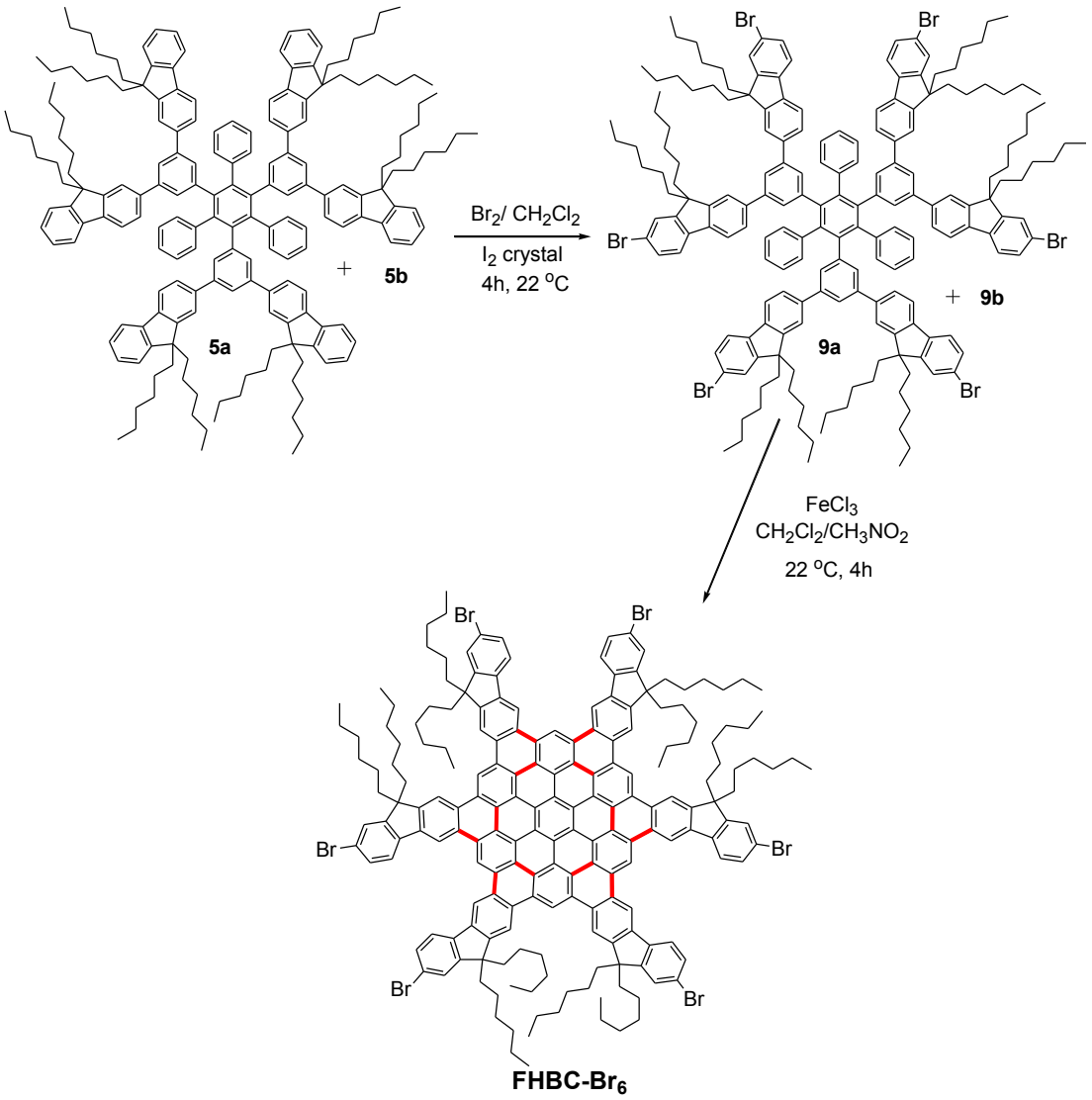

Successful preparation of **FHBC-Br$_6$** allows easy attachment of various aryl groups by using six fold Suzuki coupling with the corresponding boronic acids. A Pd(0) catalyzed reaction of **FHBC-Br$_6$** with 2,5-dimethoxy-4-methylphenylboronic acid, thus produces highly soluble **FHBC-Ar$_6$** in excellent yield (Scheme 7). **FHBC-Ar$_6$** was easily characterized by ^{1}H and ^{13}C NMR spectroscopy (Figure 12).

Scheme 7. Synthesis of **FHBC-Ar$_6$** by a six fold Suzuki coupling of **FHBC-Br$_6$**.

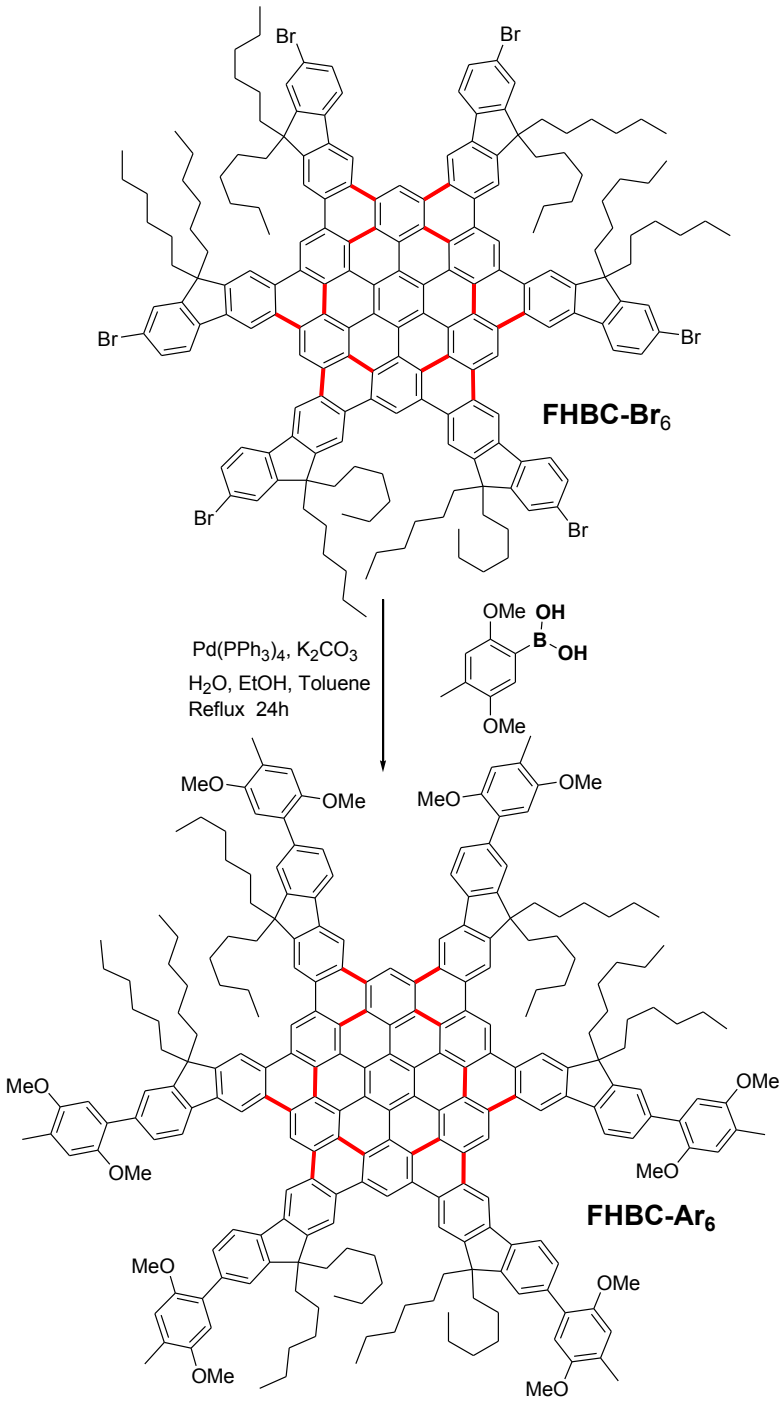
Br
Br
Br
Br
Br
Br
FHBC-Br6
Pd(PPh3)4, K2CO3
H2O, EtOH, Toluene
Reflux 24h
OMe
OH
B
OH
OMe
MeO
OMe
MeO
OMe
MeO
OMe
MeO
OMe
MeO
OMe
MeO
OMe
FHBC-Ar6

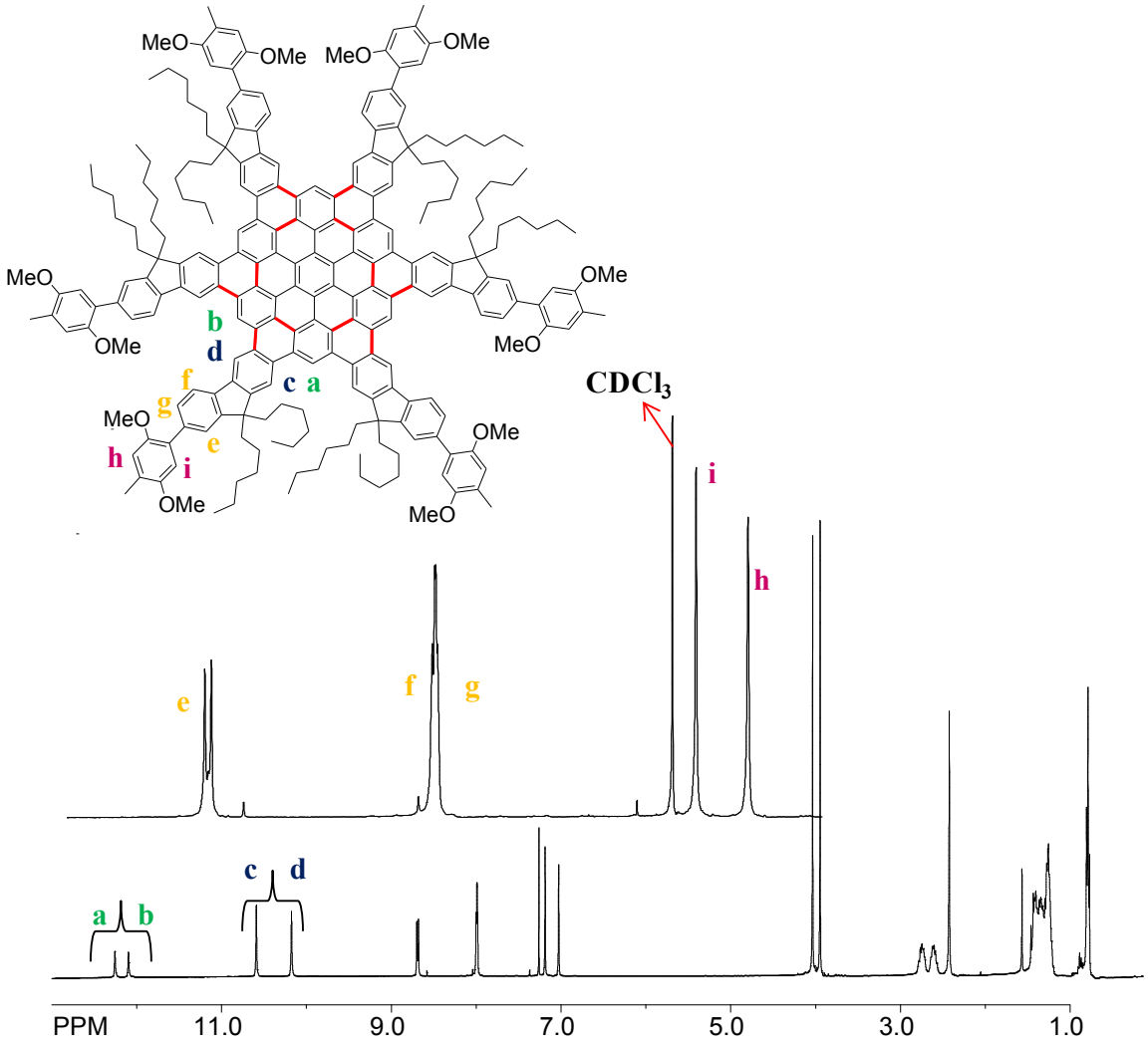

Figure 12. ^{1}H NMR spectra of FHBC-Ar$_6$ in $CDCl_3$ at 20 ^{o}C

High solubility of **FHBC-Ar$_6$** in commonly employed organic solvents again allowed us to investigate its optoelectronic properties in solution.

Electrochemistry of FHBC-Ar$_6$ The electron donor strength of **FHBC-Ar$_6$** was evaluated by electrochemical oxidation at a platinum electrode as a 4.0 x 10^{-5} M solution of **FHBC-Ar$_6$** in dichloromethane containing 0.2 M *n*-Bu_4NPF_6 as the supporting electrolyte. Cyclic voltamogram of **FHBC-Ar$_6$**, when terminated before the third oxidation event, showed two reversible oxidation waves (Figure 13A), which were

reversible over 100-500 mV scan rate. Third, fourth and fifth oxidation waves were quasi reversible (see Figure 5B). The reversible oxidation potentials of **FHBC-Ar$_6$** were calibrated with ferrocene as internal standard (E_{ox} = 0.45 V vs SCE) and were found to be 0.85, 1.16, 1.30, 1.60, and 1.71 V *vs.* SCE corresponding to monocation, hexacation, heptacation, octacation, nonacation and decacation respectively.

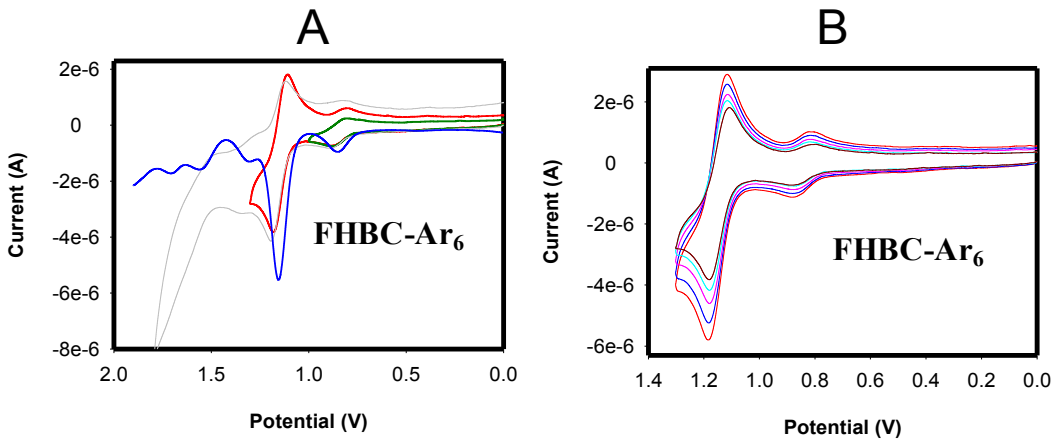

Figure 13. (**A**) Cyclic voltammogram (green/red/gray trace) and square wave (blue trace) of 4.0 x 10^{-5} M **FHBC-Ar$_6$** in CH_2Cl_2 containing 0.2 M *n*-Bu_4NPF_6 at a scan rate of 200 mV/s and (**B**) Cyclic voltammogram of **FHBC-Ar$_6$** at scan rates of 100-500 mV at 22 ^oC.

The low oxidation potential and electrochemical reversibility of **FHBC-Ar$_6$** permitted ready oxidation to the corresponding cation radical using either a hydroquinone ether (**CRET**$^{+\bullet}$ $SbCl_6^-$; E_{red} = 1.11 V *vs*. SCE)[10], magic blue (**MB**$^{+\bullet}$ $SbCl_6^-$; E_{red} = 1.15 V *vs*. SCE)[11] or hindered naphthalene cation radical (**NAP**$^{+\bullet}$ $SbCl_6^-$; E_{red} = 1.34 V *vs*. SCE)[12] as 1 e^- oxidants.

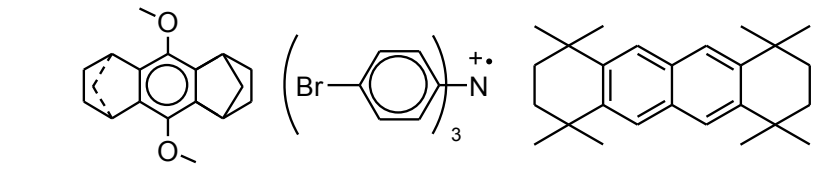

CRET$^{+\bullet}$ **MB**$^{+\bullet}$ **NAP** $^{+\bullet}$

E^{o}_{red} 1.11 1.15 1.34 (V *vs.* SCE)

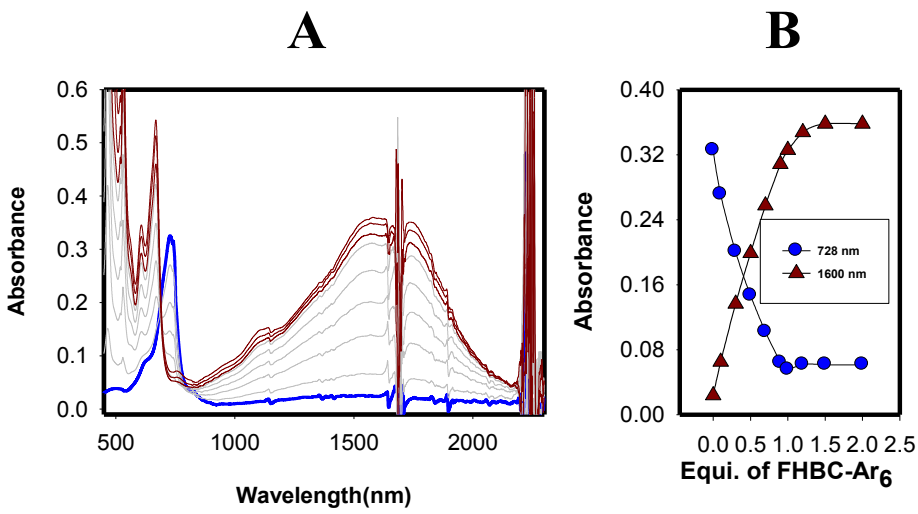

Figure 14. (**A**) The spectral changes observed upon the reduction of 1.13 x 10^{-5} M **MB**$^{+\bullet}$ by an incremental addition of sub-stoichiometric amounts of **FHBC-Ar$_6$** in CH_2Cl_2 at 22 ^{o}C. (**B**) A plot of depletion of absorbance of **MB**$^{+\bullet}$ (blue circles, at 728 nm) and an increase of the absorbance of **FHBC-Ar$_6$**$^{+\bullet}$ (brown rectangles, at 1600 nm) against the equivalents of added neutral **FHBC**.

Figure 14A shows the spectral changes attendant upon the reduction of blue-colored **MB**$^{+\bullet}$ (λ_{max} = 728 nm, log ε_{728} = 4.45) by incremental addition of sub-stoichiometric amounts of **FHBC-Ar$_6$** in dichloromethane at 22 °C. Furthermore, a plot of formation of **FHBC-Ar$_6$**$^{+\bullet}$ (i.e. an increase in the absorbance at 1600 nm against the increments of added **FHBC-Ar$_6$**, (Figure 13B) established that **MB**$^{+\bullet}$ was completely consumed after the addition of 1 equiv of **FHBC-Ar$_6$**; and the resulting highly intense and structured absorption band of **FHBC-Ar$_6$**$^{+\bullet}$ in near IR region (ε_{1600}

= 28,300 $M^{-1}cm^{-1}$) and in the visible region (ε_{670} = 48,000 $M^{-1}cm^{-1}$) showed a marginal increase upon further addition of neutral **FHBC-Ar$_6$**.

Oxidation of **FHBC-Ar$_6$** to its monocation can also be carried out with **CRET$^{+\bullet}$**, but unfortunately a clean spectral titration plot with isosbestic point could not be obtained due to an overwhelming overlap of the absorption band of **CRET$^{+\bullet}$** at 518 nm with that of **FHBC-Ar$_6^{+\bullet}$**. It is further noted that the intensely colored solution of **FHBC-Ar$_6^{+\bullet}$**, obtained either from **MB$^{+\bullet}$** (as per the stoichiometry shown below) or by using **CRET$^{+\bullet}$**, was stable at ambient temperature and did not show any decomposition during a 48-h period at 22 ^{o}C, as confirmed by UV-vis spectroscopy. Moreover, a reduction of **FHBC-Ar$_6^{+\bullet}$** with zinc dust regenerated the neutral **FHBC-Ar$_6$** quantitaitively as confirmed by ^{1}H NMR spectroscopy.

$$\textbf{FHBC-Ar}_6 + \textbf{MB}^{+\cdot} \longrightarrow \textbf{FHBC-Ar}_6^{+\cdot} + \textbf{MB}$$

In order to obtain polycation, **FHBC-Ar$_6$** was then oxidized using **NAP$^{+\bullet}$**$SbCl_6^-$ (E_{red} = 1.34 V *vs.* SCE). Figure 15A shows the spectral changes attendant upon the reduction of blue-colored **NAP$^{+\bullet}$** (λ_{max} = 673 nm, ε_{673} = 9,300 $M^{-1}cm^{-1}$) by incremental additions of sub-stoichiometric amounts of **FHBC-Ar$_6$** in dichloro-methane at 22 °C. It was found that **NAP$^{+\bullet}$** was completely consumed upon addition of 0.12 equivalent of **FHBC-Ar$_6$**. Unfortunately, a clean spectral titration plot with isosbestic points could not be obtained owing to an extensive overlap of **FHBC-Ar$_6^{n+}$** absorption with **NAP$^{+\bullet}$** absorption at 673 nm. Still, a plot of formation of **FHBC-Ar$_6^{n+}$** (*i.e.* an increase in the absorbance at 1400 nm against the increments of added **FHBC-Ar$_6$**, (Figure 15B and 15C) established that the abosrption band at 1400 nm attains a steady value after addition of 0.12 equivalent of **FHBC-Ar$_6$** upto the

addition of 0.20 equivalent. However, this band increases significantly upon further addition upto 0.8 equivalents of **FHBC-Ar$_6$** suggesting extensive association of **FHBC-Ar$_6^{8+}$** with neutral **FHBC-Ar$_6$**.

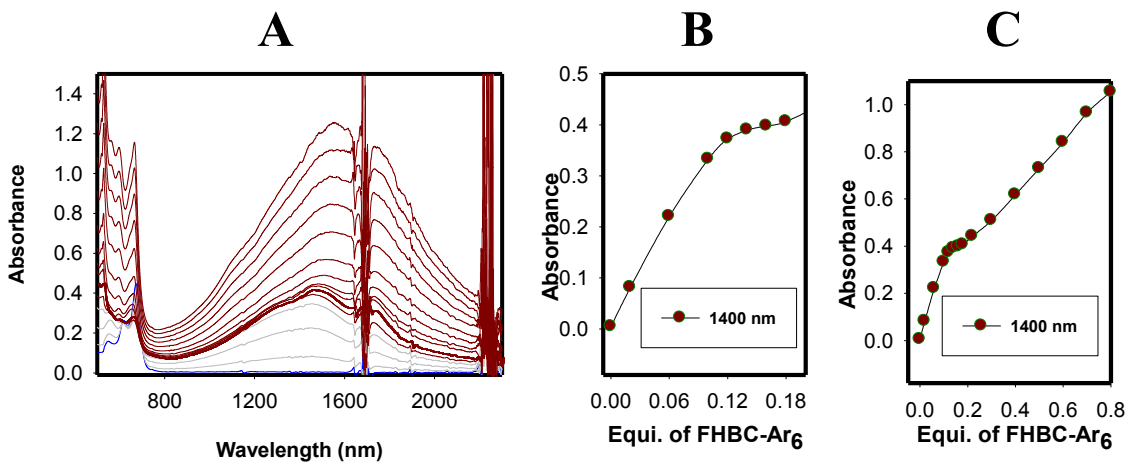

Figure 15. (**A**) The spectral changes observed upon the reduction of 4.95 x 10^{-5} M **NAP**$^{+\bullet}$ by an incremental addition of sub-stoichiometric amounts of **FHBC-Ar$_6$** in CH_2Cl_2 at 22 ^oC. (**B**) A plot of depletion of absorbance of **MB**$^{+\bullet}$ (blue circless, at 728 nm) and an increase of the absorbance of **FHBC-Ar$_6^{+\bullet}$** (brown rectangles, at 1600 nm) against the equivalents of added neutral **FHBC**.

Absorption/emission spectroscopy of FHBC-Ar$_6$ The UV-vis and fluorescence spectra of **FHBC-Ar$_6$** (1.5 x 10^{-4} M) was recorded in dichloromethane at 22 ^oC to obtain a highly structured absorption band (Figure 16A). The absorption bands at 300 - 360 nm can be accounted for fluorene and the peripheral aryl groups, while the higher wavelength bands in 400-500 nm region arises from the absorption of the **FHBC-Ar$_6$** core. Excitation of **FHBC-Ar$_6$** at 456 nm (λ_{max}) gave an emission in the region from 550 nm to 660 nm with sharp emission peak at 583 nm while the however excitation at 337 nm (the absorption region of fluorene and dimethoxytolyl) gave similar emission as obtained by

excitation at 456 nm, in addition to the bands at 404, 425 and 450 nm (Figure 15B), which suggest energy transfer from the peripheral aryl groups to the core of the molecule.

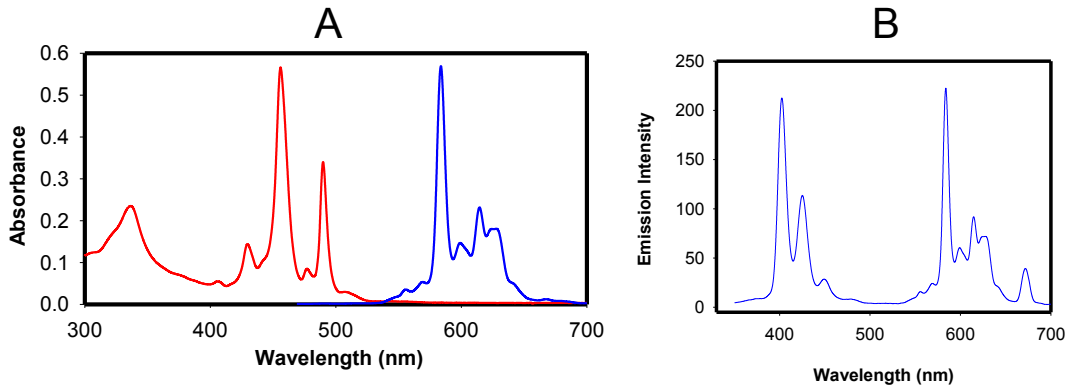

Figure 16. (**A**) Absorption (red trace) and emission (blue trace) of **FHBC-Ar$_6$** (**B**) Emission of **FHBC** (blue trace) and (grey trace) obtained with excitation at 325 nm and 337 respectively

SUMMARY and CONCLUSIONS

In conclusion, a highly soluble HBC based polycyclic aromatic hydrocarbon (**FHBC**) has been synthesized. Deployment of fluorenes at the periphery of the **FHBC** core not only imparted solubility to the structure, but also allowed it to be functionalized further allowing the attachment of electroactive groups in order to study the intramolecular charge transport phenomena. Exceptional solubility of **FHBC** and **FHBC-Ar$_6$** should allow easy processing of the molecule for their use in molecular electronics devices. Well resolved $^{1}H/^{13}C$ NMR spectra show the absence of aggregate formation in solution state. Lower oxidation potential, high molar extinction coefficient and a low band gap make **FHBC** and **FHBC-Ar$_6$** interesting candidates for their potential use in solar cells.

EXPERIMENTAL

Materials: All reactions were performed under argon atmosphere unless otherwise stated. DDQ, anhydrous ferric chloride, liquid bromine, *n*-butyl lithium, trimethylborate, trimethylsilyl acetylene, copper(I) iodide, $Pd(PPh_3)_4$ and anhydrous diethyl ether were commercially available and were used without further purification.

Anhydrous tetrahydrofuran (THF) was prepared by refluxing commercial THF over lithium aluminum hydride under an argon atmosphere for 24 hours followed by distillation under an argon atmosphere. It was stored in a Schlenk flask equipped with a Teflon valve fitted with Viton O-rings. Dichloromethane was repeatedly stirred with fresh aliquots of conc. sulfuric acid (~10 % by volume) until the acid layer remained colorless. After separation, it was washed successively with water, aqueous sodium bicarbonate, water, and aqueous sodium chloride, and dried over anhydrous calcium chloride. The dichloromethane was distilled twice from P_2O_5 under an argon atmosphere and stored in a Schlenk flask equipped with a Teflon valve fitted with Viton O-rings. The hexanes and toluene were distilled from P_2O_5 under an argon atmosphere and then refluxed over calcium hydride (~12 hr). After distillation from CaH_2, the solvents were stored in Schlenk flasks under an argon atmosphere. NMR spectra were recorded on 300 and 400 MHz NMR spectrometers.

Cyclic Voltammetry (CV). The CV cell was of an air-tight design with high vacuum Teflon valves and Viton O-ring seals to allow an inert atmosphere to be maintained without contamination by grease. The working electrode consisted of an adjustable platinum disk embedded in a glass seal to allow periodic polishing (with a fine emery

cloth) without changing the surface area (~1 mm^2) significantly. The reference SCE electrode (saturated calomel electrode) and its salt bridge were separated from the catholyte by a sintered glass frit. The counter electrode consisted of platinum gauze that was separated from the working electrode by ~3 mm. The CV measurements were carried out in a solution of 0.1 to 0.2 M supporting electrolyte (tetra-*n*-butylammonium hexafluorophosphate, TBAH) and the substrate in dry dichloromethane under an argon atmosphere. All the cyclic voltammograms were recorded at a sweep rate of 200 mV sec^{-1}, unless otherwise specified and were IR compensated. The oxidation potentials ($E_{1/2}$) were referenced to SCE, which was calibrated with added (equimolar) ferrocene ($E_{1/2}$ = 0.450 V *vs*. SCE). The $E_{1/2}$ values were calculated by taking the average of anodic and cathodic peak potentials in reversible cyclic voltammograms or directly from square-wave voltammograms in irreversible cyclic voltammograms.

Synthesis of 1,3-dibromo-5-nitrobenzene from 2,6-dibromo-4-nitrophenylamine

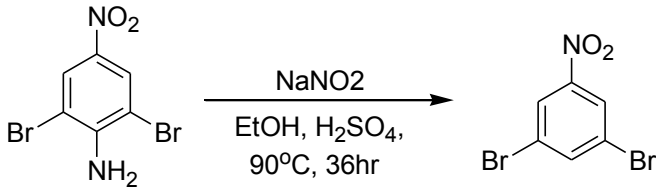

To a hot (90 ^oC) stirred solution of 2,6-dibromo-4-nitrophenylamine (40 g, 135.0 mmol) in ethanol (450 mL) and conc. H_2SO_4 (45 mL), taken in a 1000 mL three-necked round bottom flask, $NaNO_2$ (30 g, 435 mmol) was added in portions to prevent excessive foaming. The resulting reaction mixture as stirred at 90 ^oC for 36 h. The mixture was then allowed to cool to room temperature and thereafter, the contents were poured into ice-cold water. The resulting solid was filtered using a Buchner funnel and washed with

water. The filtered solid containing the product along with the inorganic salts was then dissolved in boiling ethanol and filtered hot to afford 1,3-dibromo-5-nitrobenzene as orange needles. Yield: 27.0 g, 72 %; mp 95 ^{o}C; ^{1}H NMR ($CDCl_3$) δ: 7.99 (t, 1H, J = 1.7 Hz), 8.32 (d, 2H, J = 1.7 Hz); ^{13}C NMR ($CDCl_3$) δ: 123.68, 125.79, 140.27.

Synthesis of 3,5-dibromophenylamine from 1,3-dibromo-5-nitrobenzene

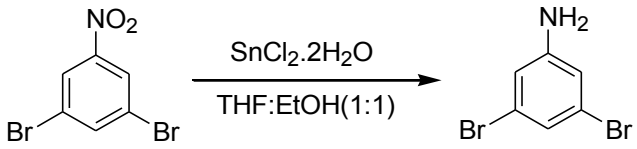

To a solution of 1,3-dibromo-5-nitrobenzene (27.0 g, 96.10 mmol) in THF (200 mL) and ethanol (200 mL), was added slowly $SnCl_2.2H_2O$ (108.40 g, 480.6 mmol). The resulting mixture was then stirred at room temperature for 20 h. The solvent was then removed *in vacuo* and aq. NaOH (2 M, 250 mL) was added to the flask. The mixture was stirred for 2 h and was then extracted with diethyl ether. The combined organic layers were dried over $MgSO_4$, filtered and the solvent was removed *in vacuo* to afford the pure product. Yield: 24.1 g, 96 %; ^{1}H NMR ($CDCl_3$) δ: 3.76 (s, 2H), 6.76 (s, 2H), 7.01 (s, 1H).

Synthesis of 1,3-dibromo-5-iodobenzene from 3,5-dibromophenylamine (1).

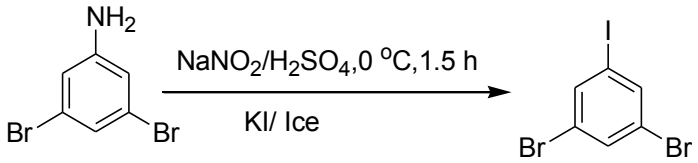

3,5-Dibromophenylamine (13.0 g, 51.80 mmol) was dissolved in conc. H_2SO_4 (100 ml) placed in a 1000 mL three-necked round bottom flask at 50 ^{o}C. The solution was cooled to 0 ^{o}C and sodium nitrite (7.85 g, 113.9 mmol) was added in portions with continuous

stirring, while maintaining the temperature below 5 ^{o}C. The reaction mixture was allowed to stir at 0 ^{o}C for 2 h. and then poured onto ice-cold solution of KI (24.9 g, 150 mmol) in water (120 mL). The suspension was heated to 80 ^{o}C (to settle down the solid) for 15 minutes. The solid was filtered and washed with cold water. Recrystallization with ethanol afforded desired product. Yield: 14.95 g, 80%. mp 123-124 ^{o}C ; ^{1}H NMR ($CDCl_3$) δ: 7.63 (s, 1H), 7.79 (s, 2H); ^{13}C NMR ($CDCl_3$) δ 94.67, 123.58, 133.85, 138.70.

Synthesis of 1,3-dibromo-5-phenylethynylbenzene from 1,3-dibromo-5-iodobenzene (2)

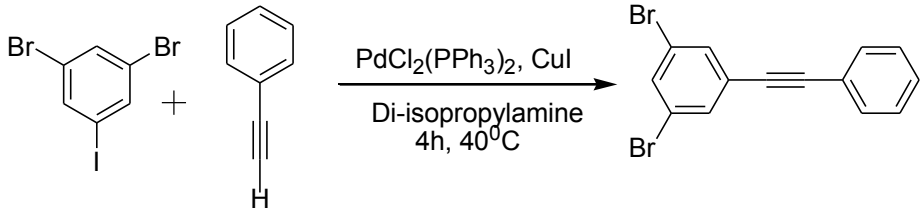

To a solution of 1,3-dibromo-5-iodobenzene (6.0 g, 16.6 mmol), $PdCl_2(PPh_3)_2$ (0.287 g, 0.40 mmol) and CuI (0.078 g, 0.40 mmol) in diisopropylamine (30 mL) under argon, was added phenylacetylene (1.82 mL, 16.58 mmol) at room temperature over a course of 5 minutes. The resulting mixture was stirred at 40 ^{o}C (water bath) for 4 h. The mixture was then cooled to room temperature and diluted with hexanes (100 mL). The contents were filtered through a short pad of silica gel and washed with hexanes. Evaporation of the solvent *in vacuo* led to a yellow oil which was purified by column chromatography using ethyl acetate and hexanes (1:9) to give the pure product as off white solid. Yield: 4.8 g, 87%; mp 106- 108 ^{o}C; ^{1}H NMR ($CDCl_3$) δ: 7.34-7.40 (m, 3H), 7.49-7.54 (m, 2H), 7.60 (d, 2H, J = 1.78 Hz), 7.63 (t, 1H, J = 1.78 Hz); ^{13}C NMR ($CDCl_3$) δ: 86.58, 92.14, 122.42, 122.82, 126.90, 128.67, 129.17, 131.94, 133.17, 134.07.

Synthesis of 4

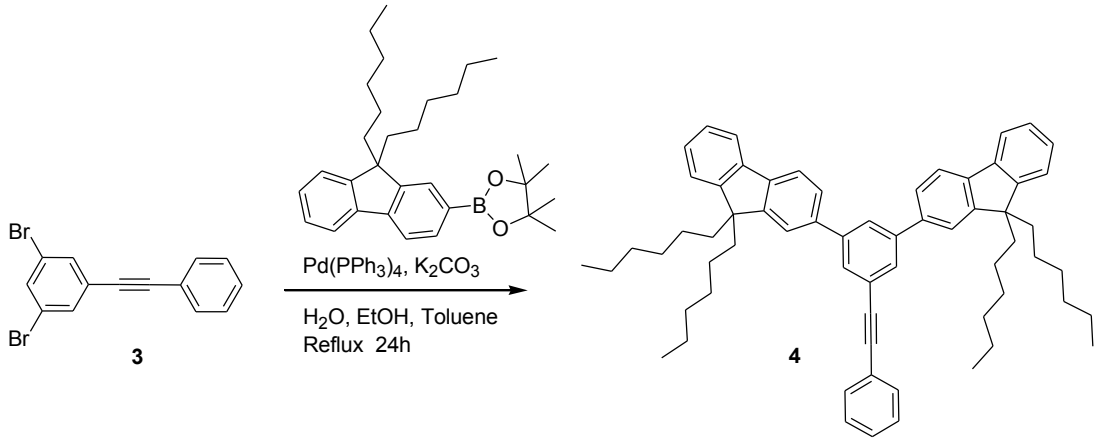

To a degassed solution of 1,3-dibromo-5-phenylethynylbenzene (1.1 g, 3.3 mmol), 2-(4,4,5,5-tetramethyl-1,3,2-dioxaborolan)-9,9-dihexylfluorene (4.0 g, 8.7 mmol), Pd $(PPh_3)_4$ (0.094 g, 0.082 mmol) in dry toluene (50 mL) and ethanol (13 mL) taken in a Schlenk flask, was added a degassed solution of potassium carbonate (2 M, 20 mL) using a syringe. The resulting mixture was refluxed for 24 hours under complete exclusion of light. The reaction mixture was then cooled to room temperature, poured into 5 % aqueous HCl (50 mL), and extracted with dichloromethane (3 x 30 mL). The combined extracts were washed with water (50 mL) and brine (50 mL) and dried over anhydrous $MgSO_4$. Removal of the solvent in *vacuo* afforded a crude product that was purified using column chromatography on silica gel with ethyl acetate and hexanes (1:99) as eluent to afford **4** as yellow viscous oil. Yield: 1.8 g, 65%; ^{1}H NMR ($CDCl_3$) δ: 0.60- 0.73 (m, 8H), 0.77 (t, 12H, J = 6.7 Hz), 1.02- 1.16 (m, 24H), 2.0- 2.08 (m, 4H), 7.32- 7.41 (m, 10H), 7.60- 7.65 (m, 4H), 7.68 (dd, 2H, J = 8.0 Hz, 1.6 Hz), 7.73- 7.77 (m, 2H), 7.80 (d, 2H, J = 8.0Hz), 7.82 (d, 2H, J = 1.7 Hz), 7.90 (t, 1H, J = 1.7 Hz); ^{13}C NMR ($CDCl_3$) δ: 14.24, 22.80, 23.96, 29.92, 31.70, 40.64, 55.45, 89.73, 89.80, 120.03, 120.05, 120.22,

123.12, 124.27, 126.30, 127.02, 127.39, 128.64, 129.22, 131.91, 139.43, 140.84,141.10, 142.76, 151.20, 151.76.

Synthesis of 7

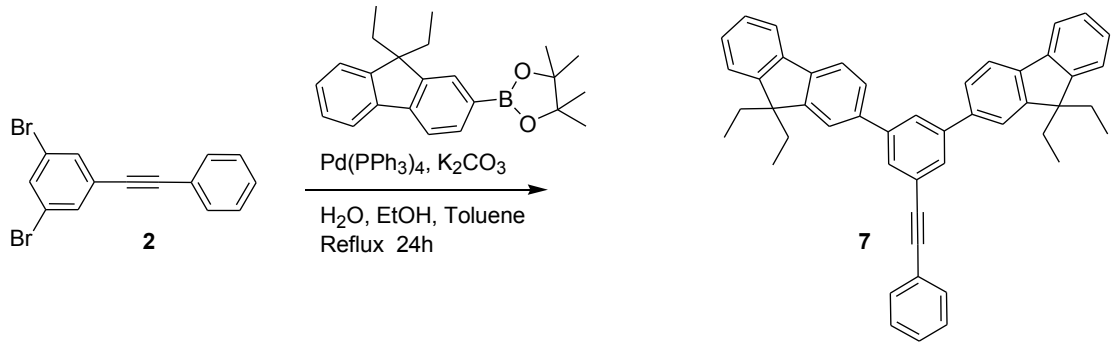

To a degassed solution of 1,3-dibromo-5-phenylethynylbenzene (1.1 g, 3.3 mmol), 2-(4,4,5,5-tetramethyl-1,3,2-dioxaborolan)-9,9-diethylfluorene (3.03 g, 8.7 mmol), Pd $(PPh_3)_4$ (0.094 g, 0.082 mmol) in dry toluene (50 mL) and ethanol (13 mL) taken in a Schlenk flask, was added a degassed solution of potassium carbonate (2 M, 20 mL) using a syringe. The resulting mixture was refluxed for 24 hours under complete exclusion of light. The reaction mixture was then cooled to room temperature, poured into 5 % aqueous HCl (50 mL), and extracted with dichloromethane (3 x 30 mL). The combined extracts were washed with water (50 mL) and brine (50 mL) and dried over anhydrous $MgSO_4$. Removal of the solvent in *vacuo* afforded a crude product that was purified using column chromatography on silica gel with ethyl acetate and hexanes (1:19) as eluent to afford **7** as colorless solid. Yield: 1.25 g, 62 %; ^{1}H NMR ($CDCl_3$) δ: 7.90 (m, 1H), 7.83 (d, 3H),7.81 (s, 1H), 7.75- 7.77 (m, 2H), 7.69 (dd, 2H), 7,61- 7.66 (m, 4H), 7.32- 7.42 (m, 9H), 2.06- 2.16 (m, 8H), 0.36- 0.42 (t, 12H); ^{13}C NMR ($CDCl_3$) δ: 8.80,

33.03, 56.49, 89.73, 89.78, 120.01, 120.20, 121.89, 123.16, 123.35, 124.27, 126.39, 126.50, 127.12, 128.63, 129.24, 131.93, 139.53, 141.26, 141.50, 142.74,150.40, 150.92.

Trimerization of 4 to 5a and 5b

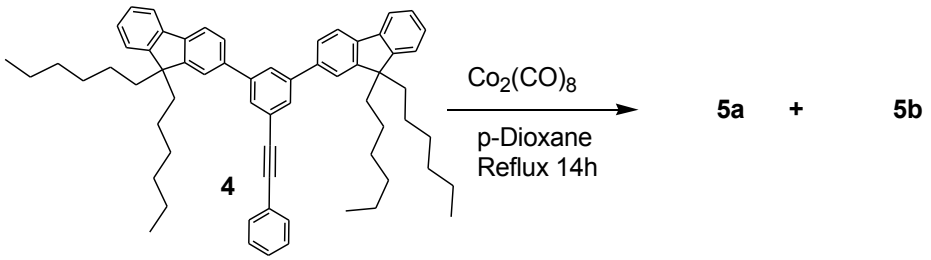

To a degassed solution of **4** (1.76 g, 2.1 mmol) in *p*-dioxane (40 mL) taken in a Schlenk flask, octacarbonyldicobalt (0.237 g, 0.7 mmol) was then added under high argon flow. The resulting mixture was refluxed for 14 hours. Upon completion, the solvent was removed *in vacuo*. The resulting solid was suspended in dichloromethane (50 mL) and filtered through a short pad of celite to get the mixture of isomers **5a** and **5b** as light brown colored solid. Yield: 1.7 g, 96 %.

Trimerization of 7 to 8a and 8b.

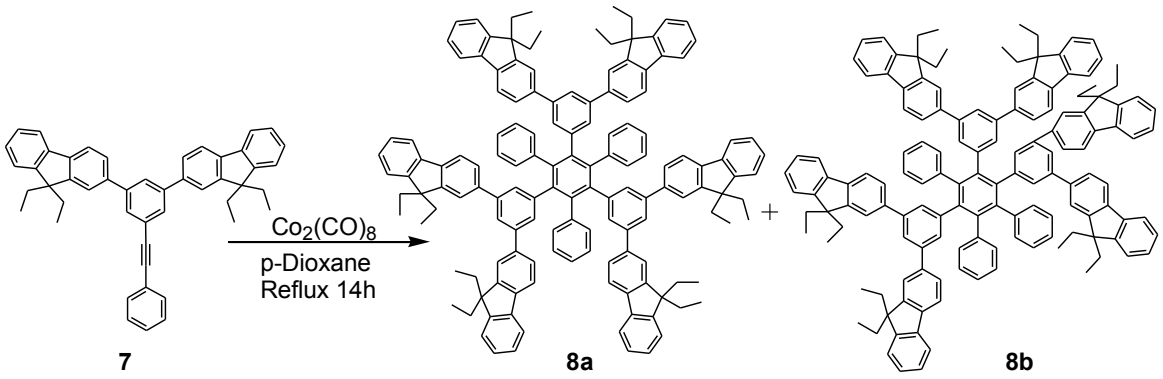

To a degassed solution of **7** (1.3 g, 2.1 mmol) in *p*-dioxane (40 mL) taken in a Schlenk flask, octacarbonyldicobalt (0.237 g, 0.7 mmol) was then added under high argon flow. The resulting mixture was refluxed for 14 hours. Upon completion, the solvent was removed *in vacuo*. The resulting solid was suspended in dichloromethane (50 mL) and filtered through a short pad of celite to get the mixture of isomers **8a** and **8b** as colorless solid. Yield: 1.19 g, 92 %. The resulting product when recrystallized using dichloro-methane and methanol (4:1) afforded the crystals of **8a ;** ^{1}H NMR ($CDCl_3$) δ: 0.35 (t, 36H, *J* = 7.3 Hz), 2.05 (q, 24H, *J* = 7.3 Hz), 6.97 (s, 6H), 7.10 (m, 3H), 7.22- 7.28 (m, 18H), 7.40 (dd, 6H), 7.57 (t, 3H),7.68- 7.74 (m, 12H); ^{13}C NMR ($CDCl_3$) δ: 8.80, 32.98, 56.31, 119.78, 119.81,.119.84, 123.11, 125.94, 127.15, 127.75, 130.55, 130.56, 132.53, 140.39, 140.70, 140.80, 140.94, 141.04, 141.22, 141.42, 141.63, 150.24, 150.63.

Synthesis of FHBC (from 5a and 5b mixture)

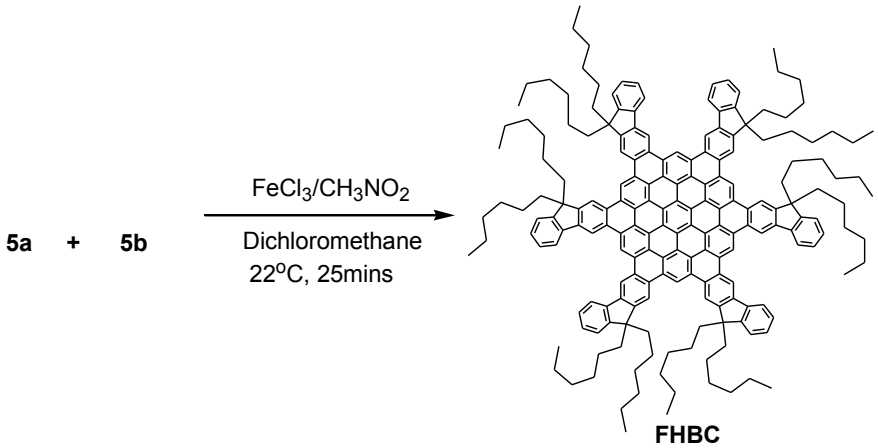

To a degassed solution of the mixture of isomers **5a** and **5b** (1.50 g, 0.60 mmol) in dry dichloromethane (50 mL), was added drop wise a solution of ferric chloride (3.31 g, 20.40 mmol) dissolved in nitromethane (30 mL). The reaction mixture was stirred for 20 minutes at 22 °C. To the resulting mixture was then added methanol (20 mL) followed by

water (40 mL). The product was extracted with dichloromethane (3 x 50 mL), washed with water and dried over magnesium sulfate. The resulting solution was then passed through a short pad of silica gel, and the solvent was evaporated under vacuum to get crude red colored solid which was purified by column chromatography using benzene and hexanes (1:19) as eluent. ; Yield: 0.38 g, 25%; mp >450 ^{o}C; ^{1}H NMR ($CDCl_3$) δ: 0.79 (s, 6H), 1.1- 1.5 (m, 14H), 2.45- 2.85 (m, 4H), 7.17 (t, 1H, *J* = 7.2 Hz), 7.79 (d, 1H, *J* = 7.2 Hz), 7.86 (t, 1H, *J* = 7.2 Hz), 8.67 (d, 1H, *J* = 7.2 Hz), 10.12 (s, 1H), 10.56 (s, 1H), 12.04 (s, 1H), 12.22 (s, 1H); ^{13}C NMR ($CDCl_3$) δ: 14.25, 22.88, 24.58, 30.25, 31.88, 41.66, 55.93, 115.57, 116.07, 118.61, 121.06, 121.12, 121.61, 122.94, 122.97, 123.77, 127.70, 127.73, 127.87, 128.58, 130.85, 131.00, 141.23, 142.20, 151.39, 152.24. MS : MALDI-TOF (M^+) = 2505.

Synthesis of 9a and 9b

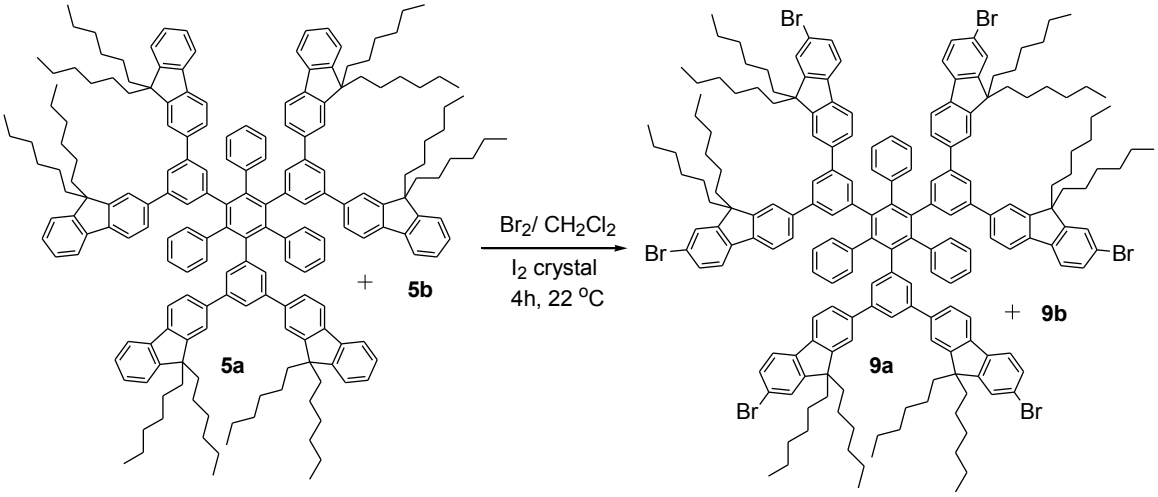

Mixture of **5a** and **5b** (1.21 g, 0.478 mmol) was dissolved in dichloromethane (100 mL) placed in a 500 mL round bottom flask and crystal of iodine was added to the resulting solution. Bromine (0.46 g, 2.86 mmol) dissolved in dichloromethane (70 mL) was taken

in a dropping funnel and added drop wise to the above solution over a period of 30 minutes. After complete addition of bromine, reaction mixture was further stirred at room temperature for 3.5 h. After completion of reaction, water (100 mL) was added slowly. The dichloromethane layer was separated and the aqueous layer was further extracted with dichloromethane (2 x 50 mL). The collected organic layers were washed with saturated solution of sodium bisulfite (2 x 30 mL), followed by water (50 mL) and brine (30 mL) and dried over magnesium sulfate. The solvent was evaporated under vacuum to afford a mixture of **9a** and **9b** as a light brown colored solid. Yield: 1.35 g, 94%.

Synthesis of FHBC-Ar$_6$

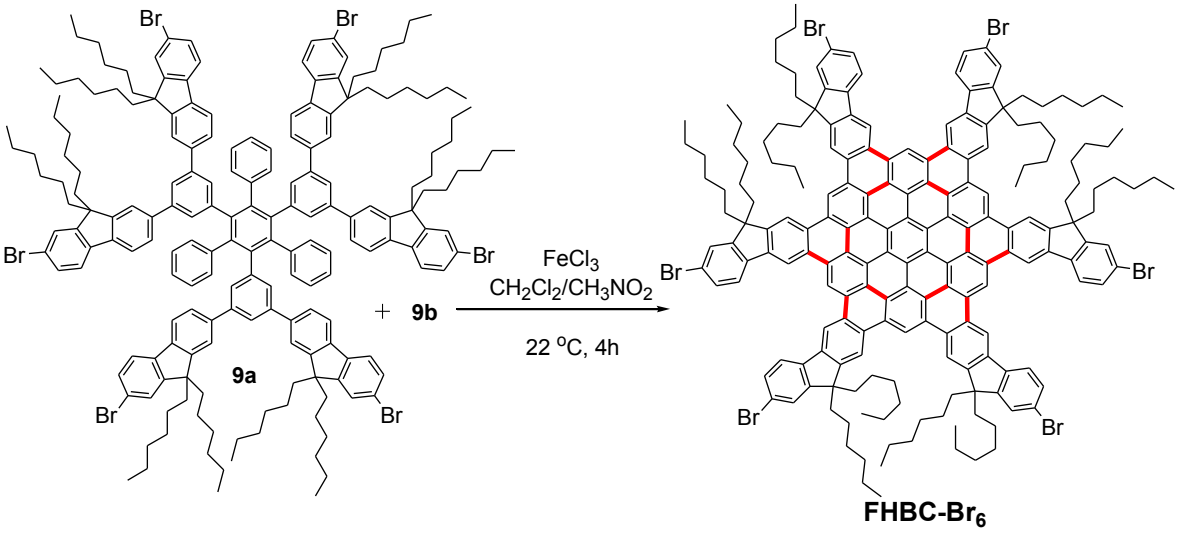

To a degassed solution of the mixture of isomers **9a** and **9b** (0.81 g, 0.27 mmol) in dry dichloromethane (100 mL), was added drop wise a solution of ferric chloride (2.67 g, 16.47 mmol) dissolved in nitromethane (30 mL). The reaction mixture was stirred for 3h at 22 °C. To the resulting mixture was then added methanol (80 mL) followed by water (40 mL). The product was extracted with dichloromethane (3 x 50 mL), washed with water and dried over magnesium sulfate. The resulting solution was then passed through

a short pad of silica gel, and the solvent was evaporated under vacuum to get crude dark red colored solid which was purified by column chromatography using ethyl acetate (elutes only undesired product) followed by dichloromethane (elutes only **FHBC-Br$_6$** selectively). mp > 450 ^{o}C; Yield: 0.16 g, 20%; ^{1}H NMR ($CDCl_3$) δ: 0.70–0.80 (m, 36H), 1.10-1.40 (m, 96H), 2.44-2.75 (m, 24H), 7.87 (s, 6H), 7.93 (d, 6H, *J* = 8.0 Hz, 1.5 Hz), 8.47 (d, 6H, J = 8.0 Hz), 10.07 (s, 6H), 10.47 (s, 6H), 12.00 (s, 3H), 12.12 (s, 3H).

Synthesis of FHBC-Ar$_6$

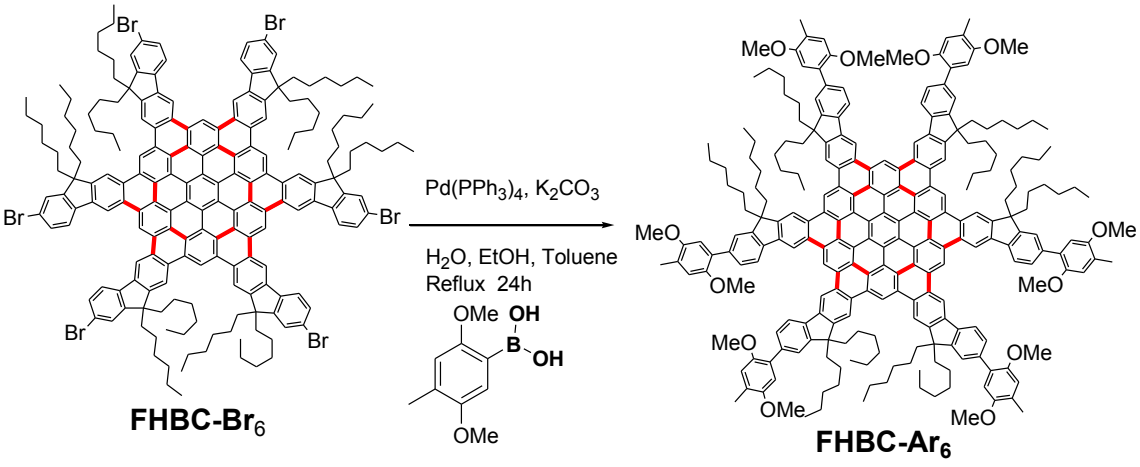

To a degassed solution of **FHBC-Br$_6$** (0.05 g, 0.017 mmol), 2,5-dimethoxy-4-methylphenylboronic acid (0.04 g, 0.20 mmol), Pd (PPh_3)$_4$ (0.06 g, 0.005 mmol) in dry toluene (25 mL) and ethanol (7 mL) taken in a Schlenk flask, was added a degassed solution of potassium carbonate (2 M, 10 mL) using a syringe. The resulting mixture was refluxed for 24 hours under complete exclusion of light. The reaction mixture was then cooled to room temperature, poured into 5 % aqueous HCl (50 mL), and extracted with dichloromethane (3 x 30 mL). The combined extracts were washed with water (50 mL) and brine (50 mL) and dried over anhydrous $MgSO_4$. Removal of the solvent in *vacuo* afforded a crude product that was purified using column chromatography on silica gel

with ethyl acetate and hexanes (1:19) as eluent to afford **FHBC-Ar$_6$** as a deep red colored solid. Yield: 0.047 g, 84%; ^{1}H NMR ($CDCl_3$) δ: 0.76- 0.84 (m, 36H), 1.20- 1.48 (m, 96H), 2.56- 2.82 (m, 24H), 3.94 (s, 18H), 4.03 (s, 18H), 7.02 (s, 6H), 7.19 (s, 6H), 7.92- 8.02 (m, 12H), 8.69 (d, 6H, J = 8.7 Hz), 10.17 (s, 6H), 10.59 (s, 6H), 12.09 (s, 3H), 12.25 (s, 3H).^{13}C NMR ($CDCl_3$) δ: 14.24, 16.64, 22.90, 24.67, 30.31, 31.89, 41.62, 55.92, 56.47, 57.26, 113.55, 115.53, 116.26, 118.73, 120.66, 121.19, 121.26, 121.62, 121.72, 123.03, 125.25, 127.17, 127.81, 127.90, 128.90, 129.52, 130.78, 131.11, 138.91, 139.87, 142.11, 150.74, 151.88, 152.54.

EXPERIMENTAL SPECTRA

Collection of NMR data for various intermediates

^{1}H NMR of 1,3-dibromo-5-nitrobenzene

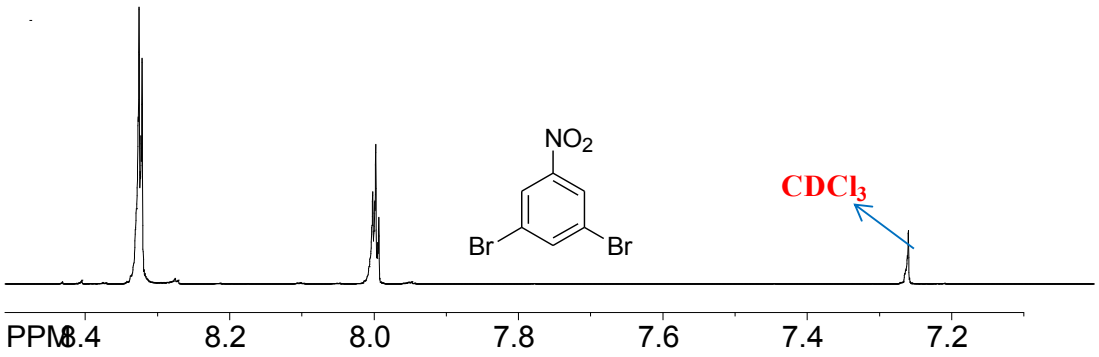

^{13}C NMR of 1,3-dibromo-5-nitrobenzene

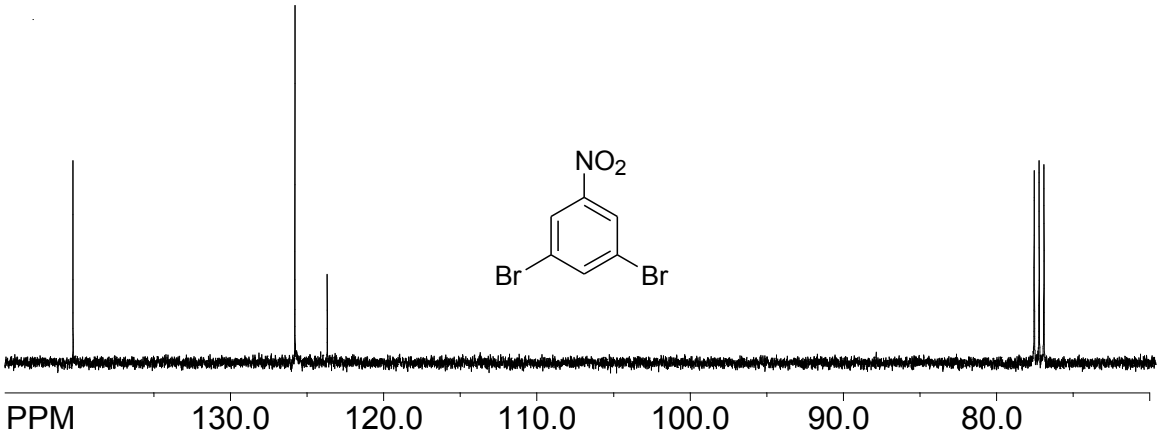

^{1}H NMR of 3,5-dibromo-phenylamine

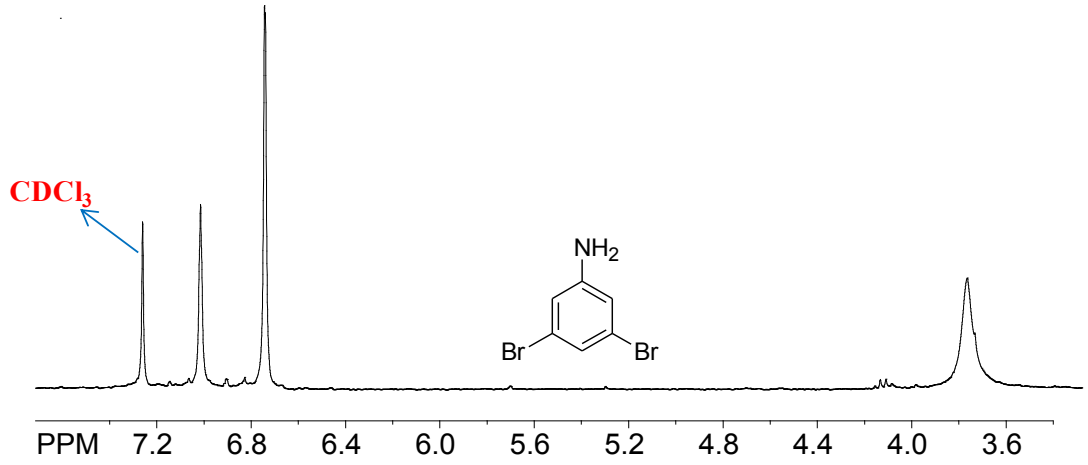

^{1}H NMR of 1,3-dibromo-5-iodobenzene (1)

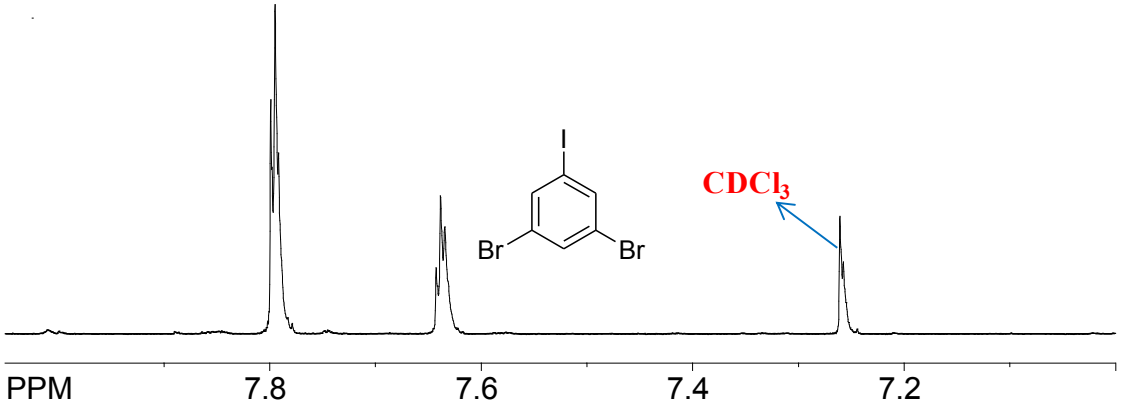

^{13}C NMR of 1,3-dibromo-5-iodobenzene (1)

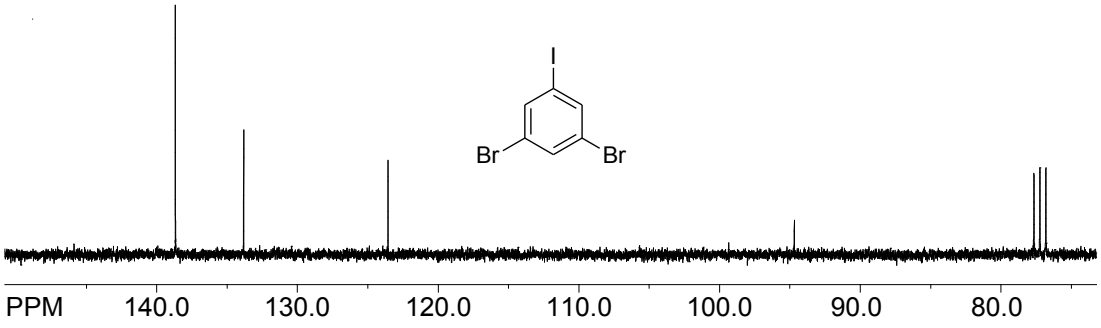

^{1}H NMR of 1, 3-dibromo-5-phenylethynylbenzene (2)

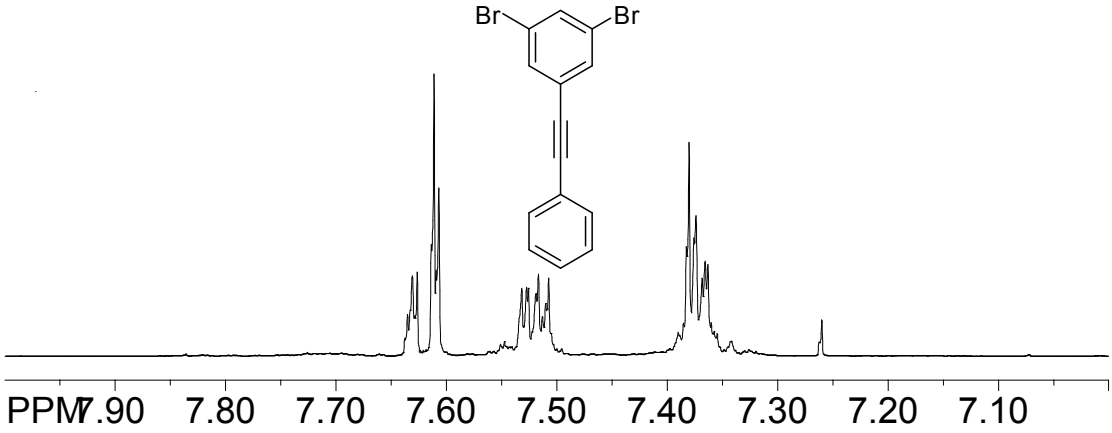

^{13}C NMR of 1, 3-dibromo-5-phenylethynylbenzene (2)

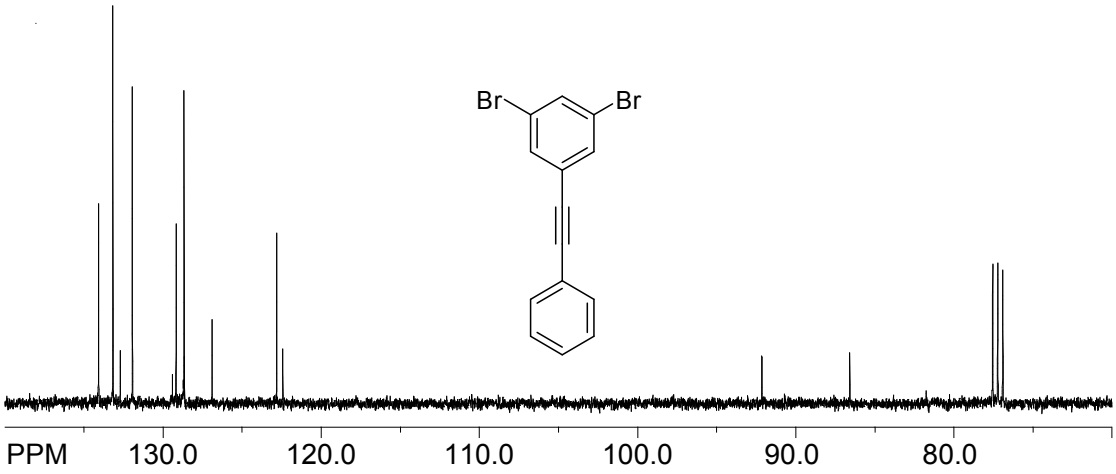

^{1}H NMR of 4

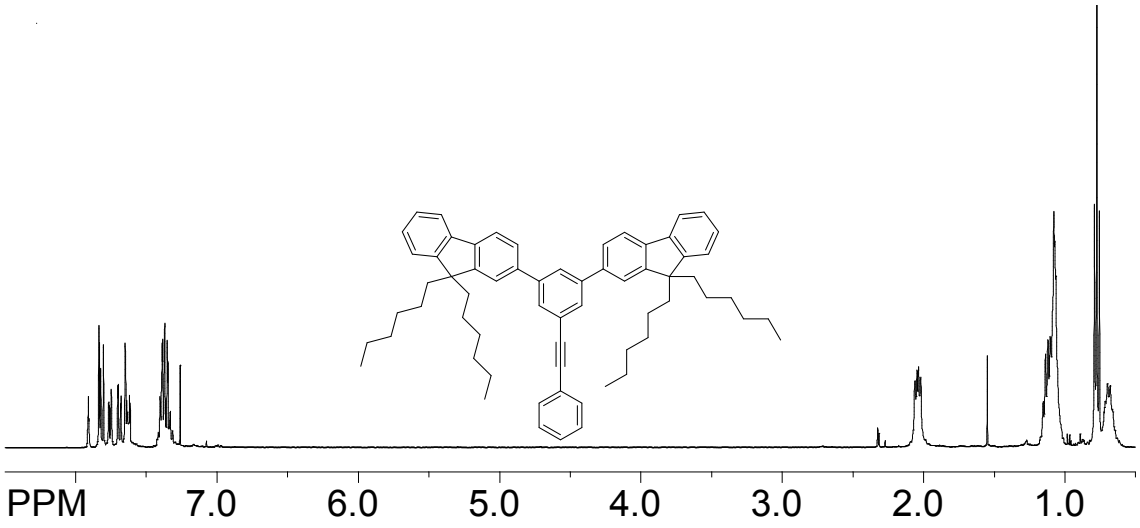

Zoomed ^{1}H NMR of 4

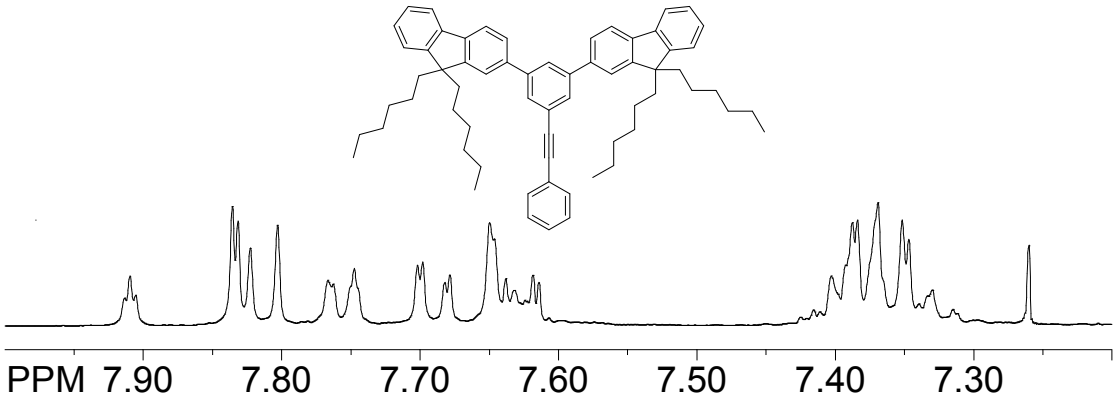

^{13}C NMR of 4

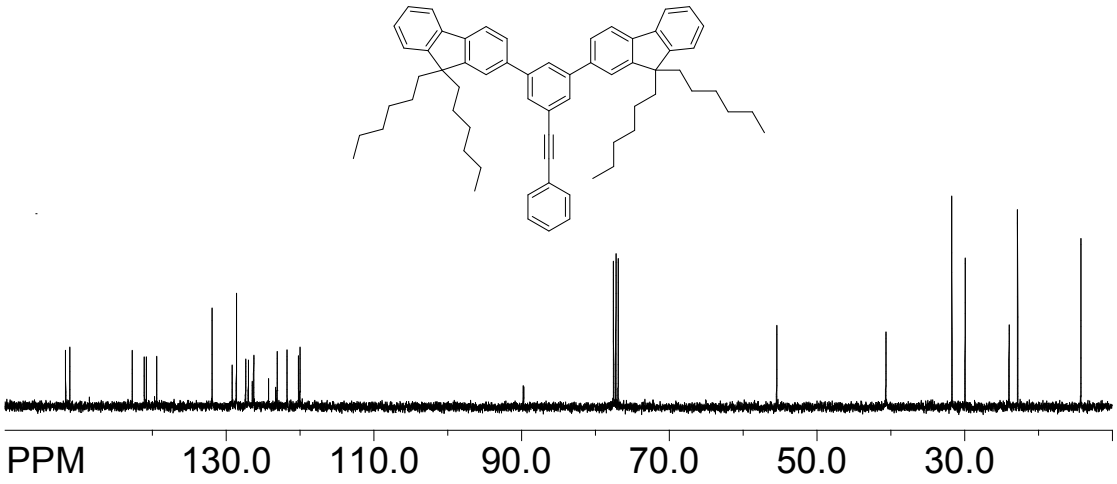

^{13}C NMR of 4

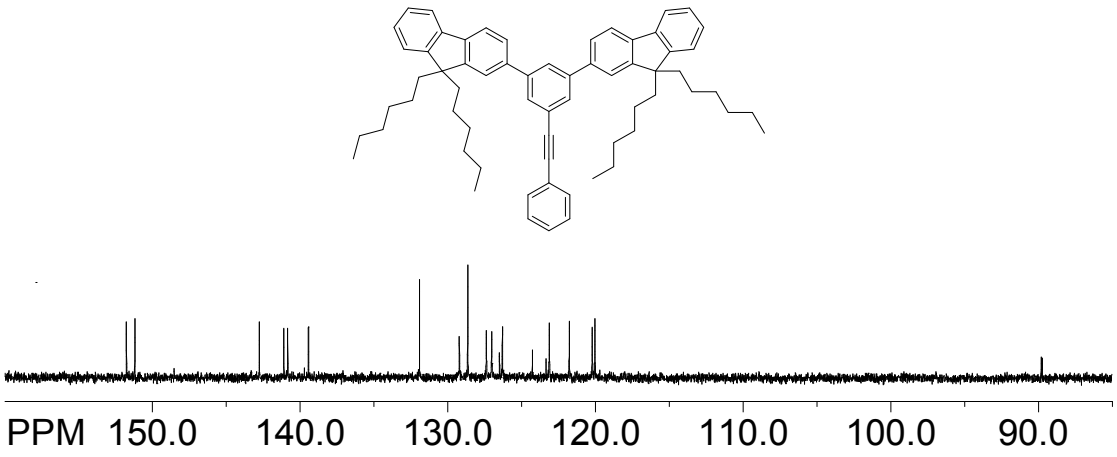

^{1}H NMR of the mixture of 5a and 5b

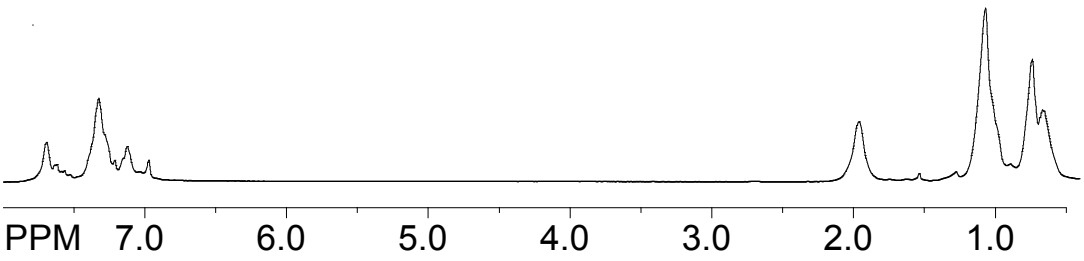

^{13}C NMR of the mixture of 5a and 5b

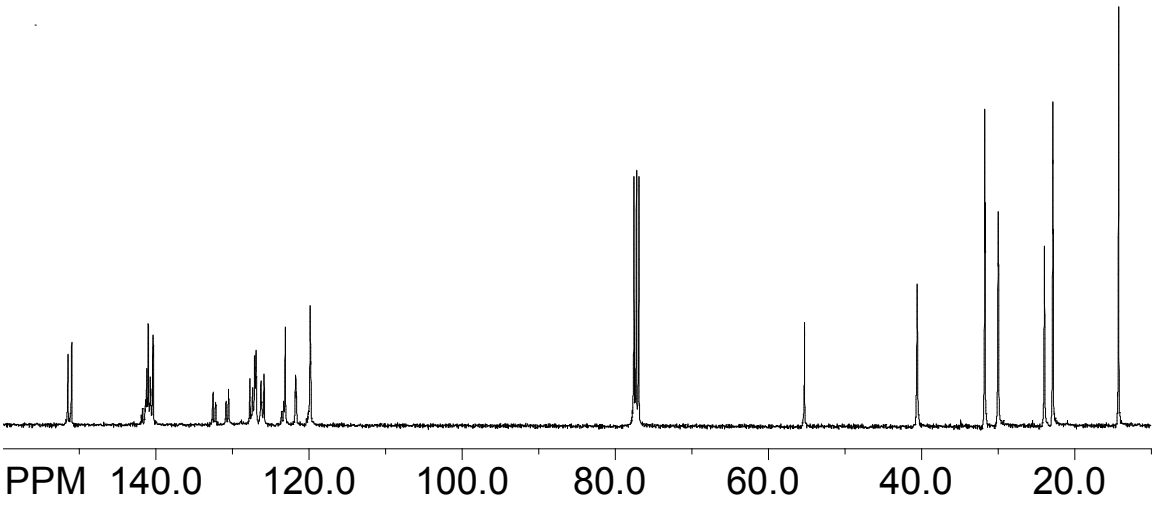

Zoomed ^{13}C NMR of mixture of 5a and 5b

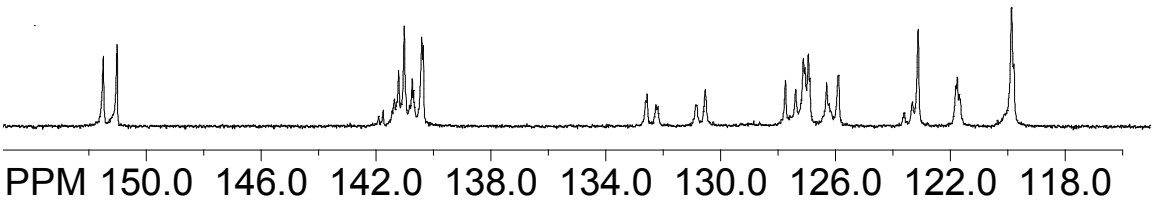

^{1}H NMR of FHBC

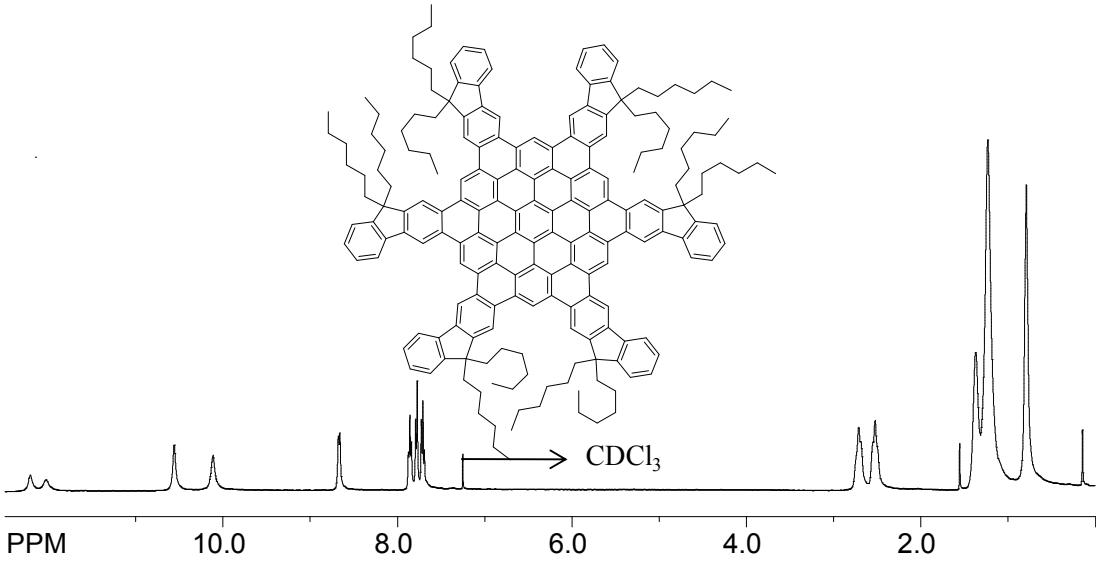

Zoomed ^{1}H NMR of FHBC

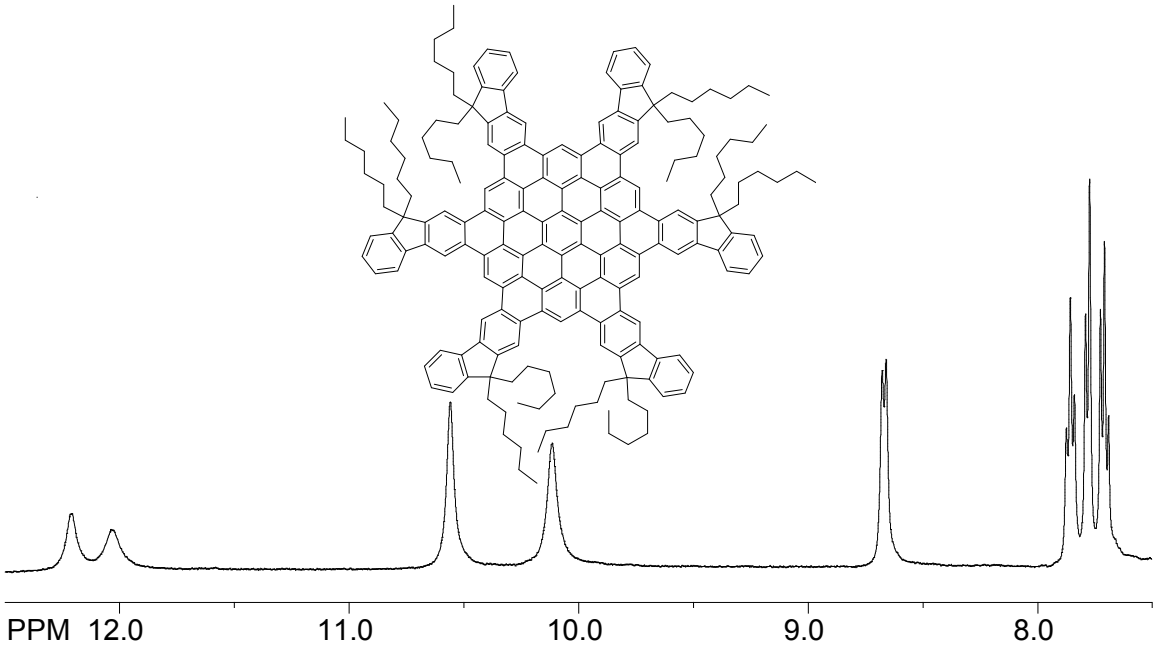

Zoomed ^{1}H NMR of FHBC

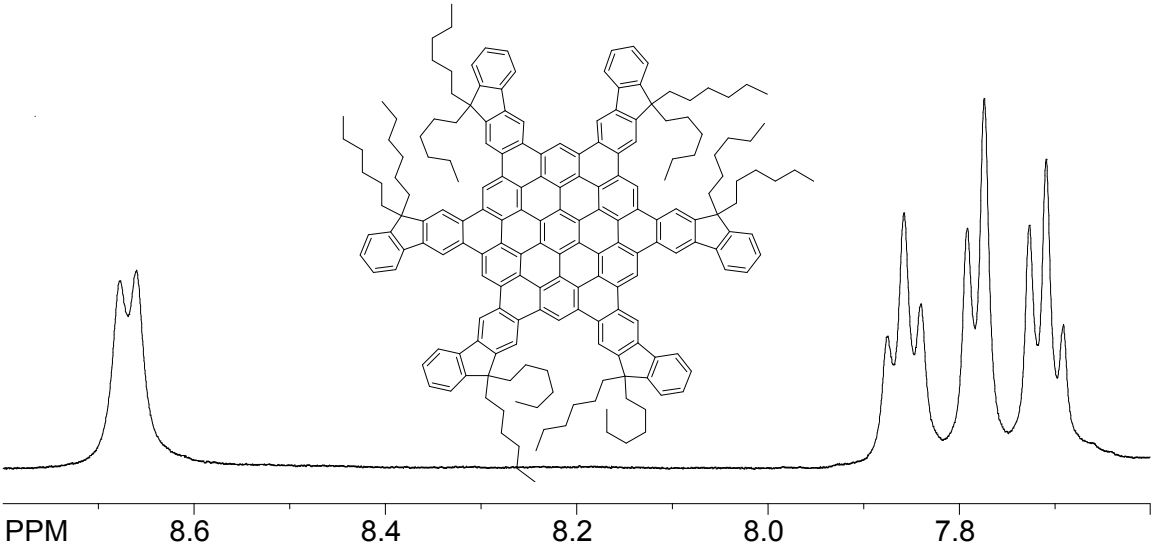

^{13}C NMR of FHBC

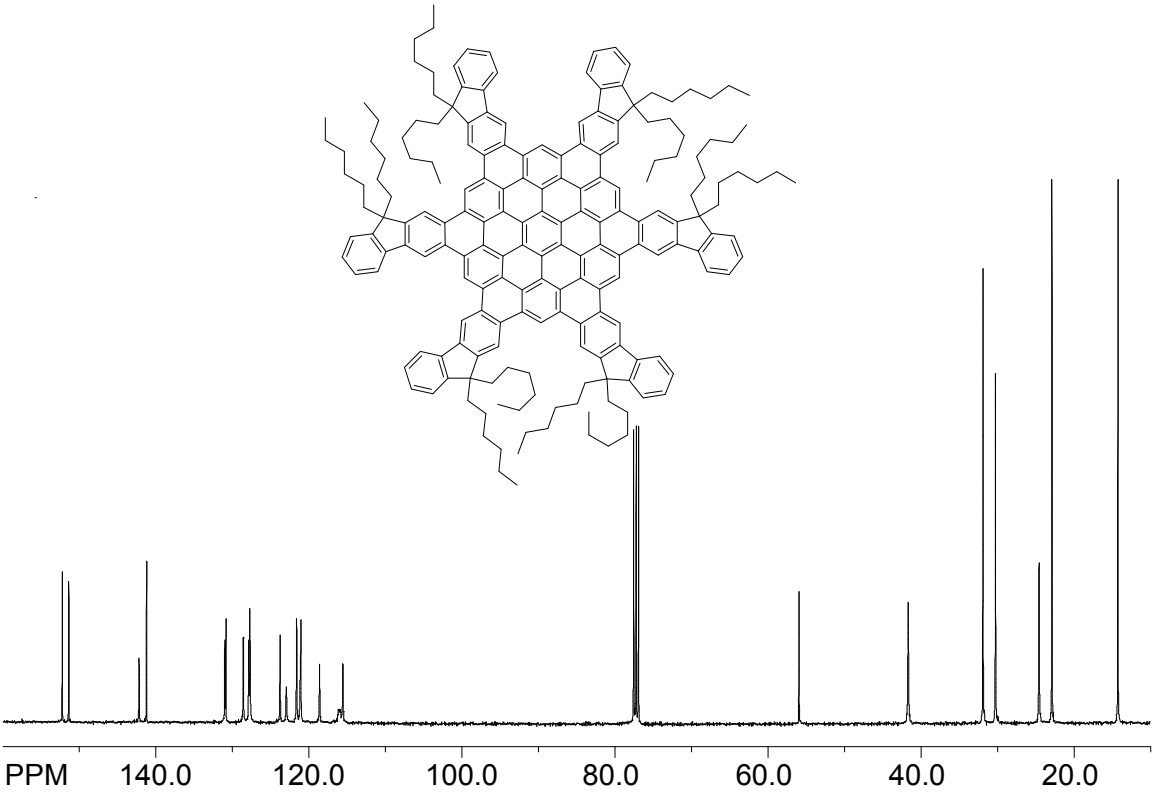

Zoomed ^{13}C NMR of FHBC

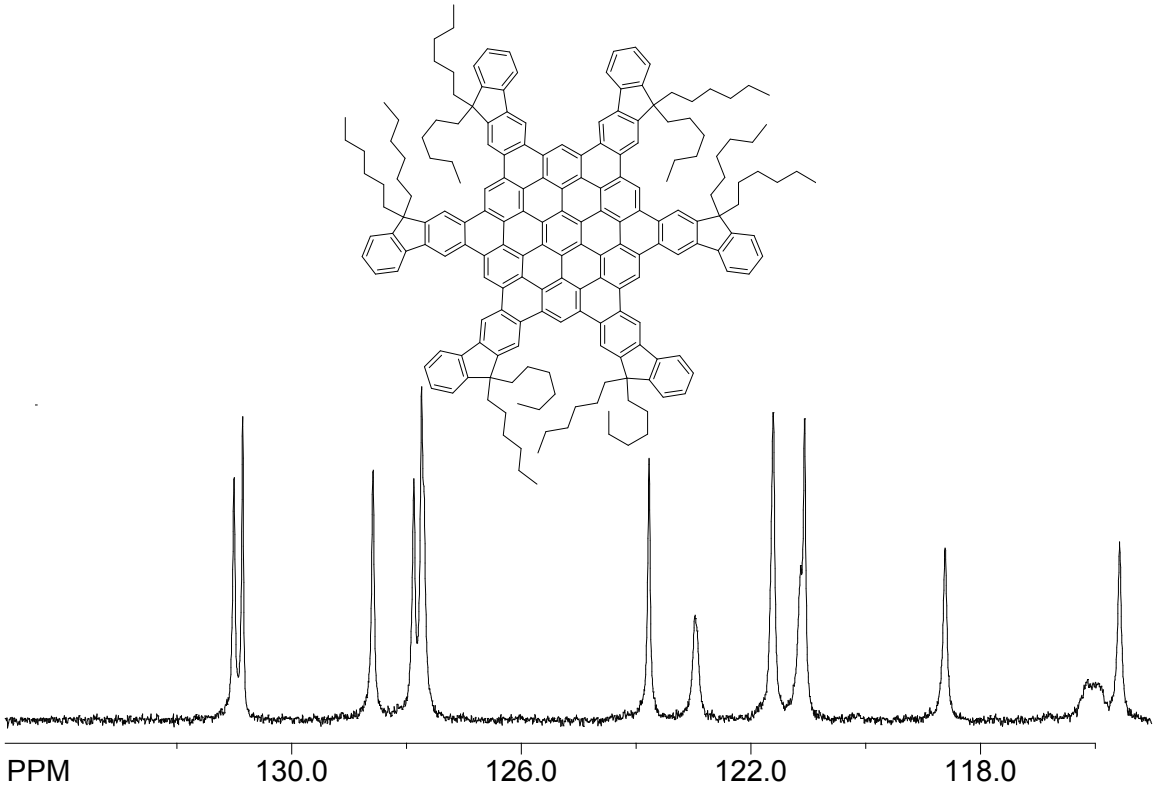

^{1}H NMR of 7

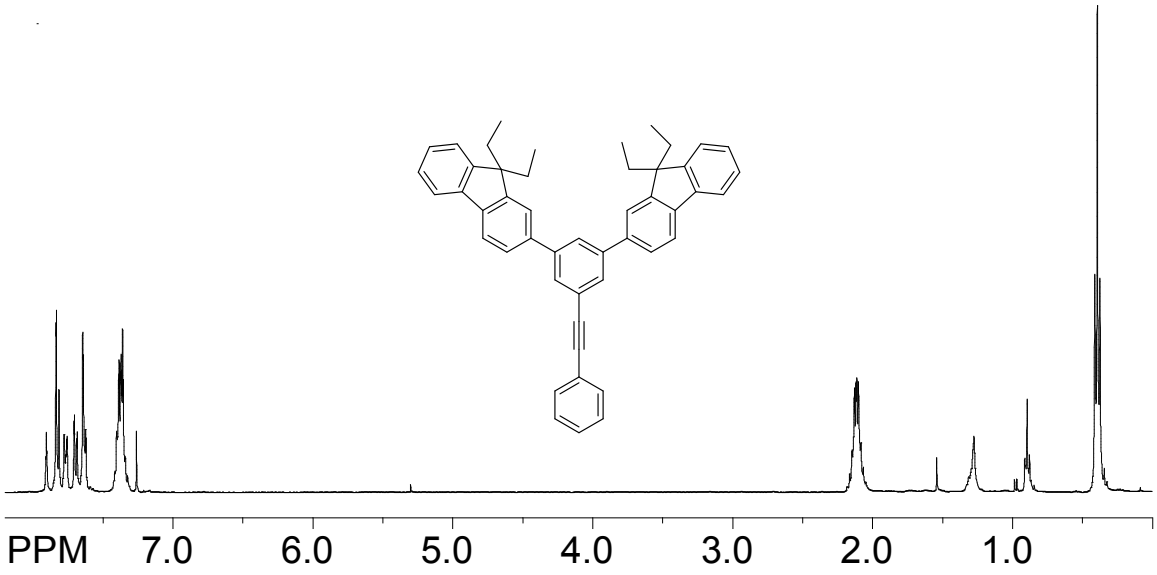

Zoomed ^{1}HNMR of 7

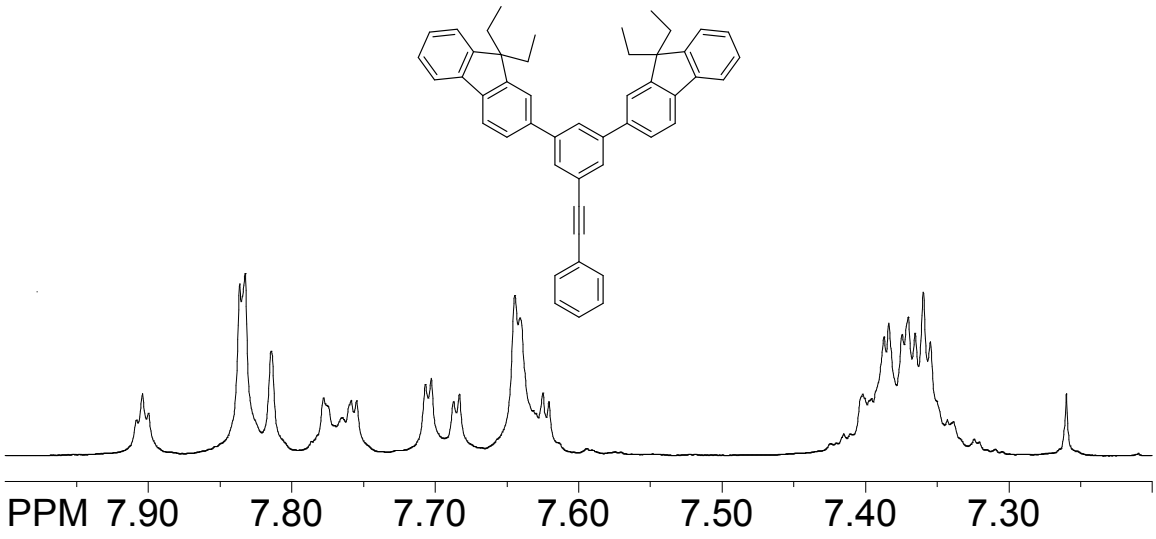

^{13}C NMR of 7

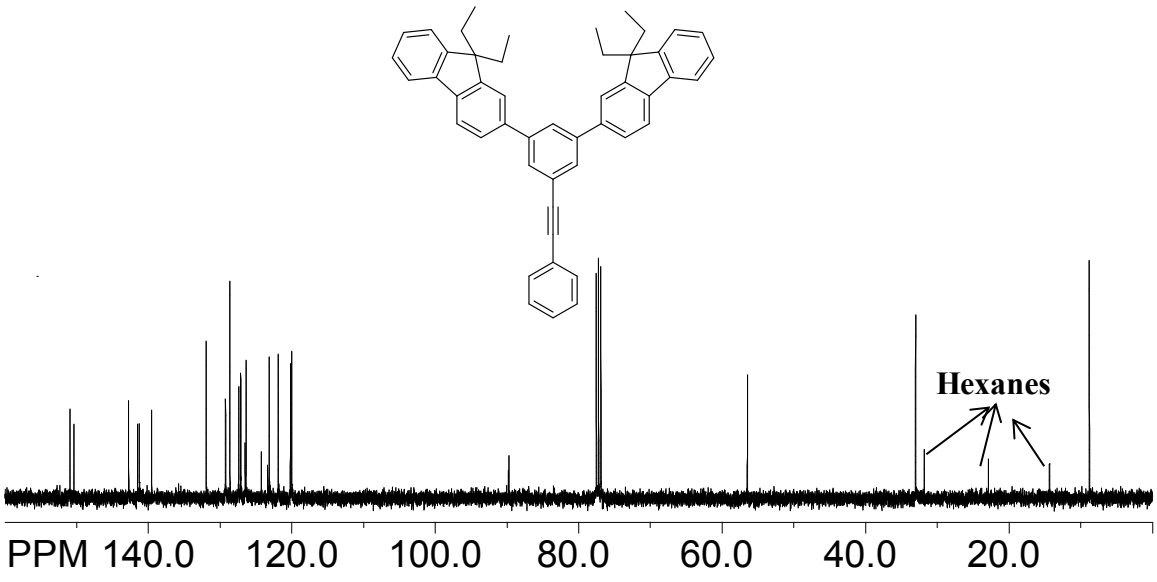

Zoomed ^{13}C NMR of 7

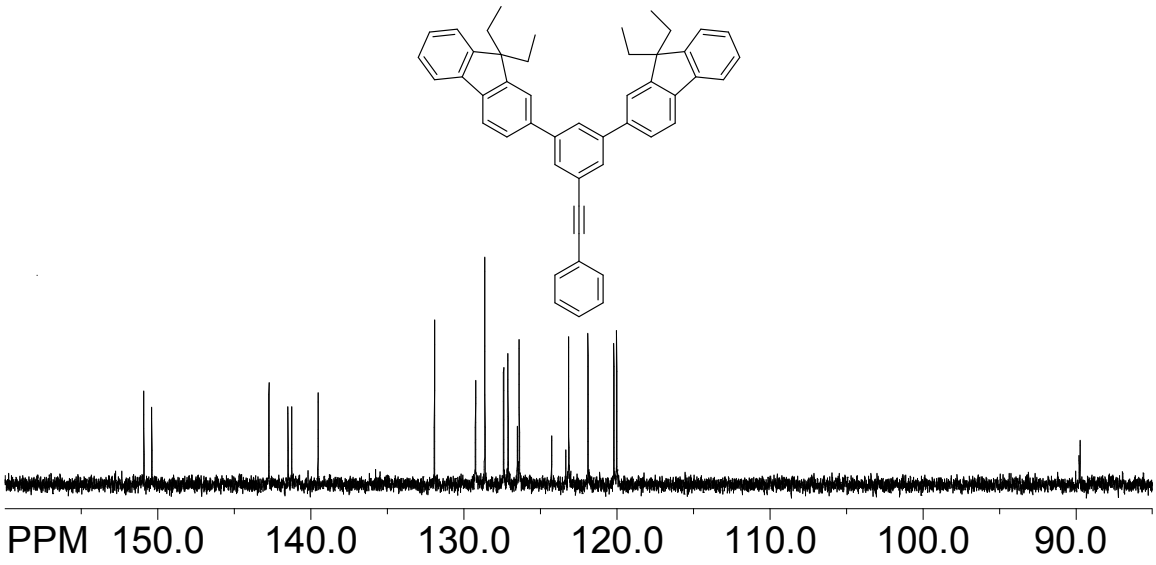

1H NMR of 8a

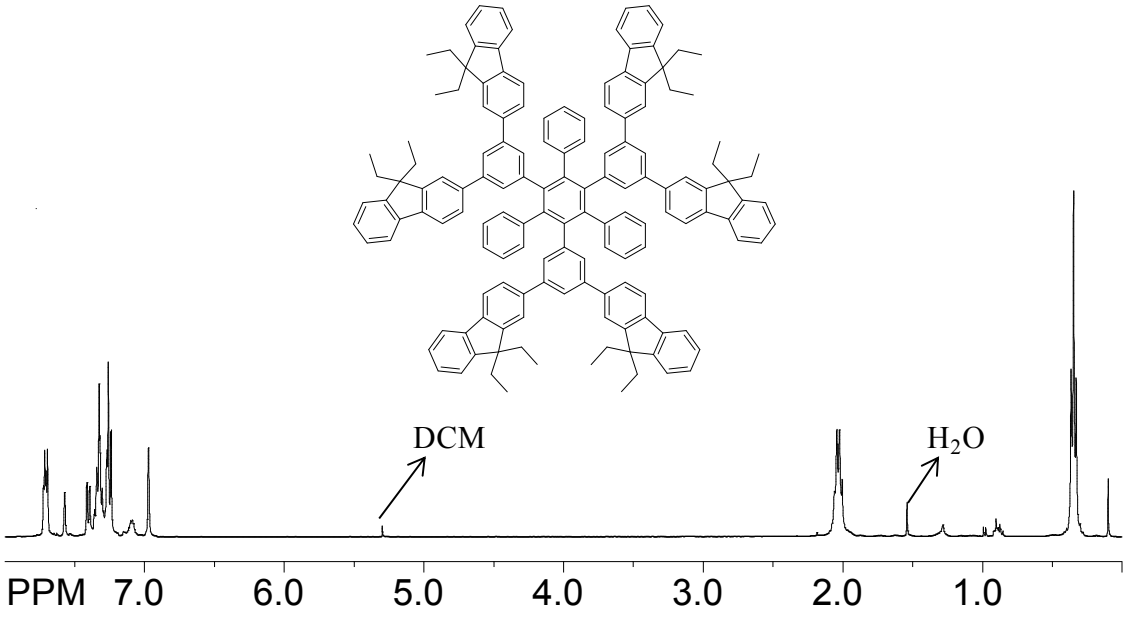

Zoomed ^{1}H NMR of 8a

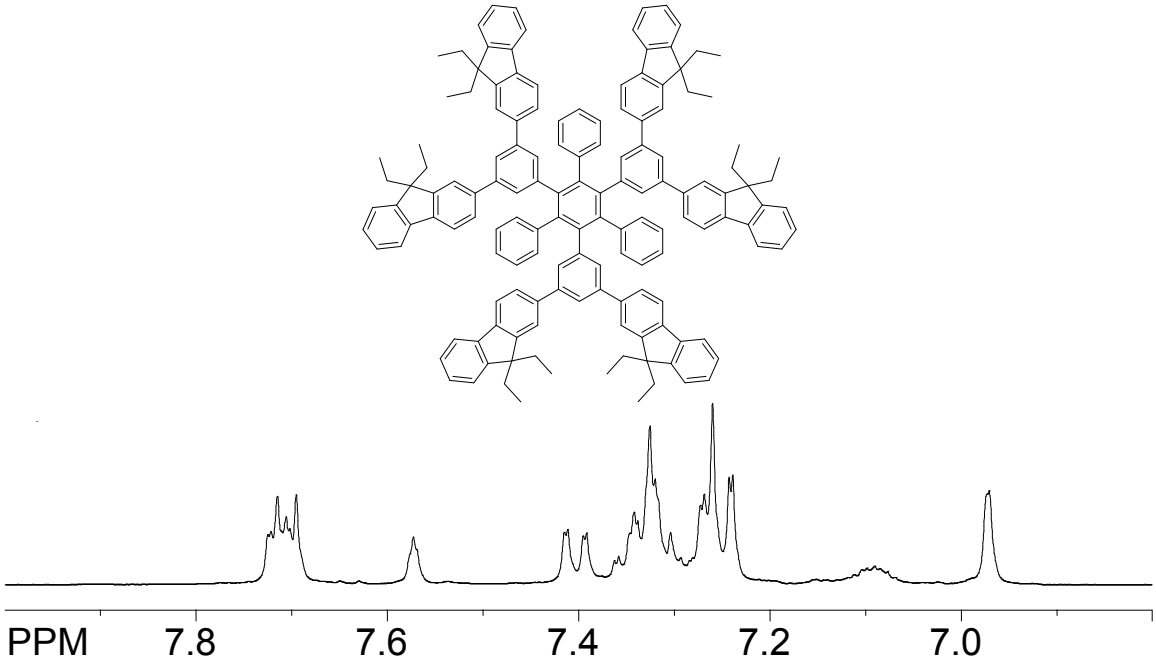

^{13}C NMR of 8a

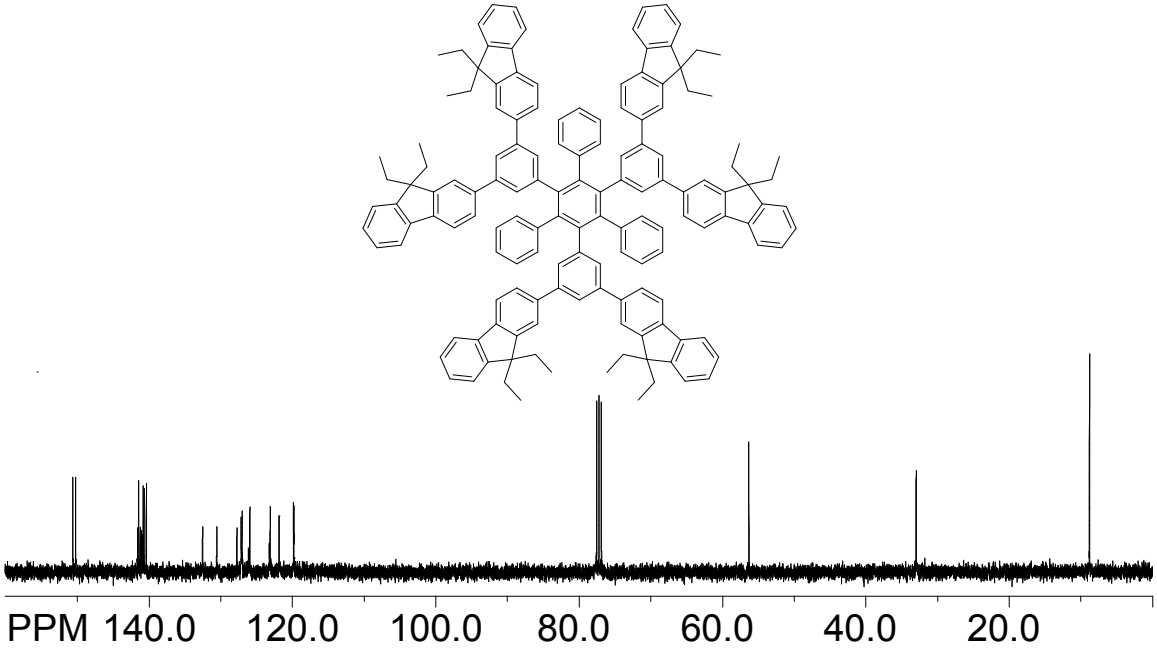

Zoomed ^{13}C NMR of 8a

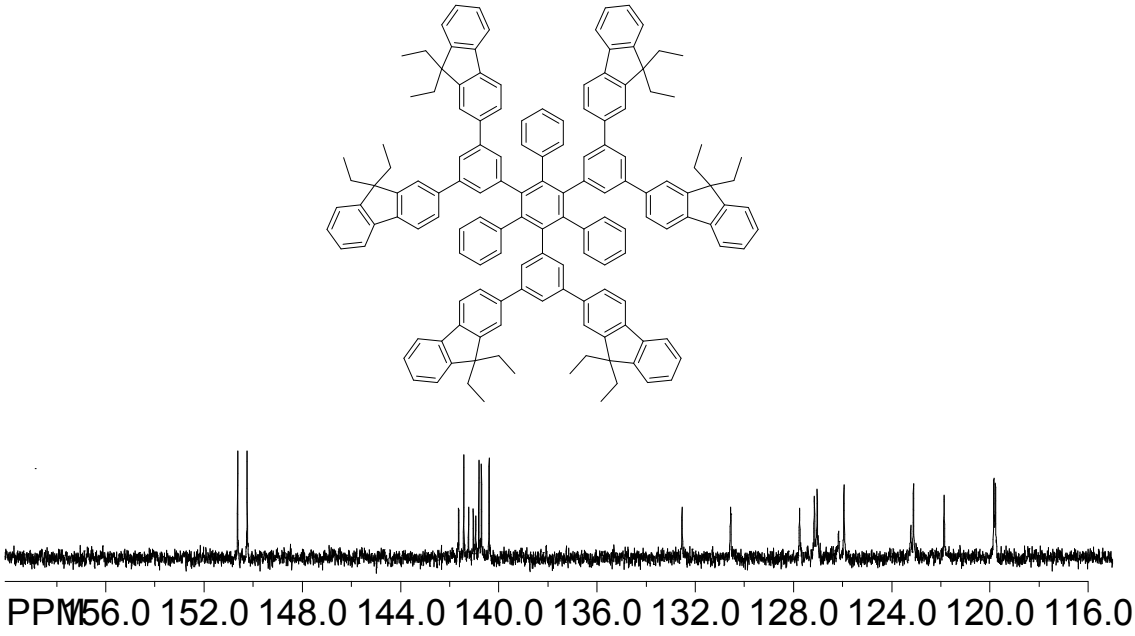

^{1}H NMR of FHBC-Br_6

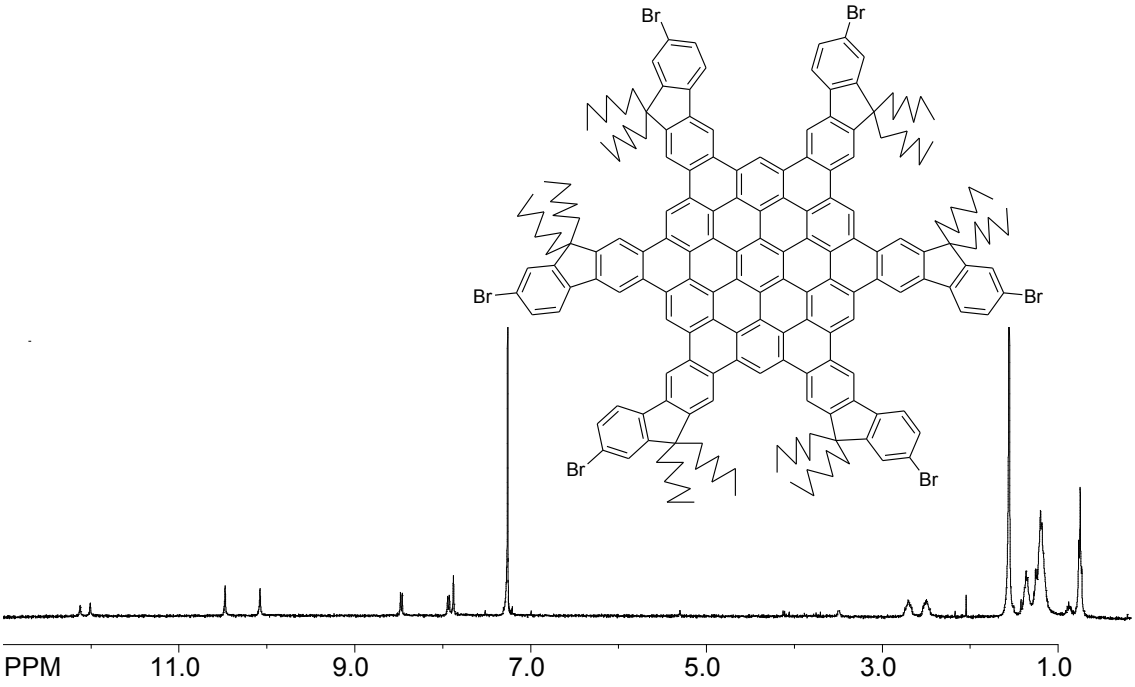

Zoomed ^{1}H NMR of FHBC-Br$_6$

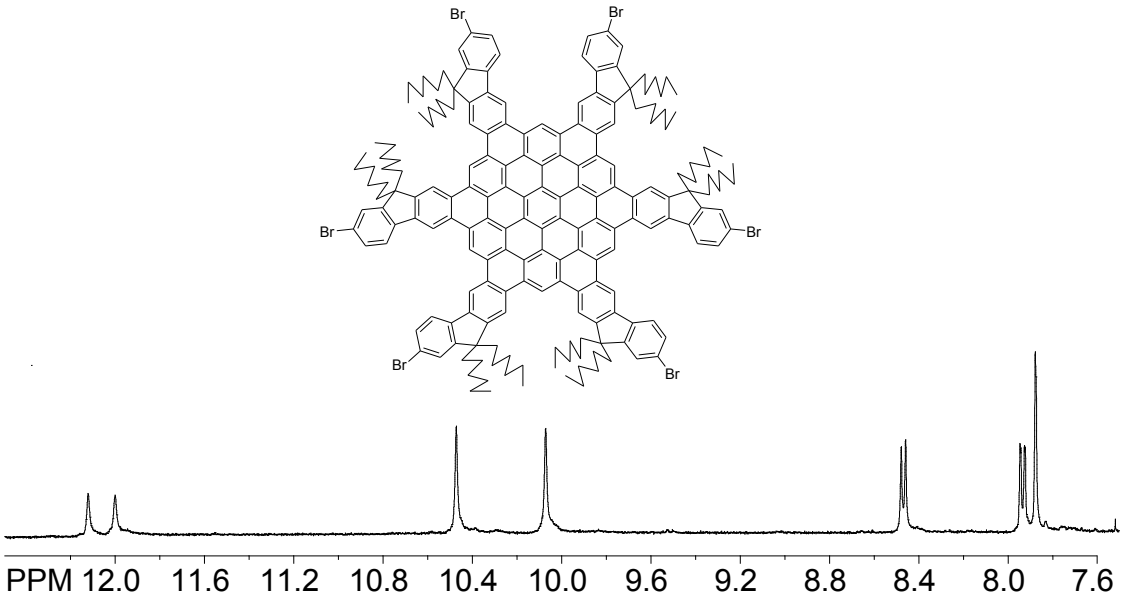

^{1}H NMR of FHBC-Ar$_6$

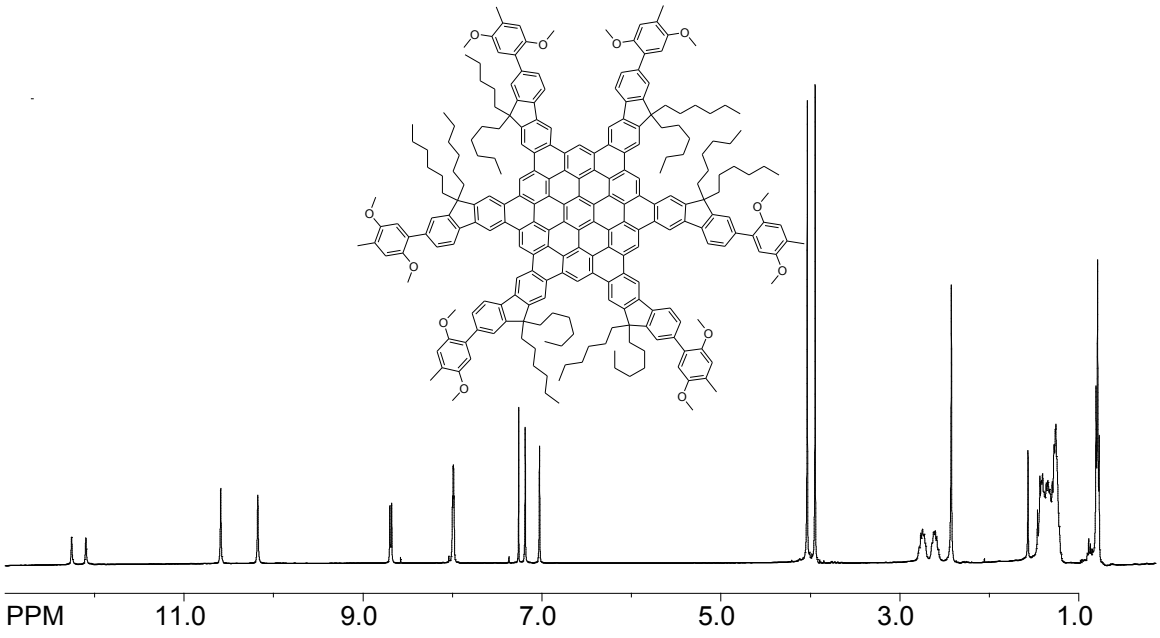

Zoomed 1, ^{1}H NMR of FHBC-Ar$_6$

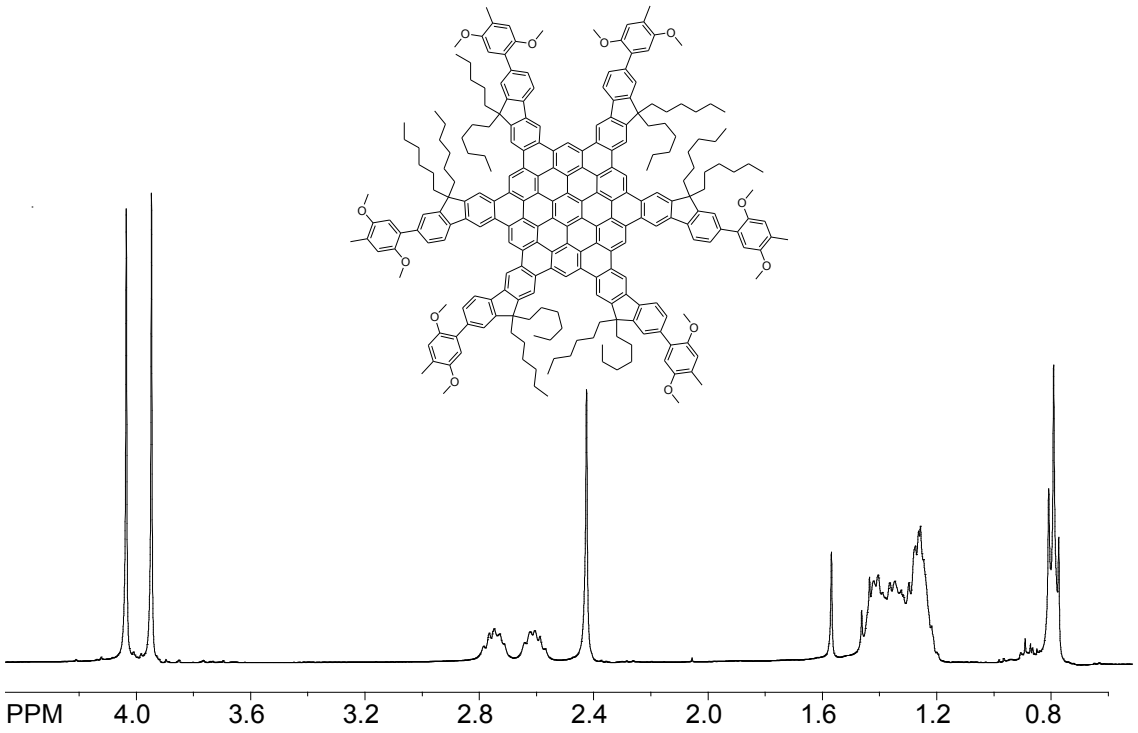

Zoomed 2,^{1}H NMR of FHBC-Ar$_6$

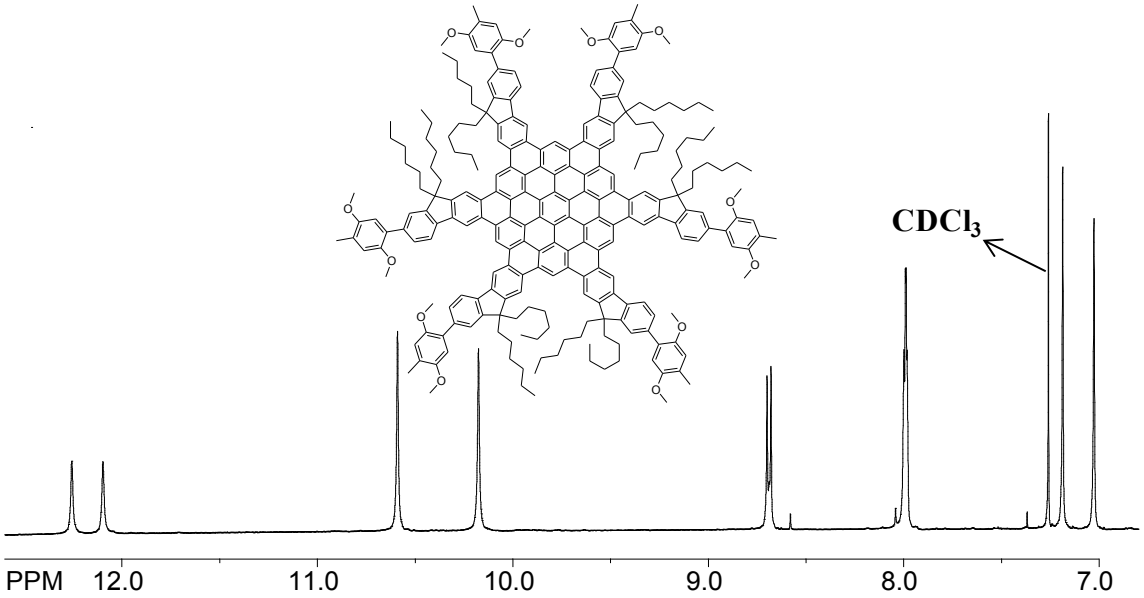

Zoomed 3, ^{1}H NMR of FHBC-Ar$_6$

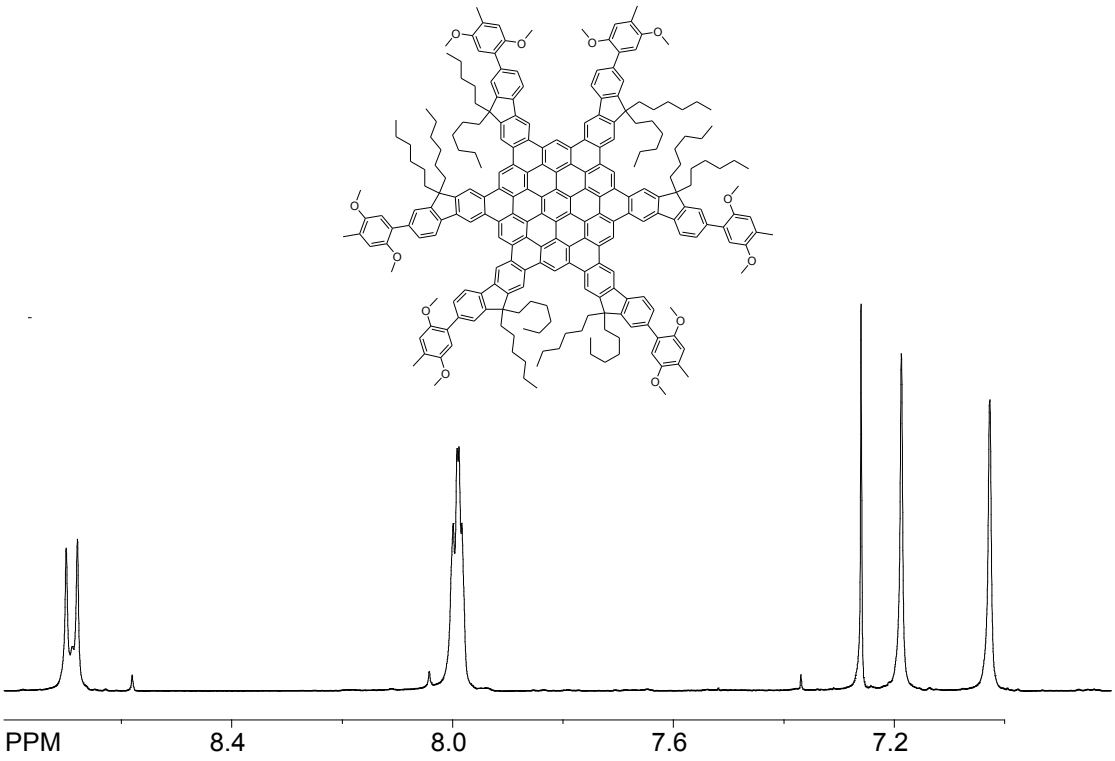

^{13}C NMR of FHBC-Ar$_6$:

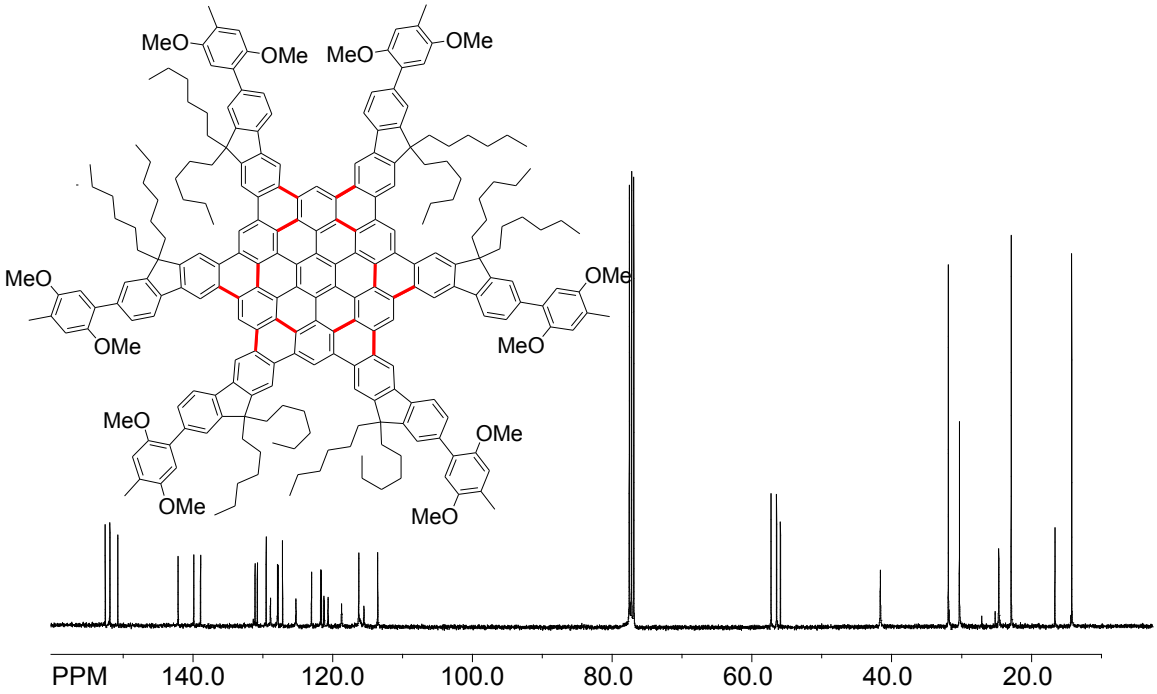

Zoomed ^{13}C NMR of FHBC-Ar6:

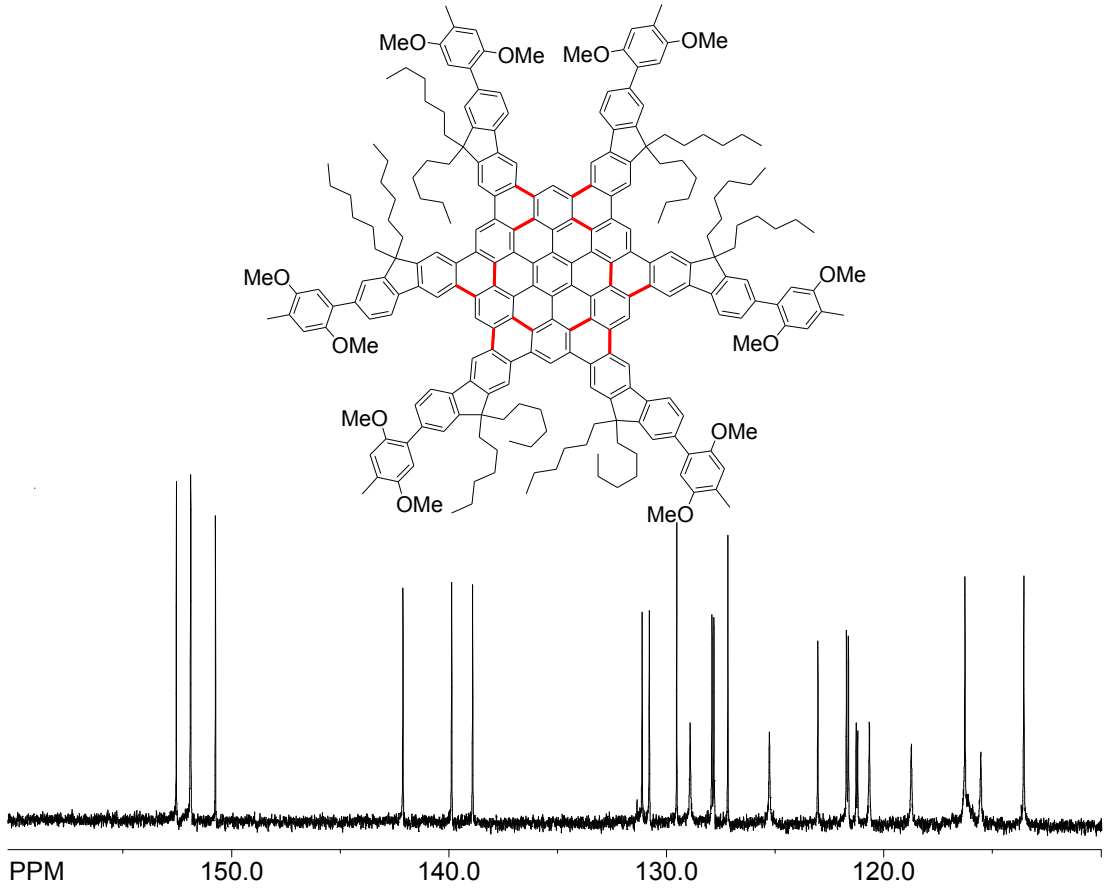

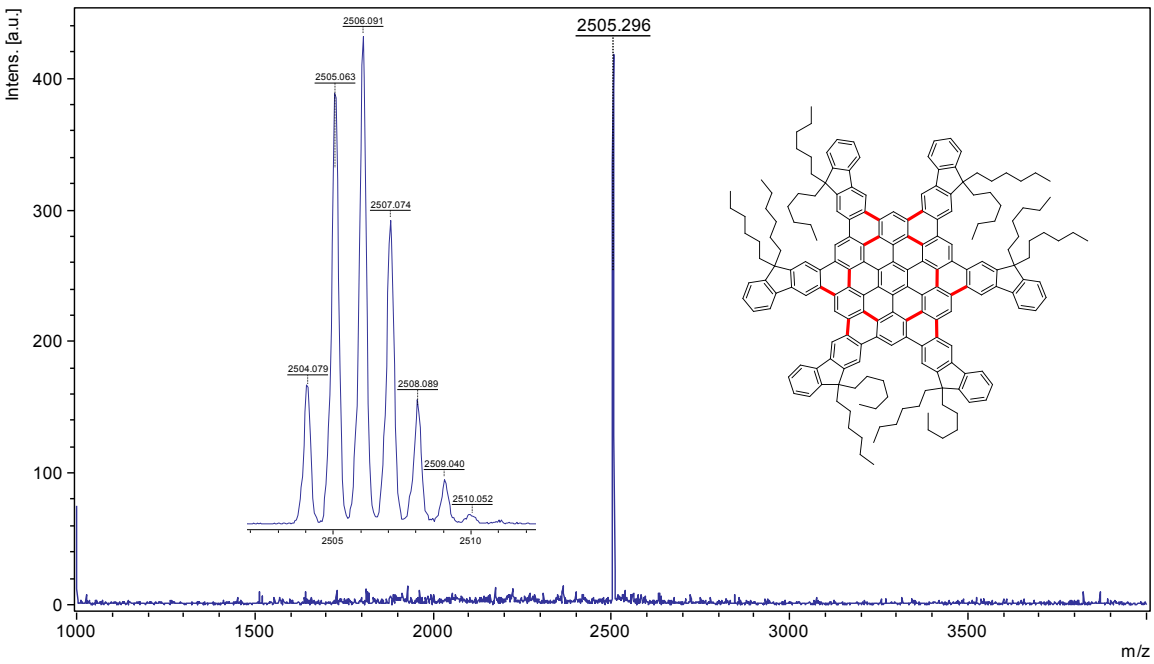

Figure 17. MALDI-TOF mass spectra of FHBC obtained using dithranol as a matrix. Inset showing the isotope distribution for the molecular ion of FHBC.

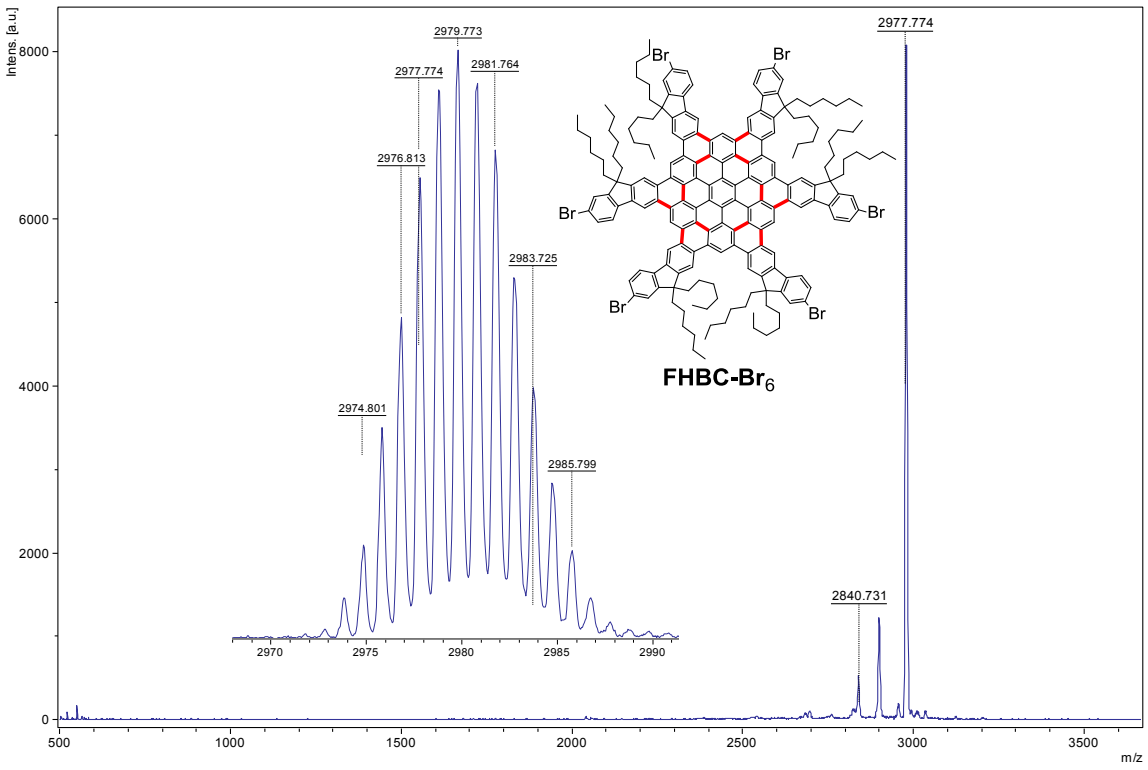

Figure 18. MALDI-TOF mass spectra of FHBC-Br_6 obtained using dithranol as a matrix. Inset showing the isotope distribution for the molecular ion of FHBC-Br_6.

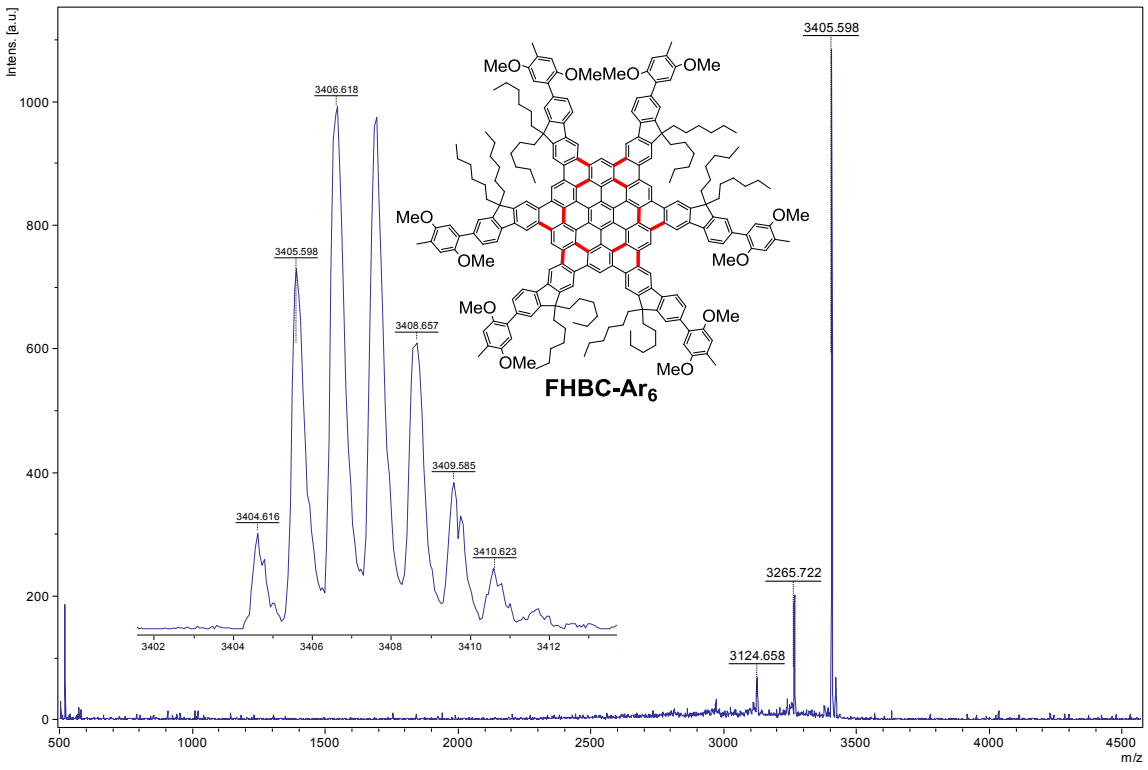

Figure 19. MALDI-TOF mass spectra of FHBC-Ar_6 obtained using dithranol as a matrix. Inset showing the isotope distribution for the molecular ion of FHBC-Ar_6.

BIBLIOGRAPHY

(General Introduction)

(1) (a) Hart, H.; Teuerstein, A.; Babin, M. A. *J. Am. Chem. Soc*. **1981**, *103*, 903. (b) bhattacharya, A.; DiMichele, L. M.; Dolling, U.-H.; Grabowski, E. J. J.; Grenda, V. J. *J. Org. Chem.* **1989**, *54*, 6118. (c) Andersen,M. L.; Handoo, K. L.; Parker, V. D. *Acta Chem. Scand.* **1991**,*45*, 983. (d) Bauld, N. L.; Bellville, D. J.; Harirchian, B.; Lorenz, K. T.; Pabon, P. A., Jr.; Reynolds, D. W.; Wirth, D. D.; Chiou, H. S.; Marsh, B. K. *Acc. Chem. Res.* **1987**, *20*, 371. (e) Kita, Y.; Tohma, H.; Hatanaka, K.; Takada, T.; Fujita, S.; Mitoh, S.; Sakurai, H.; Oka, S. *J. Am. Chem. Soc.* **1994**, *116*, 3864.

(2) (a) Chanon, M. *Bull. Soc. Chim. Fr.* **1985**, 209. (b) Eberson, L. Electron-Transfer Reactions in Organic Chemistry; Springer: New York, **1987**. (c) Dinnocenzo, J. P.; Banach, T. E. *J. Am. Chem. Soc.***1986**, *108*, 6063. (d) Richardson, T. J.; Bartlett, N. *J. Chem. Soc., Chem. Commun.* **1974**, 427. (e) Snider, B. B.; Kwon, T. *J. Org. Chem.* **1990**, *55*, 4786. (f) Panday, G. *Top. Curr. Chem.***1993**, *168*,175.

(3) (a) Connelly, N. G.; Geiger, W. E. *Chem*. *Rev*. **1996**, *96*, 877. (b) McClend, C. W. In *Synthetic Reagents*; Pizey, J. S., Ed.; *Wiley*: *New York*, **1983**; p 85. (c) Uemura, S. In *Synthetic Reagents*; Pizey, J. S., Ed.; *Wiley*: *New York*, **1983**; p 165. (d) Bock, H.; Bra¨hler, G.; Henkel, U.; Schleker, R.; Seebach, D. *Chem*. *Ber*. **1980**, *113*, 289. (e) Mijs, W. J.; deJonge, C. R. H. I. *Organic Synthesis by Oxidation by Metal Complexes*; *Plenum*: *New York*, **1986**.

(4) (a) Enkelmann, V. *Synth. Met*. **1991**, *42*, 2547. (b) Yoshizawa, K.; Chano, A.; Ito, A.; Tanaka, K.; Yamabe, T.; Yamauchi, J.; Shiro, M. *J*. *Am*. *Chem*. *Soc*. **1992**, *114*, 5994. (c) Rathore, R.; Lindeman, S. V.; Kochi, J. K. *Angew*. *Chem*. *Int*. *Ed*. **1998**, *37*, 1585.

(5) (a) Law, K. Y. *Chem*. *Rev*. **1993**, *93*, 449. (b) Baumgarten, M.; Mullen, K. *Top*. *Curr*. *Chem*. **1994**, *169*, 1.

(6) Tiwari, S.; Greenham, N. C. *Optical and Quantum Electronics*; **2009**, *41*, 69.

(7) Morisaki, Y.; Chujo, Y. *Macromolecules* **2004**, *37,* 4099.

(8) Zyss, J.; Ledoux, I.; Volkov, S.; Chernyak, V.; Mukamel, S.; Bartholomew, G. P.; Bazan, G. C. *J*. *Am*. *Chem*. *Soc*. **2000**, *122*, 11956.

(9) Bartholomew, G. P.; Bazan, G. C. *Acc*. *Chem*. *Res*. **2001**, *34*, 30.

(10) Bartholomew, G. P.; Bazan, G. C. *J. Am. Chem. Soc.* **2002**, *124*, 5183.

(11) Banerjee, M.; Shukla, R.; Rathore, R. *J. Am. Chem. Soc.* **2009**, *131*, 1780.

(12) Banerjee, M.; Lindeman, S. V.; Rathore, R. *J. Am. Chem. Soc.* **2007**, *129*, 8070.

(13) Rathore, R.; Abdelwahed, S. H.; Guzei, I. A. *J. Am. Chem. Soc.* **2003**, *125*, 8712.

(14) Stevenson, C. D.; Kiesewetter, M. K.; Reiter, R. C.; Abdelwahed, S. H.; Rathore, R. *J. Am. Chem. Soc.* **2005**, *127*, 5282.

(15) Rathore, R.; Abdelwahed, S. H.; Kiesewetter, M. K.; Reiter, R. C.; Stevenson, C. D. *J. Phys. Chem. B* **2006**, *110*, 1536.

(16) Vura-Weis, J.; Abdelwahed, S. H.; Shukla, R.; Rathore, R.; Ratner, M. A.; Wasielewski, M. R. *Science* **2010**, *328*, 1547.

(17) (a) Schmittel, M.; Burghart, A. *Angew. Chem., Int. Ed. Engl.* **1997**, *36*, 2550. (b) Albini, A.; Fasani, E.; Dalessandro, N. *Coord. Chem. Rev.* **1993**, *125*, 269.

(18) Banerjee, M.; Shukla, R.; Rathore, R. *J. Am. Chem. Soc.* **2009**, *131*, 1780-1786.

(19) Chebny, V. J.; Navale, T. S.; Shukla, R.; Lindeman, S. V.; Rathore, R. *Org. Lett.* **2009**, *11*, 2253.

(20) Navale, T. S.; Zhai, L.; Lindeman, S. V.; Rathore, R. *Chem. Commun.* **2009**, 2857.

(21) (a) Lewis, L. C.; and Singer, L. S. *Chem. Phys.* **1965**, *43*, 2712. (b) Howarth, O. W.; Fraenkel, G. K. *J. Am. Chem. Soc.* **1966**, *88*, 4514.

(22) (a)Badger, B.; Brocklehurst, B. *Trans. Faraday Soc.* **1969**, *65*, 2582 and 2588. (b) Badger, B.; Brocklehurst, B. *Trans. Faraday Soc.***1970**, *66*, 2939. (c) Badger, B.; Brocklehurst, B. *Nature* (London) **1968**, *219*, 263.

(23) Rodgers, M. A. J. *J. Chem. Soc., Faraday Trans. 1* **1972**, *68*, 1278.

(24) Kochi, J. K.; Rathore, R.; Magueres, P. L. *J. Org. Chem.* **2000**, *65*, 6826.

(25) Benesi, H. A.; Hildebrand, J. J. *J. Am. Chem. Soc.* **1949**, *71*, 2703.

(26) Rathore, R.; Kumar, A. S.; Lindeman, S. V.; Kochi, J. K. *J. Org. Chem.* **1998**, *63*, 5847.

(Chapter 1A)

(1) (a) Wu, J.; Pisula, W.; Muellen, K. *Chem. Rev.*, **2007**, *107*, 718. (b) Schenning, A. P. H. J.; Meijer, E. W. *Chem. Commun.*, **2005**, 3245.

(2) (a) Yang, J.-S.; Swager, T. M. *J. Am. Chem. Soc.*, **1998**, *120,* 5321. (b) Yamaguchi, S.; Swager, T. M. *J. Am. Chem. Soc.*, **2001**, *123*, 12087. (c) Rose, A.; Tovar, J. D.; Yamaguchi, S.; Nesterov, E. E.; Zhu, Z.; Swager, T. M. *Philos. Trans. R. Soc. London, Ser. A*, **2007**, *365*, 1589 and references therein.

(3) Kumar, S.; Varshney, S. K. *Mol. Cryst. Liq. Cryst. Sci. Technol., Sect. A*, **2002**, *378*, 59. (b) Li, C. W.; Wang, C.-I.; Liao, H.-Y.; Chaudhuri, R.; Liu, R.-S. *J. Org. Chem.*, **2007**, *72*, 9203. (c) Vincent, V. M.; Wright, J. D. *J. Chem. Soc. Perkin Trans I*, **1974**, 58. (d) Toal, S. J.; Trogler, W. C. *J. Mater. Chem.*, **2006**, *16*, 2871.

(4) (a) Aihara, J.-I. *J. Phys. Org. Chem.*, **2008**, 21, 79. (b) Mills, N. S. *J. Org. Chem.*, **1992**, 57, 1899.

(5) Forsyth, D. A.; Olah, G. A. *J. Am. Chem. Soc.*, **1976**, *98*, 4086.

(6) (a) Banerjee, M.; Lindeman, S. V.; Rathore, R. *J. Am. Chem. Soc.*, **2007**, *129*, 8070. (b) Kochi, J. K.; Rathore, R.; Magueres, P. L. *J. Org. Chem.*, **2000**, *65*, 6826. (c) Rathore, R.; Abdelwahed, S. H.; Guzei, I. A. *J. Am. Chem. Soc.*, **2004**, *126*, 13582. (d) Debroy, P.; Shukla, R.; Lindeman, S. V.; Rathore, R. *J. Org. Chem.*, **2007**, *72*, 1765 and references therein.

(7) Silvestri, M. A.; Nagarajan, M.; Clercq, E. De.; Pannecouque, C.; Cushman, M. *J. Med. Chem.*, 2004, **47**, 3149.

(8) Rathore, R.; Burns, C. L.; Deselnicu, M. I. *Org. Synth.*, **2005**, 82, 1.

(9) (a) Bell, F. A.; Ledwith, A.; Sherrington, D. C. *J. Chem. Soc. C*, **1969**, *13*, 2719. (b) Bell, F. A.; Ledwith, A.; Sherrington, D. C. *J. Org. Chem.*, **1976**, *13*, 155.

(10) (a) Sun, D.; Lindeman, S.V.; Rathore, R.; Kochi, J. K. *J. Chem. Soc. Perkin Trans*. *2*, **2001**, 1585. (b) Rathore, R.; Lindeman, S.V.; Kumar, A.S.; Kochi, J. K. *J. Am. Chem. Soc.* **1998**, *120*, 6931.

(11) Compare: Magueres, P. L.; Hubig, S. M.; Veya, P.; Kochi, J. K. *J. Am. Chem. Soc.*, **2000**, *122*, 10073.

(Chpater 1B)

(1) (a) Navale, T. S.; Thakur, K.; Rathore, R. *Org. Lett.* **2011**, *13*, 1634. (b) Modjewski, M. J.; Shukla, R.; Lindeman, S. V.; Rathore, R. *Tetrahedron Lett*. **2009**, *50*, 6687. (c) Wadumethrige, S. H.; Rathore, R. *Org. Lett*. **2008**, *10*, 5139. (d) Banerjee, M.; Shukla, R.; Rathore, R. *J. Am. Chem. Soc.* **2009**, *131*, 1780. (e) Banerjee, M.; Lindeman, S. V.; Rathore, R. *J. Am. Chem. Soc.* **2007**, *129*, 8070. (f) Banerjee, M.; Vyas, V. S.; Lindeman, S. V.; Rathore, R. *Chem. Commun*. **2008**, *19*, 1889. (g) Navale, T. S; Zhai L.; Lindeman S. V; Rathore, R. *Chem. Commun*. **2009**, *20*, 2857. (h) Rathore, R.; Abdelwahed, S. H.; Guzei, I. A. *J. Am. Chem. Soc.* **2003**, *125*, 8712. (i) Chebny, V. J.; Gwengo, C.; Gardinier, J. R.; Rathore, R. *Tetrahedron Lett.* **2008**, *49*, 4869.

(2) (a) Chiriboga, X.; Gilardoni, G.; Magnaghi, I.; Finzi, P. V.; Zanoni, G.; Vidari, G. *J. Nat. Prod.* **2003**, *66*, 905. (b) Boniface, P. J.; Cambie, R. C.; Carroll, D. R.; Marsh, N. F.; Milbank, J. B. J.; Rutledge, P. S.; Woodgate, P. D. *Aust. J. Chem.* **1994**, *47*, 441. (c) Springer, J. W.; Moore, T. A.; Moore, A. L.; Gust, D.; Groy, Thomas L. *Acta.Crystallogr*. **2002**, *E58*, 1145. (d) Cory, R. M.; McPhail, C. L.; Dikmans, A. J. *Tetrahedron Lett.* **1993**, *34*, 7533. (f) Quast, H.; Fuchsbauer, H. L. *Chem. Ber.* **1986**, *119*, 2414.

(3) (a) Lou, K.; Prior, A. M.; Wiredu, B.; Desper, J.; Hua, D. H. *J. Am. Chem. Soc.* **2010**, *132*, 17635. (b) Jing, C.; Zhu, X-Z.; Chen, C-F. *J. Org. Chem.* **2010**, *75*, 7420.

(4) (a) Zhu, X.-Z.; Chen, C.-F. *J. Org. Chem.* **2005**, *70*, 917. (b) Pei, B-J.; Chan, W-H.; Lee, A. W-M. *Org. Lett.* **2011**, 13(7), 1774.

(5) (a) Norvez, S. *J. Org. Chem.* **1993**, *58*, 2414. (b) Gaeta, C.; Vysotsky, M. O.; Bogdan, A.; Boehmer, V. *J. Am.Chem. Soc.* **2005**, *127*, 13136.

(6) (a) Norvez, S.; Tournilhac, F-G.; Bassoul, P.; Herson, P. *Chem. Mat*. **2001**, 13(8), 2552. (b) Norvez, S.; Simon, J. *Chem. Commun.* **1990**,1398.

(7) Quast, H.; Fuchsbauer, H. L. *Chem. Ber*. **1986**, 119(3), 1016.

(8) Almlof, J. E.; Feyereisen, M. W.; Jozefiak, T. H.; Miller, L. L. *J. Am. Chem. Soc.* **1990**, *112*, 1206.

(9) Fitzgerald, J. J.; Drysdale, N. E.; Olofson, R. A. *Syn.Commun*. **1992**, *22*, 1807.

(10) (a) Fitzgerald, J. J.; Drysdale, N. E.; Olofson, R. A. *J. Org. Chem.* **1992**, *57,* 7122.(b) Prinz, H.; Burgemeister, T.; Weigrebe, W.; Muller, K. *J. Org. Chem*. **1996**, *61*, 2857.

(11) Lu, L.; Chen, Q.; Zhu, X.; Chen, C. *Synthesis* **2003**, 2464.

(12) Shyamasundar, N.; Caluwe, P. *J. Org. Chem.* **1981**, *46*, 809.

(13) (a) Cameron, D. W.; Schutz, P. E. *J. Chem. Soc.* **1967**, 2121. (b) Hui, C. W.; Mak, T. C. W.; Wong, H. N. C. *Tetrahedron* **2004**, 60, 3523.

(14) (a) Nishio, M.; Hirota, M.; Umezawa, Y. The CH/π Interaction. Evidence, Nature, and Consequences, Wiley-VCH, New York, 1998. (b) Shukla, R.; Lindeman, S. V.; Rathore, R. *Chem. Commun*. **2007**, 3717 and references cited therein.

(15) (a) Banerjee, M.; Shukla, R.; Rathore, R. *J. Am. Chem. Soc.* **2009**, *131*, 1780-1786. (b) Chebny, V. J.; Navale, T. S.; Shukla, R.; Lindeman, S. V.; Rathore, R. *Org. Lett.* **2009***, 11,* 2253.

(16) *Introduction to Molecular Electronics*, Petty, M. C.; Bryce, M. R.; Bloor, D., Eds.; Oxford Univ. Press: New York, 1995.

(17) *Organic Electronics*; Klauk, H., Ed.; Wiley-VCH: Weinheim, **2006**.

(18) Rathore, R.; Burns, C. L.; Deselnicu, M. I. *Org. Synth.* **2005**, *82*, 1.

(19) (a) Sun, D.; Lindeman, S. V.; Rathore, R.; Kochi, J. K. *J. Chem. Soc. Perkin Trans*. *2*, **2001**, 1585. (b) Rathore, R.; Lindeman, S.V.; Kumar, A. S.; Kochi, J. K. *J. Am. Chem. Soc.* **1998**, *120*, 6931.

(Chapter 2A)

(1) (a) Wu, J.; Pisula, W.; Müllen, K. *Chem. Rev.* **2007**, *107*, 718. (b) Haddon, R. C.; Chi, X.; Itkis, M. E.; Anthony, J. E.; Eaton, D. L.; Siegrist, T.; Mattheus, C. C.; Palstra, T. T. M. *J. Phys. Chem. B* **2002**, *106*, 8288. (c) Plass, K. E.; Grzesiak, A. L.; Matzger, A. J. *Acc. Chem. Res.* **2007**, *40*, 287. (d) Newman, C. R.; Frisbie, C. D.; da Silva Filho, D. A.; Brédas, J.-L.; Ewbank, P. C.; Mann, K. R. *Chem. Mater.* **2004**, *16*, 4436. (e) Rathore, R.; Maguères, P. Le; Kochi, J. K. *J. Org. Chem*. **2000**, *65*, 6826.

(2) (a) Lewis, F. D.; Letsinger, R. L.; Wasielewski, M. R. *Acc. Chem. Res*. **2001**, *34*, 159. (b) Dekker, C.; Ratner, M. A. *Physics World* **2001**, *14*, 29. (c) Grinstaff, M. W. *Angew. Chem. Int. Ed. Engl.* **1999**, *38*, 3629.

(3) (a) Rathore, R.; Burns, C. L.; Abdelwahed, S. H. *Org. Lett.* **2004**, *6*, 1689. (b) Chebny, V. J.; Shukla, R.;. Rathore, R. *J. Phys. Chem. B* **2006**, *110*, 13003. (c) Shukla, R.; Lindeman, S. V.; Rathore, R. *Org. Lett.* **2007**, *9*, 1291. (d) Chebny, V. J.; Dhar, D.; Lindeman, S. V.; Rathore, R. *Org. Lett.* **2006**, *8*, 5401.

(4) (a) Sun, D.; Rosokha, S. V.;. Kochi, J. K. *Angew. Chem. Int. Ed.* **2005**, *44*, 5133. (b) Rosokha, S. V.; Neretin, I. S.; Kochi, J. K. *J. Am. Chem. Soc.* **2006**, *128*, 9394. (c) Lambert, C. *Angew. Chem. Int. Ed.* **2005**, *44*, 7337 and references cited therein.

(5) (a) Quast, H.; Fuchsbauer, H. L. *Chem. Ber.* **1986**, *119*, 1016. (b) Russell, G. A.; Suleman, N. K.; Iwamura, H.; Webster, O. W. *J. Am. Chem. Soc.* **1981**, *103*, 1560. (c) Kobayashi, T.; Kubota, T.; Ezumi, K. *J. Am. Chem. Soc.* **1983**, *105*, 2172.

(6) (a) Swager, T. M. *Acc. Chem. Res.* **2008**, *41*, 1181. (b) Thomas III, S. W.; Joly, G. D.; Swager, T. M. *Chem. Rev.* **2007**, *107*, 1339. (c) Zhu, X.-Z.; Chen, C.-F *J. Am. Chem. Soc.* **2005**, *127*, 13158. (d) Zhu, X.-Z.; Chen, C.-F. *J. Org. Chem.* **2005**, *70*, 917.

(7) (a) *Introduction to Molecular Electronics*, Petty, M. C.; Bryce, M. R.; Bloor, D. Eds.; Oxford Univ. Press: New York, 1995. (b) Maiya, B. G.; Ramasarma, T.; *Current Science* **2001**, *80*, 1523.

(8) (a) Rathore, R.; Chebny, V. J.; Kopatz, E. J.; Guzei, I. A. *Angew. Chem. Int. Ed.* **2005**, *44*, 2771. (b) Rathore, R.; Abdelwahed, S. H.; Guzei, I. A. *J. Am. Chem. Soc.* **2003**, *125*, 8712. (c) Stevenson, C. D.; Kiesewetter, M. K.; Reiter, R. C.; Abdelwahed, S. H.; Rathore, R. *J. Am. Chem. Soc.* **2005**, *127*, 5282. (d) Rathore, R.; Abdelwahed, S. H.; Kiesewetter, M. K.; Reiter, R. C.; Stevenson,

C. D. *J. Phys. Chem. B* **2006**, *110*, 1536. (e) Chebny, V. J.; Rathore, R. *J. Am. Chem. Soc.* **2007**, *129*, 8458. (f) Debroy, P.; Lindeman, S. V.; Rathore, R. *Org. Lett.* **2007**, *9*, 4091 and references cited therein.

(9) Note that the removal of the first electron from **2** and **3** results in the corresponding cation radicals where a charge is delocalized over two (pre-organized) cofacial veratrole moieties in **2** and over three veratrole moieties in **3**, and thereby rendering the ejection of the second electron from both $\mathbf{2}^{+\bullet}$ and $\mathbf{3}^{+\bullet}$ difficult by roughly ~280 and 290 mV, respectively. It is also noted that owing to the delocalization of charges in the dicationic $\mathbf{3}^{+2}$ makes the ejection of the third electron much more difficult (i.e. by 490 mV).

(10) Rathore, R.; Burns, C. L.; Deselnicu, M. I. *Org. Synth*. **2005**, *82*, 1.

(11) Rathore, R.; Burns, C. L.; Deselnicu, M. I. *Org. Lett.* **2001**, *3*, 2887.

(12) It should be noted that the addition of neutral **3** (up to 10 equiv.) to the solution of $\mathbf{3}^{+\bullet}$ or increasing the concentration of $\mathbf{3}^{+\bullet}$ by 10-fold did not show any change in its absorption spectrum.

(13) (a) Nelsen, S. F. *Chem. Eur. J.* **2000**, *6*, 581. (b) Badger, B.; Brocklehurst, B. *Nature* **1968**, *219,* 263. (c) Kochi, J. K. ; Rathore, R. ; Le Magueres, P. *J. Org. Chem.* **2000**, *65*, 6826.

(14) A suitable crystal (0.33 x 0.20 x 0.10 mm^3) of **3** was obtained from a mixture of dichloromethane-acetonitrile solution at 22 ^oC, see Table 3. A suitable crystal (0.22 x 0.05 x 0.04 mm^3) of [$\mathbf{3}^{+\bullet}\mathbf{SbCl_6}^-$] was obtained from a mixture of dichloromethane-toluene solution at 22 ^oC, see Table 4.

(15) The observation of effective electronic coupling (as judged by the lowering of oxidation potentials and observation of the intense NIR intervalence transitions) amongst the cofacially-oriented veratrole moieties with the interplanar angles of ~120^o in **2** and **3**, suggests that minimal orbital overlap between the interacting π-systems is sufficient for effective electronic coupling to occur. Compare: Rathore, R.; Kochi, J. K. *Can. J. Chem.* **1999**, *121*, 913.

(16) Compare: Banerjee, M.; Vyas, V. S.; Lindeman, S. V.; Rathore, R. *Chem. Commun.* **2008**, 1889.

(17) Davidson, I. M.; Musgrave, O. C. *J. Chem. Soc.* **1963**, 3154.

(18) Rathore, R.; Burns, C. L. *J. Org. Chem.* **2003**, *68*, 4071.

(Chapter 2B)

(1) (a) *Introduction to Molecular Electronics*; Petty, M. C., Bryce, M. R., Bloor, D., Eds.; Oxford University Press: New York, 1995. (b) Maiya, B. G.; Ramasarma, T. *Curr. Sci.* **2001**, *80*, 1523–1530. (c) Gross, M.; Muller, D. C.; Nothofer, H.-G.; Scherf, U.; Neher, D.; Brauchle, C.; Meerholz, K. *Nature* **2003**, *405*, 661–665. (d) *Organic Electronics*; Klauk, H., Ed.; Wiley-VCH: Weinheim, 2006.

(2) (a) Weiss, E. A.; Tauber, M. J.; Kelley, R. F.; Ahrens, M. J.; Ratner, M. A.; Wasielewski, M. R. *J. Am. Chem. Soc.* **2005**, *127*, 11842. (b) Berresheim, A. J.; Muller, M.; Mullen, K. *Chem. Rev.* **1999**, *99*, 1747.

(3) (a) Scherf, U.; List, E. J. W. *Adv. Mater.* **2002**, *14*, 477. (b) Li, Z. H.; Wong, M. S.; Tao, Y.; Lu, J. *Chem. Eur. J.* **2005**, *11*, 3285. (c) Goldsmith, R. H.; Sinks, L. E.; Kelley, R. F.; Betzen, L. J.; Liu, W.; Wiess, E. A.; Ratner, M. A.; Wasielewski, M. R. *Proc. Natl. Acad. Sci. U.S.A.* **2005**, *102*, 3540. (d) Perepichka, I. I.; Perepichka, I. F.; Bryce, M. R.; Palsson, L.-O. *Chem. Commun.* **2005**, 3397.

(4) (a) Davis, W. B.; Svec, W. A.; Ratner, M. A.; Wasielewski, M. R. *Nature* **1998**, *396*, 60. (b) Van Hutten, P. F.; Krasnikov, V. V.; Hadziioannou, G. *Acc. Chem. Res.* **1999**, *32*, 257.

(5) (a) Zade, S. S.; Bendikov, M. *Org. Lett.* **2006**, *8*, 5243. (b) Roncali, J. *Chem. Rev.* **1992**, *92*, 711. (c) *Handbook of Oligo- and Polythiophenes*; Fichou, D., Ed.; Wiley-VCH: Weinheim, Germany, **1999**.

(6) Shirakawa, H.; Louis, E. J.; MacDiarmid, A. G.; Chiang, C. K.; Heeger, A. *J. Chem. Soc. Chem. Commun.* **1977**, *16*, 578.

(7) (a) Berresheim, A. J.; Müller, M.; Müllen, K. *Chem. Rev.* **1999**, *99*, 1747. (b) Watson, M. D.; Fechtenkotter, A.; Müllen, K. *Chem. Rev.* **2001**, *101*, 1267 and references therein. (c) Baumgarten, M.; Müllen, K. *Top. Curr. Chem.* **1994**, *169*, 1 and references therein. (d) Cao, X.-Y.; Zi, H.; Zhang, W.; Lu, H.; Pei, J., *J. Org. Chem.* **2005**, *70*, 3645. (e) Rathore, R.; Burns, C. L. *J. Org. Chem.* **2003**, *68*, 4071-4074. (f) Chebny, V. J.; Gardinier, J. R.; Rathore, R. *Tetrahedron. Lett.* **2008**, *49*, 4869. (g) Wadumethrige, S. H.; Rathore, R. *Org. Lett.* **2008**, *10*, 5139. (h) Zhai, L.; Shukla, R.; Rathore, R. *Org. Lett.* **2009**, 11, 3474.

(8) Rathore, R.; Burns, C. L.; Deselnicu, M. I. *Org. Synth.* **2005**, *82*, 1.

(9) Rathore, R.; Kochi, J. K. *J. Org. Chem.* **1995**, *60*, 4399.

(10) Li, X.; Upton, T. G.; Gibb, L. D.; Gibb, B. C. *J. Am. Chem. Soc.,* **2003**, *125*, 650.

(11) Copper(II) is known to oxidize hydroquinones to quinones. See (a) Rockcliffe, D. A.; Martell, A. E. J. Chem. Soc., Chem. Commun. **1992**, 1758. (b) Kitajima, N.; Koda, T.; Iwata, Y.; Moro-oka, Y. *J. Am. Chem. Soc,* **1990***, 112,* 8833.

(12) Chebny, V.; Navale, T. S.; Lindeman, S. V.; Rathore, R. *Org. Lett*. **2009**, *11*, 2253.

(13) **4R:** (Anisole)**, 6R:** (1,4-dimethoxybenzene)**, 7R:** (1,4-dimethoxy-2,5-dimethylbenzene) Rathore, R.; Bosch, E.; Kochi, J. K. *Tetrahedron*, **1994**, *50*, 6727. **5R:** (4-methylanisole) a) Bystron, T. *J. Electrochem. Soc.* **2009**, *156*, 1. b) Toshiki, T. *Chem. Eur. J.* **2005**, *11*, 6192. c) Toshiki, T. *Electrochim. Acta.* **2009**, 54, 5959. **9R**: (4-methoxybenzophenone) E_{ox1}= 1.98 V vs SCE, (**10R [**(1-methoxy-4-(1,2,2-triphenyl)benzene] Banerjee, M.; Emond, S. J.; Lindeman, S. V.; Rathore, R. *J. Org. Chem.,* **2007**, *72*, 8054. **8R**: (1,2,4-trimethoxy-5-methylbenzene) 0.98V *vs* SCE. **8R** was prepared by treating 4-bromo-2,5-dimethoxytoluene with sodium methoxide in refluxing toluene using catalytic Cu(I)Br as a catalyst.

(14) Rathore, R.; Burns, C. L.; Deselnicu, M. I. *Org. Lett.* **2001**, *3*, 2887.

(15) Rathore, R.; Kumar, A. S.; Lindeman, S. V.; Kochi, J. K. *J. Org. Chem*. **1998**, *63*, 5847. (b) Kochi, J. K.; Le Magueres, P.; Rathore, R. *J. Org. Chem*. **2000**, *65*, 6826.

(16) Compare: a) Rathore, R.; Kochi, J. K. *Can. J. Chem*. **1999**, *121*, 913. b) Rathore, R.; Burns, C. L.; Abdelwahed, S. A. *Org. Lett*. **2004**, *6*, 1689. C) Rathore, R.; Abdelwahed, S. A.; Guzei, I. A. *J. Am. Chem. Soc.* **2003**, *125*, 8712 d) Chebny, V.; Navale, T. S.; Shukla, R.; Lindeman, S. V.; Rathore, R. *Org. Lett*. **2009**, *11*, 2253.

(17) Navale, T. S.; Zhai, L.; Lindeman, S. V.; Rathore, R. *Chem. Commun*. **2009**, 2857.

(Chapter 3)

(1) (a) *Introduction to Molecular Electronics*, Petty, M. C.; Bryce, M. R.; Bloor, D. Eds.; Oxford Univ. Press: New York, 1995. (b) Maiya, B. G.; Ramasarma, T. *Current Science* **2001**, *80*, 1523.

(2) (a) Watson, M. D.; Fechtenkotter, A.; Müllen, K. *Chem. Rev.* **2001**, *101*, 1267. (b) Grimme, W.; Kaemmerling, H. T.; Lex, J.; Gleiter, R.; Heinze, J.; Dietrich, M. *Angew. Chem., Int. Ed. Engl.* **1991**, *30*, 205.

(3) (a) Yang, J.-S.; Swager, T. M. *J. Am. Chem. Soc*. **1998**, ***120***, 5321. (b) Yamaguchi, S.; Swager, T. M. *J. Am. Chem. Soc*. **2001**, *123*, 12087. (c) Rose, A.; Tovar, J. D.; Yamaguchi, S.;. Nesterov, E. E.; Zhu, Z.; Swager, T. M. *Philos. Trans. R. Soc. London, Ser. A* **2007**, *365*, 1589 and references therein.

(4) Kumar, S.; Varshney, S. K. *Mol. Cryst. Liq. Cryst. Sci. Technol., Sect. A* **2002**, *378*, 59. (b) Li, C.-W.; Wang, C.-I.; Liao, H.-Y.; Chaudhuri, R.; Liu, R.-S. *J. Org. Chem.* **2007**, *72*, 9203. (c) Toal, S. J.; Trogler, W. C. *J. Mater. Chem*. **2006**, *16*, 2871. (d) Chaudhuri, R.; Hsu, M.-Y.; Li, C.-W.; Wang, C.-I.; Chen, C.-J.; Lai, C. K.; Chen, L.-Y.; Liu, S.-H.; Wu, C.-C.; Liu, R.-S. *Org. Lett.* **2008**, *10*, 3053.

(5) Buckles, R. E.; Serianz, A.; Naffziger, D. *Proceedings of the Iowa Academy of Science* **1973**, *80*, 45-49.

(6) McMurry, J. E. *Acc. Chem. Res.* **1983**, *16*, 405.

(7) Banerjee, M.; Emond, S. J.; Lindeman, S. V.; Rathore, R. *J. Org. Chem.* **2007**, *72*, 8054.

(8) (a) Scholl, R.; Mansfeld, J. *Ber. Dtsch. Chem. Ges.* **1910**, *43*, 1734. (b) Kovacic, P.; Jones, M. B. *Chem. Rev.* **1987**, *87*, 357.

(9) Navale, T. S.; Zhai, L.; Sergey, V.; Rathore, Rajendra. *Chem. Comm.* **2009**, 2857.

(10) Klumpp, D. A.; Baek, D. N.; Prakash, G. K. S.; Olah, G. A. *J. Org. Chem.* **1997**, *62*, 6666. (b) Olah, G. A.; Klumpp, D. A.; Baek, D. N.; Neyer, G.; Wang, Q. *Org. Synth.* **1999**, *76*, 294.

(11) Rathore, R.; Lindeman, S. V.; Kumar, A. S.; Kochi, J. K. *J. Am. Chem. Soc.* **1998**, 120, 6931.

(12) An NMR analysis of the crude reaction mixture suggested that it contained traces of parent dibenzochrysene **1d** and 9,10-diphenylphenanthrene **1b** together with multitude of products arising from the electrophilic aromatic chlorination of **1a**, **1b**, and **1d**.

(13) (a) Zhai, L.; Shukla, R.; Rathore, R. *Org. Lett.* **2009**, *11*, 3474. (b) Zhai, L.; Shukla, R.; Wadumethridge, S. H.; Rathore, R. *J. Org. Chem*. **2010**, *75*, 4748.

(14) The blue-violet color in reaction of **1a** with DDQ/H^+ arises due to the formation of $\mathbf{1a}^{+\bullet}$ and $\mathbf{1}^{+2}$, as confirmed by comparison of the UV-vis absorption spectrum of the reaction mixture with that of the authentic spectra[11] of $\mathbf{1a}^{+\bullet}$ and $\mathbf{1}^{+2}$.

(15) (a) Brook, A. G. *J. Chem. Soc.* **1952**, 5040-5041. (b) Newman, M. S.; Khanna, V. K. *Org. Prep. Proc. Int.* **1985**, *17*, 422-423. (c) Scott, J. W.; Parrish, D. R.; Bizzarro, F. T. *Org. Prep. Proc. Int.* **1977**, *9*, 91-94.

(16) (a) Oxidative cyclizations of symmetrical TAEs to corresponding diarylphenanthrenes and diarylmethylidenefluorene have been previously observed; see: Ciminale, F.; Lopez, L.; Mele, G. *Tetrahedron* **1994**, *50*, 12685. (b) it is well known that the cation radicals and dications of TAEs are twisted aroud the ethylenic c=c bond by ~30^o-60^o and undergo ready isomerization under oxidative conditions; see ref 11.

(17) Note that (DDQ, E_{red} = +0.60 V vs. SCE), in the presence of an acid, oxidizes a variety of aromatic donors with oxidation potentials as high as ~1.6 V vs. SCE, to the corresponding cation radicals, however, rate of formation of cation radical increases with increasing oxidation potential of donors, see: (a) Rathore, R.; Kochi, J. K. *Acta. Chem. Scand.* **1998**, *52*, 114-130. (b) Rathore, R.; Zhu, C.-J.; Lindeman, S. V.; Kochi, J. K. *J. Chem. Soc., Perkin Trans 2* **2000**, 1837-1840. (c)

Handoo, K. L.; Gadru, K. *Curr. Sci.* **1986**, *55*, 920-922 and references cited therein.

(18) The bifluorenylidene formed from **2c**, after oxidative C-C bond formation, can easily be isomerizes to DBC **2d** by acid or electron-transfer catalysis, see: Suzuki, K.; Yamaguchi, U. *Bull. Chem. Soc. Japan* **1962**, *35*, 735-740 and refences cited therein.

(19) Daik, R.; Feast, W. J.; Batsanov, S. A.; Howard, A. J. *New J. Chem.* **1998**, 1047-1049.

(20) Buckles, R. E.; Hausman, E. A.; Wheeler, R. G. *J. Am. Chem. Soc.* **1998**, *120*, 2494-2496.

(Chapter 4)

(1) (a) *Introduction to Molecular Electronics*; Petty, M. C., Bryce, M. R., Bloor, D., Eds.; Oxford University Press: New York, 1995. (b) Maiya, B. G.; Ramasarma, T. *Curr. Sci.* **2001**, *80*, 1523–1530. (c) Gross, M.; Muller, D. C.; Nothofer, H.-G.; Scherf, U.; Neher, D.; Brauchle, C.; Meerholz, K. *Nature* **2003**, *405*, 661–665. (d) *Organic Electronics*; Klauk, H., Ed.; Wiley-VCH: Weinheim, 2006.

(2) (a) Berresheim, A. J.; Müller, M.; Müllen, K. *Chem. Rev.* **1999**, *99*, 1747. (b) Watson, M. D.; Fechtenkotter, A.; Müllen, K. *Chem. Rev.* **2001**, *101*, 1267 and references therein. (c) Baumgarten, M.; Müllen, K. *Top. Curr. Chem*. **1994**, *169*, 1 and references therein. (d) Cao, X.-Y.; Zi, H.; Zhang, W.; Lu, H.; Pei, J., *J. Org. Chem*. **2005**, *70*, 3645-3653.

(3) (a) Rathore, R.; Burns, C. L. *J. Org. Chem*. **2003**, *68*, 4071-4074. (b) Chebny, V. J.; Gardinier, J. R.; Rathore, R. *Tetrahedron Lett*. **2008**, 49, 4869. (c) Wadumethrige, S. H.; Rathore, R. *Org. Lett*. **2008**, *10*, 5139. (d) Zhai, L.; Shukla, R.; Rathore, R. *Org. Lett.* **2009**, *11*, 3474.

(4) (a) Herwig, P.; Kayser, C. W.; Müllen, K.; Spiess, H. W. *Adv. Mater.* **1996**, *6*, 510-513. (b) Fechtenkötter, A.; Saalwächter, K.; Harbison, M. A.; Müllen, K.; Spiess, H. W. *Angew. Chem., Int. Ed. Engl.* **1999**, *38*, 3039-3042. (c) Pisula, W.; Tomovic, Z.; Simpson, C.; Kastler, M.; Pakula, T.; Müllen, K. *Chem. Mater.* **2005**, *17*, 4296-4303.

(5) Wasserfallen, D.; Kastler, M.; Wojciech, P.; Hofer, W. A.; Fogel, Y.; Wang, Z.; Müllen, K. *J. Am. Chem. Soc.* **2006**, *128*, 1334-1339.

(6) Geng, Y.; Trajkovska, A.; Katsis, D.; Ou, J. J.; Culligan, S.W.; Chen, S.H., *J. Am. Chem. Soc.* **2002**, *124*, 8337-8347 and references cited therein.

(7) (a) Rathore, R.; Abdelwhaed, S.H.; Guezi, I.A., *J. Am. Chem. Soc.* **2003**, *125*, 8712-8713. (b) Rathore, R.; Abdelwahed, S.H.; Kiesewetter, M.K.; Reiter, R.C.; Stevenson, C.D., *J. Phys. Chem. B* **2006**, *110*, 1536-1542. (c) Stevenson, C.D.; Kiesewetter, M.K.; Reiter, R.C.; Chebny, V. J.; Rathore, R., *J. Phys. Chem. A* **2006,** *110*, 9602-9609. (d) Stevenson, C.D.; Kiesewetter, M.K.; Reiter, R.C.; Abdelwahed, S.H.; Rathore, R., *J. Am. Chem. Soc* **2005**, *127*, 5282-5283.

(8) (a) Suzuki, A. *Chem. Commun*. **2005**, 4759-4763. (b) Hassan, J.; Sevignon, M.; Gozzi, C.; Schulz, E.; Lemaire, M. *Chem. Rev.* **2002**, *102*, 1359-1469 and references therein.

(9) (a) Scholl, R.; Mansfeld, J. *Ber. Dtsch. Chem. Ges.* **1910**, *43*, 1734-1746. (b) Kovacic, P.; Ones, M. B. *Chem. Rev.* **1987**, *87*, 357-379. (c) Zhai, L.; Shukla, R.; Rathore, R. In reference 3d.

(10) Rathore, R.; Burns, C. L.; Deselnicu, M. I. *Org. Synth.* **2005**, *82*, 1.

(11) (a) Bell, F. A.; Ledwith, A.; Sherrington, D. C. *J. Chem. Soc. C* **1969**, *13*, 2719. (b) Bell, F. A.; Ledwith, A.; Sherrington, D. C. *J. Org. Chem.* **1976**, *13*, 155.

(12) Rathore, R.; Burns, C. L.; Deselnicu, M. I. *Org. Lett.* **2001**, *3*, 2887.